PERFORMANCE AND TORQUE PULSATIONS MINIMISATION OF INVERTER FED THREE PHASE INDUCTION MOTOR

A THESIS

Submitted in partial fulfilment of
the requirements for the Degree of
Doctor of Philosophy
IN THE
FACULTY OF ENGINEERING AND TECHNOLOGY

By
O.P. GARG

UNDER THE SUPERVISION OF
Dr. R.B. SAXENA

DEPARTMENT OF ELECTRICAL AND ELECTRONICS ENGINEERING
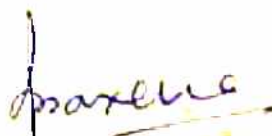BIRLA INSTITUTE OF TECHNOLOGY AND SCIENCE
PILANI (Rajasthan), INDIA
Feb. 1976

TO

ALKA	daughter
SHISHIR	son
VIJAYA	wife

CERTIFICATE

This is to certify that the thesis entitled 'Performance and Torque Pulsations Minimisation of Inverter Fed Three Phase Induction Motor' and submitted by Shri O.P. Garg, embodies original work done by him under my supervision. It is recommended that the thesis be accepted in partial fulfilment of the requirements for the degree of Doctor of Philosophy in the Department of Electrical and Electronics Engineering of the Faculty of Engineering and Technology of the Birla Institute of Technology and Science, Pilani (Rajasthan).

Thesis Supervisor

(Dr. R.B. Saxena)
Lecturer in the Department of
Electrical and Electronics Engineering
Birla Institute of Technology and Science
Pilani (Rajasthan)

ACKNOWLEDGEMENTS

ABSTRACT

The problem of torque pulsations is very severe in an inverter fed, three phase induction motor; due to the nonsinusoidal nature of inverter's output voltage. A new mathematical model, giving equations at the filter terminals of the system is developed, doing away with the normal assumption of known and fixed (stepped type) voltage waveform at the motor terminals. Effects of filter parameters, ripples present in the rectified output and inverter's periodic switching are fully accounted in the developed model. The model enables to compute the pulsating torque, various losses and other performance characteristics of the drive both under dynamic and steady state conditions. The computed results for large sets of system parameters at different frequencies establish, that the higher values of leakage and magnetising inductances reduce the torque pulsations without appreciably affecting the efficiency and power factor.

Rosenbrock's Hill Climb method has been used as min-max technique to find an optimal set of machine parameters giving minimum torque pulsations; and from therein, suitable design recommendations have been evolved. The system is found to be stable almost at all the frequencies with optimal parameters.

The computed results with normal parameters at various frequencies are found to be in close agreements with the experimental results.

CONTENTS

- o -

LIST OF COMPUTER PROGRAMS

MAIN LINE PROGRAMS

Name of the program	Purpose
GARG	For constant speed solution of the system equations. It gives, pulsating torques, average torque, power factor, efficiency, slip, current and terminal voltage steady state and transient waveforms.
GARG1	For dynamic load switching transients of phase current, torque and speed.
GARG2	Rosenbrock's Hill Climb Method used as MIN-MAX technique for optimisation of torque pulsations.
VIZI	Stability test with sinusoidal excitation, using Routh Hurwitz criterion.

Subroutines and subprograms:

R3KSH	Inversion of matrix
R4KSH	Product of two matrices
R5KSH	Fourier analysis of given waveform.
R6KSH	Average and pulsating torque calculations.
RKeSH	Numerical integration Runge-Kutta 4th order.
ALKA	Objective function (Peak pulsating torque value).
CG	Lower constraint function.
CH	Higher constraint function.
CX	Variable identification.

LIST OF TABLES:

- o -

LIST OF SYMBOLS:

Only those symbols which frequently appear in the text are given below, the others are explained when they are introduced fresh.

C_F	Filter capacitance
$[C_P^s]_k$, $[C_P^r]_k$	Transformation matrices of stator and rotor variables for a reference frame rotating at k times the fundamental speed.
$[C_P^{sr}]_k$	Combined transformation matrix of stator and rotor variables for a reference frame, rotating at k times the fundamental speed.
D_1 to D_6	Diodes
E_d	Filter input voltage.
$E_{d.c.}$	D.C. Component of filter's input voltage
$[E_j]$	System voltage matrix for jth state.
F	Objective function
G_K	Lower limit on Kth variable.
H_K	Upper limit on Kth variable.
I_i	Inverter input current.
I_{mn}	Amplitude of nth harmonic current.
I_R	Rectifier current.
J	Per unit rotational inertia of rotor.
$\bar{L}_1, \bar{L}_2$	Self inductances of stator and rotor.
L_F	Filter inductance

$[L_j]$	Inductance matrix of jth state.
M	Mutual inductance between stator and rotor.
M_1/M_2	Peak value of mutual inductance between stator/rotor phases.
N	Speed of rotation of rotor in rpm.
P	Number of poles.
R_1, R_2	Stator and rotor resistances.
R_F	Filter resistance
$[R_j]$	Resistance matrix of jth state.
S_i	Step size for ith state.
T_{avg}, T_{const}	Average torque.
T_e	Instantaneous torque.
T_{e6}, T_{e12}	6th and 12th harmonic torques.
T_L	Load torque.
T_P	Pulsating torque.
V_i	Inverter input voltage.
V_m	Peak phase voltage.
X	Independent variable.
X_{CF}, X_c	Capacitive reactance of filter.
X_{LF}, X_F	Inductive reactance of filter.
X_{L1}, X_{L2}	Leakage reactances of stator and rotor.
X_M	Magnetising reactance.
X_1, X_2	Self reactances of stator and rotor.
$[Y_j]$	State variable vector for jth state.

$[z^s_{ryb}, {}^r_{\alpha\beta\nu}]$	Impedance matrix in ryb axis of stator and $\alpha\beta\nu$ axis of rotor.
z_1 to z_6	Thyristors' forward impedances.
$[z_g]$	General system impedance matrix.
$[z^s_{qdo}, {}^r_{qdo}]_k$	Impedance matrix in qdo axis of stator and rotor for kth harmonic.
$[z_{tj}]$	Impedance matrix of jth state.
f_o	Operating frequency (Hz) .
i_1 to i_6	Thyristor currents.
$[i_g]$	General system current matrix.
$[i_j]$	System current matrix of jth state.
i^s_{qk}, i^s_{dk} $\quad$ i^r_{qk}, i^r_{dk}	q-d axis currents of stator and rotor.
$[i^s_{ryb}, {}^r_{\alpha\beta\nu}]$	Current matrix in ryb axis of stator and $\alpha\beta\nu$ axis of rotor.
i^s_{α}, i^s_{β} $\quad$ i^r_{α}, i^r_{β}	Stator and rotor currents in $\alpha\beta$ axis.
j	State number
k	Harmonic order
n	Harmonic order
p	Differential operator, pair of poles.

qdo^s, qdo^r	qdo axis of stator and rotor.
ryb^s, ryb^r	ryb axis of stator and rotor.
s	Per unit slip.
v_c	Capacitor voltage.
$[v_g]$	General system impedance matrix.
$v_{qk}^s, v_{dk}^s, v_{ok}^s$	kth harmonic voltages in q,d, and o axis of stator.
v_r^s, v_y^s, v_b^s	Stator phase voltages.
v_r^r, v_y^r, v_b^r	Rotor phase voltages.
$v_{rk}^s, v_{yk}^s, v_{bk}^s$	kth harmonic stator phase voltage.
$[v_{ryb, \alpha\beta\nu}^{s \quad r}]$	Voltage matrix in ryb axis of stator and $\alpha\beta\gamma$ axis of rotor.
w	Per unit operating frequency.
w_b	Normal angular frequency.
w_o	Operating angular frequency.
w_r	Rotor speed in electrical radians/sec.
$\alpha^r, \beta^r, \sqrt{}^r$	Rotor axes.
θ_1^n	Phase angle of nth stator harmonic.
θ_2^n	Phase angle of nth rotor harmonic.

- o -

INTRODUCTION

In many modern industries e.g. steel, textile and paper mills and for electric traction the demand is for a precise, continuous variable speed drives, capable of giving long term stability and good transient performance. The d.c. motor[23] has satisfied these requirements satisfactorily in almost all these applications; but its commutator (a mechanical frequency changer) has always been a source of numerous troubles causing frequent break downs of the drive[44]. In addition, it requires a very rigorous maintenance schedule. This causes difficulty when service interruptions cannot be tolerated or when the motor is used at inaccessible locations.

The squirrel cage induction motor is robust, rugged and permits reliable maintenance free operation. The simple rotor construction also results in a cheaper motor and a higher power/weight ratio. But its inherent constant speed characteristics has hampered its wide use as an efficient drive; which is otherwise much superior to the conventional d.c. motor. For intermittent operation, a few sub synchronous speeds are possible by stator voltage control, pole changing, pole amplitude modulation and rotor resistance control[39] (for wound rotors only). However, efficient, wide range, stepless speed control of cage induction motor is only possible when a variable frequency a.c. supply is available. The rotating converter and auxiliary,

a.c. commutator machines have been used in the past[33,80,39] to make the cage induction motor a variable speed drive. The cost of additional machines, however, make the system uneconomical when compared with d.c. motors. Also, the problem of commutation is more severe in a.c. commutator machines[33].

As a result of recent advances in solid state technology and with the availability of high power, reliable and efficient thyristor converters[22], now it has become possible to have wide speed range cage induction motor. Since its introduction in 1957 by General Electric Company[21], the thyristor has become firmly established as the active power control element of static electrical power conversion equipment of many types; ranging in power rating from a few hundred watts to several megawatts. One major application of thyristor is to control electric drives. The emergence of the thyristor in conjunction with the rapid technological advances that have been made in the area of transistors and integrated circuits, has given birth to a much wider field of applications, for the thyristor.

A. HISTORICAL DEVELOPMENT OF THYRISTOR DRIVES:

The trend during the last decade is to make the induction motor an ideal wide range variable speed drive. The thyristor is fast replacing the conventional methods of speed control of induction motor. The thyristor a.c. regulators (fig.1), consisting of two thyristors connected in parallel opposition, or a single thyristor connected across

MAIN WINDING

A.C. SUPPLY

ROTOR

AUXILIARY WINDING
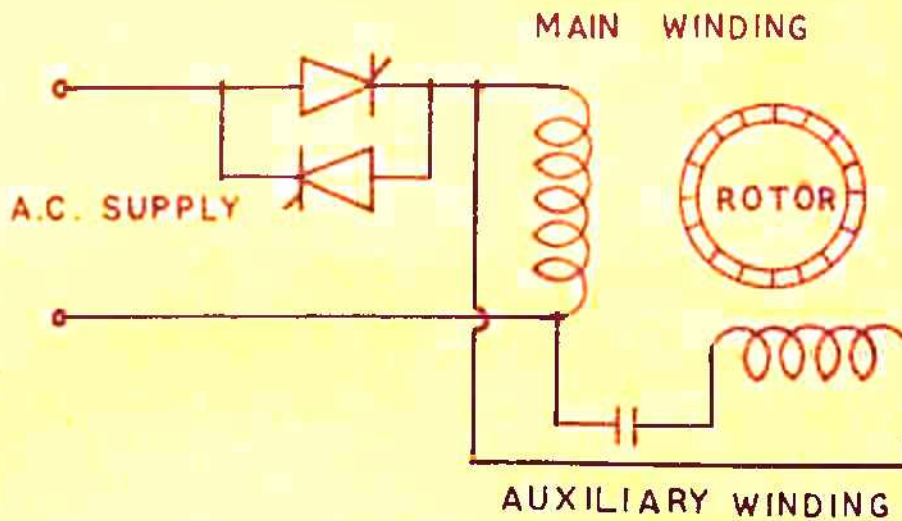
FIG.1 SPEED CONTROL OF SINGLE PHASE INDUCTION MOTOR.

L_1

L_2 STATOR (INDUCTION MOTOR)

3 PHASE SUPPLY

L_3
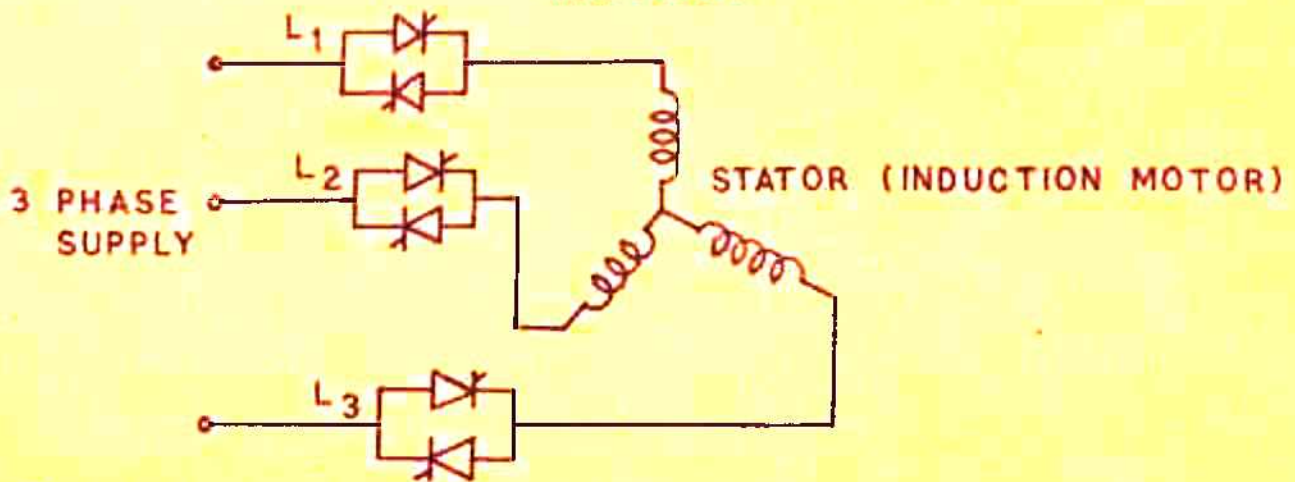
(a) THREE PHASE STAR CONNECTED MOTOR

L_1

3 PHASE SUPPLY

L_2

L_3
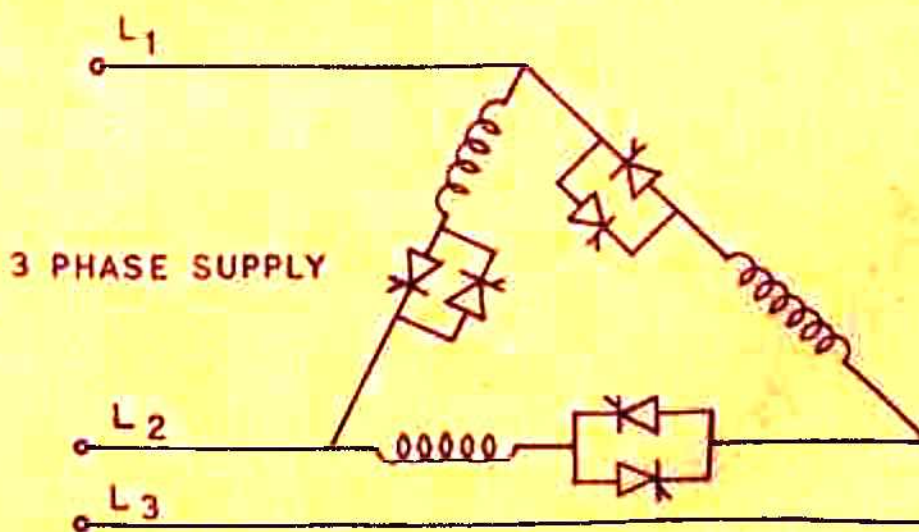
(b) THREE PHASE DELTA CONNECTED MOTOR

FIG.2 SPEED CONTROL OF THREE PHASE INDUCTION MOTOR.

INVT. A   INVT B

SLIPRINGS

STATOR ROTOR

LOAD

AUTO TRANS
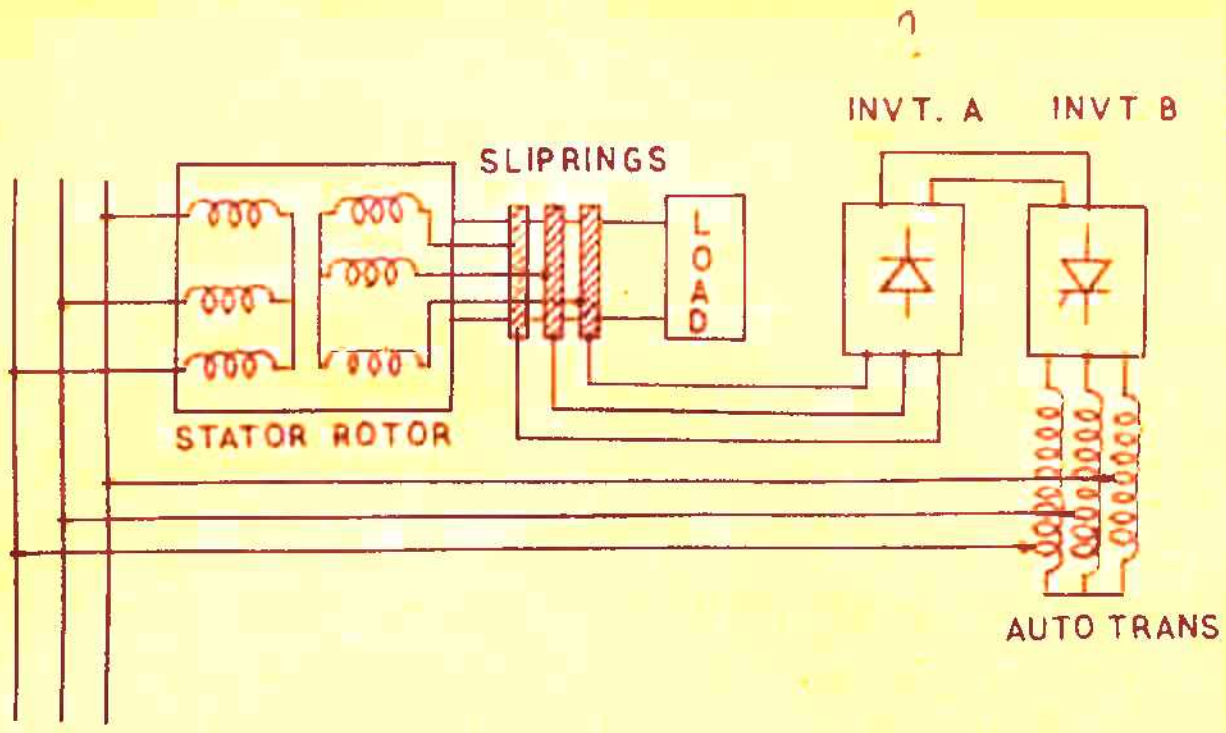
FIG. 3 SLIP POWER CONTROL OF SLIP RING
INDUCTION MOTOR.

Tmax

T LOAD

$N_1 W_1$ $N_2 W_2$ $N_3 W_3$ $N_4 W_4$
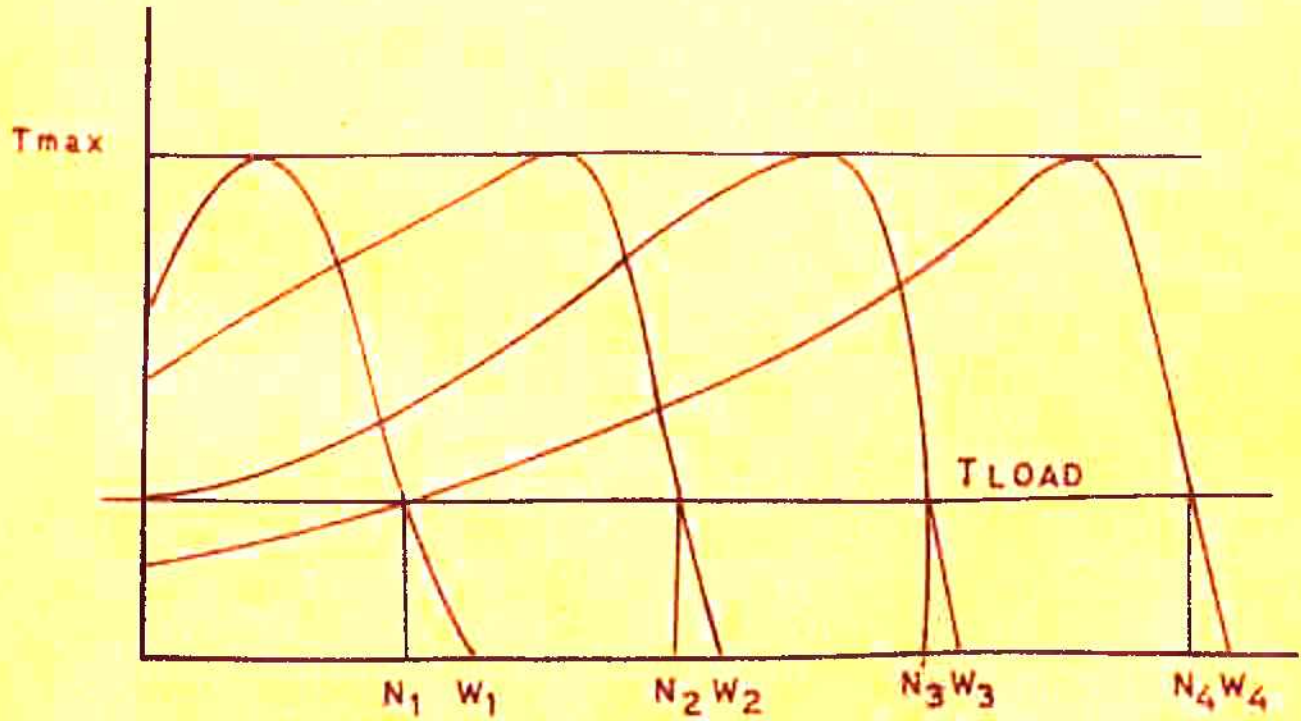
$W_1 : W_2 : W_3 : W_4 = 1 : 2 : 3 : 4$

AND APPROXIMATELY $N_1 : N_2 : N_3 : N_4 = 1 : 2 : 3 : 4$

FIG. 4   TORQUE SPEED CHARACTERISTICS

rpm to many times the normal synchronous speeds, is the frequency control of induction motor using inverter and cycloconverters. Inverter enables a supply of direct current or alternating current of one frequency to be converted to a supply of alternating current at some other frequency or frequencies. The direct conversion from a.c. at frequocy f_1 to another frequency f_2 is performed by cycloconverters[65]. The cycloconverters have not still become popular for the purpose of speed control of induction motor, mainly because of its following drawbacks.

(i) Only few limited discrete low frequency steps can be obtained.

(ii) The number of thyristors used are three times of that required for simple bridge inverter[53].

(iii) The commutation and triggering logics are very complex. A change in the supply frequency would bring a proportional change in the synchronous speed and the actual speed would follow in roughly the same manner (fig.4). An induction motor is designed to work at a particular flux density, and as the electromagnetic torque is proportional to the magnetic flux, it is necessary to have a high value of flux density without going too far into the saturation region. Therefore to keep the magnetic flux constant for any frequency, the applied voltage is adjusted in proportion to the frequency[5,11,96]

The variable frequency drive is particularly attractive in multimotor systems when large numbers of small motors are

supplied simultaneously with the same frequency. In such applications, the cost of the frequency converter is justified by the significant reduction in machine costs due to the large number of motors involved. Static frequency converters can deliver an output frequency of extremely high precision and long term stability[58,70]. Multimotor drives have found wide spread applications in the textile and synthetic fibre industries, in the paper making industry and in various processing lines where exact speed coordination is essential in order to maintain the quality of the product[27,32,72]. Many schemes have been developed to achieve a variable voltage, variable frequency supply[5,9,10,11,72,95]. In these schemes, essentially two methods have been suggested to obtain variable voltage supply, first through controlled rectifier (fig.5) and the second through variable ratio tap changing transformer and uncontrolled rectifier. The former method is superior to the latter, since any voltage can be obtained through the control of thyristor firing angle, doing away with a bulky transformer.

Bridge configurations is the obvious choice to get a balanced three phase voltages. Several commutation schemes applicable to bridge inverter have been developed in the past[17,46]. While selecting a particular commutation scheme, the operational manoeuvring and the associated cost are the major considerations. Complementary impulse commutated McMurray-Bedford[55] inverter (bridge type) is preferred

THREE
PHASE
SUPPLY AT
f_1 HZ

RECTIFIER   FILTER   INVERTER

MOTOR

TO GATES

PHASE
CONTROLLED
GATE SIGNALS

FREQUENCY
CONTROL

FREQUENCY
REFERENCE
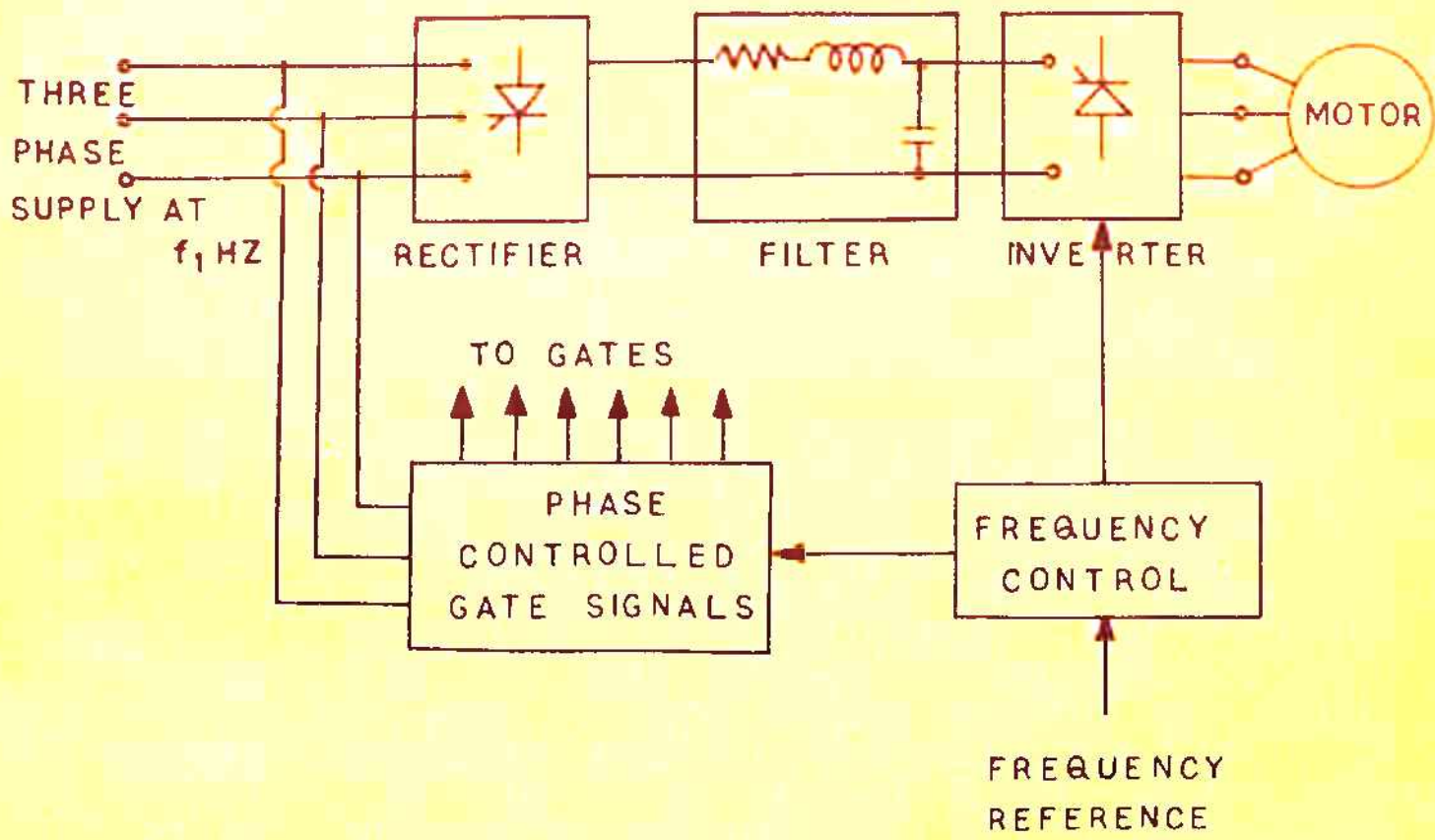
FIG.5   FREQUENCY, VOLTAGE CONVERTER.

over the McMurray's impulse commutated inverter with auxiliary thyristors; since the former is simple and requires less number of thyristors but provides as effective commutation as with auxiliary thyristors.

The most serious problem with this type of inverter is that it gives a multistep (6 steps) rectangular output voltage rich in lower order harmonic voltages. A large harmonic content in supply voltage means not a very efficient drive. This problem has been approached earlier in a number of ways by different authors by using multiple pulse width control, phase angle controlled multiple inverters and pulse width modulation. The earliest technique for voltage shaping is the multiple pulse width control[17,18], where the inverter valves are switched 'on' and 'off' a number of times during each half cycle of the inverter operating frequency. With this method of control, it is possible to substantially reduce or eliminate lower frequency harmonics[34]. Another very efficient method of voltage waveform control involves using multiple inverters, and summing their out put voltages[16]. The resulting total voltage is controlled by varying the phase angle between the individual inverters. The most effective method to reduce lower order harmonics is the pulse width modulated (PWM) inverter where both frequency and voltage are controlled in the single inverter itself[28,57]. The greater the number of steps per cycle the closer is the wave to a sinusoid. Again commutation and triggering logic and circuitry are too complex, for all the above three schemes.

The equipments are large and costly.

The choice of inverter for a particular motor depends upon the electronic trigger circuitry, associated logic circuitry and number of thyristors involved in the system. The trigger circuits for an inverter, bridge type (fig.5) with a square wave output would be the simplest, relying on a reference frequency generator and a ring counter. This system needs twelve thyristors, providing a variable voltage, variable frequency output. All other inverters need more than 12 thyristors in multiples of six. In general it might be said that more sophisticated the inverter is the more uneconomical it becomes for small and medium size drives.

The brief appraisal of thyristor a.c. drives presented here suggests that for small and medium size induction motors which constitute more than 75 percent of the total electrical drives used; the only economical way of controlling speed is by inverter fed, controlled rectifier scheme (fig. 5). Due to the simplicity[53] of six step inverter drive, researchers mostly picked this for further investigations, and continuous attempts have been made during last decade to perfect the drive.

B.   STATE OF THE ART:

The variable frequency drive has resulted in many new problems relating to the performance of an induction motor. One such problem of importance in the application of a rectifier inverter induction motor drive is that of large speed and torque pulsations specially at low frequencies[48,49].

The problem is related to the fact that most of the solid state variable frequency power supplies provide a voltage source rich in harmonics[50,56]. In certain applications e.g. machine tool drive, antenna positioning etc. uniform speed of rotation is mandatory. Therefore speed and torque pulsations should be minimum. Thus it is important to establish a method to predetermine the magnitude of electromagnetic torque pulsations and to find the ways to minimise them. In addition to the nonsinusoidal voltage waveform of the inverter; the improper machine parameters may further aggravate the torque pulsations.

The earliest work in this field is by Rogers[75] who finds the lightly damped regions of operation of variable frequency induction motor, giving a small perturbation in applied voltage and load torque. Author had shown that rotor leakage reactance and stator resistance play a dominant role specially at low frequencies when the oscillations are high. Lawrenson and Stephenson[47], using a linear two axis model of Rogers, study the dynamic performance of induction motor at various frequencies, neglecting the time harmonics in applied voltage. Effect of stator resistance and rotor inertia is considered on the settling time of the machine. The most pioneer work done on inverter fed induction motor, is by Krause and Lipo[37,38,49,50]. Many aspects of the drive like development of suitable mathematical model[37] finding

the proper computing tool[38], stability of the system using Nyquist criterion[50], speed and torque pulsation of 6th order harmonic[43], and the effects of some of the prominent system parameters (both machine and filter) on the performance[43]; have been dealt extensively. The mathematical model, developed in synchronously rotating frame is only partly successful in establishing a link between d.c. and a.c. variables. The system parameters play a deciding role in torque pulsations and improper combination of these as reported may lead to serious torque pulsations. These pulsations are found to be both frequency and load dependent. At very low frequencies the pulsating torque is reported as high as 35 percent of average torque[43]. The results published by these authors form a good guide for future researchers. Robertson and Hebbar in their publications[73,74], establish a link between a.c. and d.c. variables of composite inverter fed induction motor, by describing the machine behaviour directly in terms of the stator phase variables and three axis rotor transformed variables, retaining the computational simplicity of dq variables. Performance of PWM inverter is investigated. Sixth harmonic torque is considerably less with PWM inverter but 24th harmonic torque is found to be comparable to the average torque.

An attempt to build a different mathematical model has also been made by Ward and Kazi[97], expressing machine

variables in dq axis. The machine terminal voltage is assumed of stepped waveform and is expressed as sum of infinite number of shifted step functions. The relations developed are very complex and only suitable for fast computers. Also, the filter parameters are neglected altogether. Fallside and Wortley[20], using Routh Hurwitz criterion, predict that a normal induction motor even with sinusoidal supply, may become unstable leading to high steady state torque pulsations, at low frequencies. They suggest different design considerations and proper selection of machine parameters for a variable frequency induction motor. The other researchers, Ramamoorthy[68], Charlton[14], Harashima[24] and Hyashi[25], use a simple linear two axis model formulated at machine terminals. State variable techniques are employed to find the response of the drive with a rectangular voltage excitation applied at the motor terminals. Though the model is approximate but the results are quite encouraging. The model suggested by Sabbagh and Shewan[77] though comprehensive but unsuitable for computation, since the rotor variables are rotor position dependent. A similar approach is adopted by Takeuchi[32,93], Salihi[78] has come out with a improved version of inverter with auxiliary d.c. supply for commutation to overcome the commutation failure at low frequencies. This is ideally suited for traction purpose.

Very few papers are available dealing with the additional losses and effects on machine parameters of high frequency

excitations present in square voltage waveform. Barnes[5], Mclean and others[56] have investigated many interesting aspects of inverter fed drive. For example torque/ampere ratio is found to be fairly constant in contrast to the wide torque current ratio normally associated with induction motors operated on fixed frequency and voltage. Losses are reported to be 20 percent more in variable frequency operation.

The latest contribution to this field is the digital modelling of complex sequencing of thyristors's turn ON and OFF in a given circuit[6]. In this process, open circuit branches are removed from the associated graph to formulate the modified incidence matrix. The suggested process is ideally suited for passive load only. Topological approach has been used by Revankar[71] and Williams[100] in modelling a periodically switching networks consisting of controlled rectifier.

C.   OUTLINE OF PRESENT INVESTIGATION:

Findings of Jacovides[30] show that assumption of known voltage by earlier investigators is not sufficiently accurate for motor current waveform determination. The actual voltage waveform across the machine terminals is significantly affected by the load currents. In particular, if a rectangular voltage waveform is assumed, the difference between the actual and the assumed one is sufficient to make

prediction of the current waveform incorrect.

The present work gives a development of a near exact mathematical model of rectifier inverter fed induction motor drive (fig. 5); comprehensive enough to account for the effects of -

(i)   parameters of filter present between the controlled rectifier and inverter.

(ii)   voltage ripples normally present in the rectified output wave.

(iii) inverter's forward impedance.

These requirements necessitate the system equations formulation at filter terminals; doing away with the normal assumption of known voltage waveform at machine terminals. Thus a suitable and computationally feasible, transformation is to be evolved to establish a link between two axis d.c. variables of inverter and three axis phase variables of the motor. To enable to predict the exact torque pulsations and other performance characteristics both under transient and steady state conditions, it is essential to take into account the effects of high harmonic frequencies present along with the fundamental, over the machine parameters like rotor and stator resistances and inductances, and over the stray load losses. The works of Alger[2] and Chalmers[12,13] can prove handy for reformulating the stray loss relations for high frequencies.

The other aspect studied here is, to search for a optimal set of machine parameters giving the minimum torque pulsations at any frequency without affecting the other performance indices appreciably. The optimal machine parameters thus achieved must on one hand satisfy the stability criterion and on other hand should in no case deteriorate the transient/dynamic characteristics when compared with its corresponding normal performance. Given a optimal set of machine parameters, it may then be possible to deduce a set of viable design recommendations, to bring suitable changes at the design stage itself to make the induction motor fit for variable frequency operation with minimum torque pulsations giving fairly acceptable other performance characteristics.

Chapter 1 of the thesis deals with the development of mathematical model. A new three axis commutator transformation $C_{ryb}^{s}, {}_{\alpha\beta\gamma}^{r}$ is developed establishing a link between d.c. variables of the inverter with the a.c. variables of the machine. The transformation has all the added advantages of well known two axis commutator transformation. The system equations are formulated at the filter terminals. The system impedance matrices for all the six possible conduction states and substates are derived from generalised one using Kron's connection matrices. Relations for torque both average and pulsating, dynamic equation at mechanical

port, and the equation giving the phase voltage have also been included in this chapter.

The relations developed by Chalmers and Alger for various stray load loss components, valid for fixed frequency sinusoidal excitation; have been further modified and presented in Chapter 2 as to make them applicable for variable frequency nonsinusoidal excitations.

The computed results under steady state condition of average torque, pulsating torques, efficiency, power factor, phase current and voltage waveforms, slip and various components of losses are presented in Chapter 3. All these are computed for various frequencies covering a range of 5 Hz to 200 Hz and each for thirteen selected sets of system parameters (machine as well as filter). The range of system parameters is decided from design considerations.

The optimisation model dealt in Chapter 4, is built in multireference frames rotating at their respective harmonic synchronous speeds. The pulsating torque function, developed as function of dependent phase currents, is minimised with respect to the four selected machine parameters and simultaneously maximised with respect to the operating frequency.

In Chapter 5, the computed transient characteristics viz; torque, phase current and speed at selected frequencies with optimal machine parameters are given. These characteristics

are compared with the corresponding transient characteristics obtained with normal machine parameters.

The computed results of Chapter 3 with normal machine parameters have been verified experimentally at few frequencies and are included in Chapter 6.

- o -

CHAPTER 1

MATHEMATICAL MODEL FOR INVERTER FED THREE PHASE INDUCTION MOTOR:

This chapter deals with the development of a mathematical model for the inverter fed, variable speed, variable frequency three phase induction motor. The schematic diagram for the system is shown in fig.1.1. The system consists of three phase bridge inverter using thyristors along with their commutation circuitry, single section LC filter and the three phase cage induction motor. The inverter is normally fed from a three phase controlled bridge rectifier.

In all of the earlier studies the equations describing the system operation were formulated assuming a fixed voltage waveform of stepped nature at the machine terminals[14,19,47,48,68]. Jocovides[30] and Li[48] in their papers conclude that the assumption of a known voltage waveform as described in the literature, is not sufficiently accurate for current waveform determination. In particular if a rectangular voltage is assumed, the difference is sufficient to make prediction of the current waveform incorrect. The following reasons can be given for this:

(i) Voltages are induced in a particular phase from other phases which obviously are dependent upon the current waveform.

(ii) The duration of the turn off process and also the voltage during turn off depend on the current.

19

FILTER   INVERTER   INDUCTION MOTOR
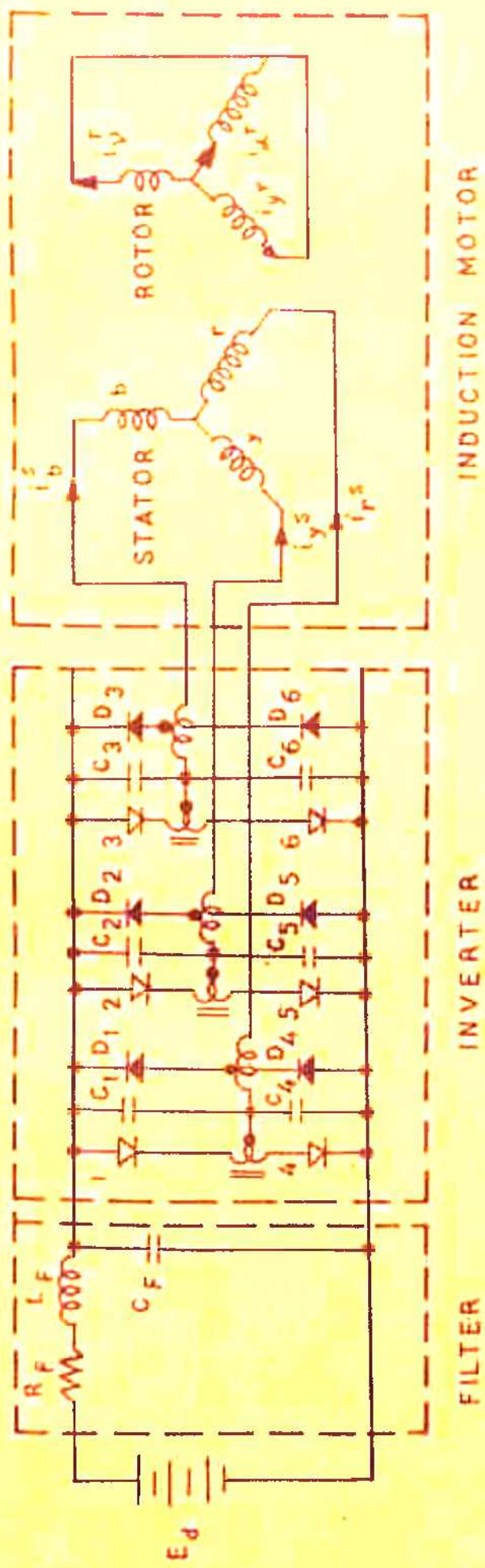
FIG. 1·1 INVERTER FED INDUCTION MOTOR
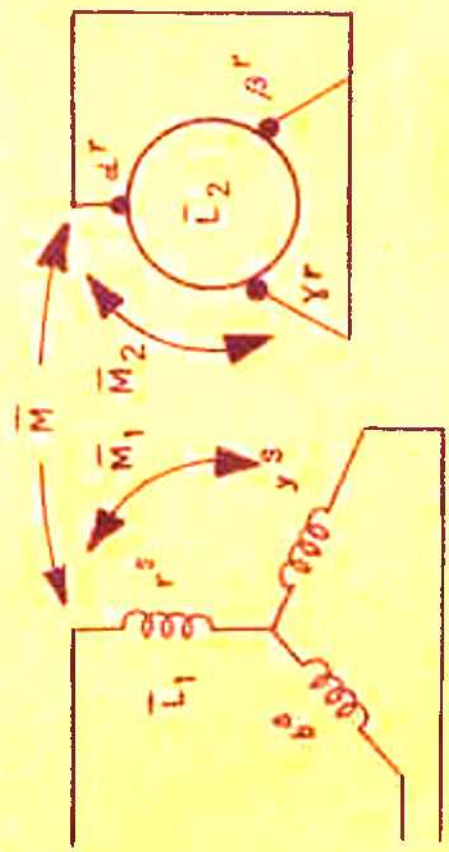
FIG. 1·2 TRANSFORMED INDUCTION MOTOR

20

(iii) There will be spikes in the voltage waveform due to
transients created by the interaction of the components
that make up the inverter and the motor as load. This
has been confirmed through experimental results by
Sabbagh and Shewan[77].

(iv) The voltage ripples in the rectifier output, the
filter inductance and the filter capacitance will also
affect the voltage wave shape at the machine terminals
to a greater extent.

The voltage appearing at the machine terminals can no
longer be of fixed nature, but it will be load dependent.
The constant speed constraint is required in these calcula-
tions so that superposition could be employed. Since the
inverter performs a series of discontinuous periodic switching
operation the behaviour of the motor is a succession of res-
ponse to these switching transients. For any system equation
formulation, to investigate induction motor performance the
inverter and filter parameters must also be included. The
mathematical model developed in the subsequent sections
includes the effects of inverters periodic switching, thyristors'
forward voltage drops, filter and the ripples in the inverter
input voltage. This necessitates the formulation of the system
equations at the d.c. terminals of the inverter giving a
model equally valid both for steady state and dynamic conditions.
Three axis commutator transformation is used to overcome the

problem of d.c., a.c. link. The system impedance matrices are developed in operational form for the six possible states of the inverter for 180° conduction mode. Using kron's connection matrices[33], the terminal equations for the independent meshes in terms of machine's phase currents are written for all possible switching states and substates. The following general assumptions are made in order to simplify the model.

(i)   Iron parts of the magnetic circuits of the machine are unsaturated.

(ii)   The space distribution of air gap flux is sinusoidal.

(iii)   The time period of output frequency is much greater than the turn off time of thyristor even at highest operating frequency.

1.1   THREE AXIS TRANSFORMATION:

To facilitate the link between d.c. terminals of the inverter with the three phase a.c. terminals of the machine it is essential to maintain the three axes of the machine. The ryb axes of rotor are transformed to $\alpha\beta\gamma$ commutator axes (fig. 1.2) which have all the added advantages of well known two axis commutator transformation[33], making all rotor impedances independent of rotor position angle θ. This transformation matrix is obtained using well known techniques[33,39]. The transformation is carried out in the following three steps.

(i) Stator and rotor phase variables in ryb axes are transformed to $0\alpha\beta$ axes using well established[33] transformation matrix.

$$
\left[C^{s}_{0\alpha\beta,\,0\alpha p}^{r}\right] = \sqrt{\tfrac{2}{3}} \quad
\begin{array}{c}
\\ r^{s} \\ y^{s} \\ b^{s} \\ r^{r} \\ y^{r} \\ b^{r}
\end{array}
\begin{bmatrix}
\frac{1}{\sqrt{2}} & 1 & 0 & 0 & 0 & 0 \\[4pt]
\frac{1}{\sqrt{2}} & -\frac{1}{2} & \frac{\sqrt{3}}{2} & 0 & 0 & 0 \\[4pt]
\frac{1}{\sqrt{2}} & -\frac{1}{2} & -\frac{\sqrt{3}}{2} & 0 & 0 & 0 \\[4pt]
0 & 0 & 0 & \frac{1}{\sqrt{2}} & 1 & 0 \\[4pt]
0 & 0 & 0 & \frac{1}{\sqrt{2}} & -\frac{1}{2} & \frac{\sqrt{3}}{2} \\[4pt]
0 & 0 & 0 & \frac{1}{\sqrt{2}} & -\frac{1}{2} & -\frac{\sqrt{3}}{2}
\end{bmatrix}
\begin{array}{c}
0 \quad \alpha^{s} \quad \beta^{s} \quad 0 \quad \alpha^{r} \quad \beta^{r}
\end{array}
$$

$$(1.1)$$

(ii) In order to eliminate the dependence of rotor terms on rotor angle θ, the rotor variables in $0\alpha\beta$ axes are transformed to $0dq$ axes keeping the stator variables intact in $0\alpha\beta$ axes. For this the following transformation is used:

$$
\left[C^{s\quad r}_{0\alpha\beta,\,0dq}\right] =
\begin{array}{c}
0 \\ \alpha^{s} \\ \beta^{s} \\ 0 \\ \alpha^{r} \\ \beta^{r}
\end{array}
\begin{bmatrix}
\begin{array}{ccc}
& & \\
& 1 & \\
& &
\end{array}
&
\begin{array}{ccc}
& & \\
& 0 & \\
& &
\end{array} \\
\begin{array}{ccc}
& & \\
& 0 & \\
& &
\end{array}
&
\begin{array}{ccc}
1 & 0 & 0 \\
0 & \cos\theta & \sin\theta \\
0 & -\sin\theta & \cos\theta
\end{array}
\end{bmatrix}
\begin{array}{c}
0 \quad \alpha^{s} \quad \beta^{s} \quad 0 \quad d^{r} \quad q^{r}
\end{array}
$$

$$(1.2)$$

With these two transformations the stator and rotor variables are transformed to two axis stationary reference frame.

(iii) In order to get the variables in three axis fixed reference frame, a two phase to three phase transformation is done using the transposed of matrix (1.1). The above three intermediate transformations can be compounded into a single one by using the relation -

$$\left[C_{ryb,\alpha\beta\nu}^{s\quad r}\right] = \left[C_{0\alpha\beta,0\alpha\beta}^{s\quad r}\right] \left[C_{0\alpha\beta,0dq}^{s\quad r}\right] \left[C_{0\alpha\beta,0\alpha\beta}^{s\quad r}\right]_{T} ,$$

giving the final transformation matrix as:

$$
\left[C_{ryb,\alpha\beta\nu}^{s\quad r}\right] =
\begin{array}{c}
\\
r^{s}\\
y^{s}\\
b^{s}\\
r^{r}\\
\\
y^{r}\\
\\
b^{r}
\end{array}
\begin{array}{ccc}
r^{s}\ y^{s}\ b^{s} & \alpha^{r} & \beta^{r} & \nu^{r}
\end{array}
\left[
\begin{array}{cccc}
[1] & & [0] & \\
& \frac{1}{3}+\frac{2}{3}\cos\theta & \frac{1}{3}+\frac{2}{3}\cos\theta_2 & \frac{1}{3}+\frac{2}{3}\cos\theta_3 \\
[0] & \frac{1}{3}+\frac{2}{3}\cos\theta_3 & \frac{1}{3}+\frac{2}{3}\cos\theta & \frac{1}{3}+\frac{2}{3}\cos\theta_2 \\
& \frac{1}{3}+\frac{2}{3}\cos\theta_2 & \frac{1}{3}+\frac{2}{3}\cos\theta_3 & \frac{1}{3}+\frac{2}{3}\cos\theta
\end{array}
\right]
$$

(1.3)

where $\theta_2 = \theta - \frac{2\pi}{3}$, $\theta_3 = \theta - \frac{4\pi}{3}$

The transformed current, voltage and impedance matrices can be easily written as follows:

$$\left[v^{s}_{ryb,\alpha\beta\nu} \right] = \left[C^{s}_{ryb,\alpha\beta\nu} \right]_{T} \left[v^{s}_{ryb,ryb} \right] \tag{1.4a}$$

$$\left[i^{s}_{ryb,\alpha\beta\nu} \right] = \left[C^{s}_{ryb,\alpha\beta\nu} \right]_{T} \left[i^{s}_{ryb,ryb} \right] \tag{1.4b}$$

and

$$\left[Z^{s}_{ryb,\alpha\beta\nu} \right] = \left[C^{s}_{ryb,\alpha\beta\nu} \right]_{T} \left[Z^{s}_{ryb,ryb} \right] \left[C^{s}_{ryb,\alpha\beta\nu} \right] \tag{1.4c}$$

The original and the transformed impedance matrices are given in appendix I.

1.2 GENERAL SYSTEM IMPEDANCE MATRIX:

There are two distinct states of inverter operation namely; conduction and commutation states. It is convenient to consider these two states separately for the purpose of formulating state impedance matrices.

(a) Conduction States:

It is assumed that each thyristor in the bridge inverter of fig. 1.1 conducts for full 180°. At any given instant three thyristors conduct; two from the upper arms and one from the lower arms of the inverter bridge (fig. 1.1) or vice versa. Also the two thyristors belonging to the same arm can never conduct simultaneously. With in the above constraints there can be six possible states of bridge inverter as shown in fig. 1.3. Table 1.1 lists these six possible conduction states.
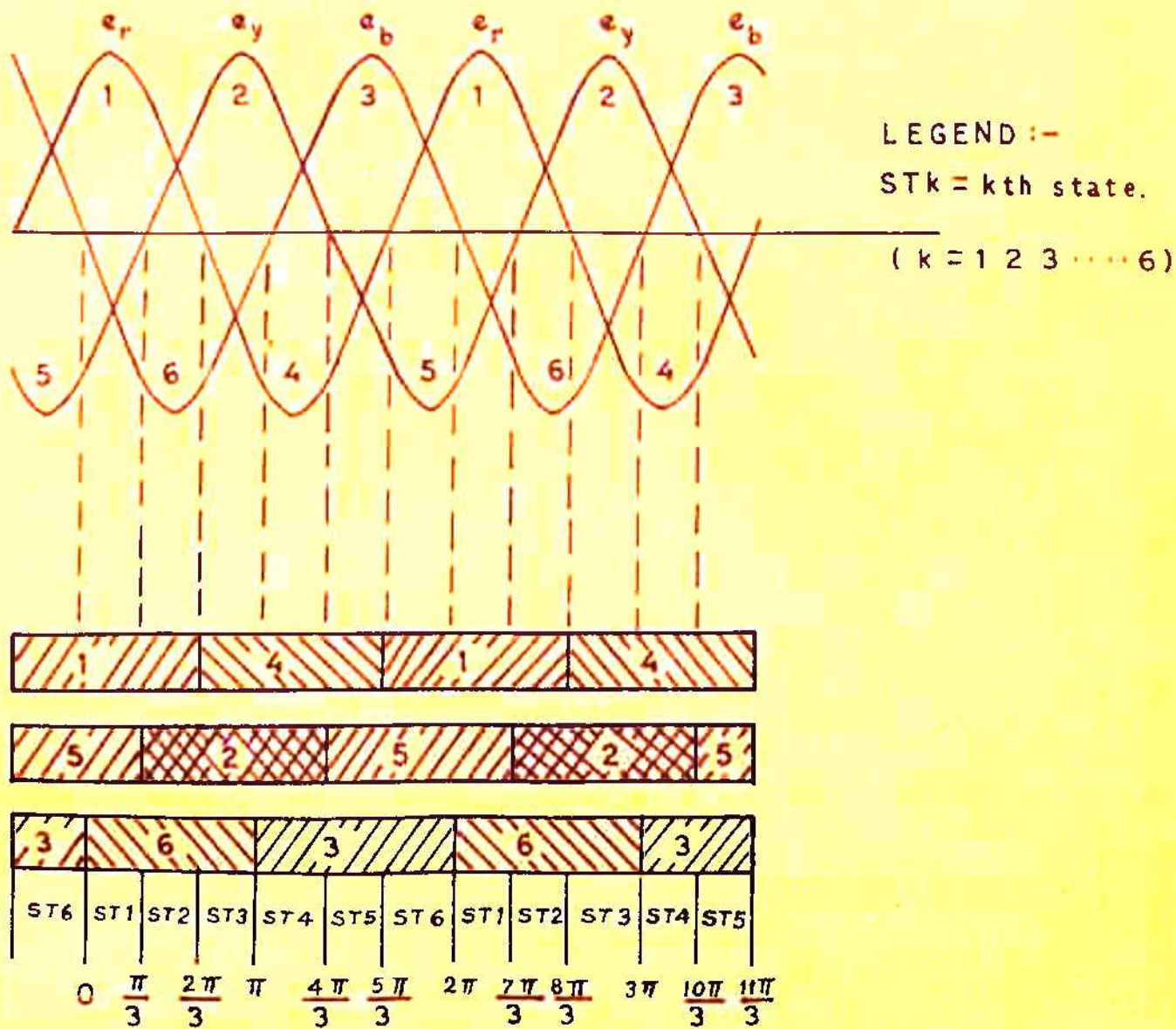
FIG. 1·3 CONDUCTION STATES.

Table 1.1   Conduction States

States	Thyristors ON	Thyristors OFF	Change of State	
			Thy. OFF	Thy. ON
1	1,5,6	2,3,4	3	6
2	1,2,6	3,4,5	5	2
3	4,2,6	1,3,5	1	4
4	4,2,3	1,5,6	6	3
5	4,5,3	1,2,6	2	5
6	1,5,3	2,4,6	4	1

(b)   System Network Topology:

The system can be considered as nonlinear network.
When any of the thyristors in the bridge changes state, the
topology of the network alters and the number of independent
meshes change[71]. The simplest approach is to consider the
topology of the network in each state. A general topology
of three phase bridge inverter can be drawn with all the
thyristors conducting[100]. The thyristors are replaced by
their respective forward finite operational impedances $z_1 - z_6$
and the motor is replaced by three phase star connected voltage
sources (fig. 1.4). The nodal analysis give the following
relations in currents.

$$i_6 = i_1 + i_2 + i_3 - i_4 - i_5 \qquad (1.5)$$
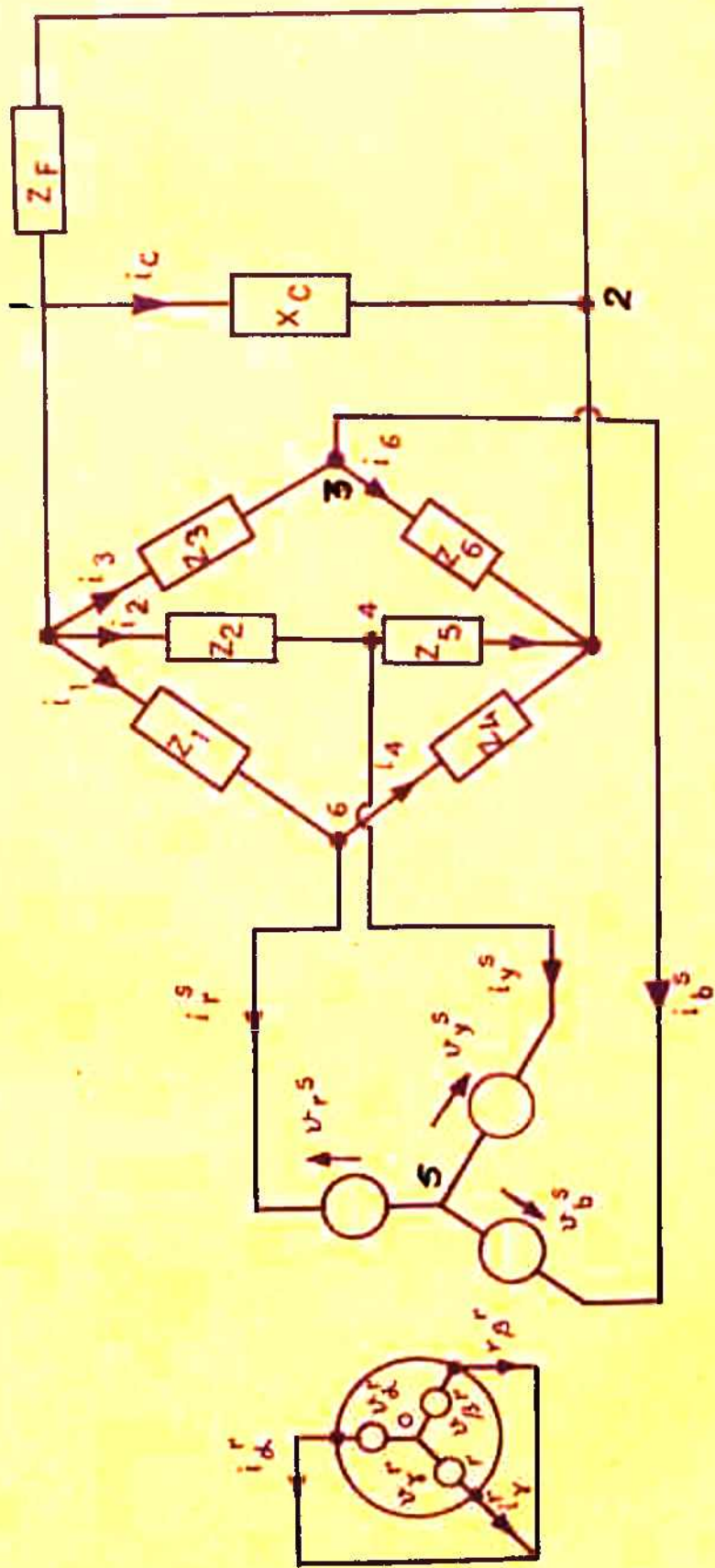
FIG. 1·4 SYSTEM NETWORK TOPOLOGY

$$i_r^s = i_1 - i_4 \tag{1.6}$$

$$i_y^s = i_2 - i_5 \tag{1.7}$$

$$i_b^s = i_4 + i_5 - i_1 - i_2 \tag{1.8}$$

For balanced system we get,

$$i_r^s + i_y^s + i_b^s = 0$$
$$i_\alpha^r + i_\beta^r + i_\gamma^r = 0 \tag{1.9}$$

(c) Selection of Independent Meshes

It is obvious from the topology of the network of fig. 1.4 that eight independent equations are required to describe the network. As well known, the thyristor acts as a unidirectional switch which allows the load current to flow in its forward direction only. The care is taken while selecting the meshes that no loop current flows against the forward directions of the thyristors falling in the mesh. The following eight independent meshes from the network (fig. 1.4) are selected.

(i) 165421   (ii) 145321   (iii) 135621   (iv) 121

(v) 16541   (vi) 453214   (vii) $\alpha^r 0\beta^r \alpha^r$ (viii) $\alpha^r 0 \gamma^r \alpha^r$

Five device currents i_1 to i_5, one capacitor current i_c and two rotor currents i_α^r, i_β^r are sufficient to describe the network. The current through the sixth device is related with rest of the five device currents as given by equation (1.5).

The eight independent mesh equations can be written in the matrix form as follows:

$$[v_g] = [z_g] \ [i_g] \tag{1.10}$$

where general voltage $[v_g]$ and current $[i_g]$ matrices are,

$$[v_g] = [E_d \ \ E_d \ \ E_d \ \ E_d \ \ 0 \ \ 0 \ \ 0 \ \ 0]_T \ , \tag{1.11}$$

$$[i_g] = [i_1 \ \ i_2 \ \ i_3 \ \ i_4 \ \ i_5 \ \ i_c \ \ i_\alpha^r \ \ i_\beta^r]_T, \tag{1.12}$$

and the general system impedance matrix $[z_g]$ is given on the next page.

1.3 CONDUCTION STATE IMPEDANCE MATRICES:

(a) Connection Matrix:

As discussed earlier only three thyristors conduct at a time while the other three remain in OFF state. Thyristors in their forward directions offer almost negligible impedances, while in their nonconducting state, they can be assumed as perfect open circuit. Thus the currents through the nonconducting thyristors can safely be assumed as zero neglecting the reverse saturation current which is quite small compared with load currents. In any practical situation, however, it is necesuary to allow for the infinite impedance of nonconducting thyristor. Several possible techniques for achieving this were considered[71,100]. The most obvious suggestion is to replace the nonconducting thyristor by high

$$[Z_g] =$$

1	2	3
$(R_1 + R_F + Z_1) + (L_4 + L_F)p$	$(R_F - R_1) + (L_F - L_4)p$	$R_F + L_F p$
$(Z_6 + R_F + R_1) + (L_4 + L_F)p$	$(2R_1 + R_F + Z_2 + Z_6) + (2L_4 + L_F)p$	$(R_F + Z_6) + L_F p$
$(R_F - 2R_1) + (L_F - 2L_4)p$	$(R_g - R_1) + (L_F - L_4)p$	$(R_g + Z_3) + L_F p$
$R_F + L_F p$	$R_F + L_F p$	$R_g + L_F p$
$(Z_1 + R_1) + L_4 p$	$-(R_1 + L_4 p + Z_2)$	$-$
$(Z_6 + R_1) + L_4 p$	$(2R_1 + Z_6 + Z_2) + 2L_4 p$	Z_6
$\frac{3}{2} M p + \frac{\sqrt{3}}{2} M w_r$	$\sqrt{3}\, M w_r$	$-$
$-\sqrt{3}\, M w_r$	$\frac{3}{2} M p - \frac{\sqrt{3}}{2} M w_r$	$-$

4	5	C	α_r	β_r
$-(R_1 + L_4 p)$	$(Z_5 + R_1) + L_4 p$	$R_p + L_4 p$	$\frac{3}{2}$ M p	$-\frac{3}{2}$ M p
$-(Z_6 + R_1) - L_4 p$	$-(Z_6 + 2R_1) + 2L_4 p$	$R_p + L_4 p$	$\frac{3}{2}$ M p	3 M p
$(2R_1 + Z_4) + 2L_4 p$	$R_1 + L_4 p$	$R_p + L_4 p$	-3 M p	$-\frac{3}{2}$ M p
-	-	$R_g + L_{gp} p + \frac{1}{C_p p}$	-	-
$-(R_1 + L_4 p)$	$R_1 + L_4 p$	$-\frac{1}{C_p p}$	$\frac{3}{2}$ M p	$-\frac{3}{2}$ M p
$-(Z_6 + R_1) + L_4 p$	$-(2R_1 + Z_6) - 2L_4 p$	-	$\frac{3}{2}$ M p	3 M p
$-\frac{3}{2}$ M p $-\frac{\sqrt{3}}{2}$ M w_r	$-\sqrt{3}$ M w_r	-	$R_2 + L_2 p + \frac{L_2}{\sqrt{3}} w_r$	$\frac{2L_2}{\sqrt{3}} w_r$
$\sqrt{3}$ M w_r	$-\frac{3}{2}$ M p $+\frac{\sqrt{3}}{2}$ M w_r	-	$-\frac{2L_2}{\sqrt{3}} w_r$	$R_2 + L_2 p + \frac{L_2}{\sqrt{3}} w_r$

$$(1.13)$$

resistance, and a value of 300 K. Ohm would normally be suitable[100]. But with this the algorithm becomes quite complex and the accuracy of the results is not appreciably improved. Also the replacement of thyristor by high backward resistance may adversely affects the system time constant, limiting the maximum step length commensurate with numerical stability. A second suggestion is to remove the thyristor impedance terms from $[Z_g]$ matrix, and by use of compensation theorem, to develop expressions for the voltages across the nonconducting thyristors which are then used to modify the voltage matrix $[v_g]$[100]. However, the substantial number of complicated terms in the thyristor voltage expressions again lead to an unacceptably long computing time. The method finally adapted is based on Kron's approach[33].

The application of Kron's approach leads to an effective method of dealing with the periodically varying topology of the network. In this approach a systematic method is developed to reduce the independent set of variables $[v_g]$, $[i_g]$ and $[Z_g]$ to the new sets valid for the new topology of the state of the network.

With the three thyristors always off (in rotation), the number of equations for each state reduce from eight to five only. For computational convenience, the five state equations are written in terms of phase currents of stator and rotor and a capacitor current. The independent currents

of equation (1.12) are related to the currents which actually flow in each branch in any jth state of the system by the connection matrix $[C_j]$ i.e.

$$[i_j] = [C_j][i_g] \qquad (1.14)$$

Here matrix $[C_j]$ can be written as:

$$[C_j] = \begin{matrix} & r^s \quad y^s \qquad c \qquad \alpha^r \qquad \beta^r \\ \begin{matrix} 1 \\ 2 \\ 3 \\ 4 \\ 5 \\ c \\ \alpha^r \\ \beta^r \end{matrix} & \begin{bmatrix} [C_{Tj}] & \qquad & [C_1'] \\ \\ \\ [C_2'] & \qquad & [U] \end{bmatrix} \end{matrix} \qquad (1.15)$$

where $[C_{Tj}]$ is the state transformation matrix of 5 x 2 for jth state.

$[C_1']$ null matrix of 5x3

$[C_2']$ null matrix of 3x2

$[U]$ unity matrix of 3x3

The general constraints valid for any state are:

$$i_1 = i_r^s = -i_4$$

$$i_2 = i_y^s = -i_5 \qquad (1.16)$$

$$i_3 = i_b^s = -(i_r^s + i_y^s)$$

The process of formulating transformation matrix $[c_{Tj}]$ may be illustrated by considering the reduced bridge topology of fig. 1.5 for state 1 when thyristors 1,5 and 6 conduct. The additional constraints for state 1 are:

$$i_2 = i_3 = i_4 = 0 \qquad (1.17)$$

The state transformation matrix $[c_{T1}]$ becomes:

$$[c_{T1}] = \begin{bmatrix} 1 & 0 & 0 & 0 & 0 \\ 0 & 0 & 0 & 0 & -1 \end{bmatrix}_T \qquad (1.18)$$

Similarly, other state transformation matrices are derived as given below:

$$[c_{T2}] = \begin{array}{c} \\ r^s \\ y^s \end{array} \overset{\begin{array}{ccccc} 1 & 2 & 3 & 4 & 5 \end{array}}{\begin{bmatrix} 1 & 0 & 0 & 0 & 0 \\ 0 & 1 & 0 & 0 & 0 \end{bmatrix}_T} \qquad (1.19)$$

$$[c_{T3}] = \begin{array}{c} r^s \\ y^s \end{array} \begin{bmatrix} 0 & 0 & 0 & -1 & 0 \\ 0 & 1 & 0 & 0 & 0 \end{bmatrix}_T \qquad (1.20)$$

$$[c_{T4}] = \begin{array}{c} r^s \\ y^s \end{array} \begin{bmatrix} 0 & 0 & -1 & -1 & 0 \\ 0 & 1 & -1 & 0 & 0 \end{bmatrix}_T \qquad (1.21)$$

ROTOR

STATOR
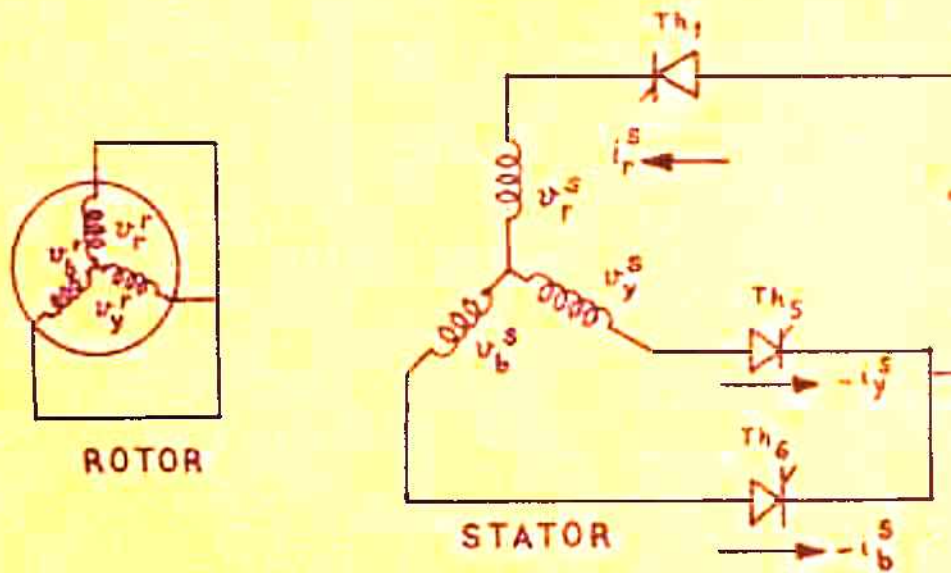
FIG. 1·5 NETWORK TOPOLOGY FOR
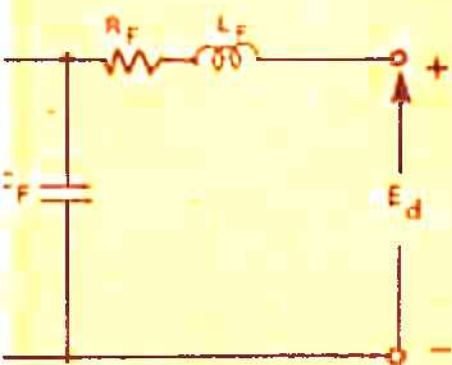
STATE 1.

$$[C_{T5}] = \begin{array}{c} r^s \\ y^s \end{array} \begin{bmatrix} 0 & 0 & -1 & -1 & 0 \\ 0 & 0 & -1 & 0 & -1 \end{bmatrix}_T \qquad (1.22)$$

$$[C_{T6}] = \begin{array}{c} r^s \\ y^s \end{array} \begin{bmatrix} 1 & 0 & -1 & 0 & 0 \\ 0 & 0 & -1 & 0 & -1 \end{bmatrix}_T \qquad (1.23)$$

(b) **States' Voltage Equations:**

The voltage, current and impedance matrices for jth
state can be obtained with the help of the connection matrix
developed in the preceding section in the following form:

$$[v_j]_T = [v_g]_T [C_j] \qquad (1.24a)$$

$$[i_j]_T = [i_g]_T [C_j] = [i_r^s \quad i_y^s \quad i_c \quad i_\alpha^r \quad i_\beta^r]_{T,} \qquad (1.24b)$$

$$[z_{tj}] = [C_j]_T [z_g][C_j] \qquad (1.25)$$

and $[v_j] = [z_{tj}][i_j]$ \qquad (1.26)

For computational simplicity, it is essential to have same
state voltage and current matrices [V] and [I] respectively for
all states. This can easily be achieved by performing linear
operations over equation (1.26) giving

$$[V] = [s_d \quad s_d \quad s_d \quad 0 \quad 0]_T \qquad (1.27a)$$

$$[I] = [i_r^s \quad i_y^s \quad i_c \quad i_\alpha^r \quad i_\beta^r]_T \qquad (1.27b)$$

$$[v] = [z_{sj}][I] \qquad (1.27c)$$

The modified impedance matrices for states 1 to 6 are:

$$[Z_{s1}] =
\begin{bmatrix}
R_p + Z_1 + R_1 + (L_p + 2L_1)p & Z_5 + R_1 + L_1 p & R_p + L_p p & \frac{3}{2}\bar{M}p & -\frac{3}{2}\bar{M}p \\
Z_1 + Z_6 + R_2 + 2R_1 + (L_p + 2L_1)p & -Z_6 - R_1 - L_1 p & R_p + L_p p & 3\bar{M}p & \frac{3}{2}\bar{M}p \\
R_p + L_p p & - & R_p + L_p p + \frac{1}{C_p p} & - & - \\
3\bar{M}p & \frac{5\sqrt{3}}{2}\bar{M}w_r + \frac{3}{2}\bar{M}p & - & 2R_2 + 2L_2 p & R_2 + \sqrt{3}L_2 w_r + L_2 p \\
-\frac{5\sqrt{3}}{2}\bar{M}w_r + \frac{3}{2}\bar{M}p & 3\bar{M}p & - & R_2 - \sqrt{3}L_2 w_r + L_2 p & 2R_2 + 2L_2 p
\end{bmatrix}$$

(1.28)

$$[Z_{s2}] =
\begin{bmatrix}
Z_6 + R_1 + R_p + (L_1 + L_p)p & Z_2 + Z_6 + 2R_1 + R_p + (2L_1 + L_p)p & R_p + L_p p & \frac{3}{2}\bar{M}p & 3\bar{M}p \\
2R_1 + R_p + Z_1 + Z_6 + (L_p + 2L_1)p & R_p + R_1 + Z_6 + (L_p + L_1)p & R_p + L_p p & 3\bar{M}p & \frac{3}{2}\bar{M}p \\
R_p + L_p p & R_p + L_p p + \frac{1}{C_p p} & R_p + L_p p & - & - \\
3\bar{M}p & \frac{5\sqrt{3}}{2}\bar{M}w_r + \frac{3}{2}\bar{M}p & - & 2R_2 + 2L_2 p & R_2 + \sqrt{3}L_2 w_r + L_2 p \\
-\frac{5\sqrt{3}}{2}\bar{M}w_r + \frac{3}{2}\bar{M}p & 3\bar{M}p & - & R_2 - \sqrt{3}L_2 w_r + L_2 p & 2R_2 + 2L_2 p
\end{bmatrix}$$

(1.23)

$$[z_{s3}] = \begin{bmatrix} R_F+Z_2+R_1+(L_F+L_1)p & R_1+Z_4+L_1p & R_F+L_Fp & -\frac{3}{2}\overline{M}p & \frac{3}{2}\overline{M}p \\ R_F+Z_2+2R_1+(L_2+2L_1)p & -R_1-Z_6-L_1p & R_F+L_Fp & \frac{3}{2}\overline{M}p & 3\overline{M}p \\ R_F+L_Fp & - & R_F+L_Fp+\frac{1}{C_Fp} & - & - \\ 3\overline{M}p & \frac{3\sqrt{3}}{2}\overline{M}w_r+\frac{3}{2}\overline{M}p & - & 2R_2+2L_2p & R_2+\sqrt{3}L_2w_r+L_2p \\ -\frac{3\sqrt{3}}{2}\overline{M}w_r+\frac{3}{2}\overline{M}p & 3\overline{M}p & - & R_2-\sqrt{3}L_2w_r+L_2p & 2R_2+2L_2p \end{bmatrix}$$

$$(1.30)$$

$$[z_{s4}] = \begin{bmatrix} R_F+Z_2+2R_1+Z_4+(2L_1+L_F)p & R_F+R_1+Z_4+(L_F+L_1)p & R_F+L_Fp & -\frac{3}{2}\overline{M}p & \frac{3}{2}\overline{M}p \\ R_F+R_1+Z_4+L_1+(L_r+L_F)p & R_F+Z_5+2R_1+Z_4+(L_F+2L_1)p & R_F+L_Fp & -3\overline{M}p & 3\overline{M}p \\ R_F+L_Fp & R_F+L_Fp & R_F+L_Fp+\frac{1}{C_Fp} & - & - \\ 3\overline{M}p & \frac{3\sqrt{3}}{2}\overline{M}w_r+\frac{3}{2}\overline{M}p & - & 2R_2+2L_2p & R_2+\sqrt{3}L_2w_r+L_2p \\ -\frac{3\sqrt{3}}{2}\overline{M}w_r+\frac{3}{2}\overline{M}p & 3\overline{M}p & - & R_2-\sqrt{3}L_2w_r+L_2p & 2R_2+2L_2p \end{bmatrix}$$

$$(1.31)$$

$$[Z_{B5}] = \begin{bmatrix}
R_F+Z_3+R_1+(L_F+L_1)p & R_F+Z_3+2R_1+Z_5+L_Fp+2L_1p & R_F+L_Fp & -\frac{3}{2}\overline{M}p & -3\overline{M}p \\
R_F+Z_3+2R_1+Z_4+(2L_1+L_F)p & R_F+Z_3+R_1+(L_1+L_F)p & R_F+L_Fp & -3\overline{M}p & -\frac{3}{2}\overline{M}p \\
R_F+L_Fp & R_F+L_Fp & R_F+L_Fp+\frac{1}{C_Fp} & - & - \\
3\overline{M}p & \frac{3\sqrt{3}}{2}\overline{M}w_r+\frac{3}{2}\overline{M}p & - & 2R_2+2L_2p & R_2+\sqrt{3}L_2w_r+L_2p \\
-\frac{3\sqrt{3}}{2}\overline{M}w_r+\frac{3}{2}\overline{M}p & 3\overline{M}p & - & R_2-\sqrt{3}L_2w_r+L_2p & 2R_2+2L_2p
\end{bmatrix}$$

$$(1.52)$$

$$[Z_{B6}] = \begin{bmatrix}
R_F+R_1+Z_5+(L_F+L_1)p & R_F+Z_3+2R_1+Z_5+L_Fp+2L_1p & R_F+L_Fp & -\frac{3}{2}\overline{M}p & -3\overline{M}p \\
R_F+Z_4+2R_1+Z_5+(L_F+2L_1)p & R_F+R_1+Z_5+(L_F+L_1)p & R_F+L_Fp & \frac{3}{2}\overline{M}p & -\frac{3}{2}\overline{M}p \\
R_F+L_Fp & R_F+L_Fp & R_F+L_Fp+\frac{1}{C_Fp} & - & - \\
3\overline{M}p & \frac{5\sqrt{3}}{2}\overline{M}w_r+\frac{3}{2}\overline{M}p & - & 2R_2+2L_2p & R_2+\sqrt{3}L_2w_r+L_2p \\
-\frac{3\sqrt{3}}{2}\overline{M}w_r+\frac{3}{2}\overline{M}p & 3\overline{M}p & - & R_2-\sqrt{3}L_2w_r+L_2p & 2R_2+2L_2p
\end{bmatrix}$$

$$(1.53)$$

40

1.4   COMMUTATION STATE IMPEDANCE MATRICES:

Whenever a change of state takes place the thyristor which is just turned on cannot take up the load current immediately after switching as the current continues to flow in its original direction due to inductive nature of the load. The transfer of the load current from off going thyristor to incoming thyristor takes normally about $\frac{1}{4}$ th to $\frac{1}{6}$ th of half cycle; this period will be named as commutation state of the system. The topology of the network changes with the change in the state.

To simplify the analysis, the following idealising assumptions are made[6].

(i)   The period of the a.c. output of the inverter is much larger than the turn off time of the thyristor.

(ii)   Series inductance included as part of the total load will maintain the load current substantially constant at a value I_L through out the commutating subinterval S. (fig. 1.6). This assumption is made irrespective of whether the net power factor of the load is lagging, unity or leading. The series inductance can include the load itself, part of a filter, and the leakage inductance of the output transformer. The total effective series inductance is normally quite large compared with the commutating inductance.

(iii)   The feed back diodes are connected to a very small

fraction 'n' of the total winding of the auto-
transformer.

(iv) The two halves of the commutating inductance L are
tightly coupled.

(v) Turn-on time of thyristor and its reverse saturation
current are negligible.

Operation with Inductive Load:

One half cycle of operation is illustrated in the
fig. 1.6. Each half cycle is divided into five subintervals,
designated A, B, C, D and E which are bounded by changes in the
state of a thyristor or a feed back diode from a non-conducting
to a conducting condition or vice versa. The subintervals are
described in sequence as follows:

SUBINTERVAL A: Thyristor 1 is ON, connected to the positive
line of d.c. supply. If the rate of change of load current
is moderate, the voltage across commutating inductance L is
a small fraction of the d.c. supply voltage E_d' and the
capacitor C_1 is charged to the voltage E_d. At the end of
subinterval A, the load current has attained a steady value I_L.

SUBINTERVAL B: Supposing the inverter changes its state from
2 to 3 (Table 1.1), then to commutate thyristor 1, thyristor 4
is gated 'ON'. Since the voltage on capacitor C_1 cannot
change instantaneously, a voltage of $2E_d$, will appear across
upper arm of commutating inductance L, causing thyristor 1

$E'_D = E_D/2. = $ D.C. VOLTAGE FROM MID POINT OF THE SOURCE.
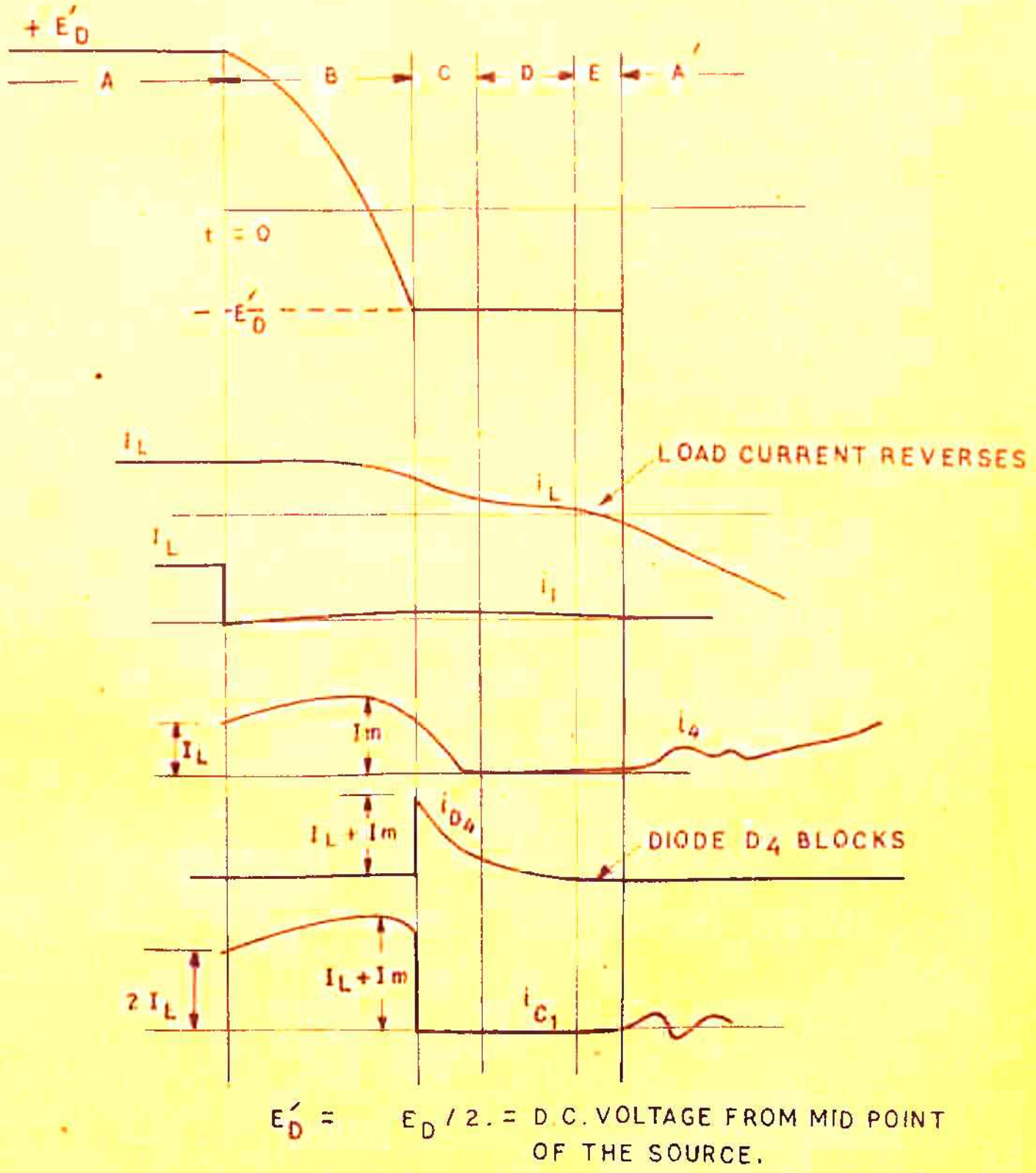
FIG. 1·6 COMMUTATION SUBINTERVALS WHEN THE INVERTER CHANGES ITS STATE FROM TWO TO THREE.

to turn off. Thus, capacitor C_1 not only supplies I_L to
load but also provides an equal current through thyristor 4.
Since the commutating subinterval t_c is very small, it is
drawn with an expanded time scale, about 10 times the scale
for other intervals. At the end of commutating subinterval
B, the voltage of r phase is reversed, and the current through
thyristor 4 has built up to a maximum value I_m.

SUBINTERVAL C: Current I_m would circulate through lower part
of commutating inductance L, thyristor 4 and diode D_4 and
the energy $\frac{1}{2} L I_m^2$ is fed back to d.c. supply through auto-
transformer action of ratio n to 1-n. Feedback diode D_4
would also carry the load current, feeding energy from the
load back to the negative side of the d.c. supply, until such
time as the load current is reversed. Diode D_4 clamps the
magnitude of the voltage impressed on (1-n) percent of auto-
transformer winding to the d.c. supply voltage E_d'. The
voltage $n \frac{E_d'}{1-n}$ induced in the n percent of auto-transformer
winding is applied to the lower arm of inductance L and reduces
the trapped circulating current linearly from I_m to zero
in time t_f:

where $t_f = \dfrac{L \, I_m (1-n)}{E_d' \, n}$ (1.34)

During this interval, the magnitude of the load voltage is
$\dfrac{E_d'}{1-n}$, and the voltage across commutating inductance raises the
reapplied forward voltage on thyristor 1 to the value $\dfrac{2 E_d'}{1-n}$.

SUBINTERVAL D: This subinterval occurs after the trapped circulating current has been reduced to zero, but the continuing feed back of energy from the inductive load keeps diode D_4 in conduction. The load voltage remains at $\frac{E_d'}{1-n}$. The voltage $\frac{n}{1-n}$ E_d, induced in n percent section of auto-transformer now appears as inverse voltage across thyristor 4.

SUBINTERVAL E: Load current reverses its polarity, diode D_4 blocks and the capacitor C_1 discharges until the potential of mid-point commutating inductance reaches the level of negative d.c. voltage.

SUBINTERVAL A':   Thyristor 4 now commences to conduct again. In order to do so, a gating signal applied at the start of subinterval B must have been maintained by using square wave geting signals. Ringing due to discharge of C_1 in the initial period is quite common. At the end of subinterval A', the load current has reached a magnitude I_L, as in the corresponding subinterval A when thyristor 1 was conducting. From the above description the following conclusions are drawn:

(i)   The impact of commutating capacitor on load current response during a very brief subinterval B is almost negligible.

(ii)   During the subintervals C and D, the load current is carried by back diode. If the forward impedance drop in back diode is assumed equal to the forward impedance drop in corresponding thyristor, then no change in the terminal equations need to be introduced.

(iii) Discharge of capacitor C_1 during subinterval E, cause
no noticeable change in the load current except ringing
which are very high frequency currents and for the
present analysis, these ringing currents can easily be
ignored.

The above conclusions lead to the fact that the impedance
matrix for commutating period will be same as that for the
conduction period. Henceforth the two impedance matrices for
commutation and conduction period will be called 'state
impedance matrix'.

1.5   SYSTEM EQUATIONS:

(a)   Terminal Equations at Electrical Ports:

The dynamic behaviour of periodically varying topology
of a network like the one shown in fig. 1.1 can conveniently
be expressed in terms of first or second order differential
equations as formulated in sections 1.3 and 1.4. State
variables selected are normally the independent currents through
inductors and capacitor voltages[42]. In our case, the phase
currents being of prime interest, are retained as state
variables in addition to the filter capacitor voltage v_c
and its derivative. The state impedance matrix in volt ampere
equation (1.27c) can be written as:

$$[Z_{sj}] = [R_j] + p[L_j] + \frac{1}{p}\left[\frac{1}{C_{Fj}}\right] \qquad (1.35)$$

where - $\begin{bmatrix} R_j \end{bmatrix}$ state resistance matrix

$\begin{bmatrix} L_j \end{bmatrix}$ state inductance matrix

$\begin{bmatrix} \dfrac{1}{C_{Fj}} \end{bmatrix}$ state capacitance matrix.

Four out of the five volt ampere equations of (1.27c) are of first order differential equations while the fifth one is of second order; which can also be reduced to first order. Taking, for instance the system of equations of state 1 (equation (1.28)) the equation

$$E_d = (R_F + L_F p) \, i_r^s + (R_F + L_F p + \frac{1}{C_F p}) \, i_c, \qquad (1.36)$$

contains a second derivative term, which can be reduced to first order by the following substitutions.

Let $p v_c = y_3 ; \quad v_c = y_6$ (1.37)

Then $E_d = (R_F + L_F p) \, i_r^s + (R_F C_F + L_F C_F p + 1) \, y_3$ (1.38)

Thus equation (1.38) replace the equation (1.36). Similar expressions can be obtained for other states as well. The following are the six state variables.

$$\begin{aligned} y_1 &= i_r^s ; \quad y_2 = i_y^s ; \quad y_3 = p v_c \\ y_4 &= i_\alpha^r ; \quad y_5 = i_\beta^r ; \quad y_6 = v_c \end{aligned} \qquad (1.39)$$

OR $\begin{bmatrix} Y_j \end{bmatrix} = \begin{bmatrix} y_1 & y_2 & y_3 & y_4 & y_5 & y_6 \end{bmatrix}_T$ (1.40)

As a result of above state reduction, the 2nd and 3rd terms of equation (1.35) get amalgamated into one giving new matrix $\begin{bmatrix} \hat{L}_j \end{bmatrix}$. The modified state impedance matrix can be written as:

$$[Z_{sj}] = [R_j] + p[\hat{L}_j]$$

Substituting this in equation (1.27c), the following relations are obtained:

$$[V] = [R_j][Y_j] + [\hat{L}_j][pY_j]$$

OR $\quad [pY_j] = -[\hat{L}_j]^{-1}[R_j][Y_j] + [\hat{L}_j]^{-1}[V] \qquad (1.41)$

Equation (1.41) is similar to the standard state space equation

$$p\dot{Y} = AY + B \qquad (1.42)$$

All the parameters and other variables involved in equation (1.41) are converted into per unit values for computational and generalisation purposes (appendix II). Let the equation (1.41) be rewritten in per unit system as:

$$[pY_j] = -[\hat{x}_j]^{-1}[R_j][Y_j] + [\hat{x}_j]^{-1}[V] \qquad (1.43)$$

Matrices $[\hat{x}]$ and $[R]$ for all the six states are:

$$[\hat{x}_1] = \begin{bmatrix} 0 & 0 & 0 & 0 & 0 & 1 \\ w(X_1+X_F) & -X_1 w & \dfrac{X_F w^2}{X_c} & \dfrac{3}{2}X_M w & -\dfrac{3}{2}X_M w & 0 \\ (2X_1+X_F)w & X_1 w & \dfrac{X_F w^2}{X_c} & 3X_M w & \dfrac{3}{2}X_M w & 0 \\ X_F w & 0 & \dfrac{X_F w^2}{X_c} & 0 & 0 & 0 \\ 3X_M w & \dfrac{3}{2}X_M w & 0 & 2X_2 w & X_2 w & 0 \\ \dfrac{3}{2}X_M w & 3X_M w & 0 & X_2 w & 2X_2 w & 0 \end{bmatrix} \qquad (1.44)$$

$$[\hat{\mathfrak{X}}_2] = \begin{bmatrix} 0 & 0 & 0 & 0 & 0 & 1 \\ (X_1+X_F)w & (2X_1+X_F)w & \dfrac{X_F^2 w^2}{X_c} & \dfrac{3}{2}X_M w & 3X_F w & 0 \\ (2X_1+X_F)w & (X_1+X_F)w & \dfrac{X_F^2 w^2}{X_c} & 3X_M w & \dfrac{3}{2}X_M w & 0 \\ \dfrac{X_F}{2}w & X_F w & \dfrac{X_F^2 w^2}{X_o} & 0 & 0 & 0 \\ 3X_M w & \dfrac{3}{2}X_M w & 0 & 2X_2 w & X_2 w & 0 \\ \dfrac{3}{2}X_M w & 3X_M w & 0 & X_2 w & 2X_2 w & 0 \end{bmatrix} \tag{1.45}$$

$$
[\hat{\mathcal{H}}_3]_m =
\begin{bmatrix}
0 & 0 & 0 & 0 & 0 & 1 \\
-X_1 w & (X_1+X_F)w & \dfrac{X_F w^2}{X_c} & -\dfrac{3}{2}X_M w & \dfrac{3}{2}X_M w & 0 \\
X_1 w & (2X_1+X_F)w & \dfrac{X_F w^2}{X_c} & \dfrac{3}{2}X_M w & 3X_M w & 0 \\
0 & X_F w & \dfrac{X_F w^2}{X_c} & 0 & 0 & 0 \\
3X_M w & \dfrac{3}{2}X_M w & 0 & 2X_2 w & X_2 w & 0 \\
\dfrac{3}{2}X_M w & 3X_M w & 0 & X_2 w & 2X_2 w & 0
\end{bmatrix}
\qquad (1.46)
$$

$$[\hat{\mathcal{H}}_4] = \begin{bmatrix} 0 & 0 & 0 & 0 & 0 & 1 \\[6pt] -(X_1+X_P)w & X_1w & \dfrac{X_Fw^2}{X_c} & -\tfrac{3}{2}X_Mw & \tfrac{3}{2}X_Mw & 0 \\[6pt] -(2X_1+X_F)w & -X_1w & \dfrac{X_Fw^2}{X_c} & -3X_Mw & -\tfrac{3}{2}X_Mw & 0 \\[6pt] -X_Pw & 0 & \dfrac{X_Fw^2}{X_c} & 0 & 0 & 0 \\[6pt] 3X_Mw & \tfrac{3}{2}X_Mw & 0 & 2X_2w & X_2w & 0 \\[6pt] \tfrac{3}{2}X_Mw & 3X_Mw & 0 & X_2w & 2X_2w & 0 \end{bmatrix} \quad (1.47)$$

$$[\hat{\mathcal{H}}_5] = \begin{bmatrix} 0 & 0 & 0 & 0 & 0 & 1 \\[6pt] -(X_1+X_P)w & -(2X_1+X_F)w & \dfrac{X_Fw^2}{X_c} & -\tfrac{3}{2}X_Mw & -3X_Mw & 0 \\[6pt] -(2X_1+X_F)w & -(X_1+X_F)w & \dfrac{X_Fw^2}{X_c} & -3X_Mw & -\tfrac{3}{2}X_Mw & 0 \\[6pt] -X_Pw & -X_Pw & \dfrac{X_Fw^2}{X_c} & 0 & 0 & 0 \\[6pt] 3X_Mw & \tfrac{3}{2}X_Mw & 0 & 2X_2w & X_2w & 0 \\[6pt] \tfrac{3}{2}X_Mw & 3X_Mw & 0 & X_2w & 2X_2w & 0 \end{bmatrix} \quad (1.48)$$

$$
[\hat{\mathcal{K}}_6] =
\begin{bmatrix}
0 & 0 & 0 & 0 & 0 & 1 \\
X_1 w & -(X_1+X_F)w & \dfrac{X_F w^2}{X_c} & \dfrac{3}{2}X_M w & -\dfrac{3}{2}X_M w & 0 \\
-X_1 w & -(2X_1+X_F)w & \dfrac{X_F w^2}{X_c} & -\dfrac{3}{2}X_M w & -3X_M w & 0 \\
0 & -X_F w & \dfrac{X_F w^2}{X_c} & 0 & 0 & 0 \\
3X_M w & \dfrac{3}{2}X_M w & 0 & 2X_2 w & X_2 w & 0 \\
\dfrac{3}{2}X_M w & 3X_M w & 0 & X_2 w & 2X_2 w & 0
\end{bmatrix}
\quad (1.49)
$$

IF $\quad a_1 = R_1 + R_F \ ; \quad a_2 = 2R_1 + R_F \ ; \quad a_3 = \dfrac{3\sqrt{3}}{2}X_M w_R$

$\qquad a_4 = \dfrac{R_F w}{X_c} \ ; \quad a_5 = \sqrt{3}X_2 w_R$

Then:

$$
[\mathcal{R}_1] =
\begin{bmatrix}
0 & 0 & 1 & 0 & 0 & 0 \\
-(Z_1+a_1) & Z_5+R_1 & -a_4 & 0 & 0 & 0 \\
-(a_2+Z_1+Z_6) & -(Z_6+R_1) & -a_4 & 0 & 0 & 0 \\
-R_F & 0 & -a_4 & 0 & 0 & -1 \\
0 & -a_3 & 0 & -2R_2 & -R_2-a_5 & 0 \\
a_3 & 0 & 0 & -R_2+a_5 & -2R_2 & 0
\end{bmatrix}
\quad (1.50)
$$

$$[R_2] = \begin{bmatrix} 0 & 0 & 1 & 0 & 0 & 0 \\ -(Z_6+a_1) & -(a_2+Z_2+Z_6) & -a_4 & 0 & 0 & 0 \\ -(a_2+Z_1+Z_6) & -(a_1+Z_6) & -a_4 & 0 & 0 & 0 \\ -R_F & -R_F & -a_4 & 0 & 0 & -1 \\ 0 & -a_3 & 0 & -2R_2 & -R_2-a_5 & 0 \\ a_3 & 0 & 0 & -R_2+a_5 & -2R_2 & 0 \end{bmatrix} \quad (1.51)$$

$$[R_3] = \begin{bmatrix} 0 & 0 & 1 & 0 & 0 & 0 \\ R_1+Z_4 & -(Z_2+a_1) & -a_4 & 0 & 0 & 0 \\ -(R_1+Z_6) & -(2Z_2+a_2) & -a_4 & 0 & 0 & 0 \\ 0 & -R_F & -a_4 & 0 & 0 & -1 \\ 0 & -a_3 & 0 & -2R_2 & -R_2-a_5 & 0 \\ a_3 & 0 & 0 & -R_2+a_5 & -2R_2 & 0 \end{bmatrix} \quad (1.52)$$

$$[R_4] = \begin{bmatrix} 0 & 0 & 1 & 0 & 0 & 0 \\ Z_4+a_1 & -(R_1+Z_2) & -a_4 & 0 & 0 & 0 \\ a_2+Z_3+Z_4 & R_1+Z_3 & -a_4 & 0 & 0 & 0 \\ R_F & 0 & -a_4 & 0 & 0 & -1 \\ 0 & -a_3 & 0 & -2R_2 & -R_2-a_5 & 0 \\ a_3 & 0 & 0 & -R_2+a_5 & -2R_2 & 0 \end{bmatrix} \quad (1.53)$$

$$
[\mathcal{Q}_5] =
\begin{bmatrix}
0 & 0 & 1 & 0 & 0 & 0 \\
Z_3+a_1 & Z_3+Z_5+a_2 & -a_4 & 0 & 0 & 0 \\
a_2+Z_3+Z_4 & Z_3+a_1 & -a_4 & 0 & 0 & 0 \\
R_F & R_F & -a_4 & 0 & 0 & -1 \\
0 & -a_3 & 0 & -2R_2 & -R_2-a_5 & 0 \\
a_3 & 0 & 0 & -R_2+a_5 & -2R_2 & 0
\end{bmatrix}
\tag{1.54}
$$

$$
[\mathcal{Q}_6] =
\begin{bmatrix}
0 & 0 & 1 & 0 & 0 & 0 \\
R_1+Z_3 & Z_3+Z_5+a_2 & -a_4 & 0 & 0 & 0 \\
-R_1-Z_1 & Z_5+a_1 & -a_4 & 0 & 0 & 0 \\
0 & R_F & -a_4 & 0 & 0 & -1 \\
0 & -a_3 & 0 & -2R_2 & -R_2-a_5 & 0 \\
a_3 & 0 & 0 & -R_2+a_5 & -2R_2 & 0
\end{bmatrix}
\tag{1.55}
$$

and

$$
X_1 = \tfrac{3}{2}X_M + X_{L1} \tag{1.56}
$$

$$
X_2 = \tfrac{3}{2}X_M + X_{L2} \tag{1.57}
$$

(b) <u>Terminal Equations at Mechanical Port:</u>

The well established torque balance equation under dynamic condition at mechanical port of the system is given as:

$$
J\frac{dw_R}{dt} + \alpha w_R + T_L = T_e \tag{1.58}
$$

where all variables in the above equation are in per unit values and the expression for electromagnetic torque T_e is given by equation (1.62).

(c) <u>Torque Relation:</u>

(i) <u>General Expression:</u>- The relation for the instantaneous electromagnetic torque as function of stator and rotor phase currents is[33],

$$
T_e = \frac{1}{2} \left[i_{ryb,ryb}^{s\ r} \right]_T \left[\frac{\partial L_{ryb,ryb}^{s\ r}}{\partial \theta} \right] \left[i_{ryb,ryb}^{s\ r} \right] \quad , \tag{1.59}
$$

where [i] and [L] are the current and inductance matrices in ryb axis both for the stator and rotor. The expression for the instantaneous torque in ryb, $\alpha\beta\nu$ reference frame can be obtained by using the following relations; relating the old and new currents.

$$
\left[i_{ryb,ryb}^{s\ r} \right] = \left[C_{ryb,\alpha\beta\nu}^{s\ r} \right] \left[i_{ryb,\alpha\beta\nu}^{s\ r} \right] \tag{1.60}
$$

From equation (1.59) and (1.60) we get -

$$
T_e = \frac{1}{2} \left[i_{ryb,\alpha\beta\nu}^{s\ r} \right]_T \frac{\partial}{\partial \theta} \left[L_{ryb,\alpha\beta\nu}^{s\ r} \right] \left[i_{ryb,\alpha\beta\nu}^{s\ r} \right] \tag{1.61}
$$

Simplifying the above relation, it becomes.

$$
T_e = \frac{2\sqrt{3}}{2} X_M \left(i_\alpha^r i_y^s - i_\beta^r i_r^s \right) \tag{1.62}
$$

(11)   Steady State Torques:

For the system under consideration the steady state phase currents are nonsinusoidal and can be expressed as:

$$i_r^s = \sum_n I_{mn}^s \sin(n\omega t + \theta_1^n)$$

$$i_y^s = \sum_n I_{mn}^s \sin(n\omega t + \theta_1^n - \frac{2\pi n}{3})$$

$$i_\alpha^r = \sum_n I_{mn}^r \sin(n\omega t + \theta_2^n) \qquad (1.63)$$

$$i_\beta^r = \sum_n I_{mn}^r \sin(n\omega t + \theta_2^n - \frac{2\pi n}{3})$$

where $n = 6k \pm 1$ (k is integer)

The steady state torque developed by the motor can be considered to be consisting of two components unidirectional torque produced due to the interaction of harmonic fields of the same order, and the pulsating torque with zero average value produced due to the interaction of harmonic fields of different orders. The frequency of pulsation of such torques depend upon the order of interacting fields. Fundamental and fifth harmonic fields, for instance give rise to the pulsating torque varying with a frequency six times the fundamental. Similarly it can be shown that all pulsating torques are of the order six and its integral multiples. But it is found[49] that pulsating torques of higher order especially of the order 18 and above are of insignificant amplitudes, therefore, can be ignored. Thus the resultant steady state torque developed

is the sum of unidirectional constant torque T_{const}, 6th and 12th order pulsating torques T_{e6} and T_{e12} respectively, giving –

$$T_e = T_{const} + T_{e6} + T_{e12} \tag{1.64}$$

Since the pulsating torques of order greater than 12 are neglected, it is sufficient to consider the fundamental, 5th, 7th, 11th and 13th harmonics of phase currents. Substituting the steady state currents of equation (1.63) into equation (1.62) we get –

$$T_{const} = \frac{3\sqrt{3}}{2} X_M \sum_n \left[I_{mn}^s \, I_{mn}^r \, \text{Sin} \left(\theta_2^n - \theta_1^n \right) \right] \text{Sin}(G_1 \frac{2\pi}{3}) \tag{1.65}$$

where

$$G_1 = -1 \quad \text{for } n = 1,7,13$$

$$G_1 = +1 \quad \text{for } n = 5,11$$

$$T_{e6} = \frac{3\sqrt{3}}{2} X_M \, \text{Sin} \frac{2\pi}{3} \sum_i K_i \, \text{Sin} (6wt + \alpha_i) \tag{1.66}$$

$$(i = 1,2,3,\ldots\ldots 8)$$

$$T_{e12} = \frac{3\sqrt{3}}{2} X_M \, \text{Sin} \frac{2\pi}{3} \sum_j G_j \, \text{Sin}(12wt + \beta_j) \tag{1.67}$$

$$(j = 1,2,3,\ldots\ldots 6)$$

and $\quad T_p = T_{e6} + T_{e12} \tag{1.68}$

where –

$$K_1 = - I_{m1}^s I_{m5}^r \qquad K_2 = - I_{m1}^s I_{m7}^r \qquad K_3 = I_{m5}^s I_{m1}^r$$
$$K_4 = I_{m5}^s I_{m11}^r \qquad K_5 = I_{m7}^s I_{m1}^r \qquad K_6 = -I_{m7}^s I_{m13}^r \quad \Big| \tag{1.69}$$
$$K_7 = -I_{m11}^s I_{m5}^r \qquad K_8 = I_{m13}^s I_{m7}^r$$

$$\alpha_1 = \theta_1^1 + \theta_2^5 \qquad \alpha_2 = \theta_2^7 - \theta_2^1 \qquad \alpha_3 = \theta_1^5 + \theta_2^1$$

$$\alpha_4 = \theta_2^{11} - \theta_1^5 \qquad \alpha_5 = \theta_1^7 - \theta_2^1 \qquad \alpha_6 = \theta_2^{13} - \theta_1^7 \qquad (1.70)$$

$$\alpha_7 = \theta_1^{11} - \theta_2^5 \qquad \alpha_8 = \theta_1^{13} - \theta_2^7$$

$$G_1 = -I_{m1}^s \, I_{m11}^r \qquad G_2 = -I_{m1}^s \, I_{m13}^r \qquad G_3 = I_{m5}^s \, I_{m7}^r$$

$$G_4 = -I_{m7}^s \, I_{m5}^r \qquad G_5 = I_{m11}^s \, I_{m1}^r \qquad G_6 = I_{m13}^s \, I_{m1}^r \qquad (1.71)$$

$$\beta_1 = \theta_1^1 + \theta_2^{11} \qquad \beta_2 = \theta_2^{13} - \theta_1^1 \qquad \beta_3 = \theta_1^5 + \theta_2^7$$

$$\beta_4 = \theta_1^7 + \theta_2^5 \qquad \beta_5 = \theta_1^{11} + \theta_2^1 \qquad \beta_6 = \theta_1^{13} - \theta_2^1 \qquad (1.72)$$

(d)   Steady State Voltage and Power Factor:

The volt ampere equation for 'r' phase of the stator can be written from phase impedance $[Z_{ryb, \alpha\beta v}^{s \quad r}]$ (appendix IB) as:

$$v_r^s = (R_1 + L_1 p) \, i_{r1}^s + \frac{3}{2} M p \, i_\alpha^r \qquad (1.73)$$

Under steady state the phase voltage can be expressed as:

$$v_r^s = \sum_n \sqrt{2} \; V_{rn}^s \, \sin(nw_0 t + \beta_n) \qquad (1.74)$$

The nth harmonic steady state voltage V_{rn}^s (rms) as obtained from equations (1.63), (1.73) and (1.74) is:-

$$V_{rn}^s \underline{/\beta_n} = (R_1 + jwn \, X_1) \, I_{rn}^s \underline{/\phi_n} + \frac{3}{2} jwn \, X_M \, I_{\alpha n}^r \underline{/\alpha_n} \qquad (1.75)$$

where $X_1 = w_b L_1$; $X_M = w_b M$

ϕ_n, α_n are phase angles.

Rewriting equation (1.75) we get –

$$V_{rn}^s \underline{/\beta_n} = \left\{ \left[I_{rn}^s \sqrt{R_1^2 + (nwX_1)^2} \cos(\phi_n + \theta_n) \right.\right.$$
$$\left. + \frac{3}{2} nwX_M I_{\alpha n}^r \cos\left(\frac{\pi}{2} + \alpha_n\right) \right]^2$$
$$+ \left[I_{rn}^s \sqrt{R_1^2 + (nwX_1)^2} \sin(\phi_n + \theta_n) \right.$$
$$\left.\left. + \frac{3}{2} nwX_M I_{\alpha n}^r \sin\left(\alpha_n + \frac{\pi}{2}\right) \right]^2 \right\}^{1/2} \qquad (1.76)$$

where $\theta_n = \tan^{-1} \dfrac{nwX_1}{R_1}$

$$\beta_n = \frac{I_{rn}^s \sqrt{R_1^2 + (nwX_1)^2}\, \sin(\phi_n + \theta_n) + \frac{3}{2} nwX_M I_{\alpha n}^r \sin\left(\frac{\pi}{2} + \alpha_n\right)}{I_{rn}^s \sqrt{R_1^2 + (nwX_1)^2}\, \cos(\phi_n + \theta_n) + \frac{3}{2} nwX_M I_{\alpha n}^r \cos\left(\frac{\pi}{2} + \alpha_n\right)}$$

$$(1.77)$$

The rms phase voltage V_r^s as available at machine terminal is:

$$V_r^s = \sqrt{\sum_n (V_{rn}^s)^2} \qquad (1.78)$$

Similarly the rms stator phase current is:

$$I_r^s = \sqrt{\sum_n (I_{rn}^s)^2} \qquad (1.79)$$

Thus the effective power factor $\cos\phi$ is:

$$\cos\phi = \sum_n V_{rn}^s I_{rn}^s \cos(\phi_n - \beta_n)\, \frac{1}{(V_r^s I_r^s)} \qquad (1.80)$$

1.6 RESUME:

The system equations are formulated at the d.c. terminals of inverter fed three phase induction motor. Three axis commutator transformation has been developed, to retain the three phase axes and to establish the link with two terminal d.c. source. Due to the periodic switching, the network topology of the system differs from state to state. A generalised system impedance matrix is developed assuming all the thyristors in conduction mode. The system impedance matrix for any state is derived from the generalised one using Kron's approach.

The mathematical model developed includes the effects of inverter's periodic switching, filter parameters, ripples present in the inverter input voltage given by controlled rectifier bridge, thyristors' commutation and their forward impedances. The system equations are converted into standard form of first order state space equations; for computational ease and simplicity. The phase currents are retained as state variables in addition to filter capacitor voltage.

The model developed here is simple and close to physical system. The model is even suitable for dynamic/transient response and for simulation of any type of fault condition either in motor or in inverter. The model along with other relations developed in this chapter enable us to evaluate the power factor, rms values of voltage and currents, torques both the constant and the pulsating types over the wide frequency range of operation with varying system parameters.

CHAPTER 2

LOSSES IN THREE PHASE INDUCTION MOTOR WITH NONSINUSOIDAL EXCITATION:

Variable frequency operation over a wide frequency range brings in many problems unseen in its normal operation at fixed frequency. The nonsinusoidal voltage when fed to an induction motor, modifies the motor operation considerably from that under conditions of pure sinusoidal applied voltage.

High frequency excitations due to variable frequency nonsinusoidal inverter output lead to the stray load losses, reducing the available torque and increasing the temperature of the machine. If these losses are of significant order, it is necessary to know their nature, locations and relationship to the motor and converter design features. In some of the earlier publications[1,2,13] the losses and torque produced in cage induction motors owing to distorted supply waveform have been considered; the results of these publications indicate that the resultant additional steady state torque and losses are insignificant. But more recently[13,36] it has been shown that, if the input waveforms have high harmonic content as in the case of inverter output voltage, the additional losses are quite high compared to the losses contributed by the fundamental voltage and currents. Fluxes and currents resulting from the input harmonic voltages are of relatively high frequencies, and effects of these

must be taken into account in both I^2R and core loss calculations. No previous publication has considered the effects on losses produced by skew leakage fluxes; Jordan and Kilingshirn[36] alone have given a little attention to end leakage losses.

In this chapter an attempt is made to formulate the relations for various losses in induction motor with variable frequency nonsinusoidal excitations. The various well established loss formulae[2,3,12,82] are modified to take into account the high frequency effects.

The following types of losses are investigated for variable frequency operation.

(i)   Core losses.

(ii)   Stray losses both at no load and at load.

(iii) Frictional losses.

The following assumptions have been made to get simpler relations;

(i)   Saturation of iron parts of the machine is neglected; thus each time harmonic can be considered independently except in special case of synchronous locking which is not considered here.

(ii)   All formulae are developed for small value of slip, so it is dropped at convenient points without affecting the results.

(iii) The nonsinusoidal output voltage from three phase bridge inverter is balanced.

2.1 HARMONIC FIELDS:

The inverter's output voltage of stepped waveform consists of harmonics of $6k \pm 1$ order (k is positive integer number). Triplen harmonic voltage and currents cannot exist in a three phase balanced system with star connected motor with its neutral isolated. Therefore, only $6k \pm 1$ orders of harmonics along with fundamental are considered for loss computations.

Operation of the machine is considered as constant torque drive upto the normal frequency and constant horse power drive for frequencies above normal, giving operating frequency,

$$f_o = wf_b,$$ (2.1)

where f_b is base (Normal) frequency;

$$w \leq 1.0 \text{ for constant torque,}$$
and $$w > 1.0 \text{ for constant horse power.}$$ (2.2)

2.2 CORE LOSSES:

Hysteresis and eddy current losses in stator and rotor with operating frequency f_o are[59,80],

STATOR

$$w_h^s = \eta_h \, B_m^{1.6} \, f_o \, ,$$ (2.3)

$$w_e^s = \eta_e \, B_m^2 \, f_o^2 \, ,$$ (2.4)

ROTOR

$$w_h^r = \eta_h \, B_m^{1.6} \, sf_o \, ,$$ (2.5)

$$w_e^r = \eta_e \, B_m^2 \, (sf_o)^2 \, .$$ (2.6)

The total iron losses are;

$$W_1 = \eta_h \; B_m^{1.6} \; f_o \; (1+s) + \eta_e \; B_m^2 \; f_o^2 \; (1+s^2) \qquad (2.7)$$

where η_h, η_e are the hysteresis loss and eddy loss constants.

B_m maximum value of air gap flux density.

s   slip of the motor.

The peak value of the air gap flux density of nth harmonic field $B_{m(n)}$, can be related to that of the fundamental flux density by assuming that the nth harmonic voltage is $\frac{1}{n}$ times that of the fundamental, but its frequency is n times the fundamental. The nth harmonic flux density then is $\frac{1}{n^2}$ times the fundamental flux density i.e.,

$$B_{m(n)} = \frac{1}{n^2} \; B_{m(1)} \; , \qquad (2.8)$$

and the nth harmonic slip s_n is,

$$s_n = \frac{n-1}{n} \quad , \quad (n = 1,7,13...etc.)$$

$$s_n = \frac{n+1}{n} \quad , \quad (n = 5,11 ....etc.)$$

then the iron losses for nth harmonic become;

$$W_{1(n)} = \eta_h \; B_{m(1)}^{1.6} \; f_o \; (1+s_n) \; (\frac{n}{n^{3.2}}) + \eta_e \; B_{m(1)}^2 \; f_o^2 (1+s_n^2)(\frac{n^2}{n^4})$$

$$(2.9)$$

For CONSTANT TORQUE operation when $w \leq 1.0$ the flux density is held constant by keeping $\frac{V}{f_o}$ ratio fixed,

then the nth harmonic loss becomes.

$$W_{1(n)} = k_1 \, wf_b \left(\frac{1+s_n}{n^{2.2}} \right) + k_2 \, w^2 f_b^2 \left(\frac{1+s_n^2}{n^2} \right) \tag{2.10}$$

Total iron loss summed over all the harmonics is then -

$$W_1 = k_1 wf_b \left(\sum_n \frac{1}{n^{2.2}} + \sum_n \frac{s_n}{n^{2.2}} \right) + k_2 \, w^2 f_b^2 \left(\sum_n \frac{1}{n^2} + \sum_n \frac{s_n^2}{n^2} \right) \tag{2.11}$$

OR

$$W_1 = k_1 \, wf_b \, (K_1 + G_1) + k_2 w^2 \, f_b^2 \, (K_2 + G_2) \tag{2.12}$$

where $k_1 = \eta_h \, B_{m(1)}^{1.6}$ (2.13)

$$k_2 = \eta_e \, B_{m(1)}^2 \tag{2.14}$$

and

$$K_1 = \sum_n \frac{1}{n^{2.2}} \tag{2.15}$$

$$K_2 = \sum_n \frac{1}{n^2} \tag{2.16}$$

$$G_1 = \sum_n \frac{s_n}{n^{2.2}} \tag{2.17}$$

$$G_2 = \sum_n \frac{s_n^2}{n^2} \tag{2.18}$$

For CONSTANT HORSE POWER operation when $w > 1.0$ the voltage applied is held constant therefore the fundamental flux density vary as:

$$B_{m(1)} \text{ (at frequency } f_o) = \frac{B_{m(1)} \text{ (at frequency } f_b)}{w} \tag{2.19}$$

From equations (2.9) and (2.19), nth harmonic loss is:

$$W_{1(n)} = \eta_h \left(\frac{B_{m(1)}}{w} \right)^{1.6} \frac{f_o}{n^{2.2}} (1+s_n) + \eta_e \frac{B_{m(1)}^2}{w^2} x$$

$$\frac{f_o^2}{n^2} (1 + s_n^2). \tag{2.20}$$

and the total iron loss is,

$$W_1 = \frac{k_1 f_b}{w^{0.6}} (K_1 + \xi_1) + k_2 f_b^2 (K_2 + \xi_2) \tag{2.21}$$

2.3 STRAY LOSSES:

The stray load losses are defined as the excess of the total losses actually occuring in a motor at a given load current over the sum of the calculated I^2R losses for that current, the no load core loss, and the friction and windage loss. They are caused by the magnetomotive forces (mmf) of the motor load currents, which divert some of the no load magnetic flux into leakage paths; there-by creating flux pulsations and eddy current losses in core plates, the conductors, and the adjacent metal parts. These losses are difficult to measure and they may vary materially in individual motors, as a result of manufacturing variations.

These losses are assumed to be independent of the main flux. Since many of the components of iron losses and stray load losses are produced by flux variations and eddy currents in the same physical components, some discrepancy is bound to be introduced by the assumption of super-position. Nevertheless,

for all practical purposes, it is assumed that the separate losses be added directly. The quasi-empirical relations to find the stray losses with sinusoidal excitations are widely reported in the literature[2,12,13].

When nonsinusoidal voltage is applied to the stator winding, the space harmonics must be viewed with respect to the principal time harmonic of the applied waveform and not simply to the fundamental.

This approach coupled with linearity of magnetic circuit leads to the superposition of each time harmonic's interaction with all the principal space harmonics including the fundamental. The following components of stray losses are considered here.

(i)   end leakage flux

(ii)   zigzag leakage flux, which normally cause high frequency surface losses in stator and rotor.

(iii) high frequency rotor flux pulsations.

(iv)   skew leakage flux.

(a)   <u>Losses Due to End Leakage Flux:</u>

The eddy currents set up in the end structure of the machine by leakage fluxes which enter the laminations in an axial direction, and also penetrate the end fingers, flanges, and other parts cause end leakage losses. They are significant when the coil overhang is large, the distance between the centers of the peripheral currents (fig. 2.1) in the stator and rotor end windings is large, and when the ventilating

shields etc. are close to the end turns. It is not possible to develop a formula for the end loss, due to the wide variations in design except possibly for large machines. However, it has been found by Alger[2] that satisfactory results are yielded by assuming that the end loss is equal to that portion of the kilo volt amperes (kva) of end leakage reactance that is due to flux entering the stator laminations axially multiplied by an empirical constant power factor. Chalmers[12,13] also supports Alger's semi-empirical formula in his publication and comes to the same conclusions from the results obtained by modified 'rotor removed test'. The end loss formula as developed by Alger is:

$$W_E = C_E \ I^2 f_o \qquad (2.22)$$

where

$$C_E = H m \ \frac{0.63 \ m \ T^2 \ D}{10^5 \ P^2} \ \log \left(1 + \frac{A^2}{Y_1 Y_2} \right)$$

H   end loss power factor (for medium sized and big machines   H = 0.3 and for small machines H < 0.3)

I   phase load current

T   effective number of turns per phase

P   number of poles

D, A, Y_1, Y_2 are shown in fig. 2.1

r_1 nearly equal to half of the stator slot depth

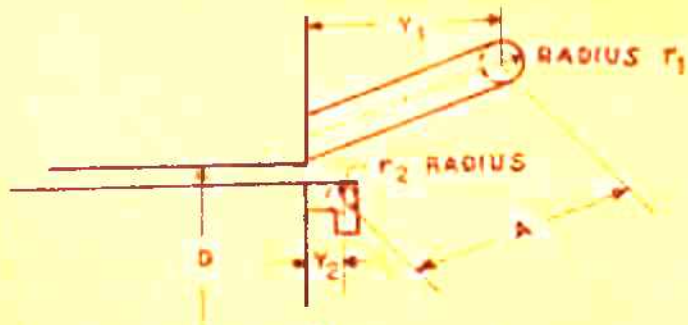r_2 nearly equal to half of the rotor slot depth.

FIG. 2·1 GEOMTRY OF END WINDING
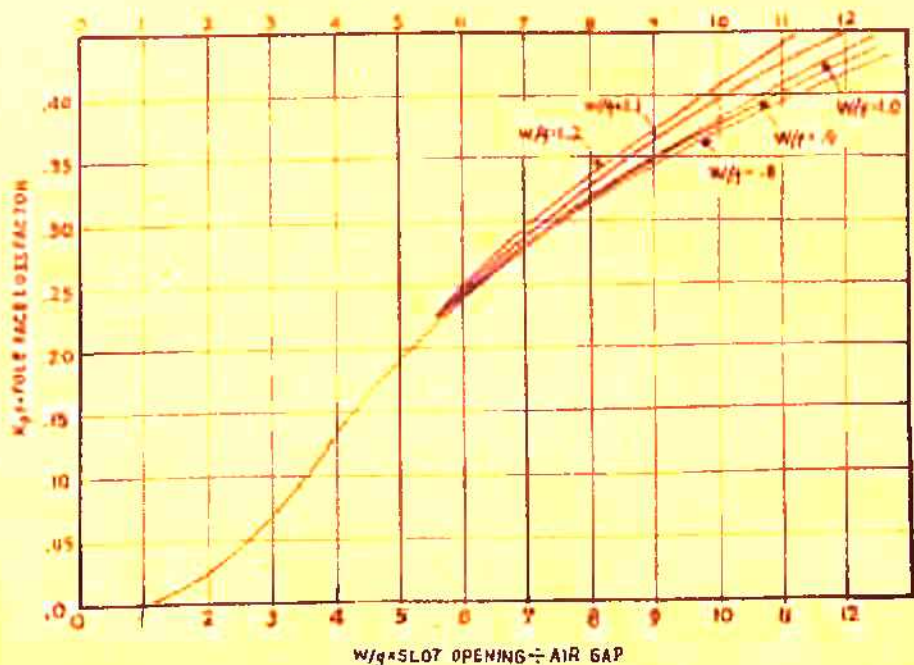
FIG. 2·2 REPRODUCED FROM REFERENCE 2.
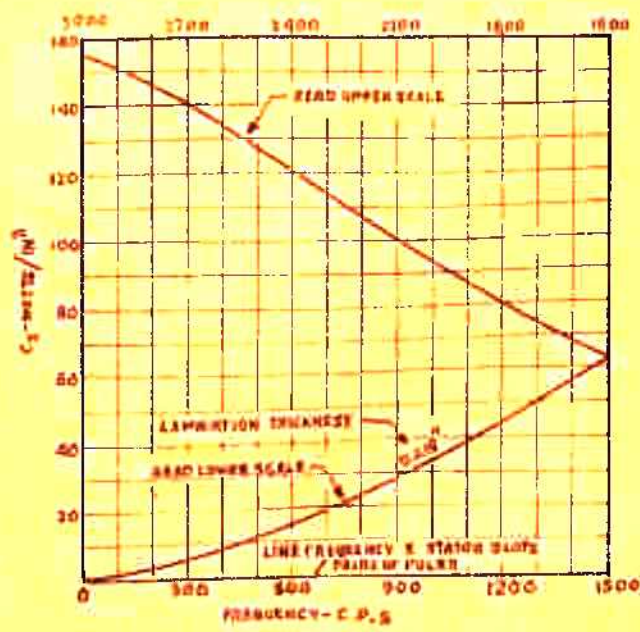
FIG. 2·3 REPRODUCED FROM REFERENCE 2.

The machine is considered to be excited by series connected
voltage sources of different frequencies. The total end
losses can be obtained from equation (2.22) by applying the
principle of superposition.

$$W_E = C_2 \sum_n \left[(I_n^2) nwf_b \right] \qquad\qquad (2.23)$$

(b) High Frequency Surface Losses:

(i) At No Load: Due to the presence of slot openings
on stator and rotor surfaces, dips in the flux distribution
around the air gap are caused; causing slot frequency pulsa-
tions in the radial flux density. These pulsations cause
eddy current losses in the laminations that are usually
called surface losses due to zig zag leakage flux. Some of
the flux pulsations pass down the rotor teeth and induce
circulating currents in the rotor winding, causing additional
rotor losses. For convenience in analysis, the peripheral
air gap flux density distribution is analysed into a series
of rotating space harmonic fields, the principal ones,
besides the fundamental being the stator and rotor slot
harmonics, with number of poles equal to $2s' \pm 1$ and $2r' \pm 1$
times the fundamental poles, where s' and r' are the numbers
of slots per pole in stator and rotor respectively. The slot
harmonic fields are partly due to permeance variations
caused by the slot openings and partly due to the nature of
mmf wave. The permeance variations cause losses at no load

while the mmf steps cause losses at load. Since these two
components have same number of poles and same frequency, the
resultant losses are proportional to the square of their
vector sum. Considering first the effects of the no load
permeance variations, the loss in the rotor surface is given
by the following relation[2].

$$W_{so} = 79 \ DL \ B_m^2 \ K_{pf} \ C_{s2} \lambda_1 \ \text{watts} \qquad (2.24)$$

where   L   core length in meters

         K_{pf} pole face loss coefficient for stator slot
openings, from fig. 2.2.

         C_{s2} rotor iron loss coefficient from fig. 2.3
in watts per inch^3 for stator slot frequency
which is equal to $\text{wmf}_b \dfrac{S_1}{p}$.

         λ_1 tooth pitch for stator in meters.

The values of C_s in fig. 2.3 are based on constant impressed
mmf, assuming the permeability equal to 800 a constant value.

(ii)   <u>At Load</u>: When the machine is loaded, space harmonics
produce harmonic fields of nature similar to permeance
harmonics except for magnitude and phase angles. Alger
produces an acceptable form of ratio (R_t) of mmf harmonic at
load to permeance harmonic at no load as:

$$R_t = \frac{\text{mmf harmonic at load}}{\text{permeance harmonic at no load}} = \frac{I^2}{s'I_o^2 K_{pf}} \qquad (2.25)$$

Therefore when the equation (2.24) is multiplied with ratio R_t, an expression for rotor surface is obtained as:

$$W_{s2} = 79 \ DL \left(\frac{I}{s'I_o} \right)^2 B_m^2 \ C_{s2} \ \lambda_1 \quad \text{(for rotor)} \quad (2.26)$$

To find the actual surface loss under load, the phase angle between the permeance and mmf ripples of the same order should be determined. However, the best approximation is obtained by addition of no load losses W_{so} and load losses W_{s2}[2,13].

By analogy to equation (2.26), the stator surface loss under load is:

$$W_{s1} = 79 \ DL \left(\frac{I}{r'I_o} \right)^2 B_m^2 \ C_{s1} \lambda_2 \quad (2.27)$$

Since the nth harmonic flux density $B_{m(n)} = \dfrac{B_m(1)}{n^2}$ the surface losses for nth harmonic are,

For $w \leq 1.0$

$$W_{s1(n)} = 79 \ DL \left(\frac{B_m(1)}{r'} \right)^2 \left[\left(\frac{I_n}{I_{on}} \right)^2 \frac{1}{n^4} \ C_{s1n} \right] \lambda_2 \cdot \quad (2.28)$$

$$W_{s2(n)} = 79 \ DL \left(\frac{B_m(1)}{s'} \right)^2 \left[\left(\frac{I_n}{I_{on}} \right)^2 \frac{1}{n^4} \ C_{s2n} \right] \lambda_1 \cdot \quad (2.29)$$

and for $w > 1.0$,

$$W_{s1(n)} = 79 \ DL \left(\frac{B_m(1)}{wr'} \right)^2 \left[\left(\frac{I_n}{I_{on}} \right)^2 \frac{1}{n^4} \ C_{s1n} \right] \lambda_2 \cdot \quad (2.30)$$

$$W_{s2(n)} = 79 \ DL \left(\frac{B_m(1)}{ws'} \right)^2 \left[\left(\frac{I_n}{I_{on}} \right)^2 \frac{1}{n^4} \ C_{s2n} \right] \lambda_1 \cdot \quad (2.31)$$

Hence, total surface losses are:

$$W_s = \sum_n W_{s1(n)} + \sum_n W_{s2(n)}$$

$$W_s = C_{sL} \left[\sum_n C_{K(n)} \left(\frac{I_n}{I_{on}} \right)^2 \right] \quad \text{(for } w \leq 1.0\text{)} \qquad (2.32a)$$

and

$$W_s = \frac{C_{sL}}{w^2} \left[\sum_n C_{K(n)} \left(\frac{I_n}{I_{on}} \right)^2 \right] \quad \text{(for } w > 1.0\text{)} \qquad (2.32b)$$

where –

C_{s1n}, C_{s2n} the iron loss coefficients at harmonic slot frequency, which is equal to $wnf_b \dfrac{S_1}{p}$ and $wnf_b \dfrac{S_2}{p}$ for stator and rotor respectively. These coefficients can be determined from fig. 2.3.

I_{on} no load current for nth harmonic

λ_2 tooth pitch for rotor

S_1 stator slots

S_2 rotor slots

p pair of poles

r' rotor slots per pole

s' stator slots per pole

$C_{sL} = 79 \; DL \; B_{m(1)}^2$

$$c_{K(n)} = \frac{\lambda_2}{r'^2} \quad \frac{c_{s1n}}{n^4} + \lambda_1 \frac{c_{s2n}}{s'^2 n^4}$$

(c)   High Frequency Rotor Pulsation Losses:

When the rotor and stator have equal number of slots, then no appreciable part of slot harmonic field would go down the rotor teeth, and no currents would be induced in the rotor winding. The maximum flux goes down in the rotor slots linking with rotor winding when -

(i) either the slots are open

(ii) or number of rotor slots are of the order of two times the number of stator slots.

In a cage rotor too, the net rotor tooth flux remains almost constant and the flux pulsation loss is negligible unless the rotor slots are skewed. If the slots are skewed by one stator slot pitch, each rotor bar spans nearly 360 degrees of the stator slot harmonics, regardless of the slot ratio, and the net voltage induced in each bar will be nearly zero. However, there will then be a considerable voltage acting from bar to bar at the midpoint of the core length, and this will cause current to flow through the laminations in this region to a extent depending on the level of bar insulation. In this case there will be some pulsation loss in the teeth and also I^2R loss in the bars and the rotor iron. As has been shown, the actual losses will vary widely with the insulation level, as well as the slot ratio, the

amount of skew and other factors[62]. The fraction of the load current that will flow in the rotor for each harmonic is determined by the ratio of zig zag leakage reactance for slot harmonic to the fundamental mmf magnetising reactance. The well established equivalent circuit for space harmonics is used to formulate a relation for rotor pulsation losses[3], given as:

$$W_z = C m I^2 k_s R_{2(d.c.)} \qquad (2.33)$$

If the effects of time harmonics present in the current waveform are included then the total rotor pulsation losses are :

$$W_z = C m R_{2(d.c.)} \left(\sum_n k_{sn} I_n^2 \right) \qquad (2.34)$$

where -

    C   the loss factor (fig. 2.4)

    k_{sn} skin effect ratio for rotor bars at stator slot frequency.

Similarly the no load rotor pulsation losses can be written as :

$$W_{zo} = C m R_{2(d.c.)} \left(\sum_n k_{sn} I_{on}^2 \right) \qquad (2.35)$$

As I_{on}, the no load current for nth harmonic is very small, the no load rotor harmonic pulsations are of little significance.
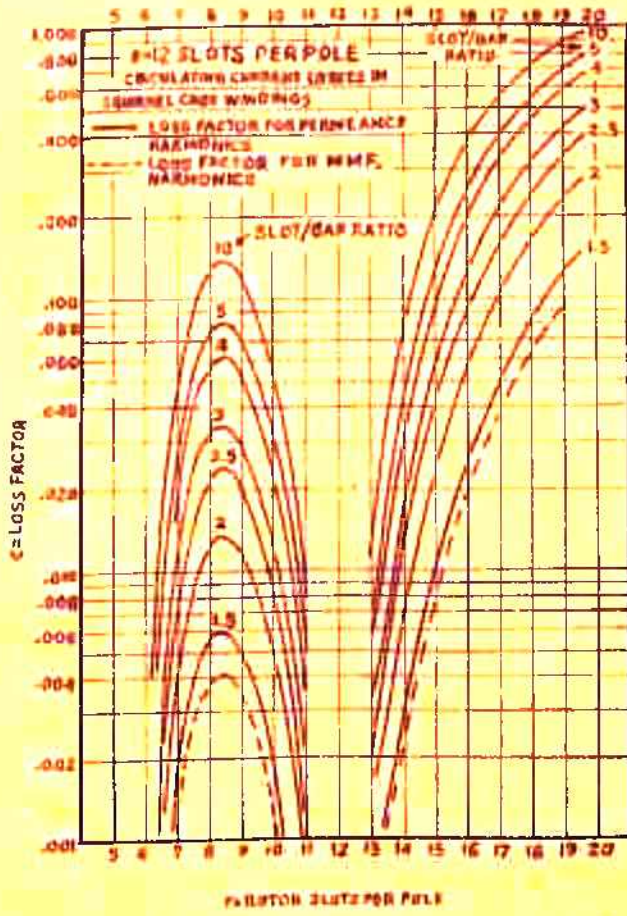
FIG. 2·4 REPRODUCED FROM REFERENCE 2.

(d)   Losses Due to Skew Leakage Flux:

In the case of a motor with skew of either of its stator or rotor slots, the skew leakage flux may be appreciable. The skew mmf is zero at the centre of the core and increases approximately linearly along with the length of the core, reaching its greatest value at the core ends[26]. The overall phase change in the skew leakage flux over the full core length is 180°. As the distance from the core center increases, the difference of stator and rotor mmfs increases linearly, and there is a corresponding increase in the radial flux density. Since the load component of the stator current is displaced nearly by 90° from the magnetising component, this increase in flux due to the skew may be considered as independent of the no load flux, to the first order of approximation. With s' slots per pole in the stator and one slot pitch skew, the ratio of the extra mmf at each end of the core to the no load magnetising mmf is[2,51,62],

$$\frac{\text{skew mmf}}{\text{fundamental mmf}} = 2 \left(\text{Sin } \frac{\pi}{4s'}\right) \frac{I'}{I_0} \simeq \frac{\pi I'}{2s' I_0} \tag{2.36}$$

where

$$I' = |I - I_0| \tag{2.37}$$

The average loss over the whole core length is approximated as:

$$W_{sK} = \frac{\pi^2}{12} \left(\frac{I'}{s' I_0}\right)^2 \times (\text{Iron losses in the stator}) \tag{2.38}$$

Accounting the effects of time harmonics, the equation (2.38) is modified to -

$$W_{sK} = C_K \left[\sum_n \left(\frac{I_n}{I_{on}} \right)^2 W_{1(n)} \right] \tag{2.39}$$

Where $W_{1(n)}$ is given by equations (2.10 and (2.20) and

$$C_K = \frac{\pi^2}{12} \frac{\sigma^2}{s'^2} \tag{2.40}$$

σ ratio of skew to one stator slot pitch.

2.4   EDDY CURRENT LOSSES IN CONDUCTORS:

When a conductor of finite section lies in a pulsating magnetic field, it becomes the seat of induced emf, which cause parasitic circulating currents precisely similar to those in steel plates under the same conditions. The additional losses from this cause may be quite large, the actual losses are increased by a loss factor K_d defined as:

$$K_d = \frac{\text{Actual } I^2 R \text{ loss}}{\text{d.c. } I^2 R \text{ loss}} = 1 + \frac{\text{extra eddy loss}}{\text{d.c. } I^2 R \text{ loss}} \tag{2.41}$$

It can be shown that the above eddy loss ratio K_d depends upon the geometry of the conductor[41]. The average loss ratio for 'l' layers is given

$$K_{davg} = 1 + (\alpha h)^4 \left(\frac{l^2}{9} \right) \tag{2.42}$$

where

$$\alpha = 2\pi \sqrt{\left(\frac{bf_0}{\int 10}\right)}$$

(2.43)

l   number of layers in the slot

b   ratio of width of copper to slot width

$\int$ resistivity of the conductor material in ohms/cm^3

If $f_0 = wnf_b$, the average loss factor for nth harmonic becomes.

$$K_{davgn} = 1 + \left(\frac{bwf_b}{\int 10^9}\right)^2 h^4 l^2 n^2$$

(2.44)

2.5 FRICTIONAL LOSSES:

The frictional losses are approximated as:

$$W_F = AN + BN^2 = AN_s(1-s) + BN_s^2(1-s)^2$$

(2.45)

where N_s = fundamental synchronous speed.

For small slip values, the relation can be further modified as:

$$W_F = A_1 wf_b + B_1 w^2 f_b^2$$

(2.46)

Coefficients A_1 and B_1 can be determined experimentally by variable voltage test (appendix V)

2.6 RESUME:

The various components of additional losses produced in

induction motor having nonsinusoidal supply waveform have been elucidated. In particular, the importance of losses due to end leakage flux, high frequency flux pulsations and skew leakage flux has been well demonstrated. The methods of calculations of losses with sinusoidal excitations whose accuracy have been well established by the experimental results by the earlier researchers; are used to formulate expressions for losses with nonsinusoidal excitations.

- o -

CHAPTER 3

STEADY STATE PERFORMANCE CHARACTERISTICS AND TORQUE PULSATIONS:

In applications where a wide speed range electrical drives are required but with mandatory uniform speed of rotation, such as paper and steel industry to produce paper and billets respectively of uniform thicknesses; it is important to establish a method for predetermining the magnitude of torque and speed pulsations of the drive. One problem of importance in the application of a rectifier inverter induction motor is that of steady state torque pulsations due to nonsinusoidal voltage at the machine terminals as discussed in chapter 1. It has also been shown by Krause[50] that instability can occur over a wide speed range if the system parameters are improperly selected, and the other obvious concern is the resulting increase in motor losses as has been discussed in Chapter 2. Thus the steady state torque pulsations are originated not only by nonsinusoidal voltages but also by improper system parameters. The speed oscillations is a natural consequence of the torque pulsations. In previous studies considerable attention has been given to the calculations of these harmonic electromagnetic torques.

Jain[31] by neglecting stator resistance, has established a general equation only for average torque with a balanced set of voltages of arbitrary waveform. Lipo and Krause[49]

consider only the 6th harmonic torque in a synchronously rotating reference frame for inverter fed induction motor. These authors assume an ideal voltage of stepped waveform at machine terminals, a constant d.c. current in inverter neglecting sixth harmonic and its multiples. Also the system equations are linearised, assuming small perturbations about a fixed point of operation.

The rectifier inverter drive system of fig. 1.1 is generally equipped with a filter between the rectifier and the inverter. Storage of energy in the filter inductance and capacitance and subsequently the exchange of energy between the filter components and magnetic field and rotor of the motor may cause the motor to develop even high magnitude pulsating torques which may even lead the system to instability at low operating frequencies[50]. Therefore it is very essential to investigate the effect of filter parameters on torque pulsations along with machine parameters specially at low frequencies. This chapter endeavours the investigation of the effects of system parameters not only on pulsating torques but also on the other important performance characteristics e.g. power factor, losses, efficiency, current etc. The maximum and the minimum limits of the system parameters are fixed from design considerations. Torque pulsations and other performance indices are computed varying one parameter at a time and keeping the others fixed at their normal values. Computer algorithm along with important

subroutines are also given.

3.1 SALIENT COMPUTATIONAL FEATURES:

(a) Critical Voltage:

If the motor is desired for constant torque operation, it is essential that the applied voltage at first approximation changes linearly with the operating frequency[96]. But it is not advisable and also not possible sometimes to run the motor at more than its normal voltage, when its operating frequency is larger than the normal frequency. Thus it is decided to consider the motor as constant torque drive upto the normal frequency and constant horse power drive for frequencies greater than normal. This type of drive is ideally suited for the traction purposes[78]. A fixed normal voltage should be applied for all frequencies equal to or greater than normal value . But since considerable voltage is lost, both at very low operating frequencies and at high frequencies greater than normal frequency; therefore it becomes essential to find the minimum voltage required to be applied, to develop a required amount of torque. The critical fundamental voltage 'V'$_{phase}$ can be determined from the well known equivalent circuit[80] of the motor given as:

$$V_{phase} = \sqrt{\frac{2wT}{P} \left[R_1 + \sqrt{R_1^2 + w^2 (X_{L1} + X_{L2})^2} \right]} \tag{3.1}$$

wT = constant for constant horse power

T = constant equal to load torque value for constant torque.

A plot of critical voltage against frequency for different machine parameters is shown in fig. 3.1. It clearly establish that $\frac{V}{f}_0$ ratio is not a fixed value for all operating frequencies. This ratio is much higher than its normal value for low frequencies, since applied terminal voltage needs to be boosted up to make up for the high stator resistance drop. Similarly, more than normal voltage may be required to be applied at machine terminals at high frequency operation even for constant horse power operation[29]. The quantum of boost up required depends mainly on stator resistance and leakage inductances. As shown in fig. 3.1, the boost up is as high as 125 percent at 5 Hz with maximum stator resistance.

(b) Applied Voltage to Inverter:

In normal applications the inverter is connected to the controlled rectifier through a filter. To maintain generality and to study the effects of ripples normally present in a rectified voltage, the inverter input voltage E_d is considered of the form:

$$E_d = E_{d.c.} + C_6 \sin 6 w_s t + C_{12} \sin 12 w_s t \qquad (3.2)$$

where –

C_6 and C_{12} amplitudes of 6th and 12th harmonic ripples.

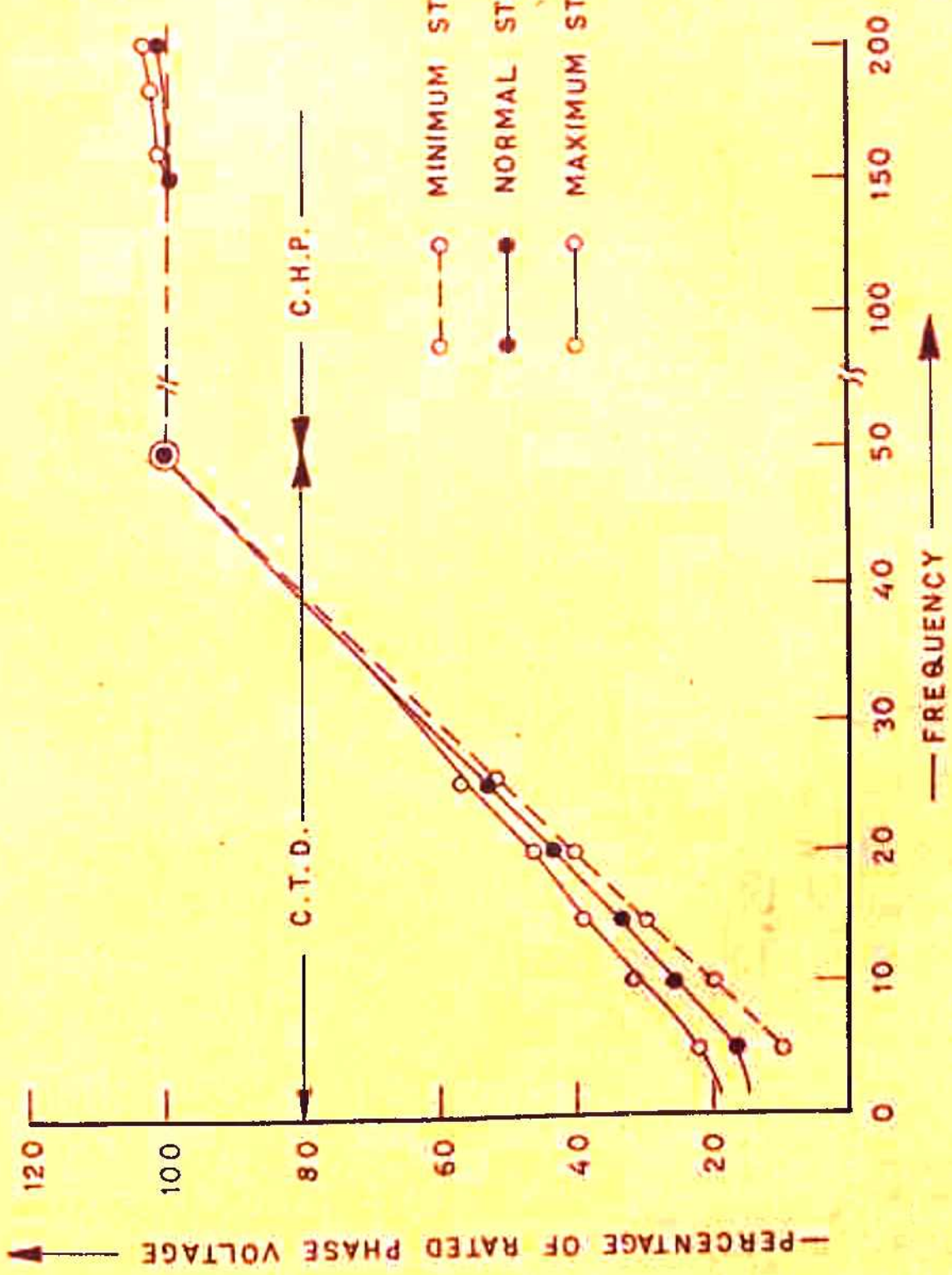w_s is the angular frequency of supply voltage.

FIG. 3·1 CRITICAL VOLTAGE.

MINIMUM STATOR RESISTANCE

NORMAL STATOR RESISTANCE

MAXIMUM STATOR RESISTANCE

C.H.P.

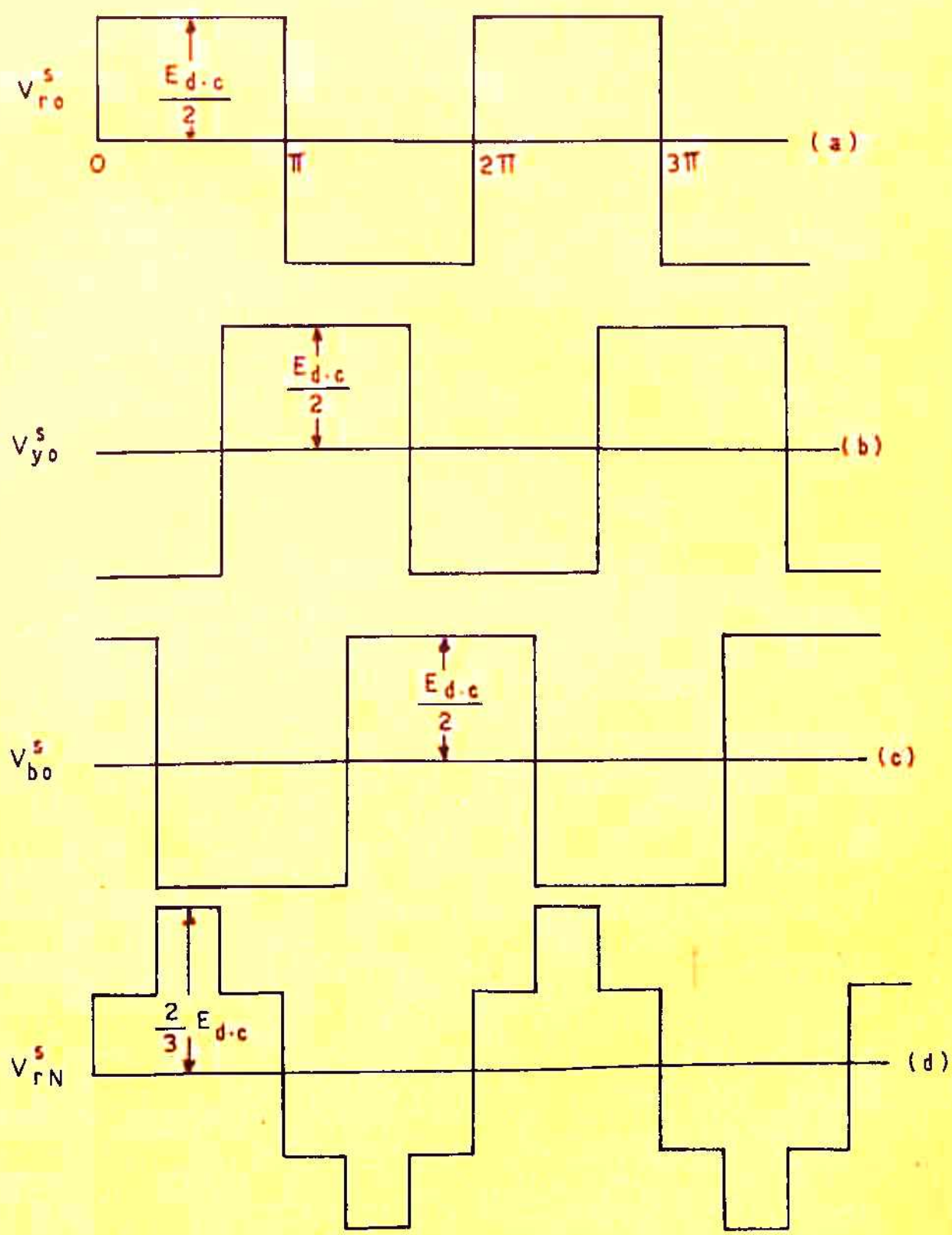C.T.D.

— FREQUENCY

—PERCENTAGE OF RATED PHASE VOLTAGE

84

FIG. 3·2 IDEAL VOLTAGE WAVEFORM.

The bridge rectifier with 6 states will have ripples of
frequencies,multiples of six in its rectified output voltage.
For practical computation, it is sufficient to consider the
sixth and 12th harmonics only, contributions due to the
higher harmonics being negligible.

In fig. 3.2 an ideal voltage waveform at the machine
terminals with respect to the mid point of d.c. voltage is
shown. The line and phase voltages are -

$$V_{ry}^s = V_{ro}^s - V_{yo}^s = V_{rN}^s - V_{yN}^s$$

$$V_{yb}^s = V_{yo}^s - V_{bo}^s = V_{yN}^s - V_{bN}^s \qquad (3.3)$$

$$V_{br}^s = V_{bo}^s - V_{ro}^s = V_{bN}^s - V_{rN}^s$$

$$V_{ry}^s = V_{br}^s = 2V_{ro}^s - (V_{yo}^s + V_{bo}^s) = 3V_{rN}^s \qquad (3.4)$$

where V_{rN}, V_{yN}, V_{bN} are the phase voltages and V_{ro}, V_{yo},
V_{bo} are the voltages of respective phase with respect
to the mid point of d.c. supply.

Equation (3.4) gives, that the amplitude of the phase
stepped voltage at the machine terminals is only $\frac{2}{3}$rd of
inverter's voltage. From fourier analysis machine phase
voltage waveform V_{rN}^s, it can be seen that the amplitude of
its fundamental is $\frac{2}{\pi} E_{d.c.}$ which should be equal to the
rated peak phase voltage V_m.

$$V_m = \frac{2}{\pi} E_{d.c.}$$

or

$$E_{d.c.} = \frac{\pi}{\sqrt{2}} \, V_{phase} \tag{3.5a}$$

And in a normal three phase bridge rectifier the ripple content is given as:

$$C_6 = .05 \, E_{d.c.} \quad \text{and} \quad C_{12} = .02 \, E_{d.c.} \tag{3.5b}$$

3.2   COMPUTER ALGORITHM:

(a)   Subroutines:

The system equation for jth state obtained in Chapter 1 (equation(1.41)) are of first order as reproduced below:

$$[pY_j] = [\hat{L}_j]^{-1} [R_j][Y_j] + [\hat{L}_j]^{-1}[V] \tag{3.6}$$

These equations are solved with the assumption of constant rotor speed. This assumption of constant speed solution is fairly valid, since the inertia of the rotor is quite high and the speed pulsations will only produce a current response of second order which can easily be ignored for pulsating torques of 6th and 12th harmonics. The dynamic response obtained in Chapter 5 justifies this assumption. Therefore the dynamic equation at mechanical port given by equation (1.58) does not form the part of state vector [Y] .

For constant speed operation these equations become a system of simultaneous first order linear differential

equations; for the solution of which only numerical methods
are best suited. The computer program for the solution of
these equations may be divided into the following subroutines.

(i) R3KSH   Inversion of matrix to find $\left[\hat{L}_j\right]^{-1}$

(ii) R4KSH   Product of two matrices to find $\left[\hat{L}_j\right]^{-1}\left[R_j\right]$

                      and $\left[\hat{L}_j\right]^{-1}\left[V\right]$

(iii) RKSSH   Numerical integration of simultaneous
                    differential equations.

Different numerical integration techniques have been
used, e.g. predictor corrector method by Jorden[34] and
Wiederhold[101], and Runge-Kutta method of/4th order by
Smith[85] and Sarkar[79]. Runge-Kutta method, enables the
increments in a set of dependent variables (currents) corres-
ponding to a small increment in the independent variable
(time) to be determined, provided the differential coefficients
of the dependent variables are known with respect to the
independent variable.

The accuracy of this method depends on the step length,
a smaller step length gives increased accuracy but needs more
computational time. The variable step length method takes care
of the accuracy as well as the computing time. In this method
a relatively large step length may be selected initially
which will automatically be adjusted during course of computa-
tion depending upon the slope of variables. A subroutine
RKSSH was developed for the solution of system

equations using Runge-Kutta method of 4th order with variable step length.

The other subroutines used in the program for evaluation of performance characteristics are -

(iv) R5KSH   Fourier analysis of one of the stator and rotor phase currents (steady state values) to resolve the current waveforms into their fundamental, 5th, 7th, 11th and 13th harmonics. Phase angles associated with each harmonic can also be determined by the same subroutine. For accurate results, the half cycle period is divided into large number of segments of equal intervals.

(v)   R6KSH   Computation of average and pulsating torques.

(b)   Main Line Algorithm:

The program has been written in a general form, so that it can be used for any machine whose differential equations can be expressed in the form as given by equation (3.6), and various input and output requirements are catered for. A substantial part of the program is devoted to the many logical decisions, although the major part of the computing time is spent on the numerical integration, which is performed repeatedly. All computations are carried over IBM 1130. Usual techniques as listed by Louden[52] are used for core memory savings. A flow diagram showing the main part of the program is given in fig. 3.3. The program 'GARG' accounts the voltage ripples in the rectified output voltage.

START

READ FIRST SET OF MACHINE PARAMETERS

READ INITIAL VALUES OF STATE VARIABLES

READ NEXT SET OF MACHINE PARAMETERS

FREQUENCY F_1

CALCULATE CRITICAL VOLTAGE AND CRITICAL SLIP

DETERMINE STATE MATRICES A AND B

CYCLE = 1

SOLVE STATE EQUATIONS USING RUNGE KUTTA 4 TH. ORDER METHOD

ARE THE CURRENTS IN STEADY STATE ?

CYCLE = CYCLE + 1   NO

YES

PERFORM FOURIER ANALYSIS OF STATOR AND ROTOR PHASE CURRENTS

FIND AVERAGE AND HARMONIC TORQUES

ARE TORQUES CALCULATED FOR ALL THE FREQUENCIES ?

GIVE AN INCREMENT TO FREQUENCY   NO

YES

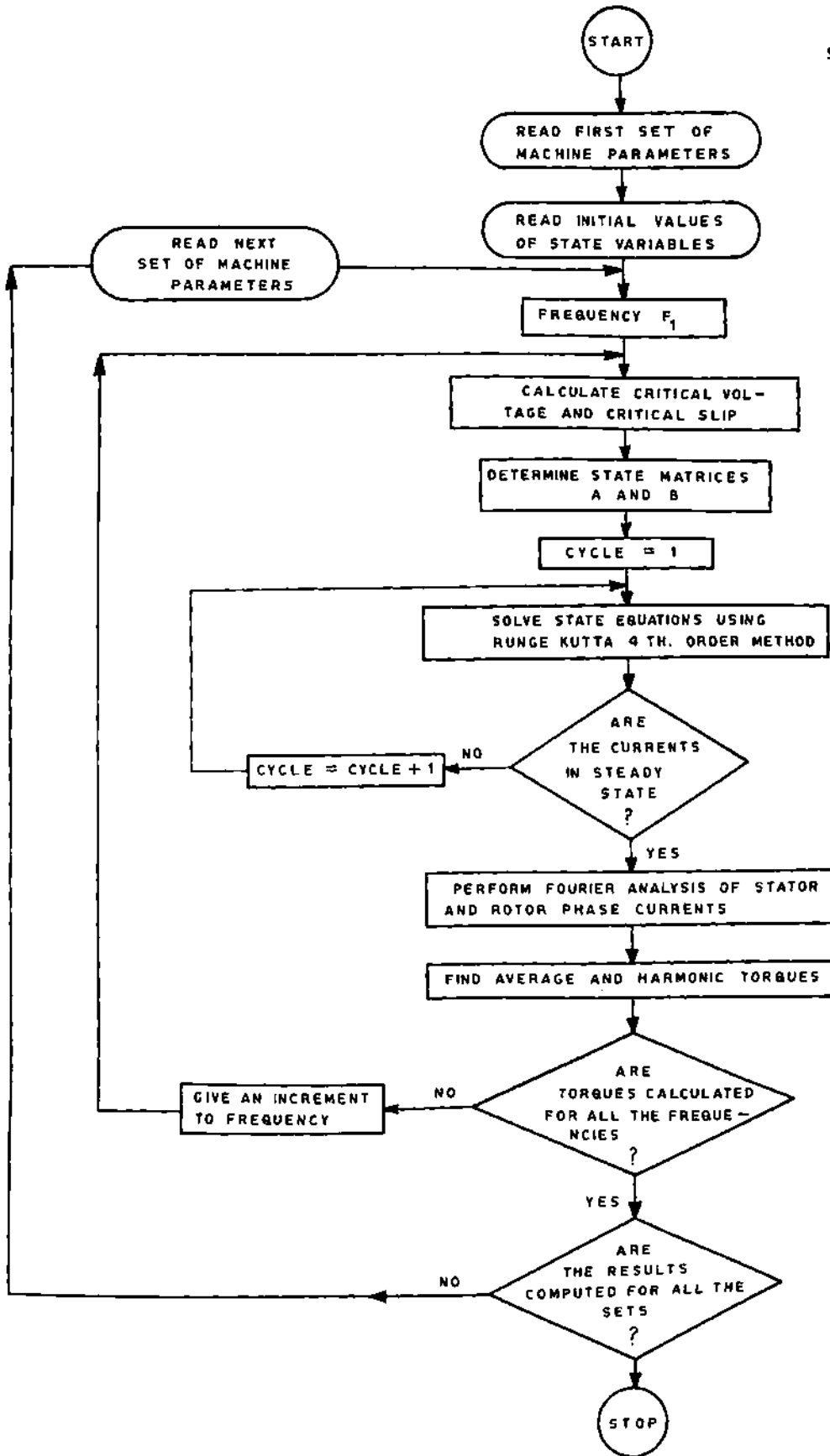ARE THE RESULTS COMPUTED FOR ALL THE SETS ?   NO

STOP

FIG. 3·3   FLOW   DIAGRAM   (constant speed solution)

3.3   SYSTEM PARAMETERS:

The work on the effects of machine and inverter parameters on steady state torque pulsations in induction motor is reported in a very limited way[43,60]. Nelson[60] and Lipo[49], for example, have studied the effects of system parameters on the stability of induction motor. As the instability of the induction motor is very much linked with the steady state torque pulsations, the results presented in these papers though obtained from different mathematical models but form an important guidance in the present work. As reported[32,50,60,75], the most important system parameters which are likely to affect the torque pulsations both under transient and steady state conditions are:

(i)   Stator resistance

(ii) Rotor resistance

(iii) Mutual or magnetising inductance

(iv) Leakage inductance of both stator and rotor

(v)   Filter inductance

(vi) Filter capacitance

(vii) Filter resistance

(viii) Operating frequency.

Since the torque pulsations at low operating frequencies are of very high magnitude[32,50], even with most properly selected set of system parameters; it becomes imperative that the computation for torque pulsations be done over a large

frequency range for each set of system parameters. The scheme of investigation as adapted here is as follows:

Only one system parameter is varied at a time within its preselected maximum and minimum limits, keeping the other parameters fixed at their respective normal values. The computation is performed over a frequency range of 5 Hz to 200 Hz in adjustable discrete steps.

(a) Machine Parameters:

The normal values of the induction motor are determined from well established light run and blocked rotor tests (appendix III). To study the effects of machine parameters over torque pulsations and other performance characteristics, the conservative estimate of the range of variations of the selected machine parameters is decided from the following design considerations.

Since the MAGNETISING INDUCTANCE is proportional to the square of phase turns, by increasing or decreasing the number of turns with in allowable limits, it is possible to increase or decrease respectively the magnetising inductance. It can be seen that magnetising inductance is reduced to about 75 percent of its normal value by decreasing the number of turns by 18 percent , on the other hand an increase of 41 percent in phase turns can almost double the magnetising inductance.

The LEAKAGE INDUCTANCE of a rotating machine depends upon the complex geometry of the leakage flux paths. For induction motor it is common practice to divide the total leakage flux into stator and rotor slot leakage flux, end connection leakage, zig zag leakage or differential leakage, belt leakage and skew leakage. The inductance calculations are made on the assumption that these leakage flux paths are unsaturated. All the components of the leakage inductance are function of magnetising inductance and the geometry of the machine[41,8]. It may be assumed that 75 percent of the total leakage inductance is controlled by magnetising inductance and the remaining 25 percent by the machine geometry. Thus the leakage inductance may be expressed in the following form:

$$X_L = (0.75 \frac{X_M}{X_{MN}} + 0.25\ C_d)\ X_{LN} \tag{3.7}$$

where

X_{LN} Normal p.u. leakage reactance

X_{MN} Normal p.u. magnetising reactance

C_d Constant factor which can be controlled by the geometry of the leakage flux paths.

With the known limits of magnetising inductance X_M and assuming a range of C_d as 0.25 to 2.0, the lower and the higher limits of leakage inductance can be calculated.

STATOR AND ROTOR RESISTANCES can be decreased by suitably increasing the conductor's cross-sectional area

or by reducing the number of turns. By these manoeuvres,
it is possible to reduce the resistances of stator and rotor
to half of their normal values. The higher rotor resistance
can be obtained by having rotor bars of alnico—a high resis-
tivity material, and high stator resistance is no problem
as any amount of additional resistance in each phase of the
stator can be inserted externally. Since the high values
of stator and rotor resistances will cause excessive resis-
tance losses bringing down the efficiency, thus the upper
values of these resistances are fixed purely from efficiency
consideration. Three hundred percent of normal stator
resistance and two hundred percent of normal rotor resistance
are considered good enough as upper limit values. The
range of variation of machine parameters along with their
normal values are listed in table 3.1

Table 3.1   Machine Parameters (Per Unit Values)

	R_1	R_2	X_{L1}	X_{L2}	X_M
Maximum	0.357	0.138	0.25	0.25	7.128
Normal	0.119	0.081	0.113	0.113	3.564
Minimum	0.05	0.034	0.031	0.031	2.67

(b)   Filter Parameters:

The design of single section LC filter parameters is
given in appendix IV. The range of variation of these
parameters along with their normal values are given in
table 3.2.

Table 3.2 Filter Parameters (R_F in Per Unit).

	R_F	L_F	C_F
Maximum	0.25	25 mH	4000 μF
Normal	0.01	100 mH	400 μF
Minimum	0.001	312.5 mH	80 μF

3.4   COMPUTED RESULTS:

The symmetrical induction motor in most cases will not
demonstrate sustained oscillations when supplied from a
balanced set of sinusoidal voltages which are independent of
load current. But the wide range of operating voltages
and frequencies encountered in rectifier inverter drive lead
to torque pulsations which do not occur at fixed frequency
operation. It is in this context that proper selection of
system parameters is vital to avoid these torques. A syste-
matic study of the effects of machine and filter parameters
on steady state torque pulsations and on

other relevant performance indices like power factor and efficiency is carried out here using the model developed in Chapter 1.

Digital computations of performance characteristics are carried out for large sets of system parameters (appendix V) over IBM 1130, each set at different frequencies covering a range from 5 to 200 Hz. A small frequency step size of 5 Hz is selected between 5 to 35 Hz, keeping in view the widely reported fact that the machine tends to become unstable at low frequencies; whereas for constant horse power operation between 50 to 200 Hz, a frequency step length of 50 Hz is adapted. The computed loss coefficients for various losses formulated in Chapter 2, are given in appendix VI. The following performance indices are computed for each set of system parameters and for each operating frequency:

(i)   Average torque

(ii) Sixth and twelveth harmonic pulsating torques and their resultant.

(iii) Steady state phase voltage waveform at machine terminals

(iv) Steady state stator and rotor phase currents waveforms

(v)   Critical voltage and operating slip for full load torque of 1.5 per unit.

(vi) All components of stray losses, iron, copper and frictional losses

(vii) Efficiency

(viii) Power factor

(ix)   Stator phase current (rms value)

Pulsating torques as percentage of respective average torque, power factor, efficiency and phase current variations against frequency are given in fig. 3.4 through 3.22. To facilitate the comparison and to study the effects of stator resistance, rotor resistance, magnetising and leakage inductances, set of three characteristics corresponding to normal, maximum and minimum values of the concerned parameter are given in a single graph. Each characteristic has been drawn for two distinct regions of operation of the motor, i.e. constant torque and constant horse power. Different performance indices are dealt in figs. 3.4 to 3.19 when only machine parameters are varied taking into account the ripples in rectified output voltage. The computed results with variable filter and with fixed machine parameters at their normal values; are shown in figs. 3.20 and 3.21.

3.5   DISCUSSION OF RESULTS:

(a)   Effects of Stator Resistance:

Torque pulsations are considerably reduced, when the stator resistance is increased. The increased stator resistance provides sufficient dampening effect on torque pulsations (fig. 3.4). But this dampening is achieved as can be expected at the cost of efficiency of the motor. The curves of fig. 3.5 clearly establish this result, where the efficiency

considerably goes down at all the frequencies both for constant torque and constant horse power operation. The decrease in efficiency is observed to be more severe at low frequencies (fig. 3.5). However, the power factor tends to improve slightly (fig. 3.6). The stator input current is also increased marginally (fig. 3.7), practically at all the frequencies, since a part of the applied voltage is lost in additional resistance therefore, to produce the same torque that with the normal resistance value, the motor needs additional input current. Due to the deteriorated performance of the machine, the practice of using stator resistance as dampener is normally not recommended unless it becomes inevitable. On the other hand, the advantage gained in terms of efficiency by reducing the stator resistance, is not that pronounced as compared with the disadvantage of increased pulsating torques. Therefore, the motor needs to be provided with a compromisive value of the stator resistance which does not lead to unnecessary and avoidable high pulsating torques or poor efficiency.

(b) Effects of Rotor Resistance:

The rotor resistance does not seem to affect substantially the pulsating torques (fig. 3.8), efficiency (fig. 3.9), power factor (fig. 3.10), and the stator input (fig. 3.11), except at very low frequencies. It has been found from the computed results that the increased rotor resistance do cause additional rotor resistance losses but this addition is not of any significant order compared with other losses.
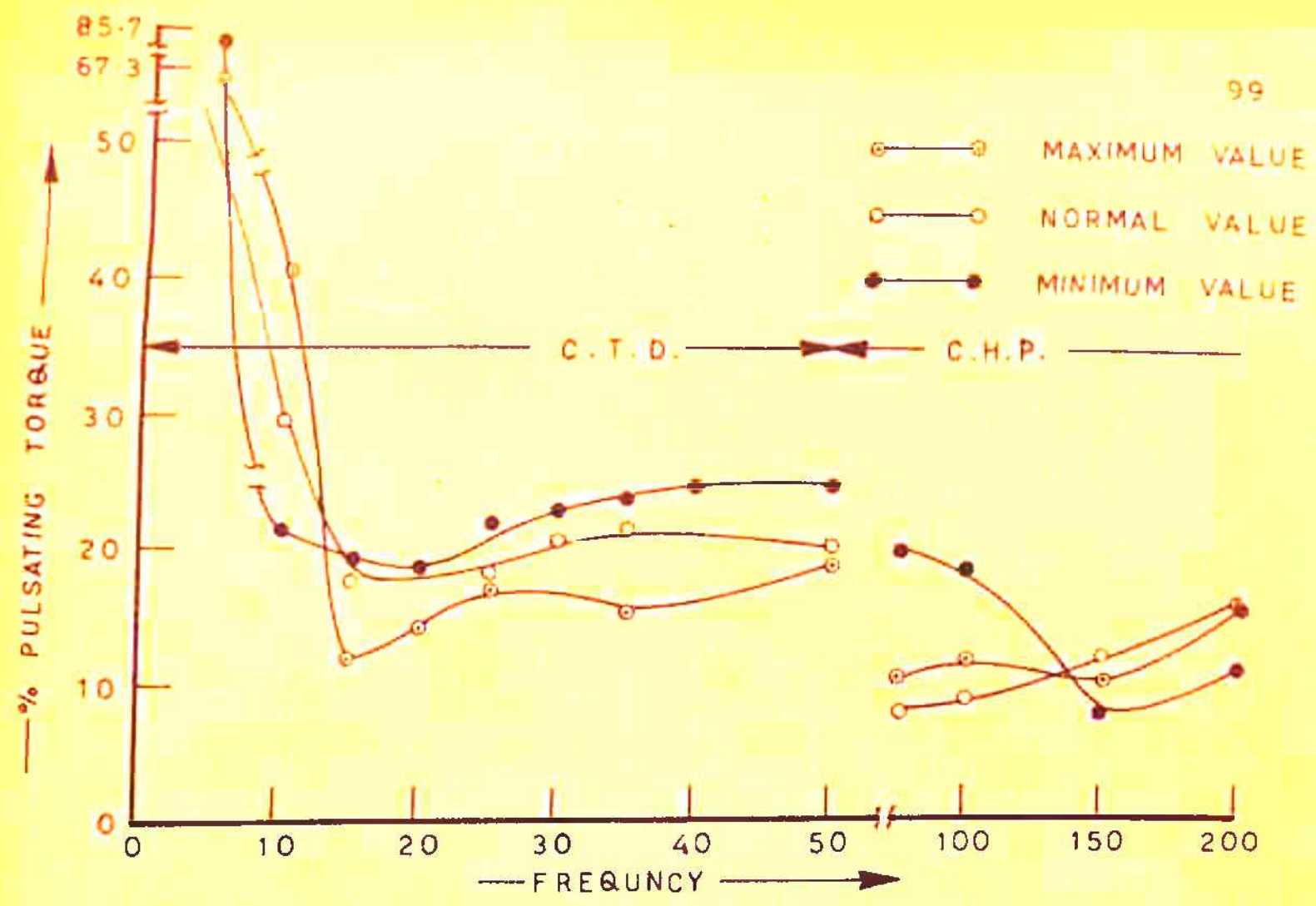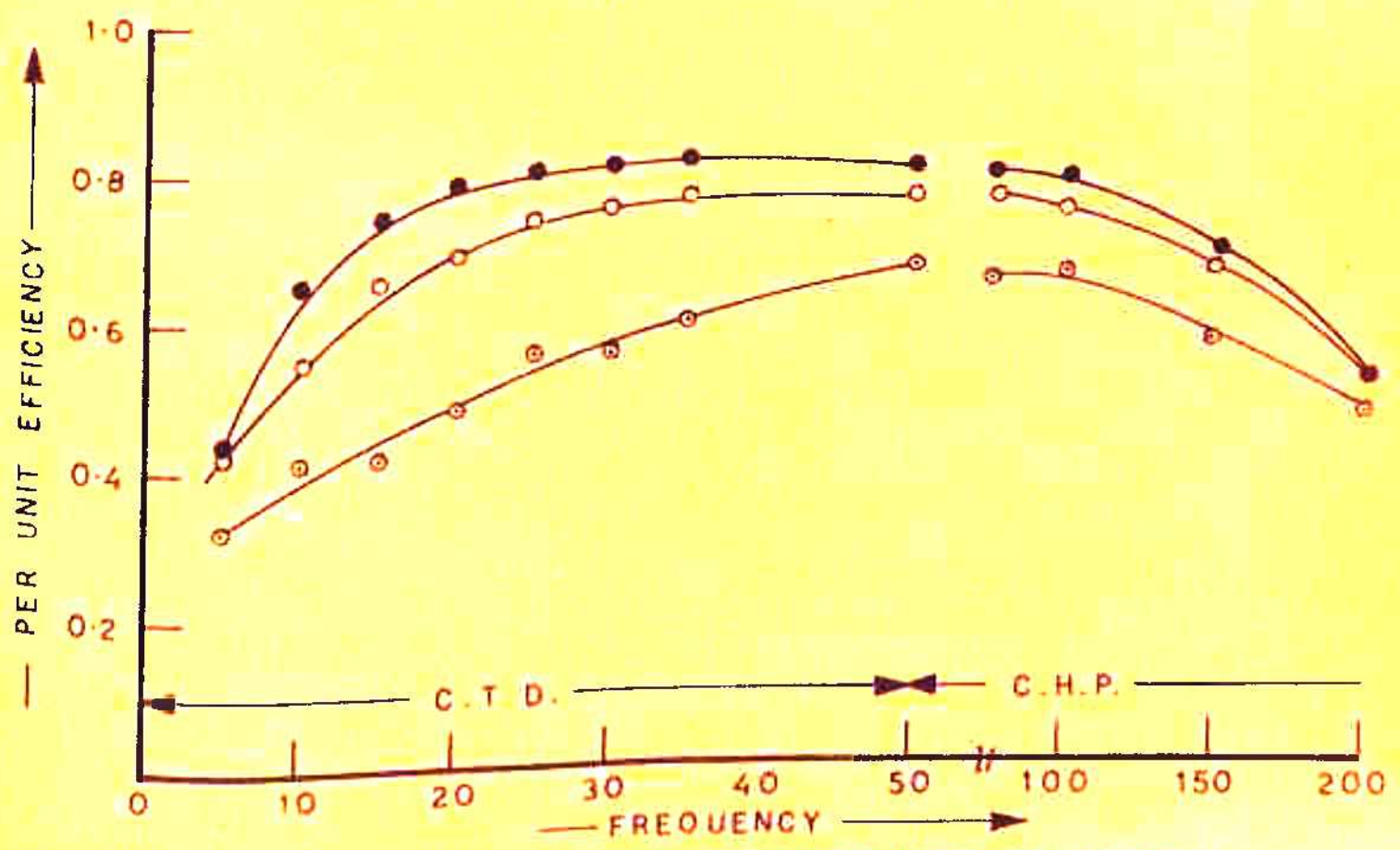
FIG.3·4 EFFECT OF STATOR RESISTANCE ON PULSATING TORQUE.

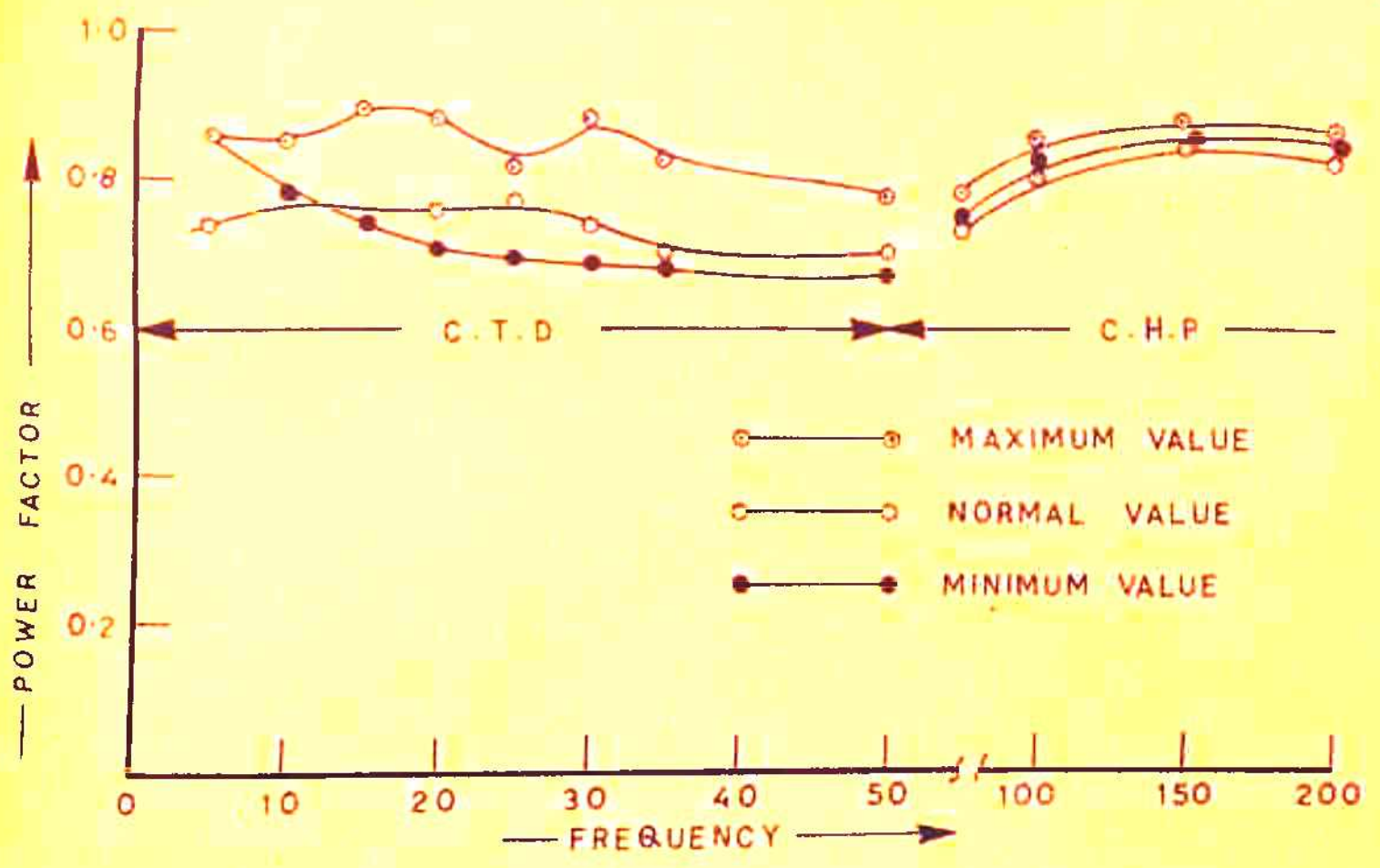FIG.3·5 EFFECT OF STATOR RESISTANCE ON EFFICIENCY.

FIG. 3·6 EFFECT OF STATOR RESISTANCE ON POWER FACTOR.
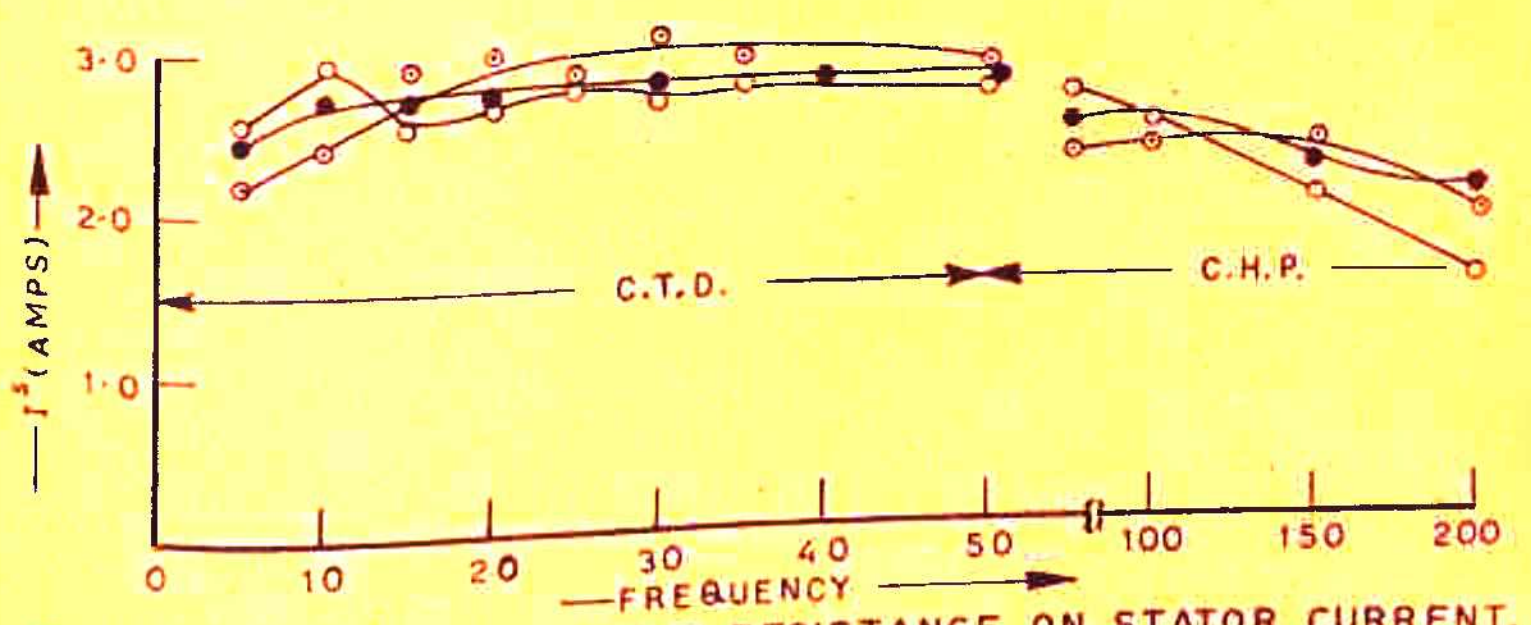

FIG. 3·7 EFFECT OF STATOR RESISTANCE ON STATOR CURRENT.

FIG. 3·8   EFFECT OF ROTOR RESISTANCE ON PULASTING TORQUE.
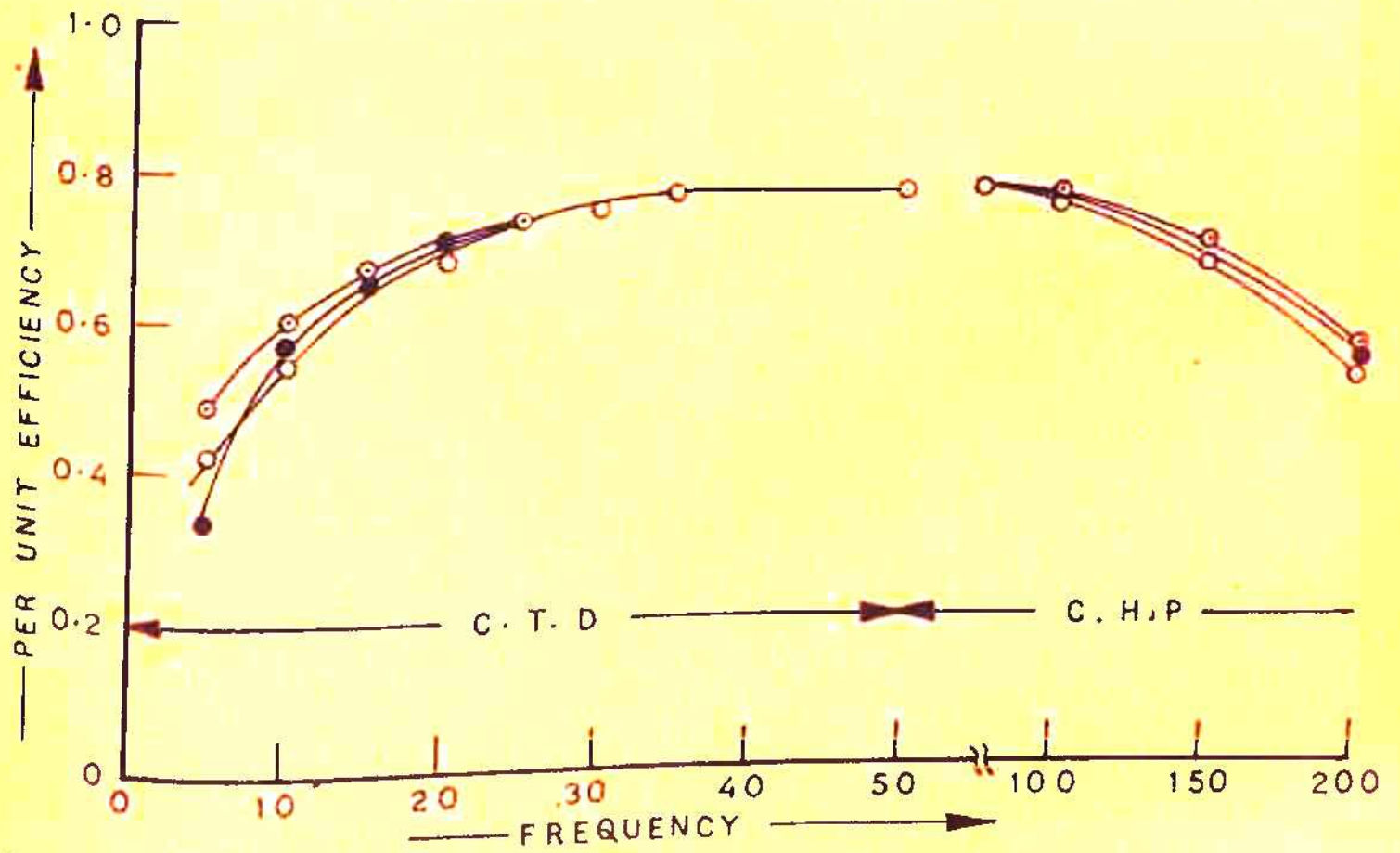
FIG. 3·9   EFFECT OF ROTOR RESISTANCE ON EFFICIENCY.
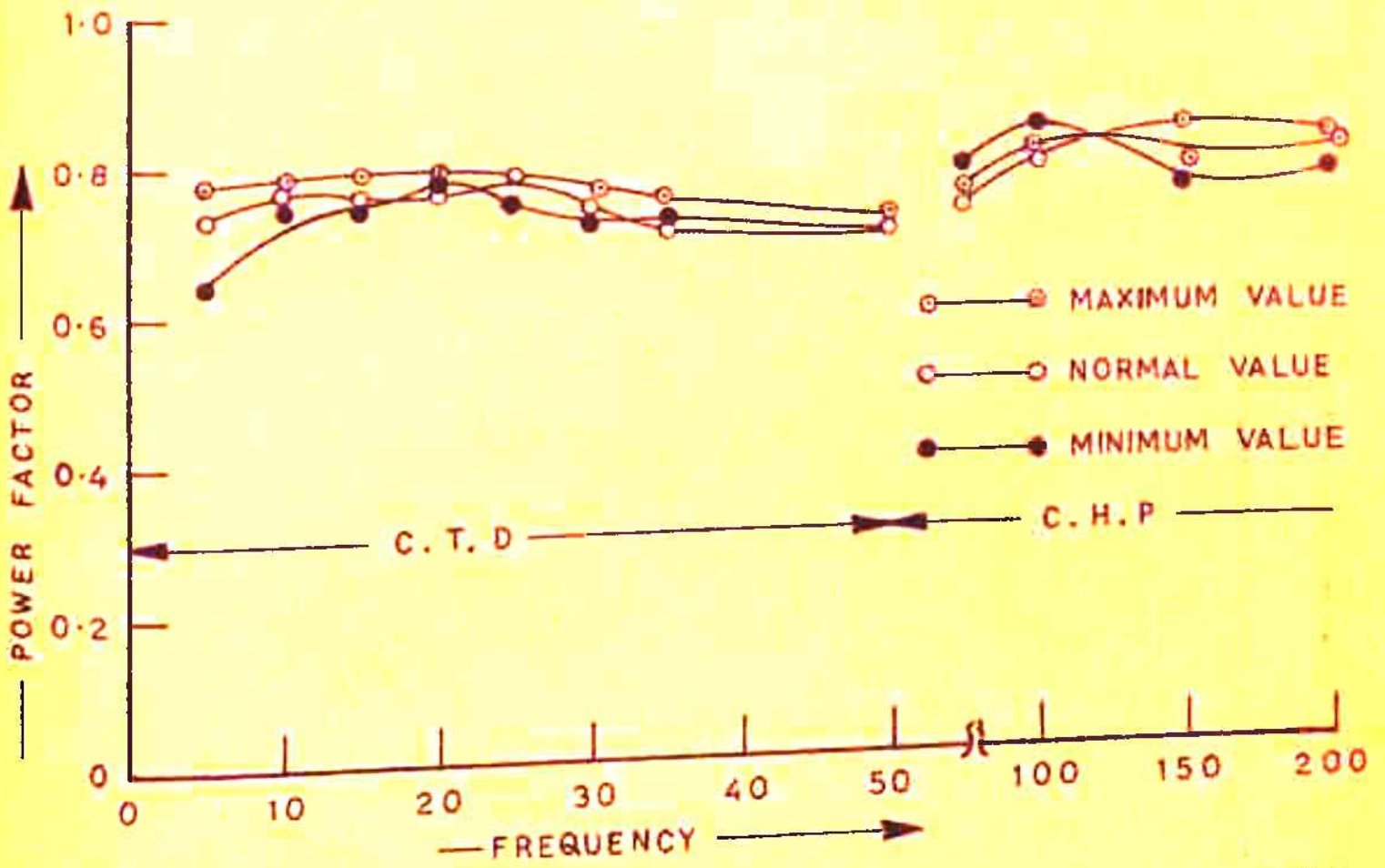
FIG. 3·10 EFFECT OF ROTOR RESISTANCE ON POWER FACTOR.
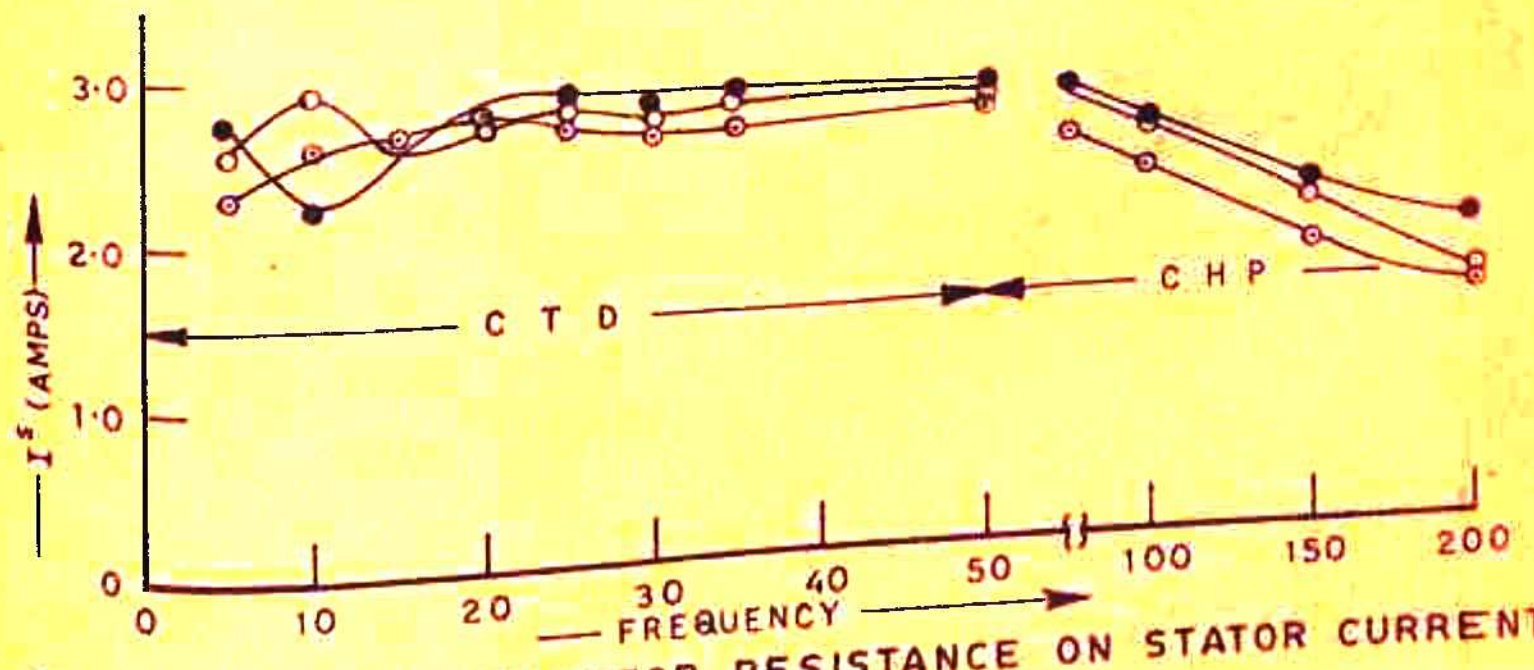
FIG. 3·11 EFFECT OF ROTOR RESISTANCE ON STATOR CURRENT.
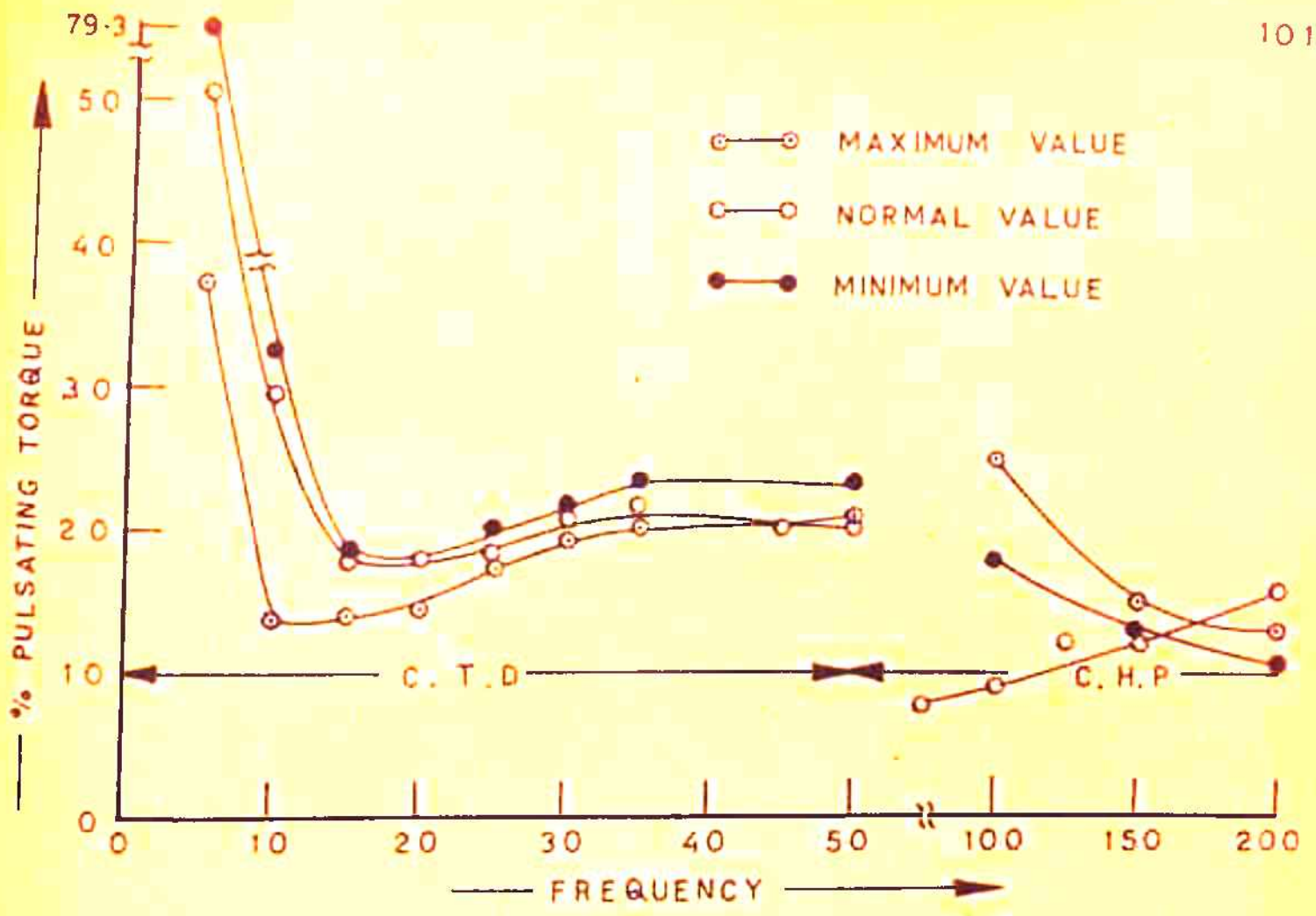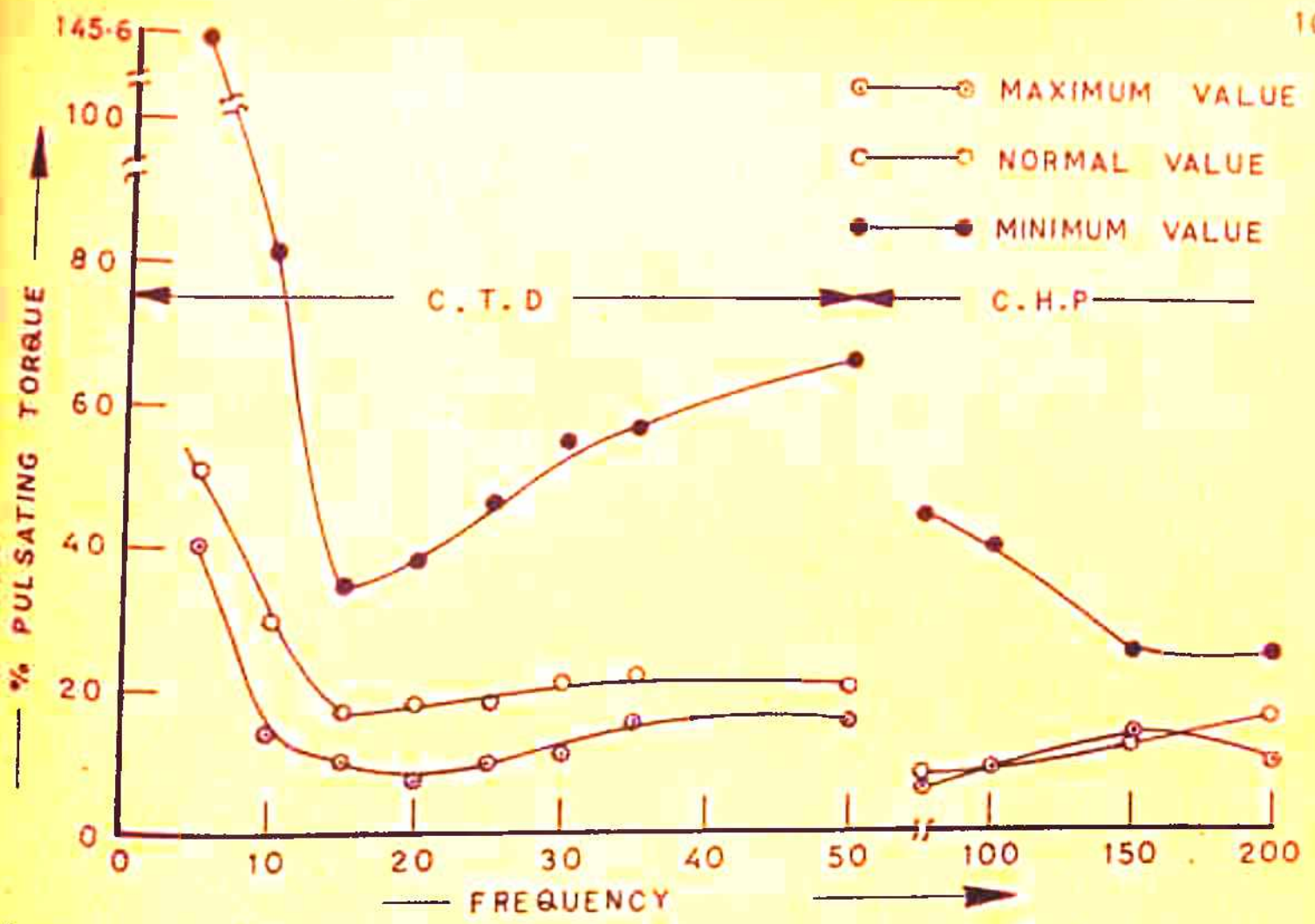
FIG. 3·12 EFFECT OF LEAKAGE INDUCTANCE ON PULSATING TORQUE.
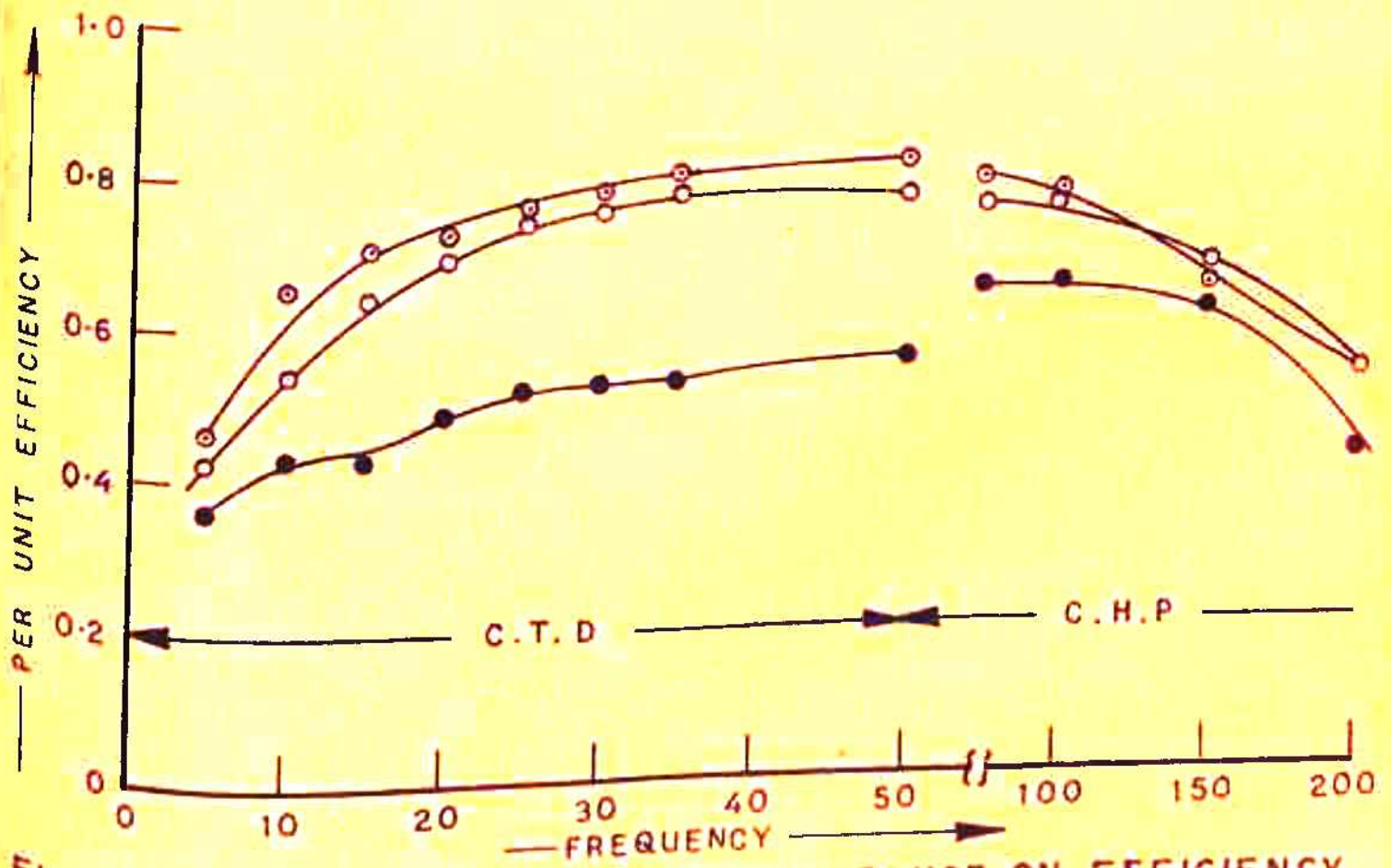
FIG. 3·13 EFFECT OF LEAKAGE INDUCTANCE ON EFFICIENCY.
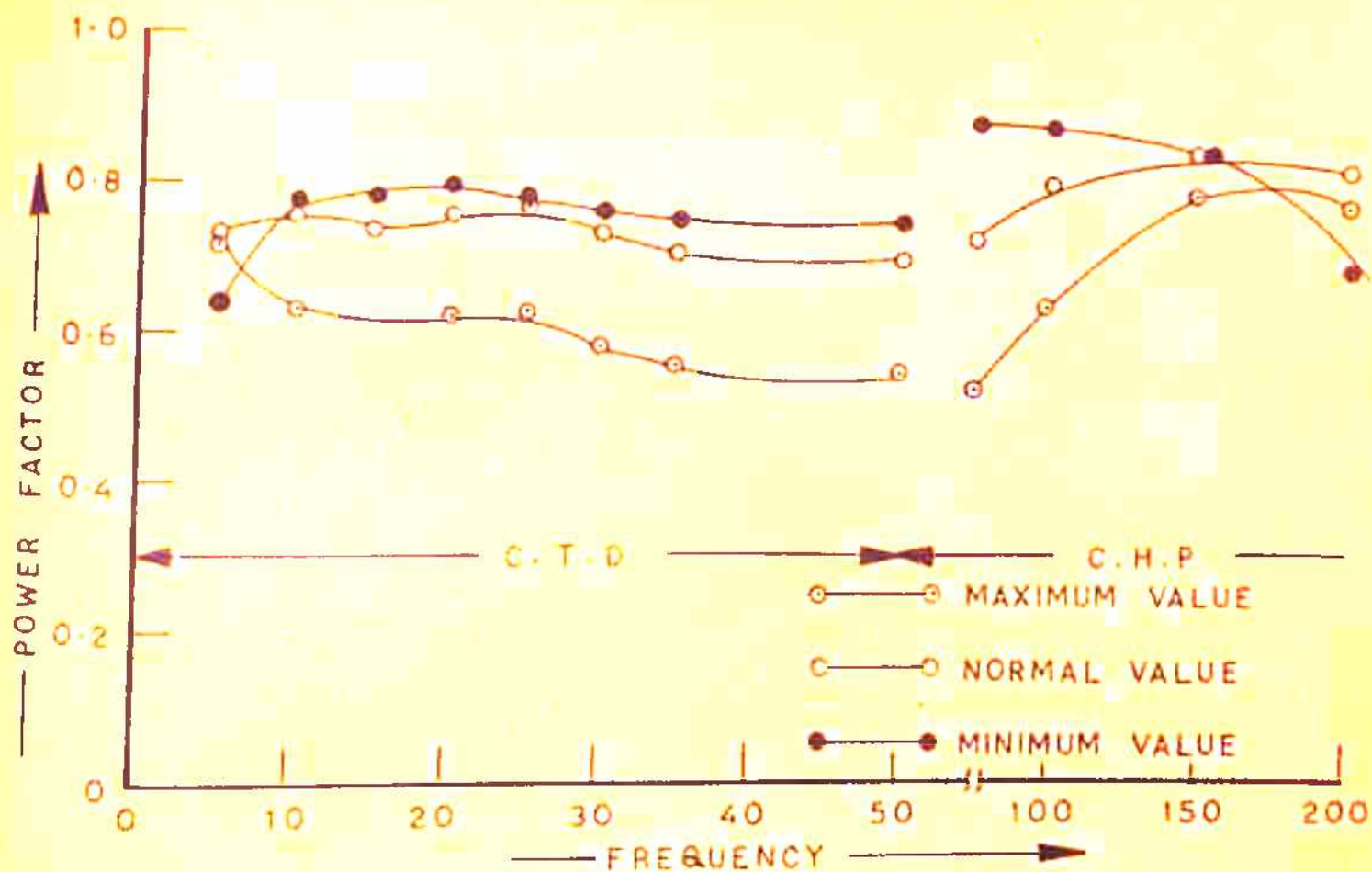
FIG. 3·14 EFFECT OF LEAKAGE INDUCTANCE ON P. F.
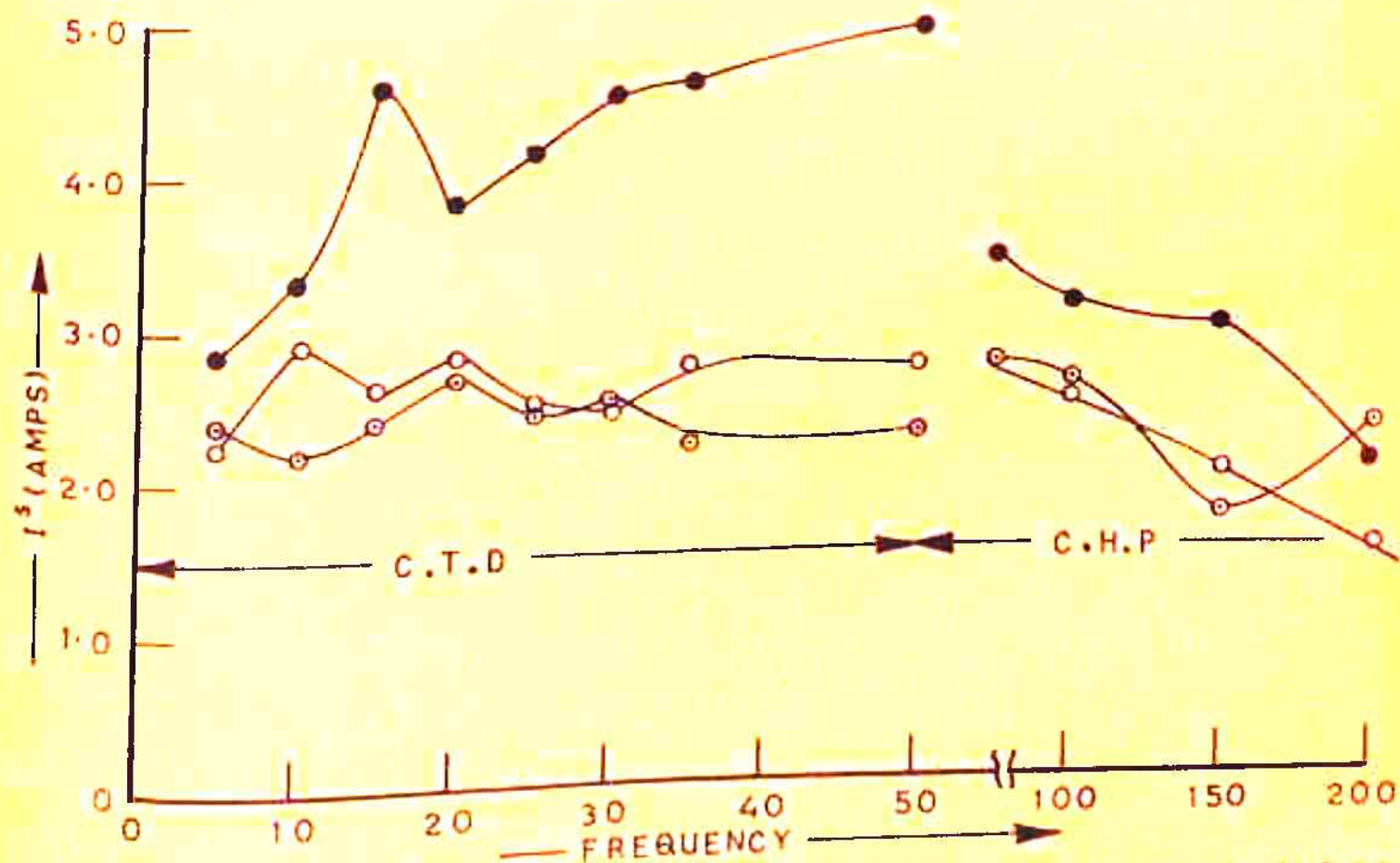
FIG. 3·15 EFFECT OF LEAKAGE INDUCTANCE ON STATOR CURRENT.
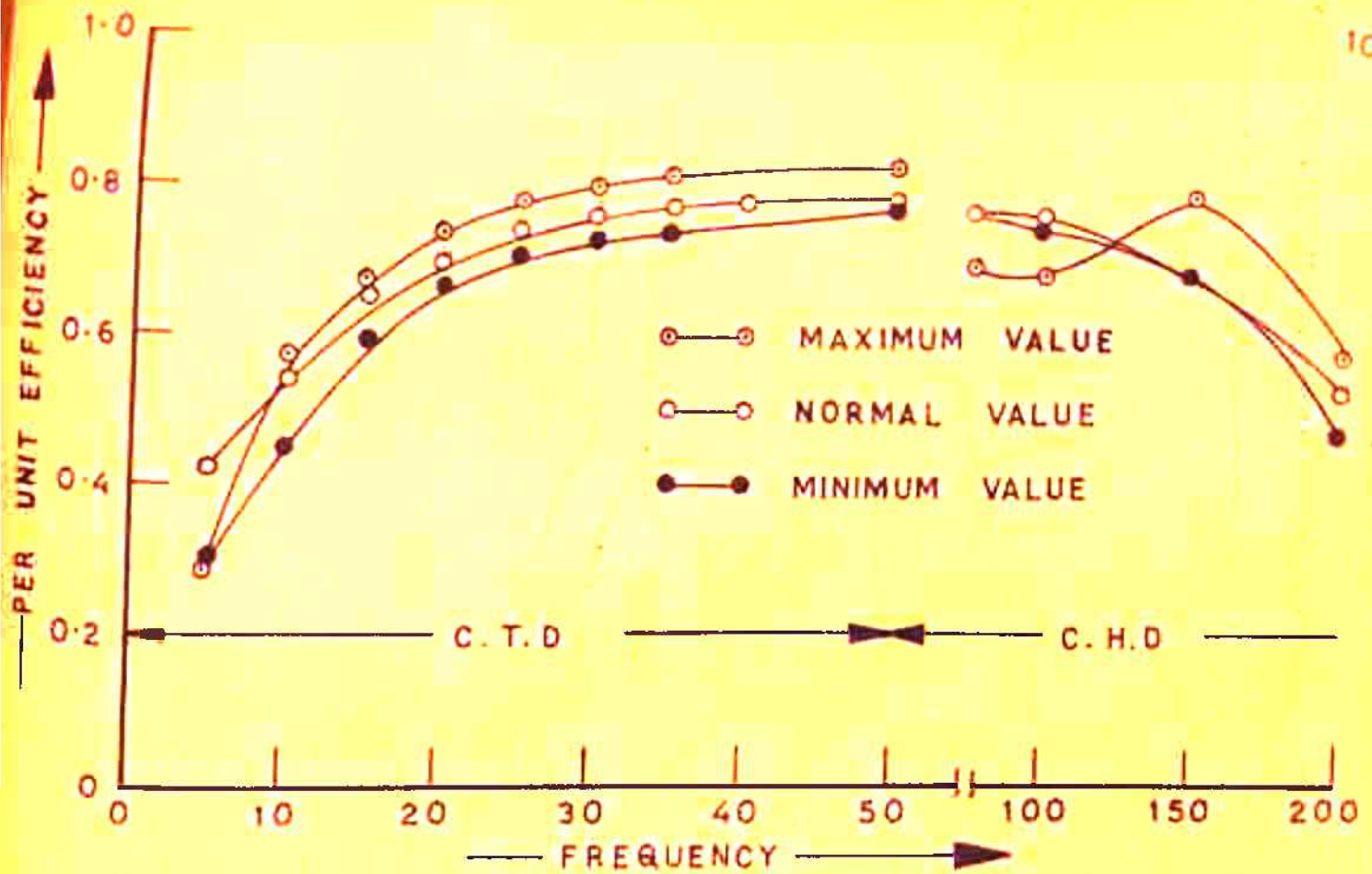
FIG. 3·17 EFFECT OF MAGNETISING INDUTANCE ON EFFICIENCY.
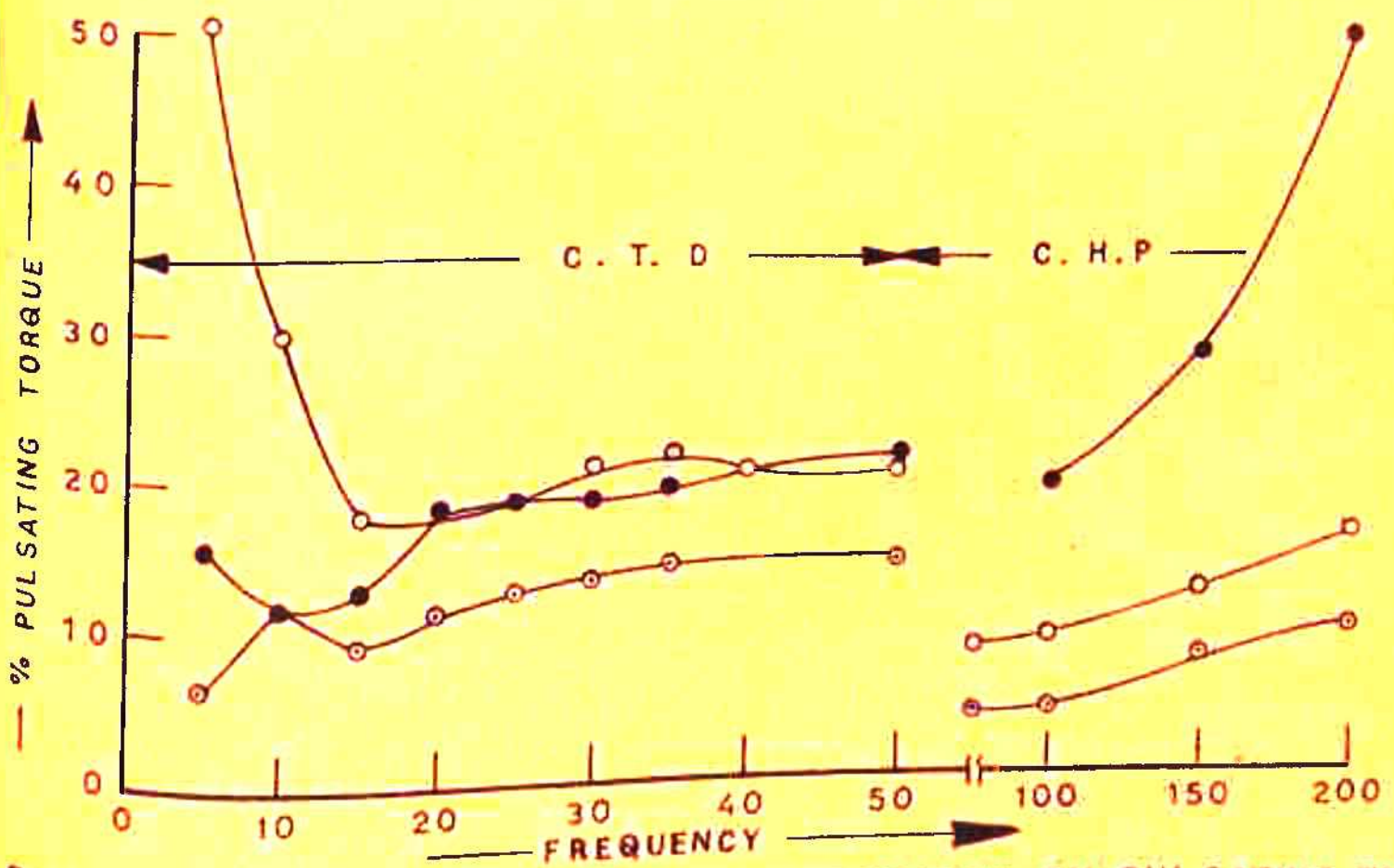
FIG. 3·16 EFFECT OF MAGNETISING INDUTANCE ON PULSATING TORQUE
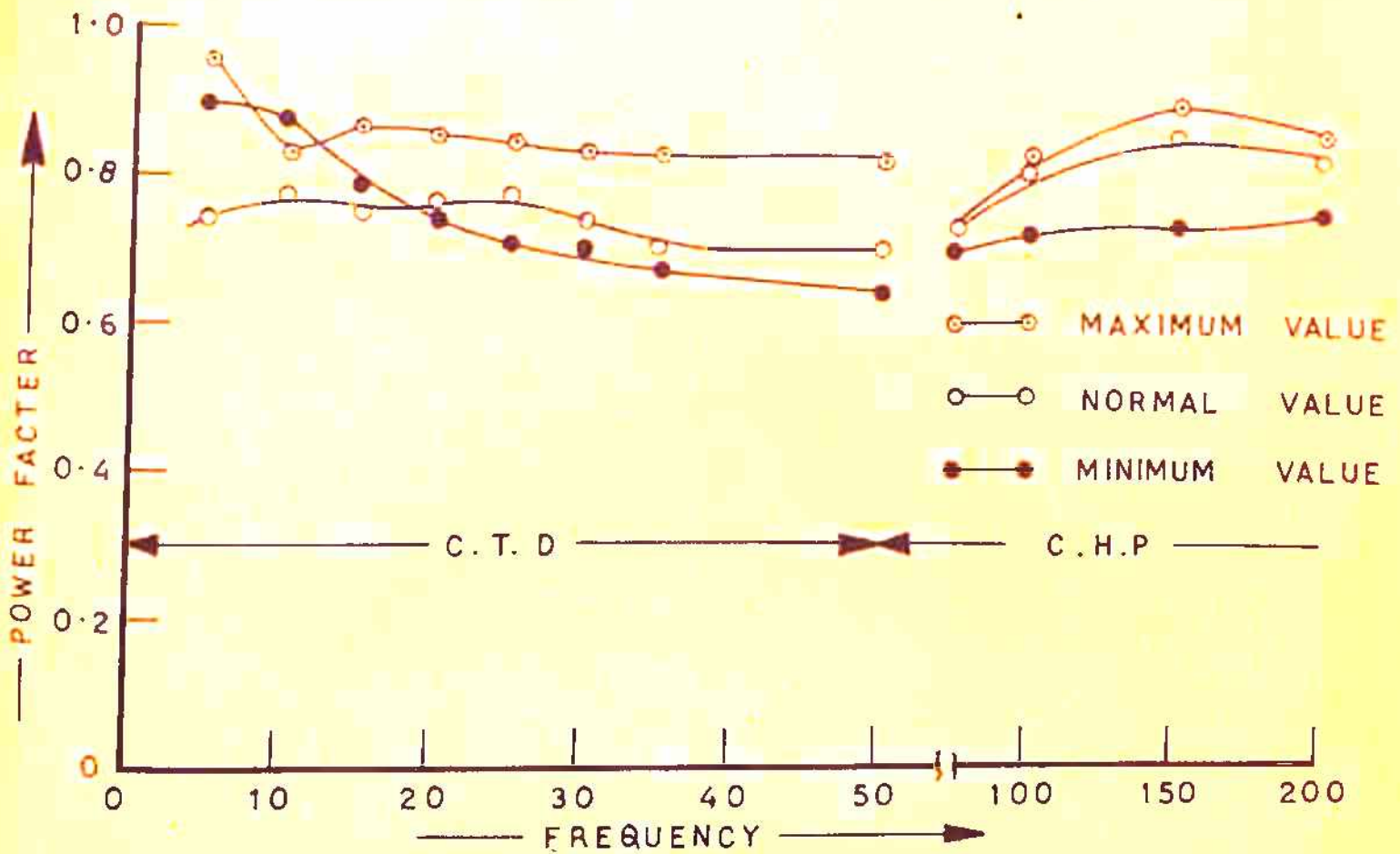
FIG. 3·18   EFFECT OF MAGNETISING REACTANCE ON P. F.
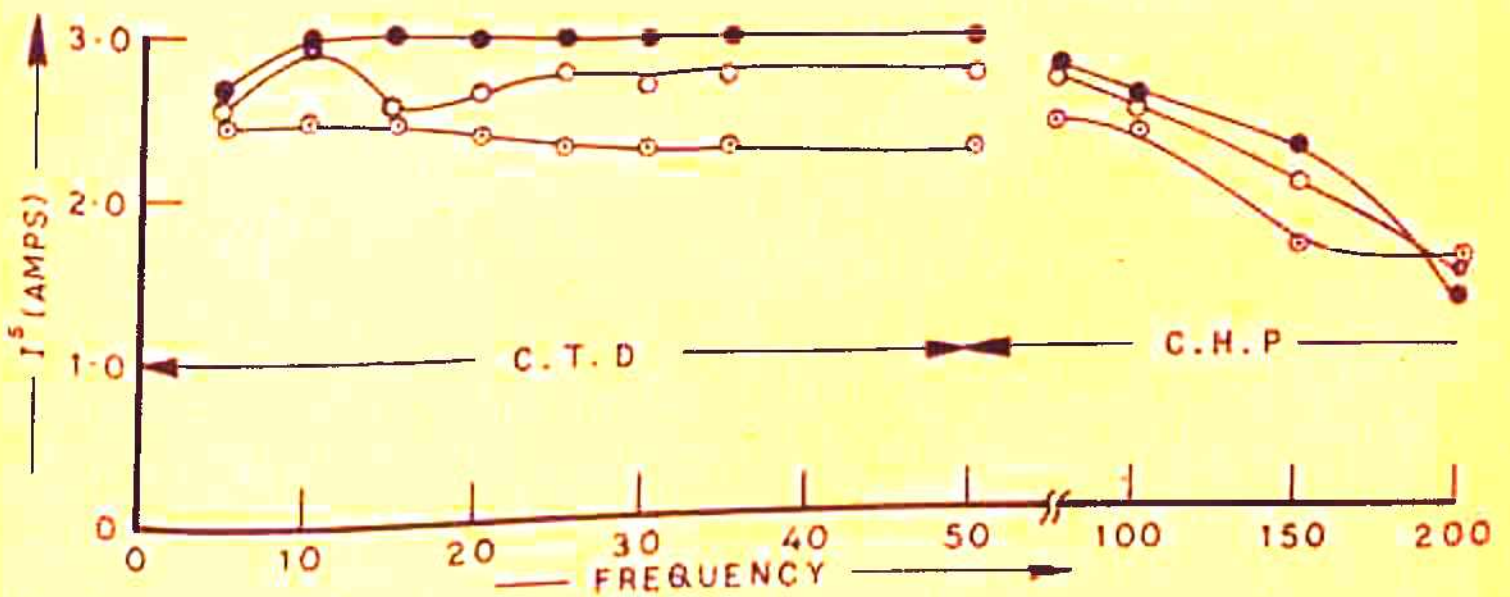
FIG. 3·19   EFFECT OF MAGNETISING REACTANCE ON STATOR
CURRENT.
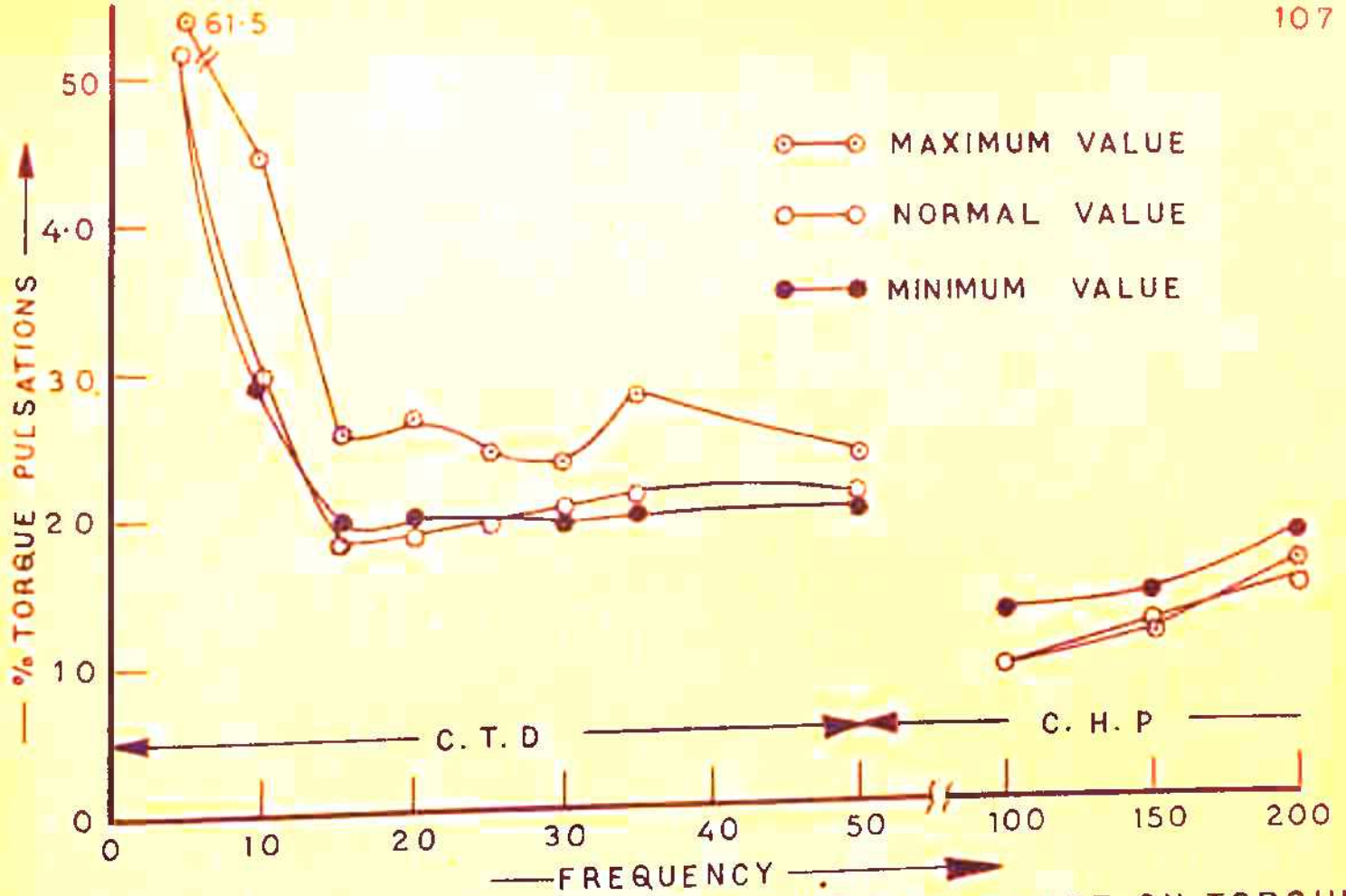
FIG. 3·20 EFFECT OF FILTER CAPACITIVE REACTANCE ON TORQUE PULSATIONS.
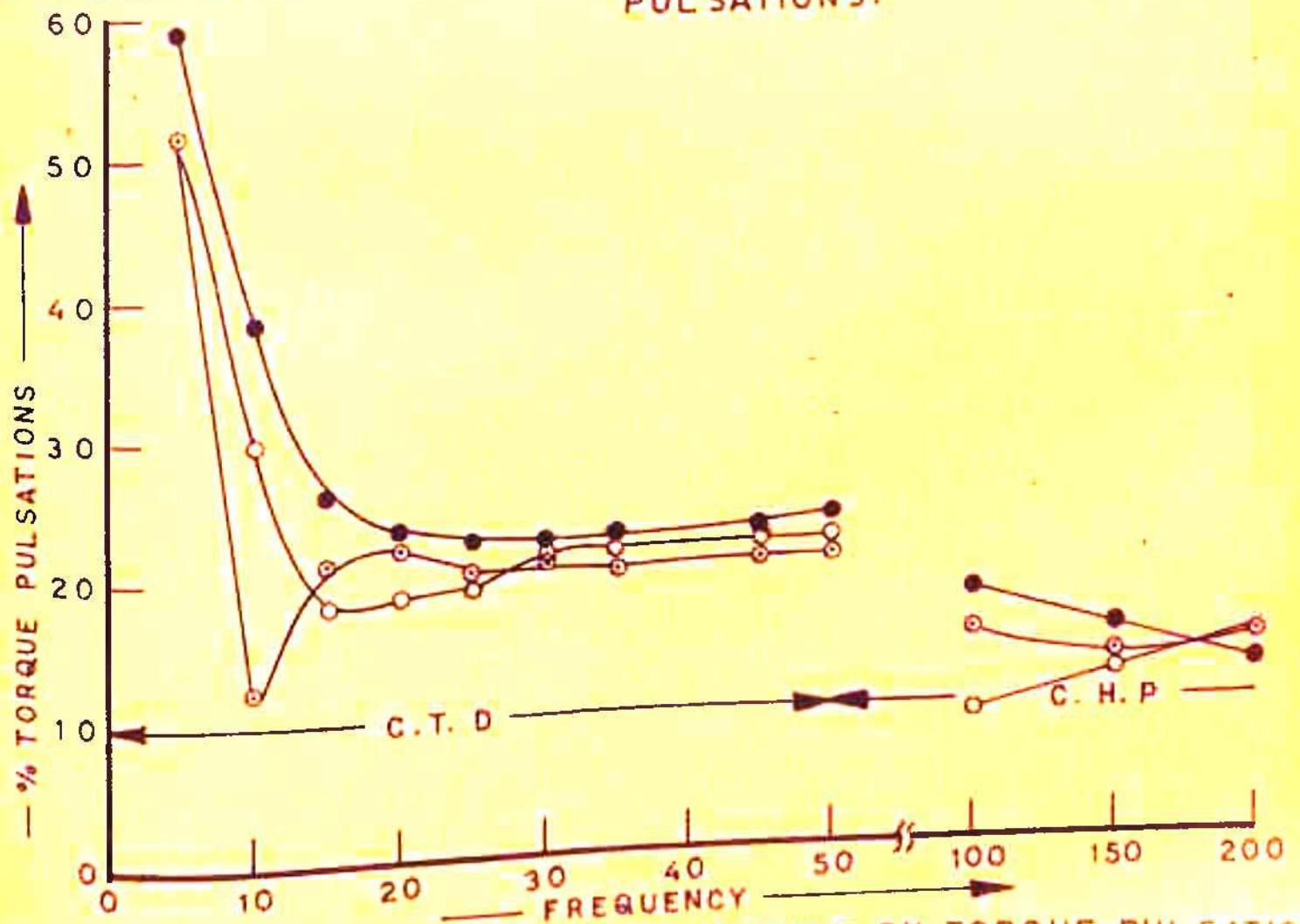
FIG. 3·21 EFFECT OF FILTER INDUCTANCE ON TORQUE PULSATIONS.
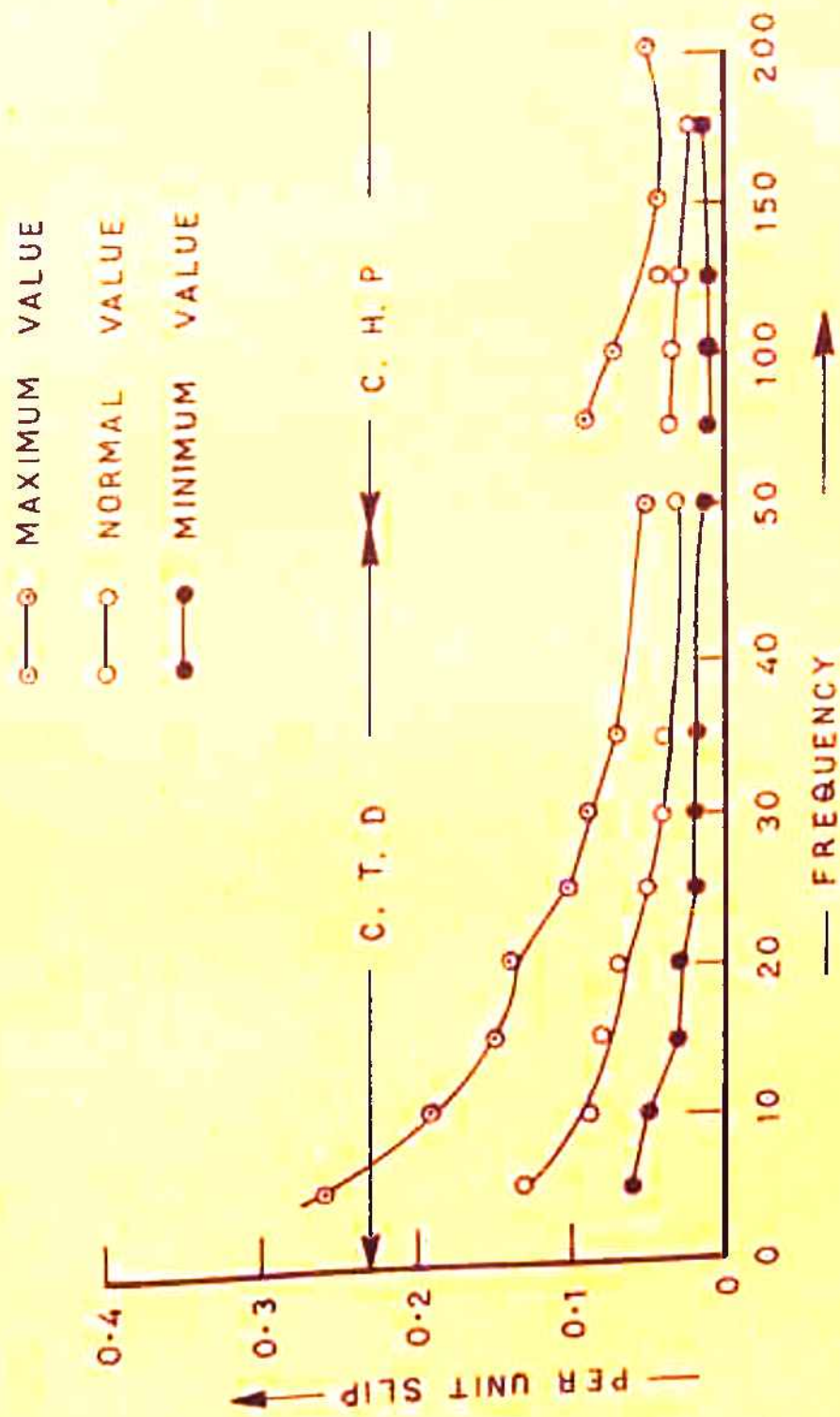
FIG. 3·22 EFFECT OF ROTOR RESISTANCE.

Therefore even in efficiency the increase in rotor resistance is not reflected. Fig. 3.8 seems to establish that harmonic pulsating torque which is produced by the interaction of stator harmonic fields with rotor harmonic fields of different orders does not change appreciably even when the rotor resistance is doubled or halved of its normal value. This happens because the apparent resistance of the rotor given by $\frac{r_2}{s_n}$ is much smaller than the apparent reactance (n times the fundamental rotor reactance). Therefore even a large perturbation of rotor resistance fails to cause a noticeable change in either pulsating torque or other performance indices. However, the power factor gets slightly improved in the frequency range of 5 to 15 Hz (fig. 3.10); where the rotor leakage reactance becomes insignificant. The fact that rotor resistance is quite dominative at low frequencies, is clear from fig. 3.8, where the pulsating torque increases considerably when the rotor resistance is decreased. Interestingly, the efficiency goes down at low frequencies (fig. 3.9), when the rotor resistance is decreased. This happens probably due to large pulsating and very little average torque. Another effect of varying rotor resistance is on slip, both for constant torque and constant horse power drives. The slip increases with high rotor resistance and vice versa (fig. 3.22).

(c)   Effects of Leakage Inductance:

The simultaneous change in stator and rotor leakage inductance are carried out both below and above their normal values. Leakage reactance being directly linked with frequency has a dominant and decisive effects on the performance and developed torque of the induction motor (fig. 3.12 to 3.15). Torque producing capacity of the machine is greatly affected by any change in leakage inductance, but constant torque condition is ensured by applying proper voltage at each operating frequency. A reduction of 10 to 15 percent in pulsating torque is achieved by doubling the leakage inductance (fig.3.12), whereas it increases by 200 percent at normal frequency and by about 300 percent at very low frequency (5 Hz), when the leakage inductance is decreased to 30 percent of its normal value. Since with the increased rotor leakage inductance the impedance seen by the harmonic rotor emf is very high, therefore only weak harmonic fields are established which ultimately lead to the considerable reduction in torque pulsations.

The power factor and efficiency both improve marginally with high leakage inductance, and deteriorates substantially with low inductance (fig. 3.13 and 3.14); all contrary to the expectation. This peculiar phenomenon can be explained as follows:

The fundamental and the harmonic currents constitute the total input current given as -

$$\bar{I} = \bar{I}_f + \sum_n \bar{I}_n \qquad\qquad (3.8)$$

The harmonic current $\bar{I}_n$ in the machine with low inductance form a nonnegligible part of the total current I, since these currents see relatively a low rotor harmonic impedances. Fig. 3.15 clearly establish this fact, where the current at 50 Hz with low inductance is 80 percent more than that with high inductance. These abnormally high values of harmonic currents cause not only the poor power factor but considerable additional losses also, bringing down the efficiency (fig.3.13). High leakage inductance is thus a big benefactor for inverter fed induction machine which curbs pulsating torque and improves the performance characteristics though marginally.

(d)   Effects of Magnetising Inductance:

Magnetising and leakage inductances are linked as given by equation (3.7). It is a very releastic relation from designer's point of view, since the magnetising and leakage fluxes cannot be thought of existing independent of each others. Thus, with the high magnetising inductance, the leakage is also high and vice versa. Therefore, it can be concluded, that the effects of leakage inductance as discussed in earlier subsection are valid here too. Figs. 3.16 to 3.19 deal with these effects, and fully confirm the results of section 3.4(o).

(e)   Effects of Filter Parameters:

When the filter capacitor is decreased to $\frac{1}{5}$th of its normal value there is a considerable increase (fig. 3.20) in torque pulsations at all the frequencies, giving a maximum increase at lowest frequency. But surprisingly a ten fold increase in the filter capacitor does not bring in any substantial change in the pulsating torques (fig. 3.20) at any frequency. These results seem to indicate that pulsating torque is almost saturated with respect to the higher capacitance values and unsaturated with respect to the lower values. This result fully conforms with the earlier results of Lipo[49,50]; where he shows the variation of torque with filter capacitor.

It is observed from fig. 3.21 that the pulsating torque is only marginally affected even by large change in the filter inductive reactance. Torque pulsations with very large filter inductance are observed to be about 1 percent less than those with normal parameters. The other performance characteristics are also not affected substantially both by filter inductive and capacitive reactances.

3.6   RESUME:

A systematic study of the effects of machine and filter parameters on steady state torque pulsations and other performance characteristics like power factor, current, slip and various components of losses; is carried out using the near exact model of Chapter 1. The motor is considered a constant

torque drive upto the normal frequency and a constant horse
power drive for frequencies greater than normal. Computed
results in convenient graphical forms are presented, for
thirteen sets of system parameters. Computations have been
done at discrete frequency steps, selecting a smaller step
for lower range and a bigger step for higher range (more
than normal).

The results establish that the leakage inductance plays
a dominant role in torque pulsations and other performance
characteristics. It is shown by decreasing the leakage induc-
tance, the torque pulsations shoots up by as much as 300 percent
specially at low frequencies. A similar effect of magnetising
inductance is also noticed. The high values of stator resis-
tance also dampens the torque pulsations but at the cost of
efficiency. The rotor resistance seems to be ineffective over
torque pulsations. The penality on efficiency and power factor
due to high leakage and magnetising inductances is of varying
degree, marginal at normal frequency and quite substantial at
low frequencies. The large filter capacitive reactance gives
large torque pulsations, but the filter inductance does not
affect either way. The computed results, clearly establish
the direction in which the machine and filter parameters be
adjusted to reduce torque pulsations without appreciably
affecting the other performance characteristics.

- o -

CHAPTER 4

OPTIMISATION OF PULSATING TORQUE:

The results of Chapter 3 and those reported in the literature[49,50,73,73] amply establish the fact that a normal induction motor is not fit for inverter fed operation, particularly with large frequency variation. It has been shown in Chapter 3 that induction motor with even normal machine parameters at normal frequency develop pulsating torque of quite high magnitude of the order of 20 to 25 percent of its full load torque. This figure is still higher for low frequency operation and aggravate further with low leakage reactance values giving as high as 50 percent pulsating torques. These torques pose a serious problem since eventually any large torque pulsation will lead to high speed pulsations under steady state condition.

Computed torque pulsations obtained for large number of sets of system parameters confirm that the design considerations for an induction motor meant for variable frequency operation have to be different than those for fixed frequency operation.

It is endeavoured here to develop a suitable optimisation technique to minimise the pulsating torque. The objective function (peak pulsating torque) is developed in the rotating multireference frames to get simpler relation as function of dependent phase current variables. Algorithm suitable for digital computation is discussed. Optimisation is carried out

with realistic design constraints and with relaxed constraints on machine parameters. Torque minimisation is carried out for the following two conditions.

(i)   Linking leakage reactance with magnetising reactance.

(ii)   Delinking leakage from magnetising reactance .

Optimal machine parameters are arrived at and complete performance indices of the machine with optimal machine parameters are reported using the near exact model of Chapter 1; and the results compared with machine's performance with normal parameters. Suitable design recommendations have been formulated to translate the optimal set of machine parameters into practice.

4.1   FORMULATION OF THE PROBLEM:

(a)   Statement of the Problem:

Pulsating torque is a very complex and nonlinear function of machine and filter parameters, operating frequency, load, and quality and magnitude of inverter input voltage. It means any technique used for optimisation will yield many optimal sets of machine parameters each valid for the given load and operating frequency. Then to recommend a single set of optimal machine parameters out of many will be an impossible task. This is overcome by optimising the pulsating torque at FULL LOAD ONLY, and adopting the optimal set so obtained. Admittedly the torque pulsations need not be minimum at all loads like at full load, but certainly these will reduce at all loads,

the only difference being the amount of reduction may be
different for different loads, the maximum reduction being at
full load. This assumption is quite fair and valid, as any
drive is expected to run at its full load for its maximum
time of operation.

The torque pulsations are also frequency dependent and
particularly at low frequencies they are quite severe. It is
clear from the results of Chapter 3, that with constant load
torque the frequency at which the maximum torque pulsations
occur is decided by the machine parameters. It is proposed
here to carry out a simultaneous search for maximum pulsating
torque with respect to the frequency along with a search for
the minimum pulsating torque with respect to the machine
parameters. Thus it becomes a MIN-MAX search. It is envisaged
that optimal set of machine parameters obtained through min-max
search will yield minimum pulsating torque at full load at any
operating frequency and considerably reduced pulsations at
other loads. The minimisation of the pulsating torque is done
with respect to the following independent variables:

(i)   Stator resistance

(ii)   Rotor resistance

(iii)   Leakage inductance assumed to be equal for stator and
        rotor and both are varied simultaneously by same amount.

(iv)   Magnetising inductance.

(b)   Multireference Frames:

Most of the optimisation techniques[4] essentially demand that the objective function be expressed as an explicit function of its independent variables. As stated earlier, the objective function under consideration is a highly complex function of its machine parameters and it is a next to impossible task even with simplest model of the machine, to develop an expression exclusively in terms of machine parameters due to multi nonlinear second order differential machine terminal equations. Using a simple and approximate mathematical model of Krause[37] it is possible to develop an expression for pulsating torque as function of phase currents the dependent variables. Even with this mathematical model, to get an explicit objective function is not possible due to the periodic nature of pulsations. Its peak occurence in terms of phase and magnitude is very much governed by machine parameters the independent variables, which are non-expressible due to trignometric product terms. Due to the very severe constraints of the highly complex, real life physical system as out lined above, one is left with no other choice but to adapt an implicit type of objective function. This can best be obtained through multireference frames[37].

The major advantage in multireference frames rotating at synchronous speed of the fundamental or of higher harmonics is that the voltage and current variables including mmfs

reduce to d.c. values and machine terminal equations are simple algebric in nature which can readily be solved. The method of multireference frames transformation assumes the excitation voltages and currents composed of fundamental and other harmonics thus allowing superposition. The fundamental variables are transformed to synchronously rotating reference frame and harmonic variables to the corresponding frames rotating at harmonic synchronous speeds. These reference frames follow the direction of their respective fields. From fig. 4.1, the Park's transformation[37] for the kth harmonic can be written as:

Stator

$$
[C_P^s]_k = \sqrt{\frac{2}{3}}
\begin{array}{c}
 \\
q^s \\
d^s \\
0
\end{array}
\begin{array}{ccc}
r^s & y^s & b^s \\
\left[\begin{array}{ccc}
\cos\delta & \cos(\delta - \frac{2\pi}{3}) & \cos(\delta + \frac{2\pi}{3}) \\
\sin\delta & \sin(\delta - \frac{2\pi}{3}) & \sin(\delta + \frac{2\pi}{3}) \\
\frac{1}{2} & \frac{1}{2} & \frac{1}{2}
\end{array}\right]
\end{array}
\qquad (4.1)
$$

Rotor

$$
[C_P^r]_k = \sqrt{\frac{2}{3}}
\begin{array}{c}
 \\
q^r \\
d^r \\
0
\end{array}
\begin{array}{ccc}
r^r & y^r & b^r \\
\left[\begin{array}{ccc}
\cos\beta & \cos(\beta - \frac{2\pi}{3}) & \cos(\beta + \frac{2\pi}{3}) \\
\sin\beta & \sin(\beta - \frac{2\pi}{3}) & \sin(\beta + \frac{2\pi}{3}) \\
\frac{1}{2} & \frac{1}{2} & \frac{1}{2}
\end{array}\right]
\end{array}
\qquad (4.2)
$$

FIG. 4·1 PARK'S TRANSFORMATION.

where

$$\beta = \delta - \theta$$

$$\delta = kw_0 t$$

$$\theta = kw_r t$$

(4.3)

k   order of harmonics (k = 1, -5, 7,-11,13)

The combined transformation matrix for stator and rotor is:

$$\left[C_P^{sr}\right]_k = \begin{bmatrix} \left[C_P^{s}\right]_k & \\ & \left[C_P^{r}\right]_k \end{bmatrix}$$

(4.4)

The machine terminal voltage is assumed to be of fixed nature having stepped waveform (fig. 3.2) and independent of load current. Resolving the voltage of fig. 3.2 in to its fourier components[66] we get,

$$v_r^s = \frac{2E_d}{\pi} \left(\sin w_0 t + \frac{1}{5} \sin 5w_0 t + \frac{1}{7} \sin 7w_0 t + \right.$$

$$\left. \frac{1}{11} \sin 11w_0 t + \frac{1}{13} \sin 13w_0 t + \dots \right)$$

(4.5a)

$$v_y^s = \frac{2E_d}{\pi} \left(\sin(w_0 t - \frac{2\pi}{3}) + \frac{1}{5} \sin(5w_0 t + \frac{2\pi}{3}) + \right.$$

$$\frac{1}{7} \sin(7w_0 t - \frac{2\pi}{3}) + \frac{1}{11} \sin(11w_0 t + \frac{2\pi}{3}) +$$

$$\left. \frac{1}{13} \sin(13w_0 t - \frac{2\pi}{3}) + \dots \right)$$

(4.5b)

$$v_b^s = \frac{2E_d}{\pi} \left(\sin(w_0 t + \frac{2\pi}{3}) + \frac{1}{5} \sin(5w_0 t - \frac{2\pi}{3}) + \right.$$

$$\frac{1}{7} \sin(7w_0 t + \frac{2\pi}{3}) + \frac{1}{11} \sin(11w_0 t - \frac{2\pi}{3}) +$$

$$\left. \frac{1}{13} \sin(13w_0 t + \frac{2\pi}{3}) + \dots \right)$$

(4.5c)

The voltage in the kth harmonic reference frame can be written as:[37]

$$
\begin{bmatrix} v_{qk}^s \\ v_{dk}^s \\ v_{ok}^s \end{bmatrix}^k = \begin{bmatrix} C_P^s \end{bmatrix}_k \begin{bmatrix} v_{rk}^s \\ v_{yk}^s \\ v_{bk}^s \end{bmatrix}
\tag{4.6}
$$

$$
v_{qk}^s = 0
$$

$$
v_{dk}^s = \frac{1}{k}\sqrt{\frac{3}{2}}\, V_{mk}
$$

where V_{mk} is amplitude of kth harmonic phase voltage.

Similarly, the phase impedance $\left[Z_{ryb,ryb}^{\,s\quad r} \right]$ (appendix IA) can be transformed to get new impedance matrix $\left[Z_{qdo,qdo}^{\,s\quad r} \right]_k$

in the kth reference frame using the following relation,

$$
\left[Z_{qdo,qdo}^{\,s\quad r} \right]_k = \left[C_P^{sr} \right]_k \left[Z_{ryb,ryb}^{\,s\quad r} \right] \left[C_P^{sr} \right]_T
\tag{4.7}
$$

expanding, simplifying and ommitting the zero sequence terms in the above relation we get -

$$
[Z_{qd,qd}^{s\ r}]_k =
\begin{array}{c c}
 & \begin{array}{cccc} q^s \quad\quad & d^s \quad\quad & q^r \quad\quad & d^r \end{array} \\
\begin{array}{c} q^s \\ d^s \\ q^r \\ d^r \end{array} &
\left[
\begin{array}{cccc}
R_1+L_1p & kw_oL_1 & Mp & kw_oM \\
-kw_oL_1 & R_1+L_1p & -kw_oM & Mp \\
Mp & (kw_o-w_r)M & R_2+L_2p & (kw_o-w_r)L_2 \\
-(kw_o-w_r)M & Mp & -(kw_o-w_r)L_2 & R_2+L_2p
\end{array}
\right]
\end{array}
\tag{4.8}
$$

where $M = \frac{3}{2}\tilde{M}$

(c) Objective Function:

Formulation of the implicit form of the objective function in terms of machine's phase currents is carried out as follows. Firstly, the harmonic and fundamental currents are determined in their respective rotating reference frames and then the currents so obtained are transformed to a common stationary reference frame. The expression for pulsating torque can then be written in terms of stationary frame currents. Since the variables both the fundamental and harmonics in their respective multireference frames are reduced to d.c. values under steady state operation, all operational terms in the impedance matrix $\left[Z_{qd,qd}^{s\ r}\right]_k$ can therefore be ignored, thus giving the following set of algebric equations[37] (all variables in per unit system),

$$
\begin{bmatrix} v_{qk}^s \\ v_{dk}^s \\ 0 \\ 0 \end{bmatrix}^k = \begin{bmatrix} R_1 & kwX_1 & 0 & kw\bar{X}_M \\ -kwX_1 & R_1 & -kw\bar{X}_M & 0 \\ 0 & (kw-w_R)\bar{X}_M & R_2 & (kw-w_R)X_2 \\ -(kw-w_R)\bar{X}_M & 0 & -(kw-w_R)X_2 & R_2 \end{bmatrix} \begin{bmatrix} i_{qk}^s \\ i_{dk}^s \\ i_{qk}^r \\ i_{dk}^r \end{bmatrix}^k
$$

(4.9)

where $\bar{X}_M = \dfrac{3}{2} X_M$

Solving for currents we get –

$$
i_{qk}^s = \left(\frac{A^k}{E^k}\right) v_{qk}^s + \left(\frac{B^k}{E^k}\right) v_{dk}^s
$$

(4.10)

$$
i_{dk}^s = -\left(\frac{B^k}{E^k}\right) v_{qk}^s + \left(\frac{A^k}{E^k}\right) v_{dk}^s
$$

(4.11)

$$
i_{qk}^r = \left(\frac{C^k}{E^k}\right) v_{qk}^s + \left(\frac{D^k}{E^k}\right) v_{dk}^s
$$

(4.12)

$$
i_{dk}^r = -\left(\frac{D^k}{E^k}\right) v_{qk}^s + \left(\frac{C^k}{E^k}\right) v_{dk}^s
$$

(4.13)

where

$$
A^k = R_1 \left[R_2^2 + (k-1+s)^2 w^2 X_2^2 \right] + k(k-1+s)R_2 w^2 \bar{X}_M^2
$$

(4.14a)

$$
B^k = k(k-1+s)^2 w^3 X_2 (\bar{X}_M^2 - X_1 X_2) - kR_2^2 wX_1
$$

(4.14b)

$$
C^k = -(k-1+s)w^2 \bar{X}_M \left[kR_2 X_1 + (k-1+s)R_1 X_2 \right]
$$

(4.14c)

$$
D^k = -(k-1+s)w\bar{X}_M \left[R_1 R_2 + k(k-1+s)w^2 (\bar{X}_M^2 - X_1 X_2) \right]
$$

(4.14d)

$$E^k = \left[R_1 R_2 + k(k-1+s)w^2 (X_m^2 - X_1 X_2) \right]^2$$

$$+ \left[kR_2 wX_1 + (k-1+s)R_1 wX_2 \right]^2 \tag{4.14e}$$

The current variables in rotating multireference frames dq are transformed to stationary reference[37] $\alpha\beta$ frame (fig.4.2) giving:

$$i_\alpha^s = \sum_{n=1,7,13} (i_{qn}^s \cos nw_o t + i_{dn}^s \sin nw_o t)$$

$$+ \sum_{n=5,11} (i_{qn}^s \cos nw_o t - i_{dn}^s \sin nw_o t) \tag{4.15a}$$

$$i_\beta^s = \sum_{n=1,7,13} (i_{dn}^s \cos nw_o t - i_{qn}^s \sin nw_o t)$$

$$+ \sum_{n=5,11} (i_{dn}^s \cos nw_o t + i_{qn}^s \sin nw_o t) \tag{4.15b}$$

$$i_\alpha^r = \sum_{n=1,7,13} (i_{qn}^r \cos nw_o t + i_{dn}^r \sin nw_o t)$$

$$+ \sum_{n=5,11} (i_{qn}^r \cos nw_o t - i_{dn}^r \sin nw_o t) \tag{4.16a}$$

$$i_\beta^r = \sum_{n=1,7,13} (i_{dn}^r \cos nw_o t - i_{qn}^r \sin nw_o t)$$

$$+ \sum_{n=5,11} (i_{dn}^r \cos nw_o t + i_{qn}^r \sin nw_o t) \tag{4.16b}$$

FIG. 4·2 TRANSFORMATION FROM ROTATING MULTI REFERENCE FRAMES TO STATIONARY FRAME.

125

And the expression for instantaneous torque T_e in terms of current variables of stationary frame is:

$$T_e = \frac{3}{2} X_M \frac{p}{2} (i_\alpha^s i_\beta^r - i_\alpha^r i_\beta^s) \tag{4.17}$$

From equations (4.15),(4.16) and (4.17) we get -

$$T_{avg} = \frac{3}{2} X_M \frac{p}{2} \left[\sum_j (i_{\beta j}^r i_{\alpha j}^s - i_{\alpha j}^r i_{\beta j}^s) \right] \tag{4.18}$$

$$
\begin{aligned}
T_{e6} = \frac{3}{2} X_M \frac{p}{2} \Big[&\sin 6w_0 t \, (i_{d1}^s i_{d5}^r + i_{q1}^s i_{q5}^r - i_{d1}^s i_{d7}^r \\
&- i_{q1}^s i_{q7}^r - i_{d5}^s i_{d1}^r - i_{q5}^s i_{q1}^r + i_{d5}^s i_{d11}^r + \\
&i_{q5}^s i_{q11}^r + i_{d7}^s i_{d1}^r + i_{q7}^s i_{q1}^r - i_{d5}^r i_{d11}^s \\
&- i_{q11}^s i_{q5}^r - i_{d13}^r i_{d7}^s - i_{q13}^r i_{q7}^s + \\
&i_{d13}^s i_{d7}^r + i_{q13}^s i_{q7}^r) + \cos 6w_0 t \, (i_{q1}^s i_{d5}^r \\
&- i_{d1}^s i_{q5}^r - i_{d1}^s i_{q7}^r + i_{q1}^s i_{d7}^r + i_{q5}^s i_{d1}^r \\
&- i_{d5}^s i_{q1}^r - i_{q11}^r i_{d5}^s + i_{d11}^r i_{q5}^s + i_{q7}^s i_{d1}^r \\
&- i_{d7}^s i_{q1}^r + i_{q11}^s i_{d5}^r - i_{d11}^s i_{q5}^r - i_{q13}^r i_{d7}^s \\
&+ i_{d13}^r i_{q7}^s + i_{q13}^s i_{d7}^r - i_{d13}^s i_{q7}^r) \Big]
\end{aligned} \tag{4.19}
$$

$$T_{e12} = \frac{3}{2} X_M \frac{P}{2} \left[\text{Sin } 12w_o t \; (i^s_{d1} \, i^r_{d11} + i^s_{q1} \, i^r_{q11} - i^r_{d13} \, i^s_{d1} \right.$$

$$- i^r_{q13} \, i^s_{q1} - i^r_{d7} \, i^s_{d5} - i^r_{q7} \, i^s_{q5} + i^r_{d5} \, i^s_{d7} + i^r_{q5} \, i^s_{q7}$$

$$+ i^s_{d11} \, i^r_{d1} - i^s_{q11} \, i^r_{q1} + i^s_{d13} \, i^r_{d1} + i^s_{q13} \, i^r_{q1} \;)$$

$$+ \text{Cos } 12w_o t \; (i^s_{q1} \, i^r_{d11} - i^s_{d1} \, i^r_{q11} - i^r_{q13} \, i^s_{d1}$$

$$+ i^r_{d13} \, i^s_{q1} - i^r_{q7} \, i^s_{d5} + i^r_{d7} \, i^s_{q5} - i^r_{q5} \, i^s_{d7} +$$

$$i^r_{d5} \, i^s_{q7} + i^s_{q11} \, i^r_{d1} - i^s_{d11} \, i^r_{q1} + i^s_{q13} \, i^r_{d1}$$

$$\left. - i^s_{d13} \, i^r_{q1} \;) \right] \tag{4.20}$$

$$T_P = T_{e6} + T_{e12}$$

The OBJECTIVE FUNCTION (OBJECT) is defined as the pulsating torque expressed as percentage of corresponding average torque rather than that of common base torque value. The justification of this definition of the objective function is that it gives better insight to the physical happening inside the machine vis a vis torque pulsations.

$$\text{OBJECT} = \left(\frac{T_{P(peak)}}{T_{avg}} \right) \times 100 \tag{4.21}$$

(d) Constraints On Independent Variables:

The independent variables as listed in section 4.1(a)

just cannot assume any values since very high or very low
values are not physically realisable. Thus the problem of
optimisation of torque is not that of unconstrained nature
but it is with finite upper and lower constraints on the
independent variables. The results given in Chapter 3 for
large number of sets of machine parameters obtained through
a more comprehensive and exact model of the system can serve
as a useful guidance in arriving at a realistic decision
about the upper and lower constraints of the independent variables.
Any decision to fix up these limits must be in fully conformity
with the effects of these parameters on the other performance
indices which are in no way of lesser significance. For
instance, pulsating torques minimisation with a set of machine
parameters leading to poor efficiency and poor power factor
cannot be accepted as a sound and viable proposition.

The upper and lower extremes of the independent variables
are decided on the following two criteria. Firstly, the values
of the concerned parameters should be obtainable keeping in
view usual design practices without involving any major
design modifications. Special materials and extraordinary
processes required if any to achieve the targeted parameters
will certainly push up the cost of the product beyond econo-
mical threshold. Secondly, the three indices of the 'goodness'
of the machine viz, efficiency, power factor and the speed
regulation should be kept in mind and imposition of any
excessive penality on any one of them may ultimately lead to

unacceptability of the drive by the customer, even the motor
may be with considerably reduced torque pulsations. Increasing
of stator resistance or leakage reactance, for instance, will
bring down the efficiency and power factor to an uneconomical
level, yet these high values are desirable to curb torque
pulsations. Keeping in view the above discussion, it may be
concluded that the upper and lower limits on the machine
parameters as evolved in section 3.3(a) and given in table 3.1
can serve as constraints on the variables.

The optimisation of the torque function is also carried out
with relaxed constraints, just to see the further improvement
(if any) in the torque function. These relaxed constraints
have no bearing with their respective physical realisation
and the exercise is just of academic interest. The following
relaxed constraints given in table 4.1 are adapted for
computation.

Table 4.1 Relaxed constraints.

Variable	R_1	R_2	$X_{L1} = X_{L2}$	X_M	w
Lower Constraint	0.0	0.0	0.0	0.0	0.05
Upper Constraint	0.5	0.5	0.5	10.0	1.0

4.2 OPTIMISATION TECHNIQUE:

The objective function (peak pulsating torque) being an implicit function of dependent variables, it is almost impossible to compute derivatives analytically or numerically. The gradient or the conjugate gradient techniques though powerful tools, are ruled out for this case. The other class of optimisation techniques fall under direct search methods. There are many well known techniques falling under sequential direct search methods. The earliest ones are of Dichotomous[88], Fibonacci[88,35] and Golden[63,87] section search techniques. All these methods are applicable for only single variable functions. A heuristic, n-dimensions method, called pattern search[4] based on intuitive exploratory search though simple but uncertain as it may get 'stuck' anywhere. The random search method[15] is effective only for discrete variables. Rosenbrock[40,76] uses a set of n mutually orthogonal directions in each cycle of exploratory moves, the method by Powell[67] searches in n conjugate directions and the method by Swann[91] is somewhere between the preceding two methods in the complexities of each strategies. Powell's method is best for small number of variables ($n \leq 4$) and for quadratic objective function giving a fast rate of convergence. But both Powell's and Swann's methods are applicable to unconstrained variables only.

The direct search method given by Rosenbrock and named as HILL CLIMB METHOD[40] is adopted for the problem under

consideration as MIN-MAX technique. This method though not as powerful as Powell's method but can find the maxima/minima of a multivariable nonlinear function subject to linear/nonlinear inequality constraints. The upper and lower constraints can either be constants or function of the independent variables. The procedure assumes a unimodal function, therefore several sets of starting values for the independent variables are to be used particularly for the pulsating torque function which is of unknown nature. The extensive results obtained from the earlier model (Chapter 1) can form a good guide to decide the best starting point.

The objective function is minimised with respect to four machine parameters, namely stator resistance, rotor resistance, magnetising inductance and leakage inductance; forming the first four variables in the above order, and maximised with respect to operating frequency the fifth variable. First, the search is carried out parallel to the axis of the variables by giving predetermined step size S_i. If the function improves the search is continued in the same direction with increased step size otherwise the direction of search is reversed and step size is halved. The improvement in the function is decided as follows:

(i)   Let F_o be the current best objective function value
        for a point where the constraints are satisfied, and
        $F*$ be the current best objective function value for a

point where the constraints are satisfied and in addition
the boundary zones (Defined below) are not voilated. F_0 and
F* are initially set equal to the objective function value
at the starting point.

(ii) The objective function is termed as 'improved' under
following two conditions.

1.   If function F evaluated with increment in any one of
      the first four variables is less than the current best
      function F_0 and constraints not violated.

2.   If function F evaluated with increment in the fifth
      variable is more than the current best function F_0
      and constraints not violated.

<u>Boundary Zones</u>   If the current point lies within a boundary
zone defined as:

Lower zone $G_K \leq X_K \leq \left[G_K + (H_K - G_K)10^{-4} \right]$

Upper zone $H_K \geq X_K \geq \left[H_K - (H_K - G_K)10^{-4} \right]$

$$(K = 1,2....,N)$$

the objective function is modified as follows:

$$F_{new} = F_{old} - (F_{old} - F*) (3\lambda - 4\lambda^2 + 2\lambda^3)$$

where

$$\lambda = \frac{G_K + (H_K - G_K)10^{-4} - X_K}{(H_K - G_K)10^{-4}}$$

(4.22a)

(Lower zone)

$$\text{(Upper Zone)} \quad \lambda = \frac{X_K - [H_K - (H_K - G_K)10^{-4}]}{(H_K - G_K)10^{-4}} \tag{4.22b}$$

At the inner edge of the boundary zone when $\lambda = 0$ the function is unaltered i.e. $F_{new} = F_{old}$. At the constraints $\lambda = 1$, and $F_{new} = F^*$. Thus the function value is replaced by the best current function value in the feasible region andnot in a boundary zone. For a function which improves as the constraint is approached the modified function has an optimum in the boundary zone.

If an improvement within the meaning of ii(1) and ii(2) are obtained without violating the boundary zones or constraints, then F^* is set equal to F_0.

<u>Axis Rotation</u>   The process is continued till the function fails to improve for all the variables. The axes are then rotated by the following equations. Each rotation of the axes is termed as <u>stage</u>.

$$M_{i,j}^{(k+1)} = \frac{D_{i,j}^{(k)}}{\left[\sum_{l=1}^{N} (D_{i,j}^{(k)})^2\right]^{1/2}} \tag{4.23}$$

where —

$$D_{i,1}^{(k)} = A_{i,1}^{(k)}$$

$$D_{i,j}^{(k)} = A_{i,j}^{(k)} - \sum_{l=1}^{j-1} \left(\sum_{n,1}^{1} M_{n,1}^{(k+1)} A_{n,j}^{(k)} M_{i,1}^{(k+1)} \right) \tag{4.24}$$

$$(j = 2,3\ldots\ldots M)$$

$$A_{i,j}^{(k)} = \sum_{l=j}^{N} d_l^{(k)} M_{i,l}^{(k)} \tag{4.25}$$

H_K higher limit of Kth variable

G_k lower limit of Kth variable

i   variable index = 1,2,3...N

j   direction index = 1,2,3...N

k   stage index

d_l sum of distances moved in the direction since

        last rotation of axes.

$M_{i,j}$ direction vector component (normalised)

N   number of independent variables

X   independent variable.

The search is made in each of the X directions using the new coordinated axes.

$$\text{New } x_i^{(k)} = \text{Old } x_i^{(k)} + S_j^{(k)} M_{i,j}^{(k)} \tag{4.26}$$

The procedure terminates when the convergence criterion is satisfied.

4.3   PROGRAM DESCRIPTION:

The program consists of a main program GARG2 and four user supplied function subprograms as given below. All input-output are executed in the main program.

SUBROUTINE ALKA specifies objective function based on the multireference frame model of section 4.1(b). This finds the critical fundamental voltage V (equation (3.1)), slip, phase currents and the current value of pulsating torque from the

values of independent variables transferred from the main program.

FUNCTION CX specifies the variable to be constrained.

FUNCTION CG specifies lower limits of constraints.

FUNCTION CH specifies higher limits of constraints.

The flow diagram for the complete program is given in fig. 4.3.

4.4 OPTIMAL MACHINE PARAMETERS:

MIN-MAX as out lined in section 4.2 and 4.3 is carried out under the following four conditions:

(i) With design constraints (table 3.1) and leakage reactance linked with magnetising reactance as given by equation (3.7).

(ii) With relaxed constraints (table 4.1) and leakage reactance linked with magnetising reactance as given by equation (3.7).

(iii) With design constraints (table 3.1) and leakage reactance delinked from magnetising reactance.

(iv) With relaxed constraints (table 4.1) and leakage reactance delinked from magnetising reactance.

The same starting point values and step sizes (table 4.2) are used each time for the above conditions.

Table 4.2 Starting Point and Step Sizes.

	R_1	R_2	$X_{L1} = X_{L2}$	X_M	f_o
Starting Point	0.119	0.0693	0.025	3.564	0.1
Starting step size	0.01	0.01	0.001	0.1	0.02
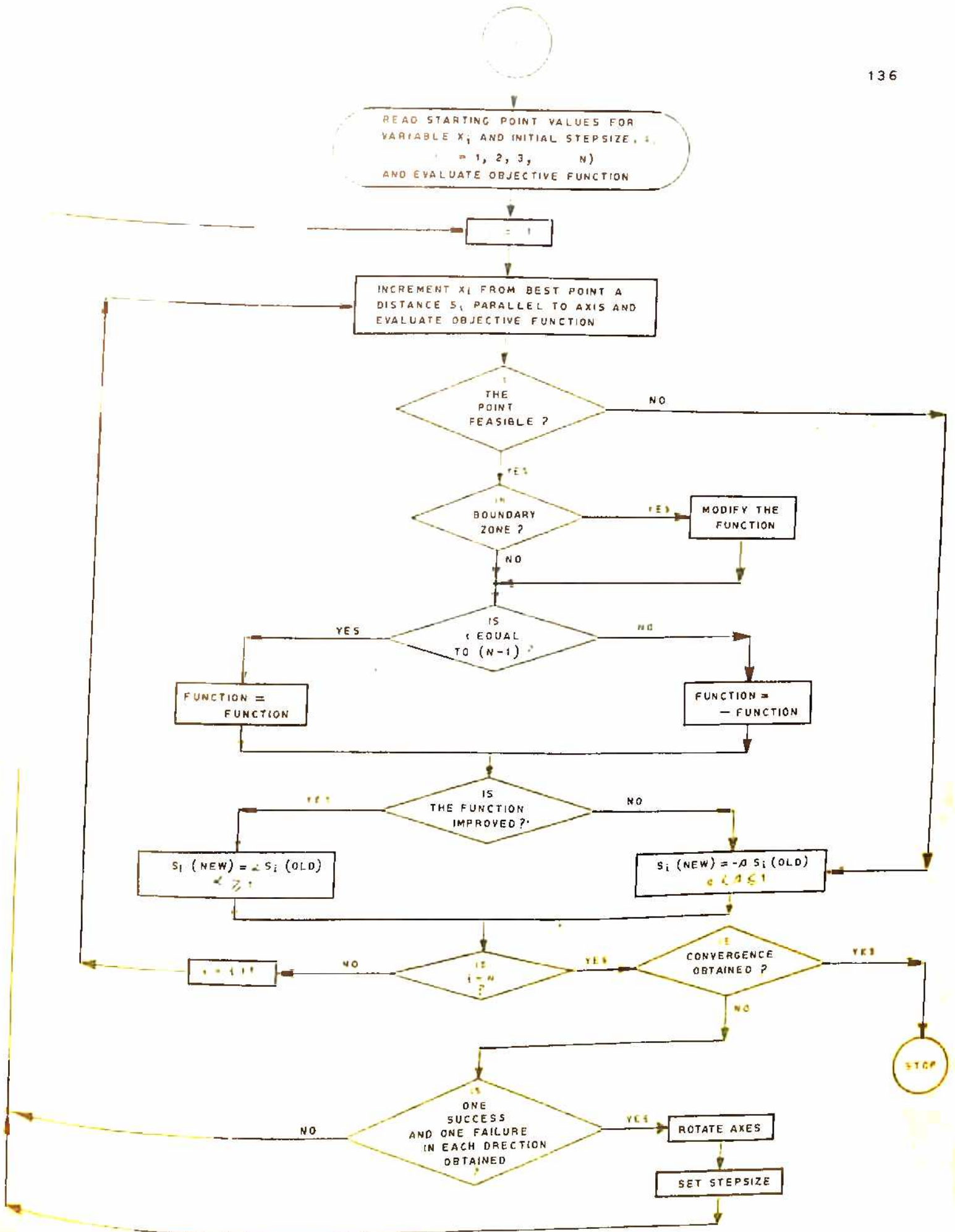
FIG. 4·3 FLOW GRAPH FOR MIN – MAX.

The four sets of optimal machine parameters along with other relevant information e.g. number of evaluations, function value etc. are listed in table 4.3. The first set of machine parameters of table 4.3 as discussed in the next section (4.5) is established as 'Feasible Optimal Machine Parameters'. The torque pulsations and other performance characteristics are computed with the feasible optimal set at different frequencies; using the near exact model developed in Chapter 1. These results alongwith those obtained with normal parameters are given in table 4.4. Comparison of these results show that torque pulsations with optimal parameters are significantly reduced over the whole frequency range of operation. Power factor and efficiency, however, are slightly reduced. This reduction is 6 to 7 percent at low frequencies and only 2 to 3 percent at 50 Hz. Thus the necessity of carrying out MIN-MAX optimisation is fully established.

From table 4.4, it may be seen that the worst torque pulsation is 16.2 at 10 Hz; which is 3.4 percent more than that predicted by MIN-MAX program. This difference in result is natural since the MIN-MAX model is an idealised one based on ideal voltage waveform.

4.5   DESIGN RECOMMENDATIONS:

Looking at table 4.3, one thing is obvious that almost all the machine parameters need to be increased to reduce torque pulsations under any condition. The best function value

Table 4.3 Sets of optimal Machine Parameters

Condition	Optimal Machine Parameters				Frequency at which worst torque pulsations occur	Objective Function value	Pulsating torque at corresponding frequency normal parameters	Percentage of Reduction of pulsating torque	No. of Sta-ges	No. of evaluations
	R_1	R_2	$X_{L1} = X_{L2}$	X_m						
(i)	0.129	0.193	0.161	5.16	7.25Hz	12.8	39.8	70.0	20	670
(ii)	0.499	0.230	0.668	8.0	45.0Hz	7.3	20.5	64.5	3	172
(iii)	0.348	0.199	0.157	5.4	48.5Hz	16.03	20.0	20.0	2	1338
(iv)	0.252	0.116	0.307	9.2	13.0Hz	4.97	17.6	72.5	1	68

Table 4.4 Comparison of Performance

Frequency	Results From Near Exact Model				Normal Parameters				MIN—MAX MODEL
	Optimal Parameters								
	ΦT_p	I	PF	Efficiency	I	ΦT_p	PF	Efficiency	
5	11.5	2.21	.600	.410	2.55	50.5	.735	.44	
10	16.2	2.18	.624	.448	2.30	29.5	.760	.55	
15	14.0	2.34	.624	.583	2.54	18.0	.760	.65	Worst
20	16.3	2.27	.646	.703	2.70	18.5	.770	.70	Torque
25	10.0	2.48	.753	.692	2.75	18.5	.780	.74	Pulsation
30	11.4	2.50	.750	.730	2.67	20.2	.740	.74	= 12.8%
35	12.1	2.40	.750	.760	2.80	21.0	.710	.75	at 7.25Hz
50	13.4	2.43	.750	.730	2.75	20.3	.700	.78	
100	4.7	2.52	.775	.747	2.50	8.0	.730	.76	
150	8.0	2.30	.800	.650	2.00	12.0	.790	.67	
200	8.75	2.50	.700	.500	1.55	16.0	.810	.52	

is achieved under condition (iv) with only about 5 percent worst torque pulsations giving a reduction of 72.5 percent. But to increase the magnetising inductance to 9.2 per unit about 260 percent of its normal value, is almost an impossible task. This necessitates an increase of about 62 percent in phase turns; and these additional turns certainly cannot be accommodated without changing the size of machine. Since the condition (iv) leads to unrealisable proposition from designer's point of view, therefore it is dropped.

The second best function value of 7.3 percent torque pulsations is obtained with relaxed constraints under condition (ii). In this set, the magnetising inductance of 8.0 per unit is quite comparable to that of condition (iv). In addition to it, stator and rotor resistances and leakage inductance are increased manifolds, which will deteriorate appreciably the performance of the drive. Thus this set too can easily be ruled out.

The third best function value of 12.8 percent torque pulsation is obtainable with practical design constraints under condition (i). Here the magnetising inductance is about 44 percent more than its normal value and the stator resistance and leakage inductance are to be increased by 12 percent and 14 percent respectively which are not at all difficult to realise. By providing extra 19 percent phase turns, not only the requisite value of the magnetising inductance is achieved but this will increase the

leakage flux also in the existing leakage paths. For higher
rotor resistance, Alnico bars may be used. The leakage induc-
tance can further be increased by having longer overhangs
and/or by having deeper rotor slots. Thus the optimal machine
parameter set under condition (i) is feasible reducing the
worst torque pulsation occuring at about 7 Hz from 40 percent
to 12.8 percent giving a reduction of nearly 70 percent. The
set under condition (iii) is not considered as the worst
torque pulsation is highest in this case.

Thus the values of parameters under condition (i) of
table 4.3 are established as the 'Feasible Optimal Machine
Parameters'.

On the basis of the above discussions, the general
design recommendations for variable frequency induction motors
of medium sizes meant for constant torque operation may be
made as follows:

(i)   The rotors should be of Alnico to get about 15 to 20
      percent extra rotor resistance from the same cross-section
      of the rotor bars.

(ii) The stator slots should be deeper, to accommodate about
      20 percent extra phase turns. For fuller utilisation
      of the rotor frame and to keep the flux density at the
      original level, the voltage rating of the machine at
      normal frequency can be increased by nearly the same
      factor of 20 percent. This will help in either reducing the

size of phase conductor or overrating the machine, thus off setting partly the additional cost due to extra phase turns.

(iii) The deeper slots and 20 percent extra phase turns will increase the leakage inductance sufficiently, but to meet an increase of about 50 percent of normal leakage inductance, the overhangs may need to be increased slightly. This of course will increase the size of motor and cost too.

(iv) No additional stator resistance needs to be inserted, since the increase of 12 percent in resistance can easily be met by extra 20 percent phase turns of step (ii).

Though the above design recommendations reduce the efficiency and power factor to the extent of 3 to 5 percent, but these are justified as the new recommended machine parameters will reduce the pulsating torque considerably.

4.6   RESUME:

A set of feasible optimal machine parameters is obtained using MIN-MAX search within feasible design constraints on the independent variables. The mathematical model used for the optimisation of torque pulsations, give the results which are fully in conformity with the results predicted by near exact model of Chapter 1.

The feasible optimal machine parameters confirm that the design considerations for a variable frequency operation of

induction motor are far more different than those of normal fixed frequency induction motor. Though the performance is deteriorated a little from the economical points of view but a motor with high leakage inductance, high stator and rotor resistance is preferable to have minimum pulsating torque.

- 0 -

CHAPTER 5

STABILITY AND DYNAMIC RESPONSE:

It has been shown by Fallside and Wortley[20], that the variable frequency induction motor may become unstable at certain operating frequencies even with sinusoidal excitation if the machine parameters are not properly selected. It has amply been established in the earlier chapters that the nonsinusoidal excitation of the bridge inverter leads to a continuous steady state torque oscillations of considerable magnitude in induction motor. These oscillations are due to imperfect system parameters; wherein some cases the point of operation even crosses over the break down torque of the motor, leading to the instability of the drive[43]. Almost similar results are obtained by Nelson[60]. He carries out stability study over symmetrical variable frequency induction motor by computing the characteristic roots or eigen values of the linearised system differential equations. Regions of lightly damped operation are identified and effects of various machine parameters over stability have been considered. The algebric equations giving necessary and sufficient conditions for stability have been formulated by Fallside.

It is intended here, to use these published results to test the drive with recommended optimal machine parameters obtained in Chapter 4, for instability at any frequency, establishing thereby the finality of optimal machine parameters.

144

The other aspect dealt in this chapter is the dynamic
response of the inverter fed drive, to establish the usefulness
of the model developed in Chapter 1, for dynamic response and
for simulation of any fault conditions[85]. The transient
phase currents, speed, and torque values are computed for
load of the machine at few selected frequencies. These results
are presented both for a machine with normal parameters and
a machine with recommended optimal parameters.

5.1   STABILITY TEST:

(a)   Perturbation Equations:

As is well known, the generalised equations of an
induction motor are nonlinear, but useful information about
steady state stability can be obtained by linearising the
equations about an operating point and investigating the
stability of the resulting linear perturbation equations. For
the given machine the steady state point is defined by supply
voltage v_{do}^s, the operating angular frequency w, and the slip
s_o. The following simplifying assumptions are made:

(i)   Inverter waveform is approximated to its fundamental value.

(ii)   All eigen values are determined for constant slip.

Equations described in synchronously rotating reference
frame are used for determining stability with fundamental
excitation only[75]. For the filter circuit (fig. 5.1), the
following relations can be written.

$$E_d = V_1 + (\frac{p}{w_b} X_{LF} + R_F) I_R \tag{5.1}$$

$$V_1 = \frac{w_b}{p} X_{CF} (I_R - I_1) \tag{5.2}$$

where $X_{LF} = w_b L_F$, $X_{CF} = \frac{1}{C_F w_b}$

Equation (4.8) developed earlier can directly be used substituting $k = 1$ for fundamental excitation; giving the following relation.

$$\begin{bmatrix} 0 \\ v_{d1}^s \\ 0 \\ 0 \end{bmatrix} = \begin{bmatrix} Z_{qd,qd}^{s} {}^{r} \end{bmatrix} \begin{bmatrix} i_{q1}^s \\ i_{d1}^s \\ i_{q1}^r \\ i_{d1}^r \end{bmatrix} \tag{5.3}$$

Equating the power expressed in d.c. and a.c. variables we get –

$$V_1 I_1 = \frac{3}{2} (v_{q1}^s i_{q1}^s + v_{d1}^s i_{d1}^s) \tag{5.4}$$

Giving a small perturbation in all voltages, currents and speed about a steady state values indicated by subscript 'o', we get –

$$\begin{aligned}
V_1 &= V_{1o} + \delta V_1 \\
E_d &= E_{do} + \delta E_d \\
I_R &= I_{Ro} + \delta I_R \\
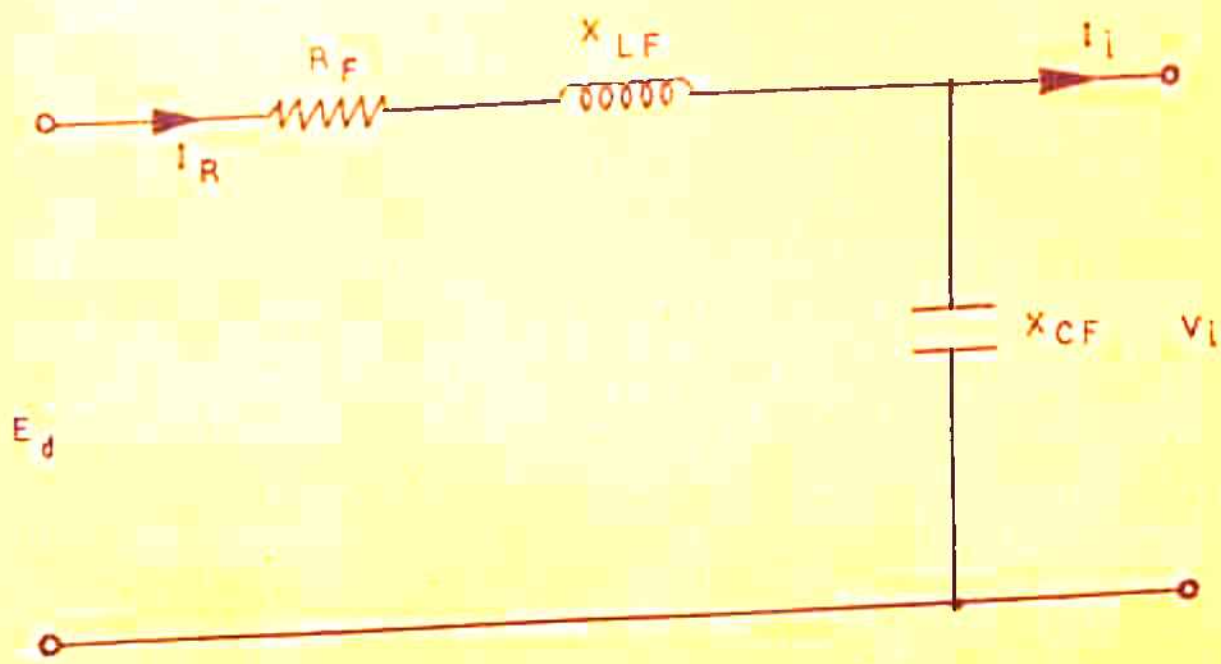I_1 &= I_{1o} + \delta I_1
\end{aligned} \tag{5.5}$$

FIG.5·1 FILTER CIRCUIT

$$i^s_{q1} = i^s_{qo} + \delta i^s_q$$

$$i^s_{d1} = i^s_{do} + \delta i^s_d$$

$$i^r_{q1} = i^r_{qo} + \delta i^r_q$$

$$i^r_{d1} = i^r_{do} + \delta i^r_d$$

$$w_R = w_{Ro} + \delta w_R$$

$$v^s_{d1} = v^s_{do} + \delta v^s_d$$

(5.5)

Using equations (5.3),(5.5) and (4.9) the steady state and
the perturbation equations can be written as:

Steady state equations: The steady state equations can be
got directly from equation (4.9) by making the following
substitutions.

$$k = 1$$
$$w_R = w_{Ro}$$
$$v^s_{q1} = 0$$
$$v^s_{d1} = v^s_{do}$$

(5.6)

Perturbation equations:

$$
\begin{bmatrix} 0 \\ \delta v^s_d \\ 0 \\ 0 \end{bmatrix}
\begin{bmatrix}
R_1+wX_1p & wX_1 & w\bar{X}_Mp & w\bar{X}_M & 0 \\
-wX_1 & R_1+wX_1p+Z_F(p) & -w\bar{X}_M & w\bar{X}_Mp & 0 \\
w\bar{X}_Mp & ws_o\bar{X}_M & R_2+wX_2p & ws_oX_2 & -\bar{X}_Mi^s_{do}-X_2i^r_{do} \\
-ws_o\bar{X}_M & w\bar{X}_Mp & -ws_oX_2 & R_2+wX_2p & \bar{X}_Mi^s_{qo}+X_2i^r_{qo}
\end{bmatrix} \times
$$

$$
\begin{bmatrix} \delta i^s_q & \delta i^s_d & \delta i^r_q & \delta i^r_d & \delta w_R \end{bmatrix}_T
$$

(5.7)

The perturbation equations for rectifier inverter are:

$$E_{do} = V_{1o} \tag{5.8}$$

$$\delta E_d = \delta V_1 + \left(\frac{p}{w_b} X_{LF} + R_F \right) \delta I_R \tag{5.9}$$

$$\delta v_d^s = \frac{2}{\pi} \delta V_1 \tag{5.10}$$

$$\delta V_1 = \frac{w_b}{p} X_{CF} (\delta I_R - \delta I_1) \tag{5.11}$$

$$I_{1o} E_{do} = \frac{3}{2} v_{qo}^s i_{qo}^s \tag{5.12}$$

$$\delta I_1 V_{1o} + \delta V_1 I_{1o} = \frac{3}{\pi} (V_{1o} \delta i_d^s + \delta V_1 i_{do}^s) \tag{5.13}$$

$$I_{1o} = \frac{3}{\pi} i_{do}^s \tag{5.14}$$

$$\delta I_1 = \frac{3}{\pi} \delta i_d^s \tag{5.15}$$

Through proper manipulations of equations (5.8) to (5.15) v_d^s can be written as:

$$\delta v_d^s = \frac{\delta E_d - \delta i_d^s \left(\frac{3}{\pi} \frac{p}{w_b} X_{LF} + \frac{3}{\pi} R_F \right)}{\frac{\pi}{2} \left[1 + \frac{p}{w_b X_{CF}} \left(\frac{p}{w_b} X_{LF} + R_F \right) \right]} \tag{5.16}$$

The equation (5.16) is unmanagable for any computational purposes. The presence of second order derivative in the denominator, makes it nonlinear. Since the filter having high value of X_{CF} are preferred (Appendix IV), the second term in the denominator of equation (5.16) can be easily neglected. Thus we get.-

$$\delta v_d^s = \frac{2}{\pi} \delta s_d - \delta i_d^s Z_F(p) \tag{5.17}$$

where $Z_F(p) = \frac{6}{\pi^2} (R_F + \frac{p}{w_b} X_{LF})$ (5.18)

Torque equation in synchronously rotating frame for fundamental excitation is[43]:

$$T_e = \overline{X}_M (i_{q1}^s i_{d1}^r - i_{d1}^s i_{q1}^r) \tag{5.19}$$

where

$$\overline{X}_M = \frac{3}{2} X_M$$

writing (5.20)

$$T_e = T_{eo} + \delta T_e$$

Substituting for currents from equation (5.5) we get –

$$T_{eo} = \overline{X}_M (i_{qo}^s i_{do}^r - i_{do}^s i_{qo}^r) \tag{5.21}$$

$$\delta T_e = \overline{X}_M \quad (i_{qo}^s \delta i_d^r + \delta i_q^s i_{do}^r)$$

$$- (i_{do}^s \delta i_q^r + \delta i_d^s i_{qo}^r) \tag{5.22}$$

The torque balance equation neglecting the frictional coefficient α (equation (158))is:

$$J \frac{dw_R}{dt} = T_e - T_L \tag{5.23}$$

where $T_L = T_{Lo} + \delta T_L$ (5.24)

Substituting equations (5.19) and (5.24) in (5.23) we get -

$$T_{eo} = T_{Lo} \tag{5.25}$$

$$Jp(\delta w_R) = \delta T_e - \delta T_L \tag{5.26}$$

Combining equation (5.26) with (5.7), the complete perturbation (linearised incremental differential relations) equation for the system can be written as:

$$
\begin{bmatrix}
0 \\[4pt]
\dfrac{2}{\pi}\delta\varepsilon_d \\[4pt]
0 \\[4pt]
0 \\[4pt]
\delta T_L
\end{bmatrix}
=
\begin{bmatrix}
R_1+wX_1p & wX_1 & w\bar{X}_M p & w\bar{X}_M & 0 \\[6pt]
-wX_1 & R_1+wX_1p+Z_F(p) & -w\bar{X}_M & w\bar{X}_M p & 0 \\[6pt]
w\bar{X}_M p & ws_0\bar{X}_M & R_2+wX_2p & ws_0X_2 & -\bar{X}_M i^s_{do}-X_2 i^r_{do} \\[6pt]
-ws_0\bar{X}_M & w\bar{X}_M p & -ws_0X_2 & R_2+wX_2p & \bar{X}_M i^s_{qo}+X_2 i^r_{qo} \\[6pt]
\bar{X}_M i^r_{do} & -\bar{X}_M i^r_{qo} & -\bar{X}_M i^s_{do} & i^s_{qo}\bar{X}_M & -\dfrac{2J}{P}p
\end{bmatrix}
\times
\begin{bmatrix}
\delta i^s_q \\[4pt]
\delta i^s_d \\[4pt]
\delta i^r_q \\[4pt]
\delta i^r_d \\[4pt]
\delta w_R
\end{bmatrix}
\tag{5.27}
$$

The above system equation can be rewritten as:

$$\frac{d}{dt} [\delta i] = [A][\delta i] + [B][\delta e] \qquad (5.28)$$

and in an open loop system where $[\delta e] = 0$, its stability can be determined from the eigen values λ of the 5 x 5 matrix $[A]$ i.e. from the roots of the characteristic equation;

$$\text{Det} \mid A - \lambda I \mid = 0 \qquad (5.29)$$

(b)   Stability Criterion:

Routh-Hurwitz criterion[42] is applied to equation (5.29) for stability test. The characteristic equation in the polynomial form is -

$$\lambda^5 + A \lambda^4 + B \lambda^3 + C \lambda^2 + D \lambda + E = 0 \qquad (5.30)$$

On applying Routh-Hurwitz criterion to equation (5.30), system is found to be stable when all $\overline{Z}_1$ to $\overline{Z}_5$ as defined below are positive.

$$
\begin{aligned}
\overline{Z}_1 &= A \\
\overline{Z}_2 &= AB - C \\
\overline{Z}_3 &= C - A(AD-E)/(AB-C) \qquad (5.31) \\
\overline{Z}_4 &= (AB - C)(CD - EB) - (AD - E)^2 \\
\overline{Z}_5 &= E
\end{aligned}
$$

The stability spectrums of the motor with normal and with optimal parameters covering a frequency range of 1 Hz to 200 Hz

are given in table 5.1

Table 5.1 Stability Spectrum.

Load (Per Unit)	Frequencies, at which the motor is UNSTABLE	
	with optimal parameters	with normal parameters
0.3	1 to 12	1 to 14
0.6	1 to 6	1 to 14
0.9	1 to 10	1 to 10
1.2	1 to 8	1 to 10
1.5 (Full load)	1 to 16	1 to 22
1.8	1 to 16	1 to 22
2.1	1 to 16	1 to 22

5.2   DYNAMIC RESPONSE:

The objective of this section is to look for any possible adverse effects on starting transients of the machine with recommended optimal parameters and compare its transient performance with that under normal parameters. While [86]

going through this exercise, it is also intended to establish the usefulness of the mathematical model, developed in Chapter 1, for the dynamical analysis of the system.

(a)   Computer Algorithm:

Using equations (1.43) and (1.58), a main line program 'GARG1' has been developed. This program uses the subroutines of earlier program 'GARG'. The computational sequence is outlined in the flowgraph (fig. 5.2).

(b)   Computed Results and Comments:

The full load switching transient phase currents, torque and speed are computed for the test motor (specifications given in appendix VI), at three selected frequencies (10,25 and 50 Hz) both with normal and recommended optimal machine parameters. The frictional loss coefficient α (equation (1.58)) being small is neglected. Figs. 5.3 to 5.14 deal with the transient characteristics e.g. phase current, torque and speed as well as torque-speed both for normal and optimal parameters.

These results can be summarised as follows:

(1)   The values of steady state pulsating torques obtained through dynamic solution establish the validity of the assumption of constant speed solution of Chapter 3. (table 5.2).
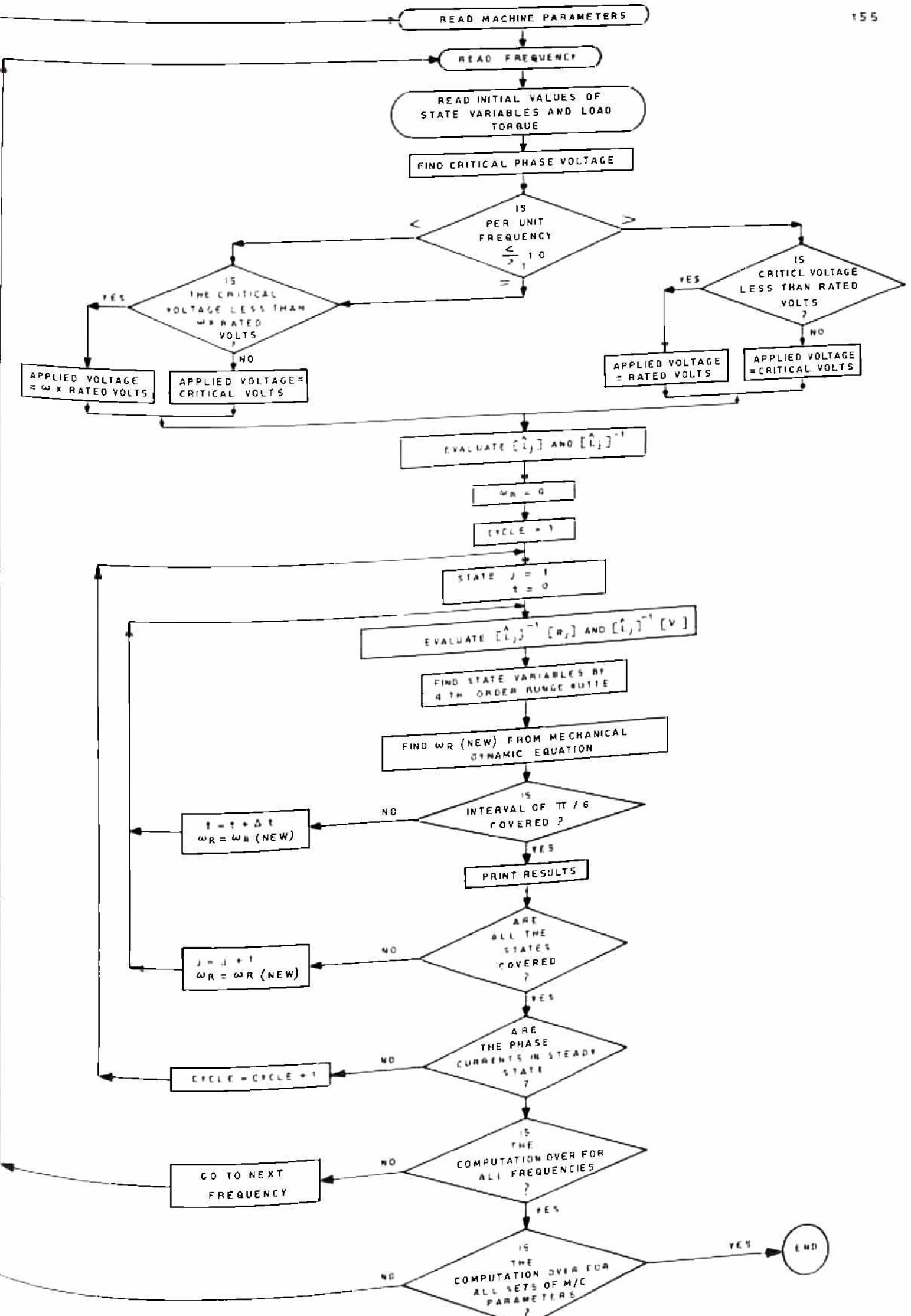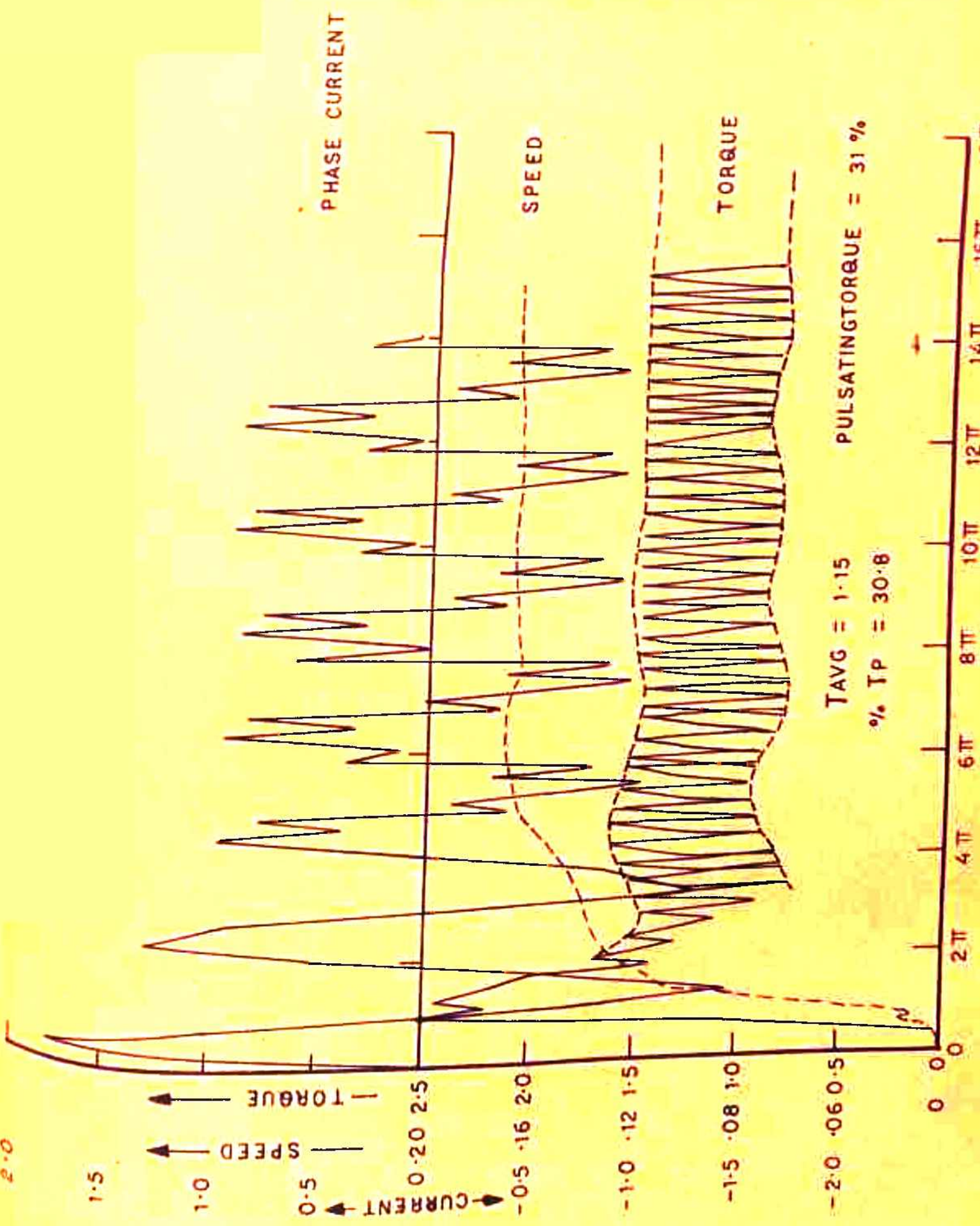
READ MACHINE PARAMETERS

READ FREQUENCY

READ INITIAL VALUES OF STATE VARIABLES AND LOAD TORQUE

FIND CRITICAL PHASE VOLTAGE

IS PER UNIT FREQUENCY $\leq \geq$ 1.0

<

=

>

IS THE CRITICAL VOLTAGE LESS THAN $\omega \times$ RATED VOLTS ?

YES

NO

APPLIED VOLTAGE = $\omega \times$ RATED VOLTS

APPLIED VOLTAGE = CRITICAL VOLTS

IS CRITICAL VOLTAGE LESS THAN RATED VOLTS ?

YES

NO

APPLIED VOLTAGE = RATED VOLTS

APPLIED VOLTAGE = CRITICAL VOLTS

EVALUATE $[\hat{L}_j]$ AND $[\hat{L}_j]^{-1}$

$\omega_R = 0$

CYCLE = 1

STATE $j = 1$ $t = 0$

EVALUATE $[\hat{L}_j]^{-1} [R_j]$ AND $[\hat{L}_j]^{-1} [V]$

FIND STATE VARIABLES BY 4 TH ORDER RUNGE KUTTE

FIND ω_R (NEW) FROM MECHANICAL DYNAMIC EQUATION

IS INTERVAL OF $\pi/6$ COVERED ?

NO

$t = t + \Delta t$ $\omega_R = \omega_R$ (NEW)

YES

PRINT RESULTS

ARE ALL THE STATES COVERED ?

NO

$j = j + 1$ $\omega_R = \omega_R$ (NEW)

YES

ARE THE PHASE CURRENTS IN STEADY STATE ?

NO

CYCLE = CYCLE + 1

IS THE COMPUTATION OVER FOR ALL FREQUENCIES ?

NO

GO TO NEXT FREQUENCY

YES

IS THE COMPUTATION OVER FOR ALL SETS OF M/C PARAMETERS ?

YES

END

NO

FIG. 5.2 FLOW GRAPH FOR DYNAMIC RESPONSE.

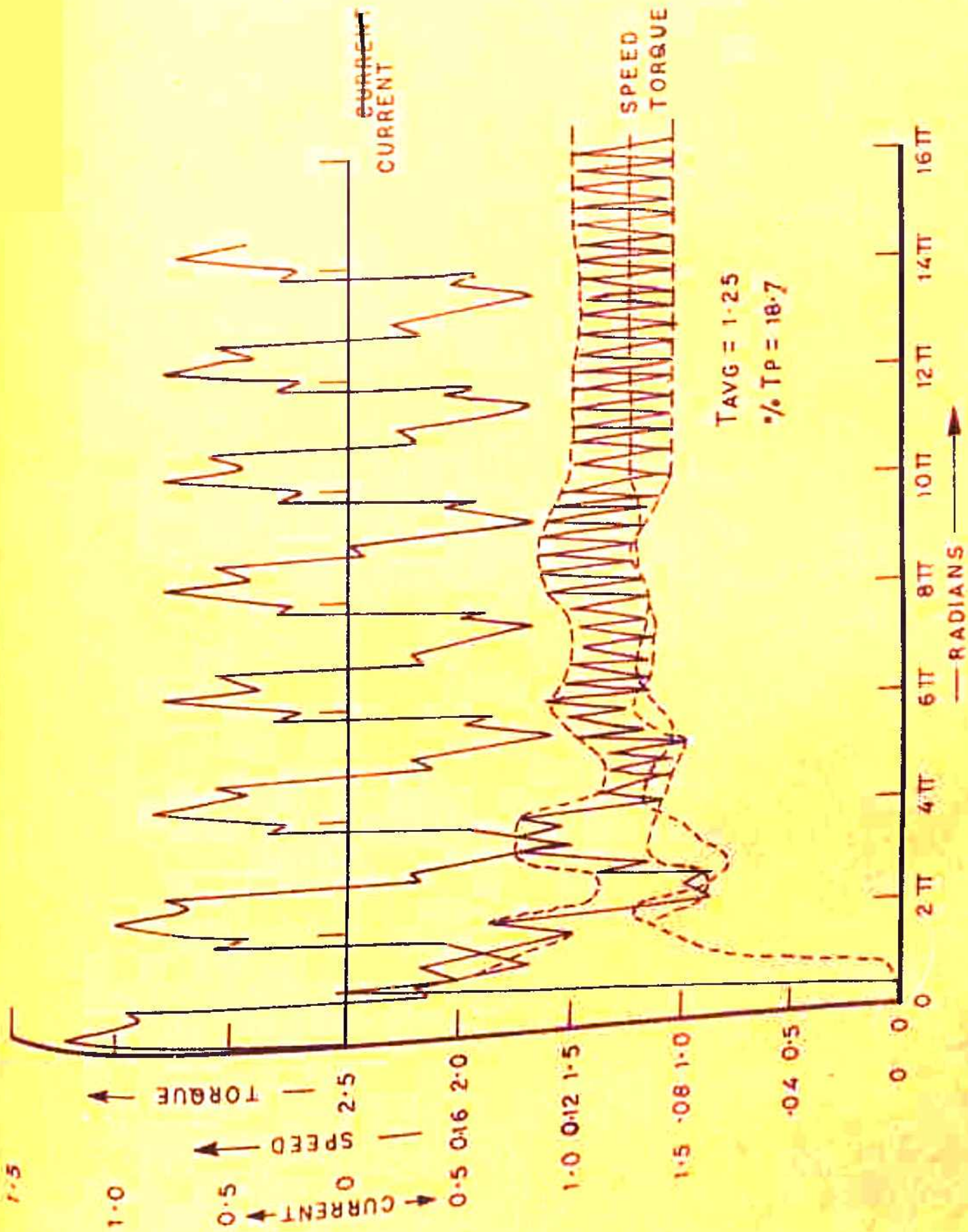FIG.5.3 TRANSIENTS AT 10 HZ WITH NORMAL MACHINE PARAMETERS AT FULL LOAD.

FIG. 5.4 TRANSIENTS CHARACTERISTIC AT 10 HZ, FULL LOAD WITH OPTIMAL PARAMETERS.
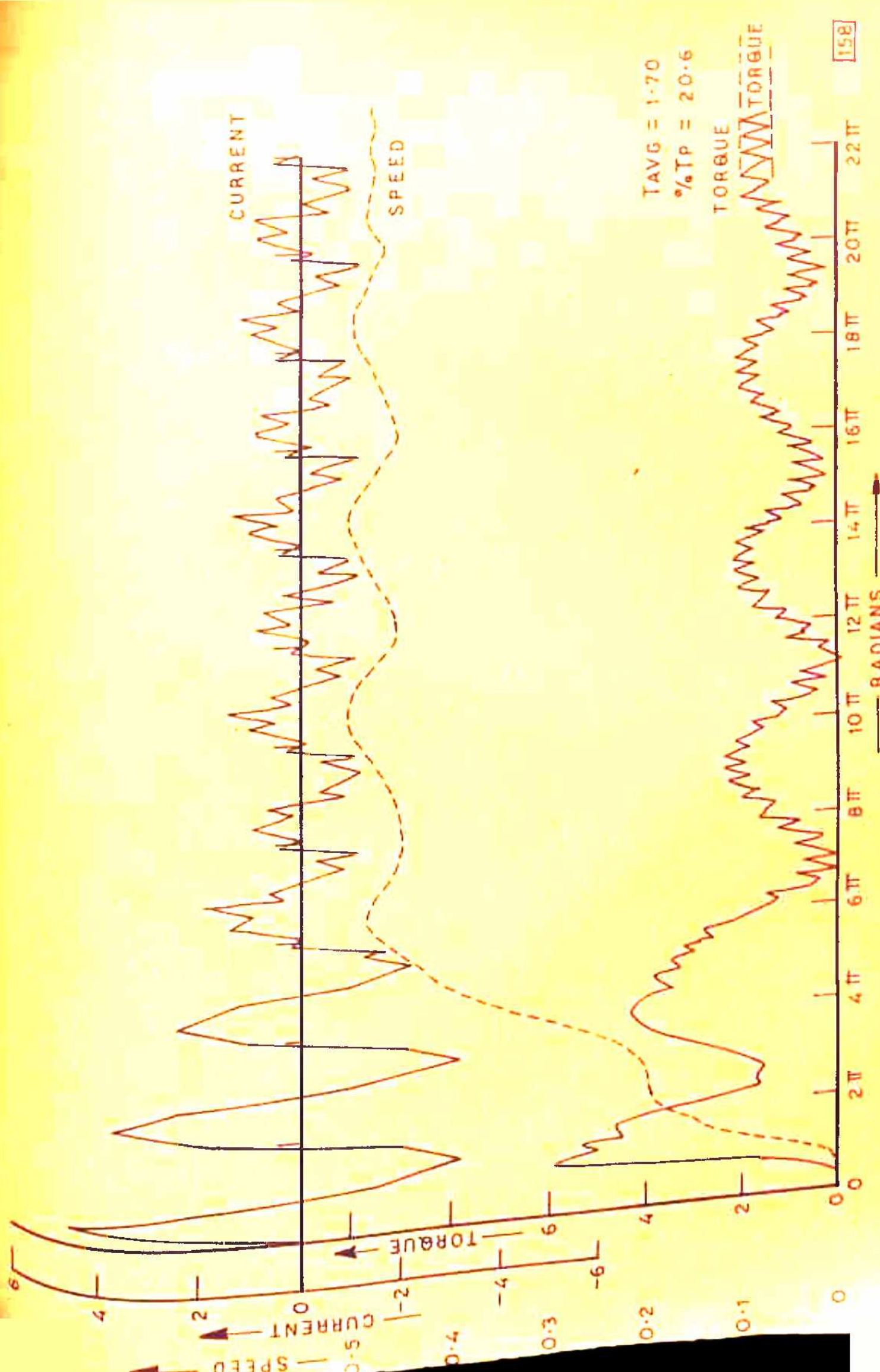
157

FIG. 5.5   TRANSIENTS AT 25 HZ, FULL LOAD WITH NORMAL PARAMETER'

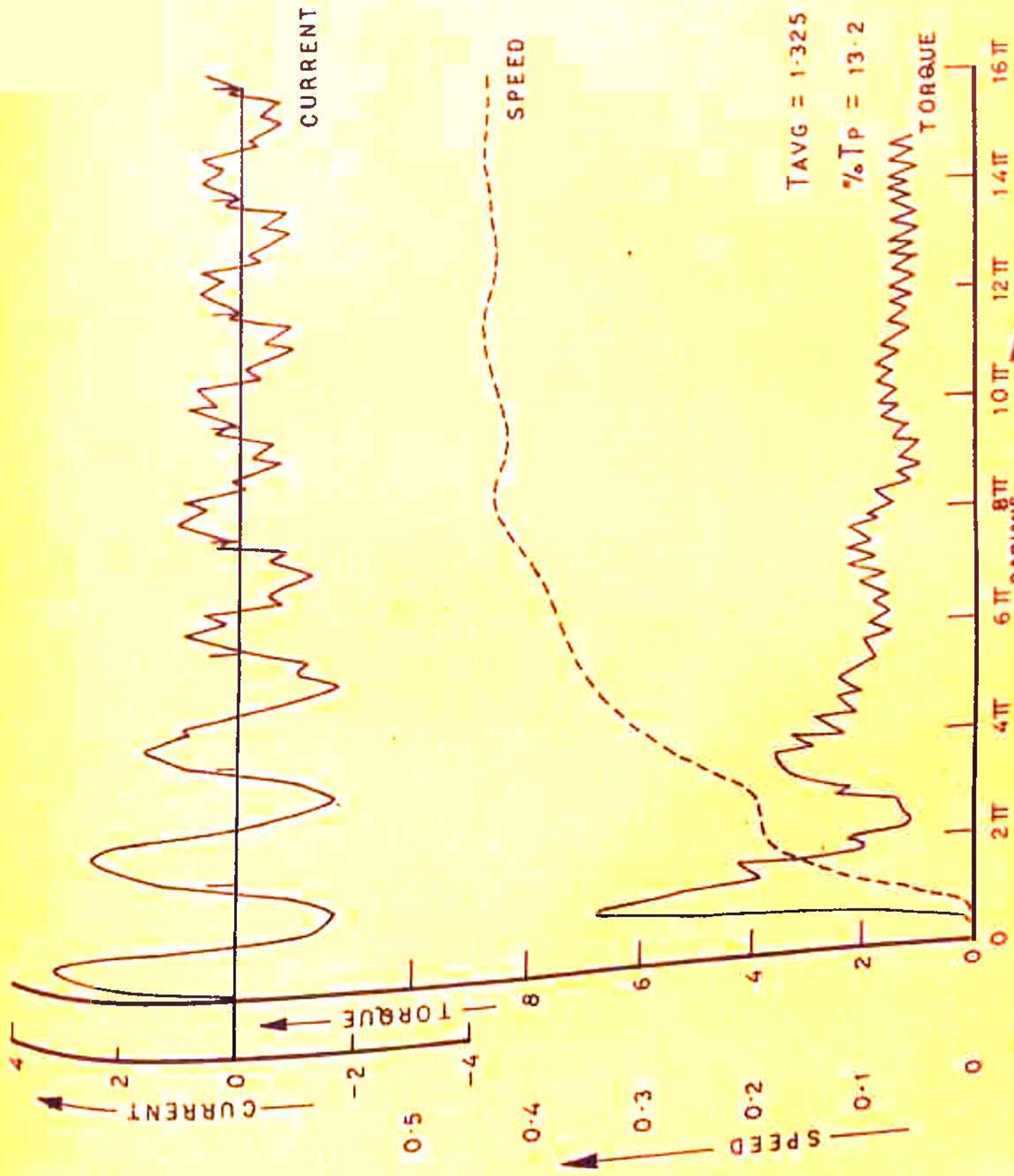FIG. 5·6 TRANSIENT CHARACTERISTICS AT 25 HZ, FULL LOAD WITH OPTIMAL PARAMETERS.

159
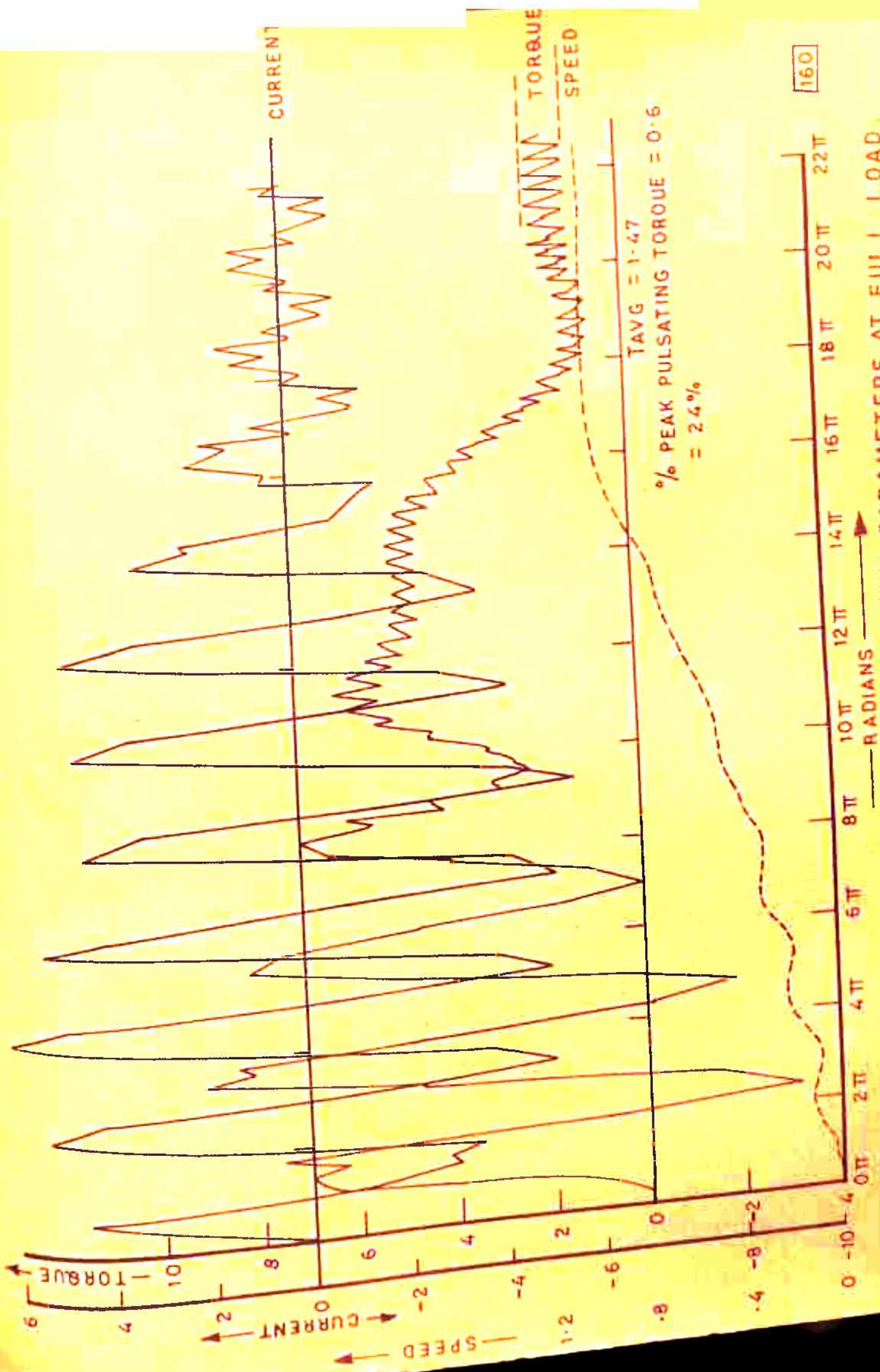
FIG. 5.7 TRANSIENTS AT 50 HZ WITH NORMAL MACHINE PARAMETERS AT FULL LOAD.

160

FIG. 5·8 TRANSIENT CHARCTERISTICS AT 50 HZ , FULL LOAD WITH OPTIMAL PARAMETERS .

TAVG = 1·65
%Tp = 15·1

CURRENT

TORQUE

SPEED

RADIANS

161

FIG. 5·9 TORQUE—SPEED CHARACTERISTIC AT 10 HZ WITH NORMAL PARAMETERS AT FULL LOAD.

162

FIG.5.10 TORQUE—SPEED CHARACTERISTICS AT 10 HZ, FULLLOAD WITH OPTIMAL PARAMETERS.

163

FIG. 5.11 TORQUE–SPEED CHARACTERISTIC AT 25 HZ, FULL LOAD WITH NORMAL PARAMETERS.
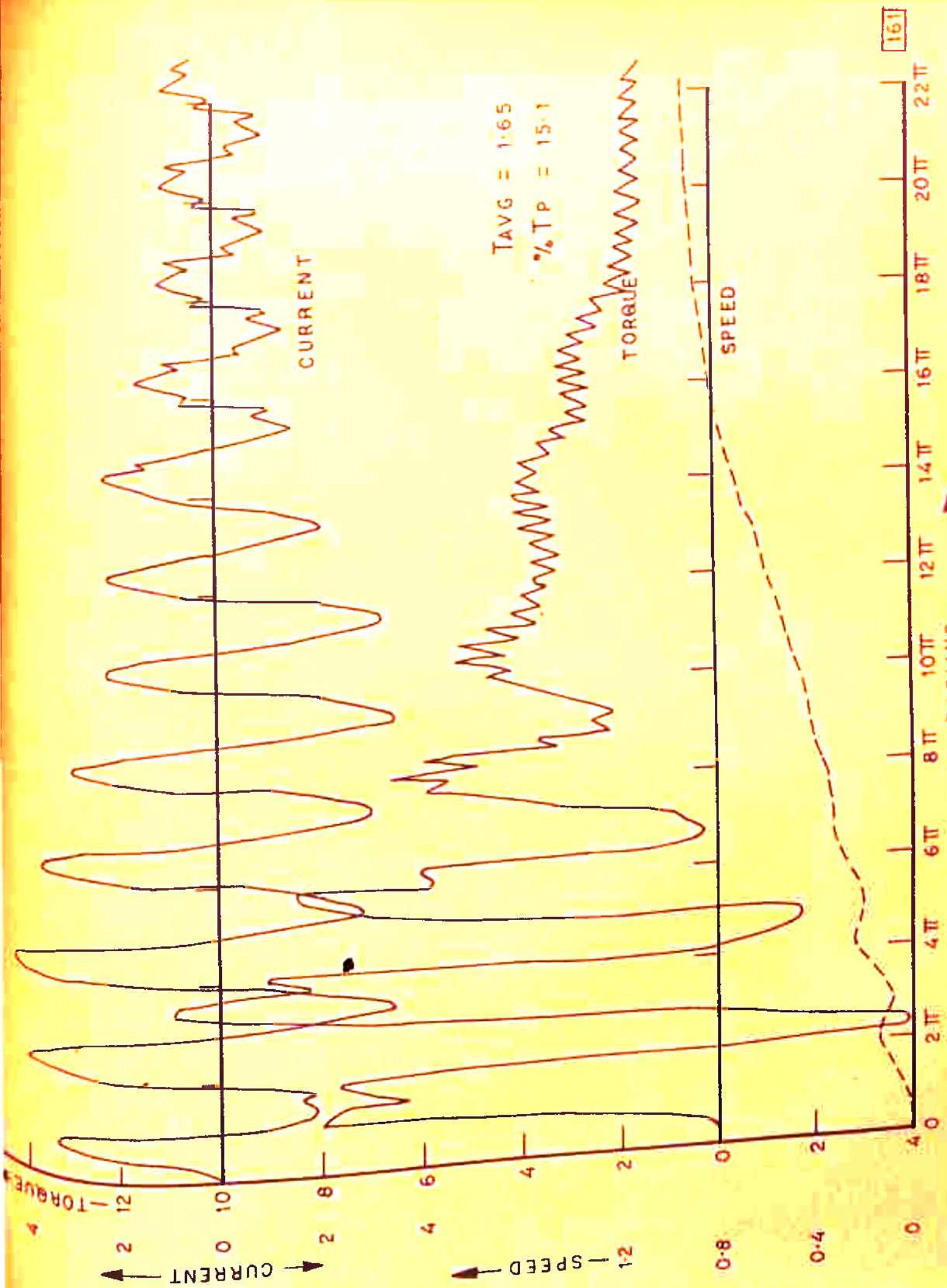
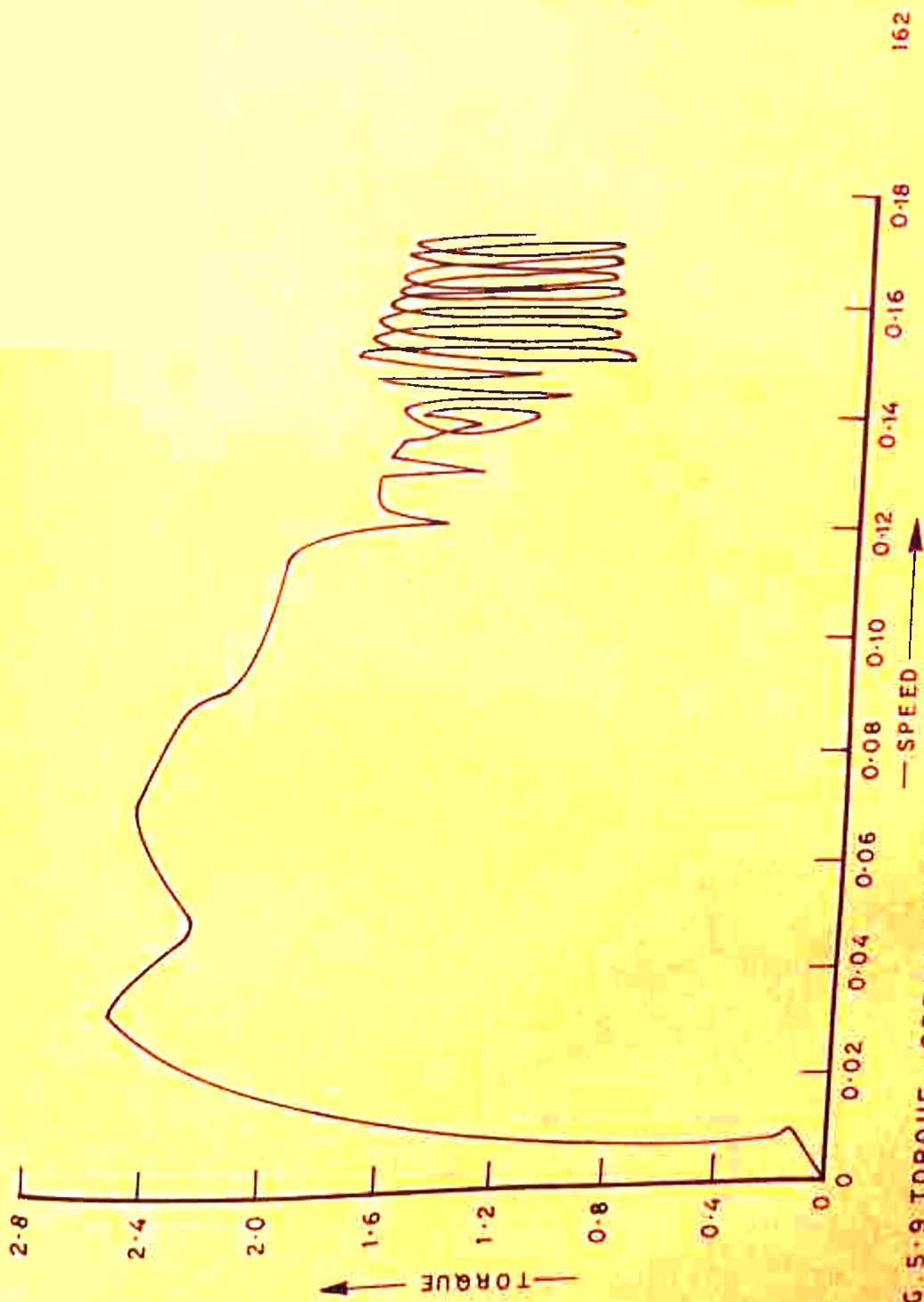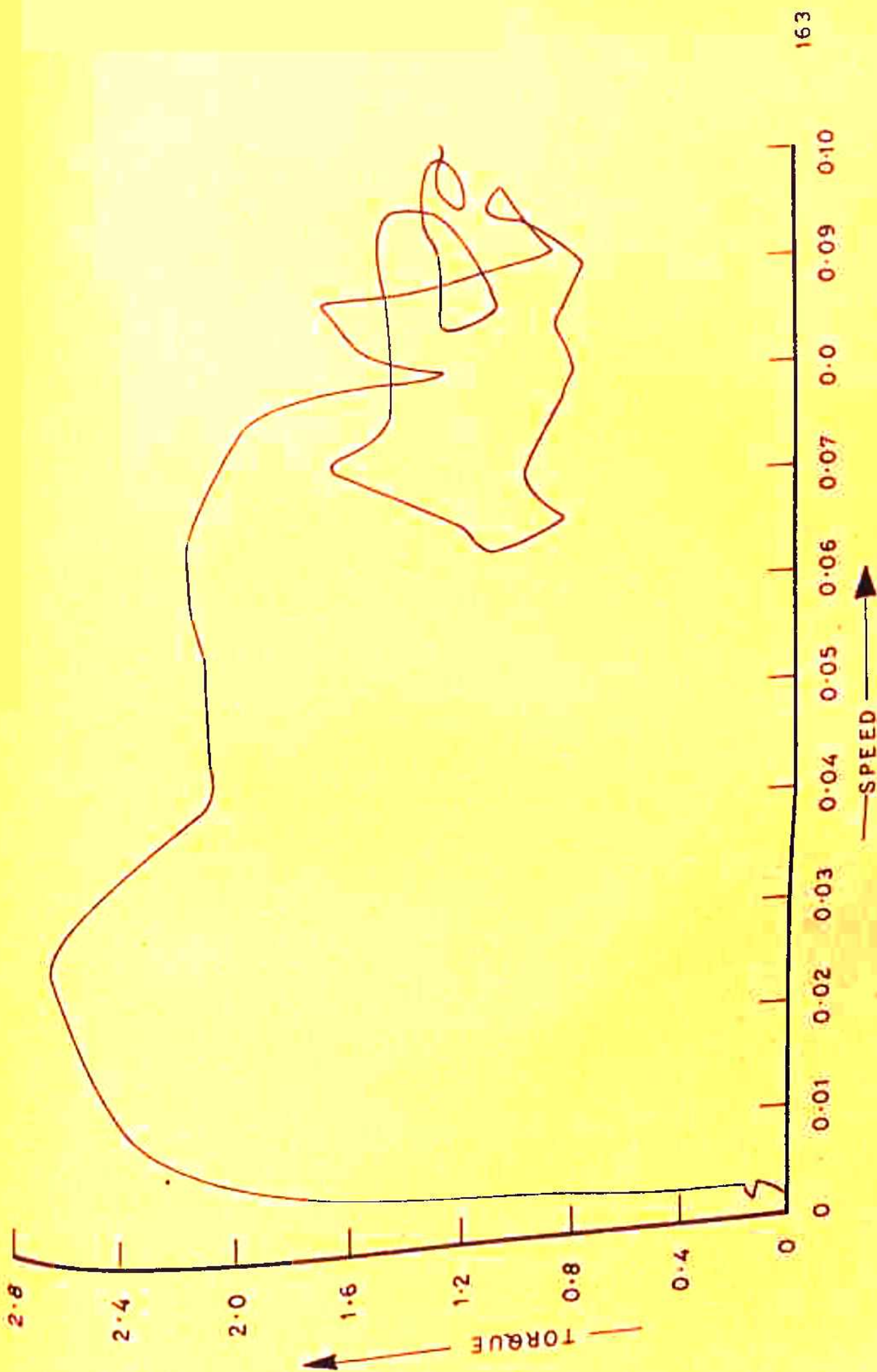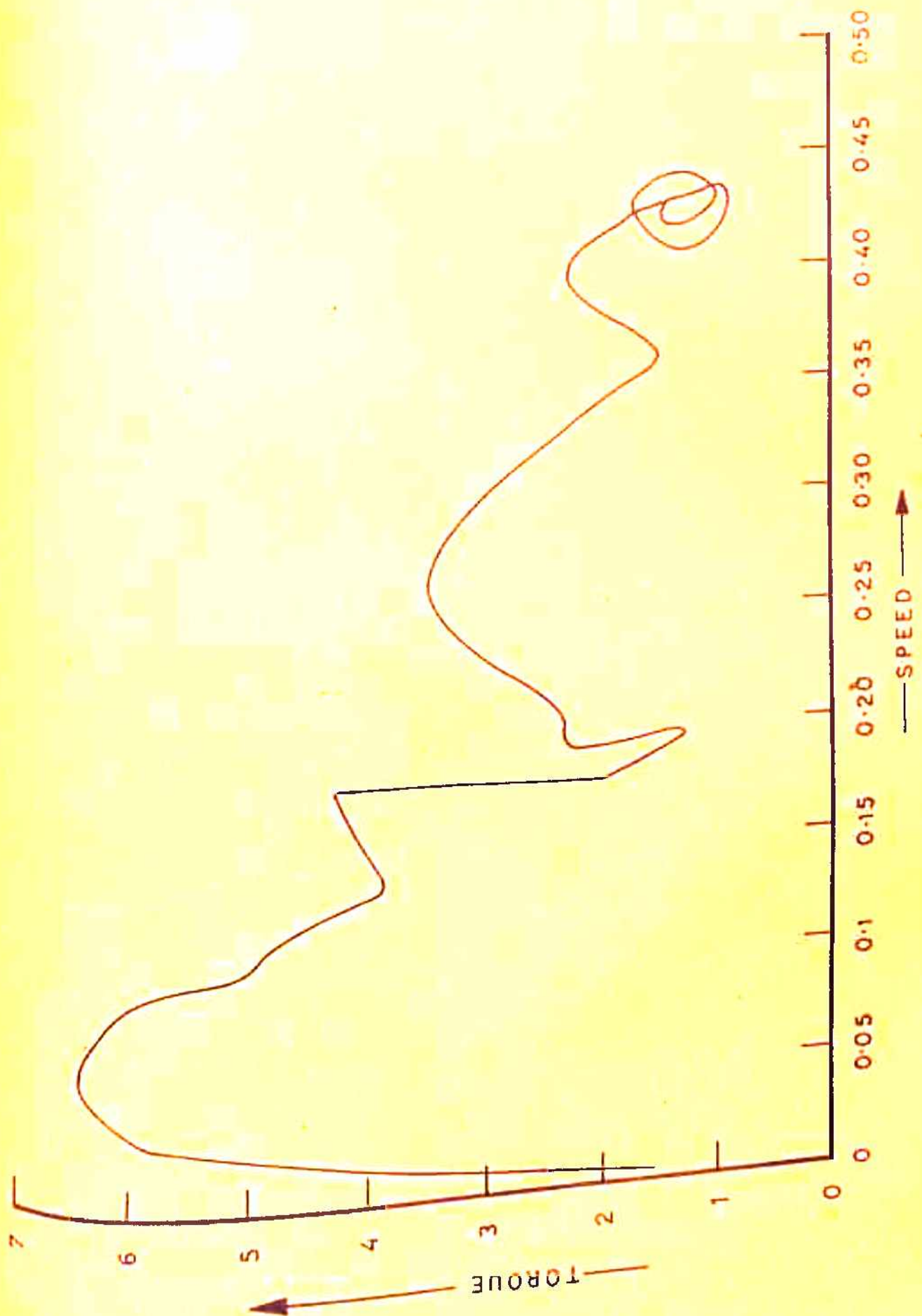FIG. 5.12 TORQUE — SPEED CHARACTERISTIC AT 25 HZ, FULLLOAD WITH OPTIMAL PARAMETERS.
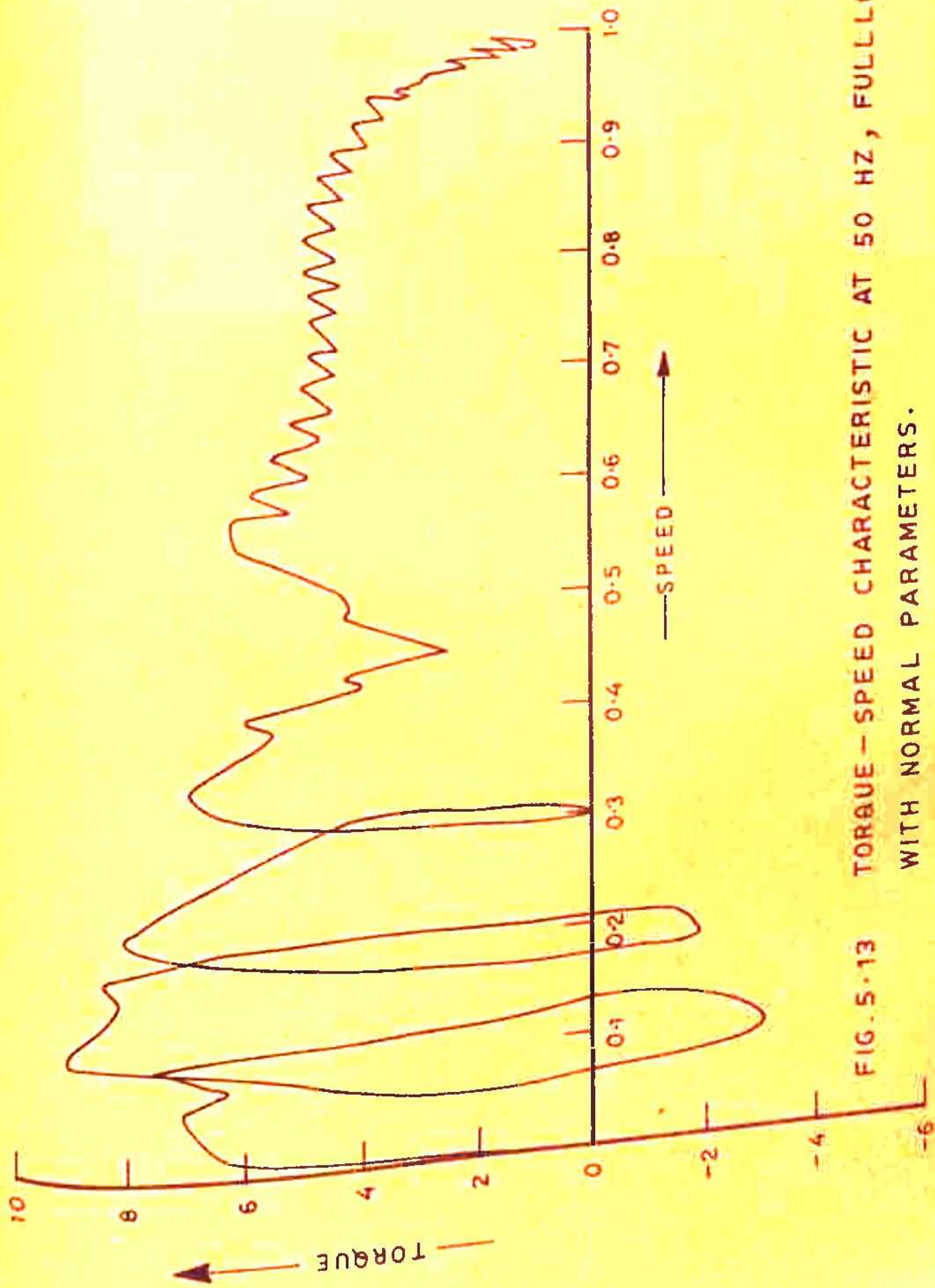
165

FIG. 5.13 TORQUE — SPEED CHARACTERISTIC AT 50 HZ, FULL LOAD WITH NORMAL PARAMETERS.

166
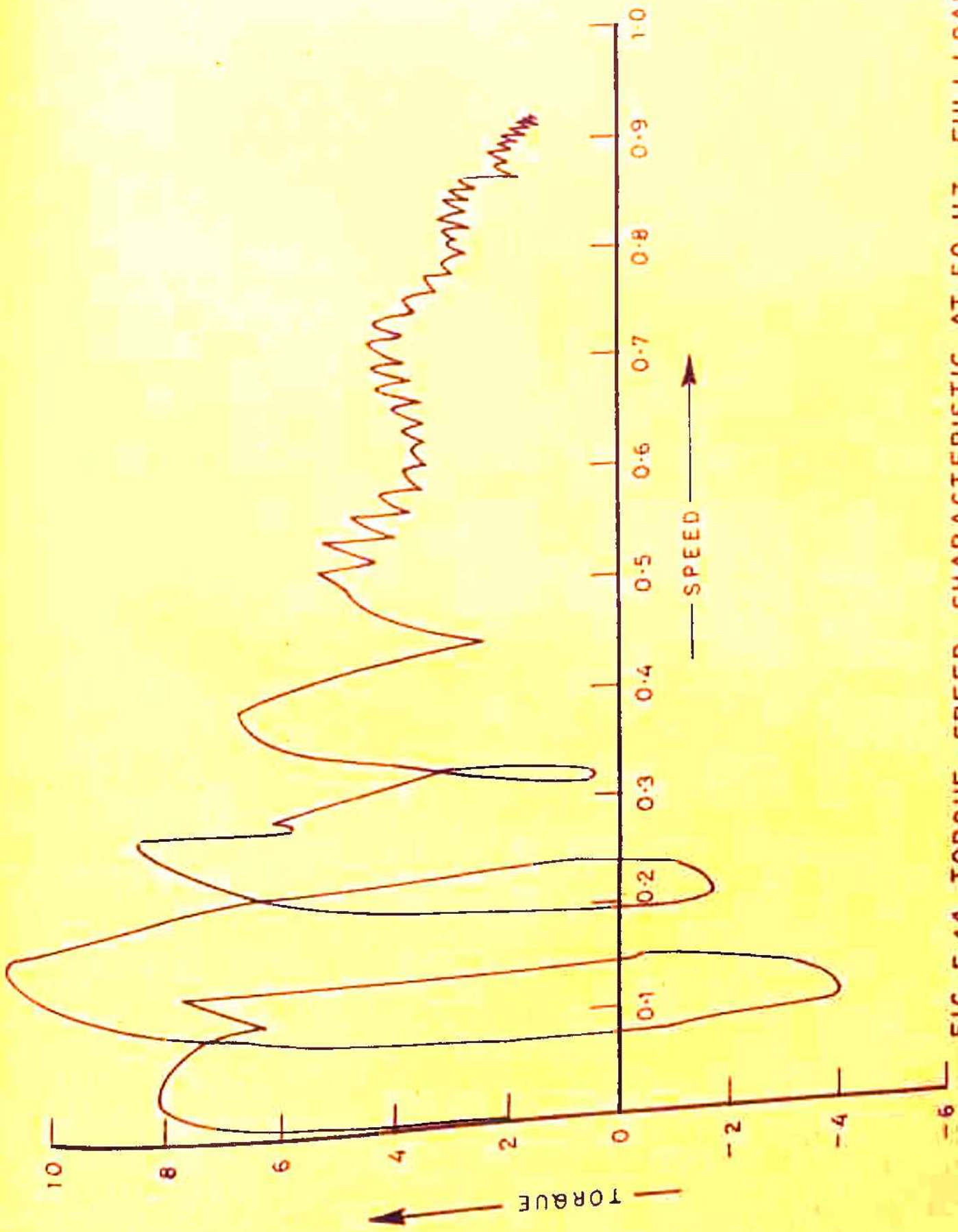
FIG. 5·14 TORQUE-SPEED CHARACTERISTIC AT 50 HZ, FULLLOAD

WITH OPTIMAL PARAMETERS.

167

Table 5.2   Comparison of dynamic and constant speed solution
torque values.

Frequency	Machine with Normal parameters			Machine with optimal parameters		
	Const.speed	Dynamic solution	% Error	Constant speed	Dynamic solution	% Error
10 Hz	23.5	30.8	-4.4	16.2	18.7	- 15.4
25 Hz	18.5	20.6	-11.2	10.0	13.2	-32.0
50 Hz	20.3	24.0	- 3.45	13.4	15.1	-12.6

(ii)   The transient peak current and peak torque get reduced
substantially in a machine with recommended optimal
parameters when compared with their respective transient
values with normal machine parameters. For example,
the current peak with optimal parameters at 10 Hz in
the transient is reduced from 1.75 p.u. to 1.25 p.u.
and in steady state from 0.9 p.u. to 0.76 p.u.
(figs. 5.3 and 5.4). The similar reductions are also
noticed at 25 Hz and 50 Hz (figs. 5.5 to 5.8).
However, the reduction in the first torque peak is only
marginal at 50 Hz (figs. 5.7 and 5.8).

(iii)   Due to higher stator and rotor resistances in the
optimal parameters set, the transients decay faster
and thus help the rotor to settle down to its steady

state values in lesser time. For instance, at 25 Hz, the settling time reduces from 10 cycles with normal parameters to 6 cycles with optimal parameters (figs. 5.5 and 5.6).

(iv) Comparing dynamic torque-speed characteristics at 10 Hz with normal (fig. 5.9) and with optimal parameters (fig. 5.10); it is noticed that number of peaks and valleys reduces considerably and the machine settles down to the steady speed without any significant oscillations in the case of optimal parameters. Torque speed characteristics at 25 Hz (figs. 5.11 and 5.12) and at 50 Hz (figs. 5.13 and 5.14) also confirm the above results.

Thus it can be concluded, that transients are less severe with optimal machine parameters, a point which goes strongly in favour of its adaptation.

5.3 RESULT:

A check is conducted for the possibility of any instability, at any operating frequency over a wide range of 1 Hz to 200 Hz using Routh-Hurwitz criterion, for a machine with recommended optimal machine parameters obtained in Chapter 4. These results are very encouraging as expected. The machine with optimal parameters become stable at almost all the frequencies.

The dynamic responses both with normal as well as optimal machine parameters have been computed. The transients are found to be less sever, the motor needs less settling time and torque speed characteristics are smoother with optimal parameters specially at low frequencies.

Thus it can be concluded that optimal machine parameters and the general design recommendations of Chapter 4, yield not only the minimum steady state torque pulsations, but an all round improvement in transient performance too. By adopting these design recommendations, stable region of operation increases considerably, and these gains offset the marginal loss incurred in terms of efficiency etc.

- o -

CHAPTER 6

EXPERIMENTAL VERIFICATION OF THE MATHEMATICAL MODEL:

To establish the validity and correctness of the computed results obtained using the near exact model developed in Chapter 1, the test motor was put to actual test under variable voltage and variable frequency condition. The inverter used for this purpose was a laboratory model designed and developed recently by Central Electronics Engineering Research Institute (CEERI), Pilani (Rajasthan).

6.1 EXPERIMENTAL SETUP:

The experimental setup consisted of the followings (fig. 6.1)

(i)   Test Motor

(ii)   3 H.P., 250 Volts, 2300 rpm, d.c. shunt generator for loading the test motor.

(iii)   Westing house's torque transducer of 8 ft.lb. capacity.

(iv)   5 KVA, 350 Volts (Line), 420 Volts (d.c.), 12 to 60 Hz, three phase bridge inverter.

(v)   Single phase bridge controlled rectifier.

(vi)   π-filter connected between the rectifier and the inverter to reduce ripple contents in the output of the rectifier.

The rectifier and the inverter controls are shown in terms of functional blocks in fig. 6.2 and 6.3.

FIG. 6.1 EXPERIMENTAL SETUP

FIG. 6-2 CONTROL FUNCTIONAL BLOCKS FOR RECTIFIER — INVERTER SYSTEM.
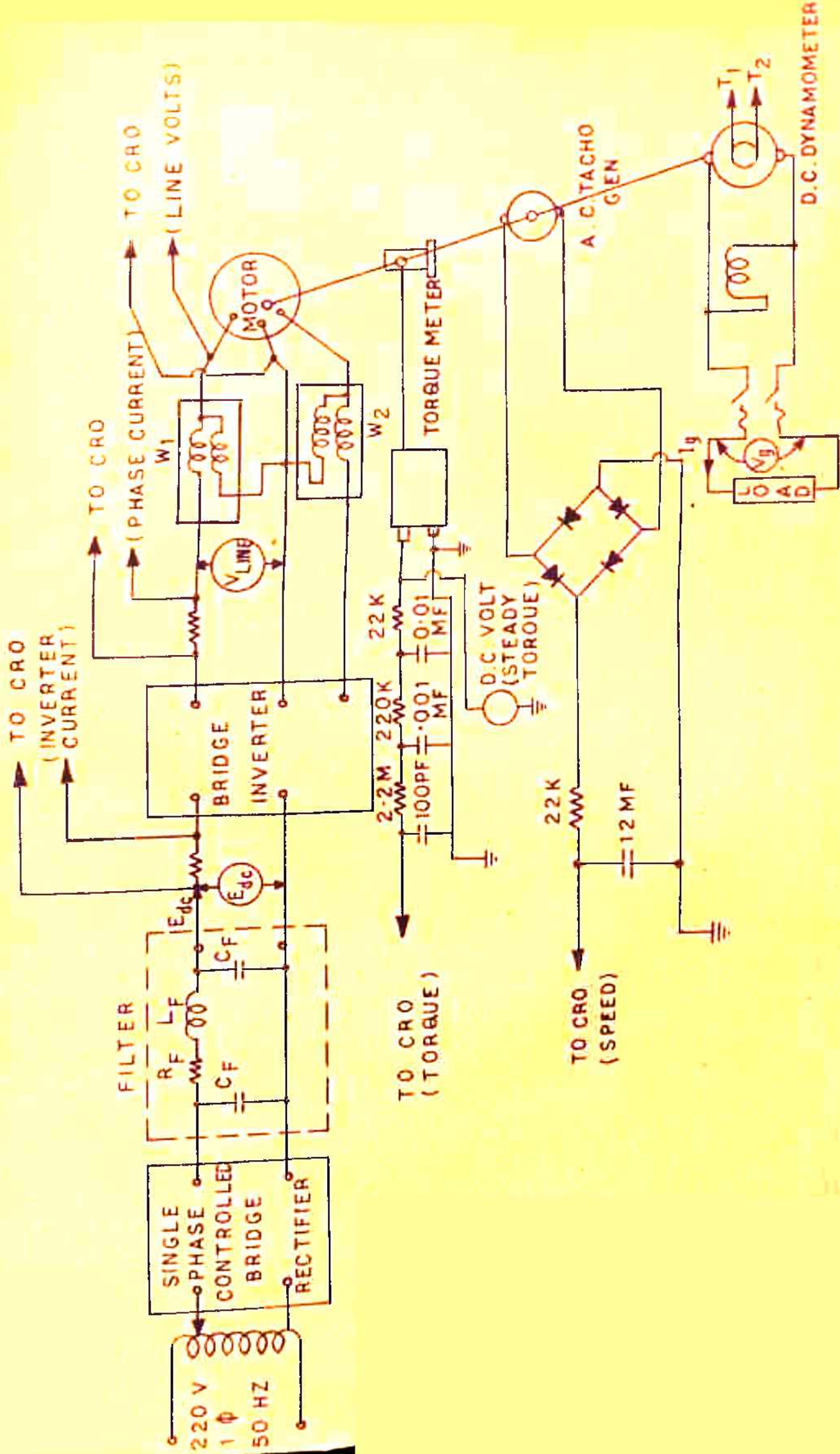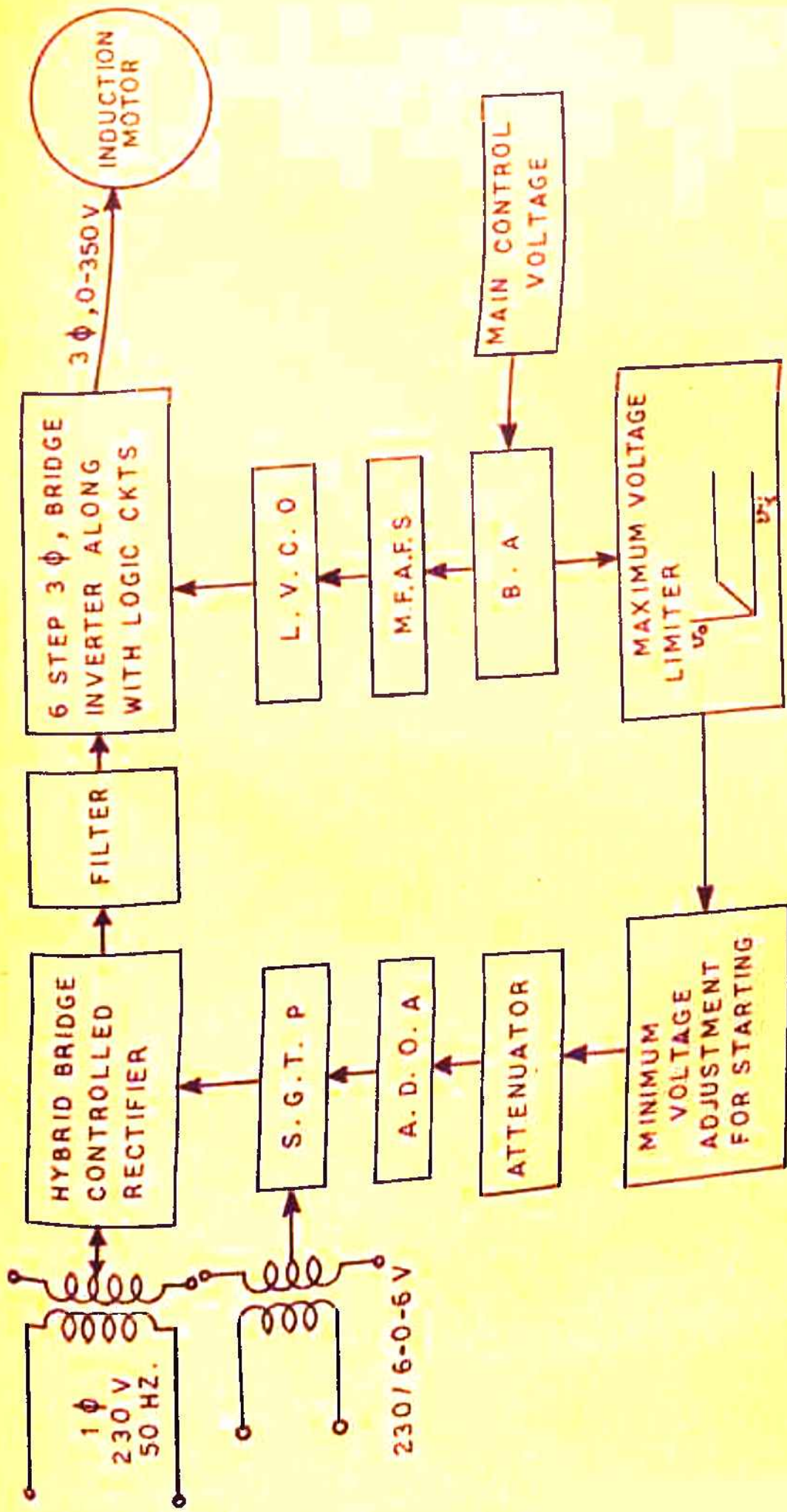
LEGEND

L. V. C. O. — LINEAR VOLTAGE CONTROLLED OSCILATOR.

M. F. A. F. S. — MINIMUM FREQUENCY ADJUSTMENT FOR STARTING.

B. A. — BUFFER AMPLIFIER.

S. G. T. P. — SYNCHRONISED GATE TRIGGER PULSE GEN.

A. D. O. A. — ADAPTIVE DIFFERENTIAL OPERATIONAL AMPLIFIER.
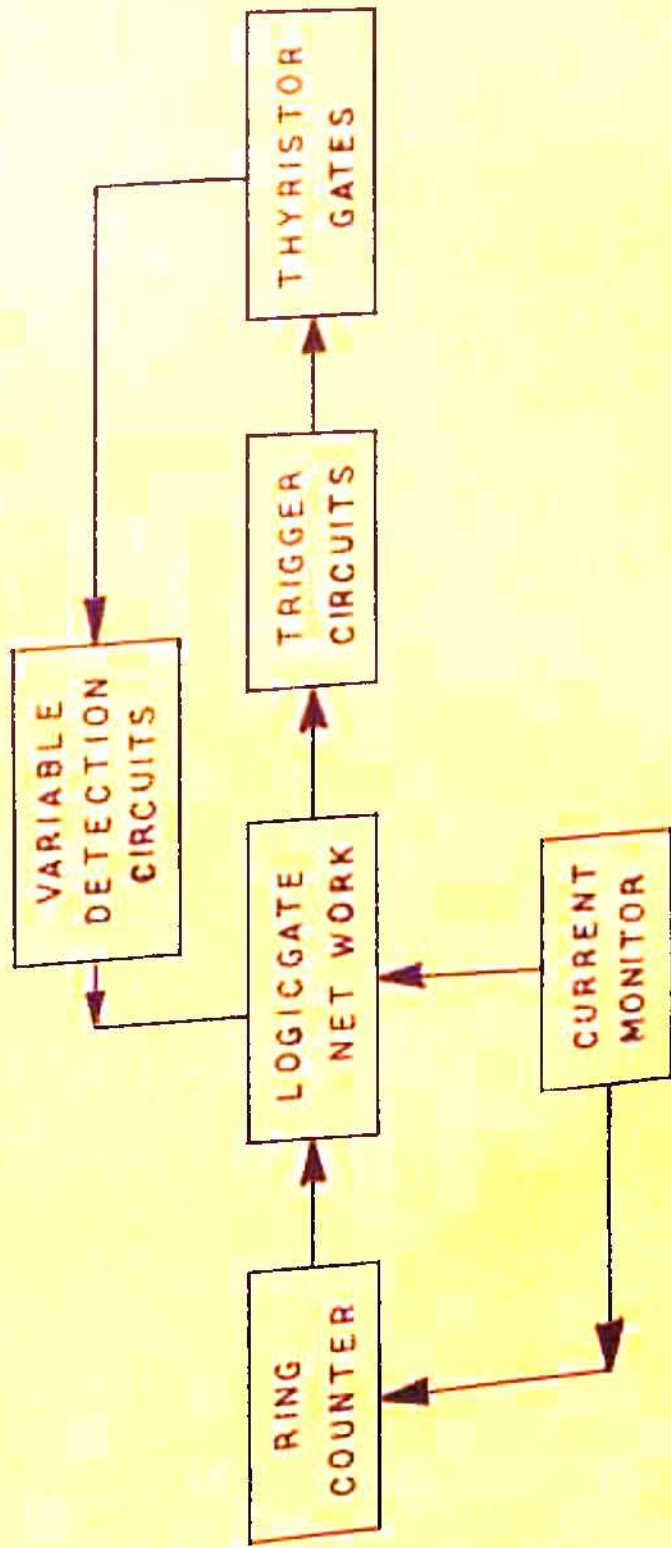
FIG. 6·3 BLOCK DIAGRAM OF LOGIC DESIGN.

The experiments were carried out under the following physical constraints, restricting the range of loading and range of operating frequency.

(i)   The thyristor used in the inverter were of 440 peak inverse voltage (PIV), restricting the maximum operating d.c. voltage to 420 volts.

(ii)   The dynamometer (d.c. shunt generator) fails to build up substantial voltage if run below 1700 rpm, thus full loading was not possible below 30 Hz operation of the induction motor.

(iii)   Commutation circuitry of the bridge inverter worked satisfactorily only in the frequency range of 12 to 60 Hz.

6.2   EXPERIMENTAL RESULTS:

The experimental performance characteristics like efficiency, power factor, slip and input phase current at constant full load torque for frequencies in the range of 30 to 42 Hz were obtained. The oscillographic displays of steady state pulsating torque, phase current, line voltage and inverter input current at various frequencies at quarter load and full load were also recorded. The results are compared with the computed ones.

(a)   Performance Characteristics:
The experiments were conducted at constant full load

output torque of 3.0 ft. lb (1.34 p.u.), for frequencies between 30 to 42 Hz. The ratio of phase voltage to frequency was kept constant. The observations were recorded for adjusted inputs. For convenience, these observations are given in table 6.1.

The calculated results along with corresponding computed results indicating the percentage error; are given in table 6.2. For overall and quick comparison the computed and the experimental results for all performance indices have been shown in graphical forms in fig. 6.4.

Table 6.1 Observations (Full Load Torque)

Torque meter gives 0.4 volt/ft.lb.

$T_{avg.}$ = Full load torque = 1.34 per unit (nearly 3 ft.lb.)

Motor input = $T_{avg.}$ x w + stator resistance losses + Iron losses.

	Adjusted Variables			Observed Variables			
Frequency	V_{phase}	Input to motor (watts)	$E_{d.c.}$	$I_{d.c.}$	Speed	$I_{a.c.}$	Torque meter reading
30	151.0	942	320	6.5	1700	2.9	1.2
32	162.0	1024	352	6.5	1800	3.0	1.2
35	177.0	1122	385	6.6	1970	3.05	1.21
37	186.0	1165	403	6.8	2120	3.0	1.18
40	197.0	1230	430	7.0	2260	3.15	1.20
42	206.0	1370	450	7.0	2420	3.1	1.22
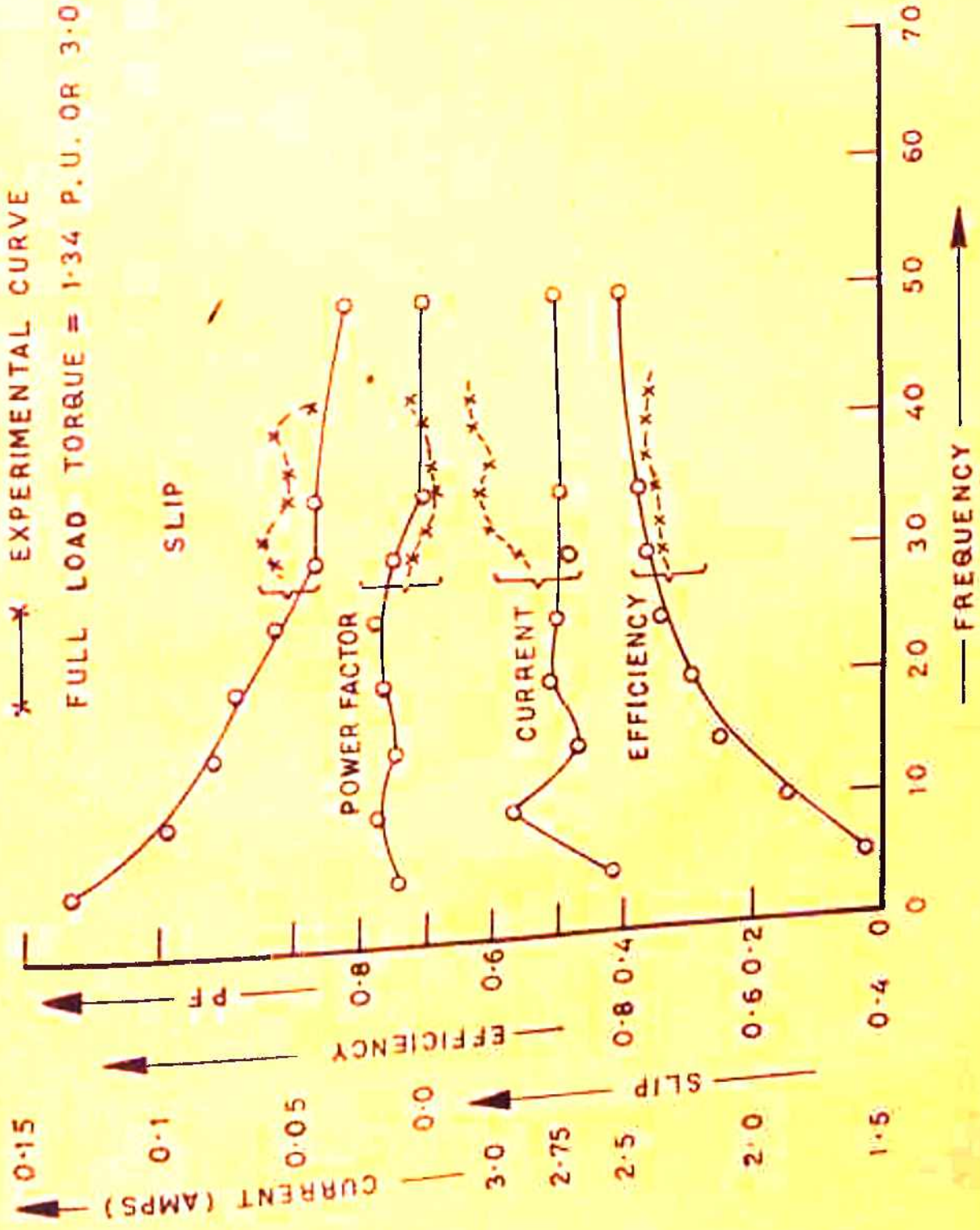
FIG. 6·4 COMPARISON OF COMPUTED AND EXPERIMENTAL RESULTS (AT CONSTANT FULL LOAD TORQUE)

177

Table 6.2 Comparison of Computed and Experimental Results (Full Load Torque)

Freq- uency	Power Factor			Efficiency			Slip			Current		
	COM	EXP	PE	COM	EXP	PE	COM	EXP	PE	COM	EXP	PE
30	.755	.72	+4.8	.76	.74	+2.7	.04	.055	-27.3	2.70	2.3	+6.90
32	.73	.70	+4.29	.77	.745	+3.5	.04	.06	-33.3	2.7	3.0	+10.0
35	.71	.69	+2.9	.775	.75	+3.3	.04	.05	-20.0	2.75	3.05	+ 9.85
37	.70	.69	+1.45	.78	.77	+1.30	.04	.05	-20.0	2.75	3.0	+ 8.35
40	.70	.70	0.0	.79	.76	+3.94	.0375	.055	-31.8	2.85	3.15	+ 9.54
42	.70	.72	-2.8	.79	.75	+5.34	.0372	.04	- 7.0	2.8	3.1	+ 9.7

COM   Computed Results

EXP   Experimental Results

PE   Percentage Error = $\dfrac{(EXP - COM)}{EXP}$ x 100

The experimental phase current is noticed to be 6 to 10 percent more than the computed values, but the actual power factors and efficiencies at various frequencies are poorer by 2 to 5 percent (table 6.2). Considering that the induction motor is coupled with 3 H.P. d.c. machine, for loading purpose which is not accounted in computation; it can be said that the computed and the experimental results are in quite close agreements with in the allowable experimental error.

(b)   Pulsating Torque Measurements:

Waveforms of pulsating torques at different loads and frequencies were recorded. Experimental values of peak pulsating torques (half of peak to peak value) are compared with the corresponding computed values (table 6.3).

Table 6.3   Torque Pulsations

Torque meter - 0.4 volt/ft.lb.

Frequency	Load torque (volts)	Exp.Peak Puls.torque		% peak puls. torque (computed)	% Error	C.R.O. display No.
		Peak value (volts)	% puls. torque			
15	0.18	0.25	140.0	125.0	+ 10.7	Fig.6.5
20	0.26	0.34	136.0	119.0	+ 12.5	Fig.6.6
25	0.30	0.36	120.0	97.5	+ 18.7	Fig.6.7
30	0.30	0.34	112.0	101.0	+ 9.8	Fig.6.8
30	1.20	0.38	31.7	20.5	+ 35.0	Fig.6.9
45	1.20	0.36	30.0	21.0	+ 30.0	Fig.6.10
50	1.20	0.32	26.7	21.4	+ 20.0	Fig.6.11

$$\% \text{ Error} = \left(\frac{\text{Experimental value} - \text{Computed value}}{\text{Experimental value}} \right) \times 100$$

The experimental results clearly establish the presence of pulsating torque of basic time period of $\frac{1}{6}$th of the operating frequency, when the induction motor is fed from nonsinusoidal voltage of the bridge inverter. The amplitude of these pulsations is as high as 140 percent of average torque at light load and at low frequencies. Torque pulsations decreases steeply as the load is increased, giving as low as 26.7 percent at 50 Hz at full load. The values of pulsating torques obtained from C.R.O. displays follow closely the computed results, giving errors in the range of + 10 percent to + 18 percent at light load and at low frequencies. But, the errors are quite substantial (+ 20 percent to + 35 percent), under full load condition. Another thing noticed from the displays of figs. 6.5 to 6.11, is that the peaks of the pulsating torques are not of uniform amplitude. This means, the torque signal is being modulated by some noise signal. The attempt to filter out the noise signal being generated by commutator brushes and mechanical coupling of the torque transducer[98], through a filter did not succeed because of the very closeness of the noise frequeney to that of torque signal. It seems that, the noise signal dominates over the actual pulsating torque signal at full load, giving erroneous results. The results

of torque pulsations at low frequencies, which are in close
agreement with the computed ones, fully establish the correct-
ness and hence the validity of the near exact model.

(c)   Phase Current and Line Voltage Waveforms:

The phase current waveforms for each frequency and
load as given in table 6.3 are shown in figs 6.12 to 6.18.
The computed current waveforms at 25 Hz, 0.75 ft. lb load
(.335 p.u.) torque and 50 Hz, 3.0 ft. lb. (1.34 p.u.) load
torque are given in figs. 6.22 and 6.23. When, compared,
the experimental waveforms (figs. 6.14 and 6.18) are found
to be in quite agreement with the computed ones.

The computed and the experimental line voltage wave-
forms as given in figs. 6.19 and 6.20 respectively, clearly
establish the earlier apprehension that the machine terminal
voltage need not remain of fixed nature at all the loads.
Fig. 6.21 gives the inverter input current, showing that the
inverter's current consists of ripples of 6th order reflected
from the motor side.

6.3   RESUME:

The limited experimental results obtained with in
many physical constraints of the immediately available
three phase, 6 step bridge inverter, are found to be
encouraging and in quite close agreement with the computed
ones. The performance indices like efficiency, power
factor, slip and current at full load are in line with their
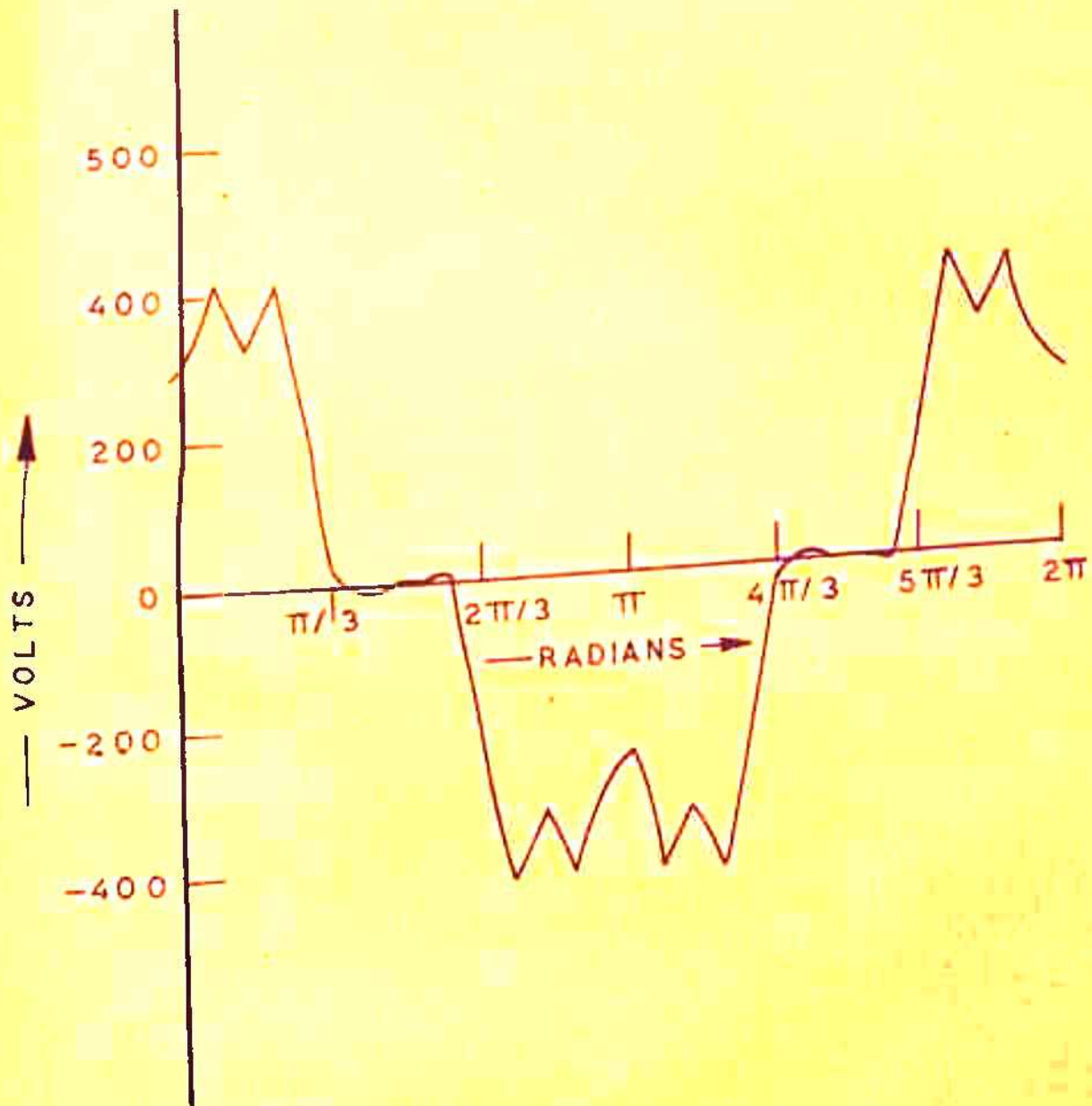
FIG. 6·19 LINE VOLTAGE, AT 50 HZ, FULL LOAD (COMPUTED)
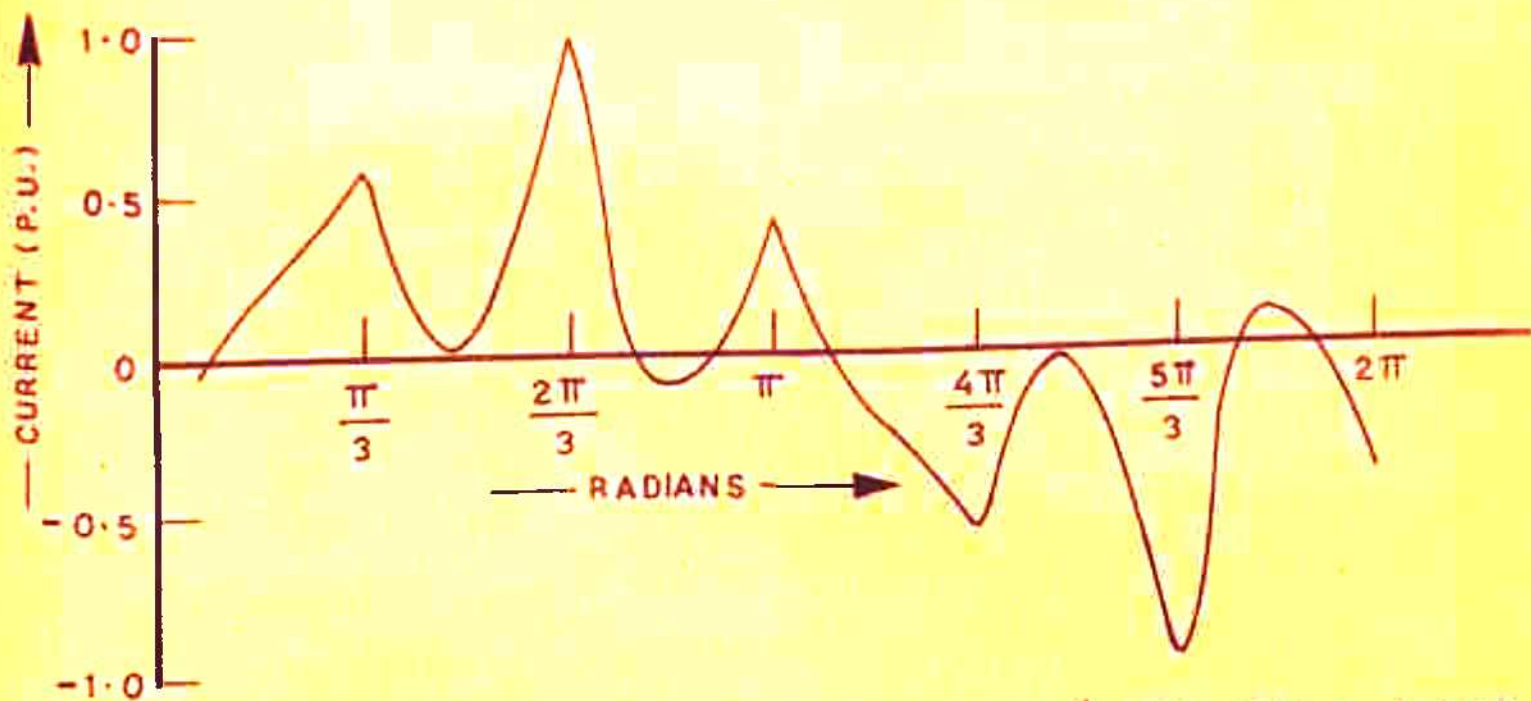
FIG. 6·22 PHASE CURRENT AT 25 HZ AT $\frac{1}{4}$ TH. FULL LOAD.
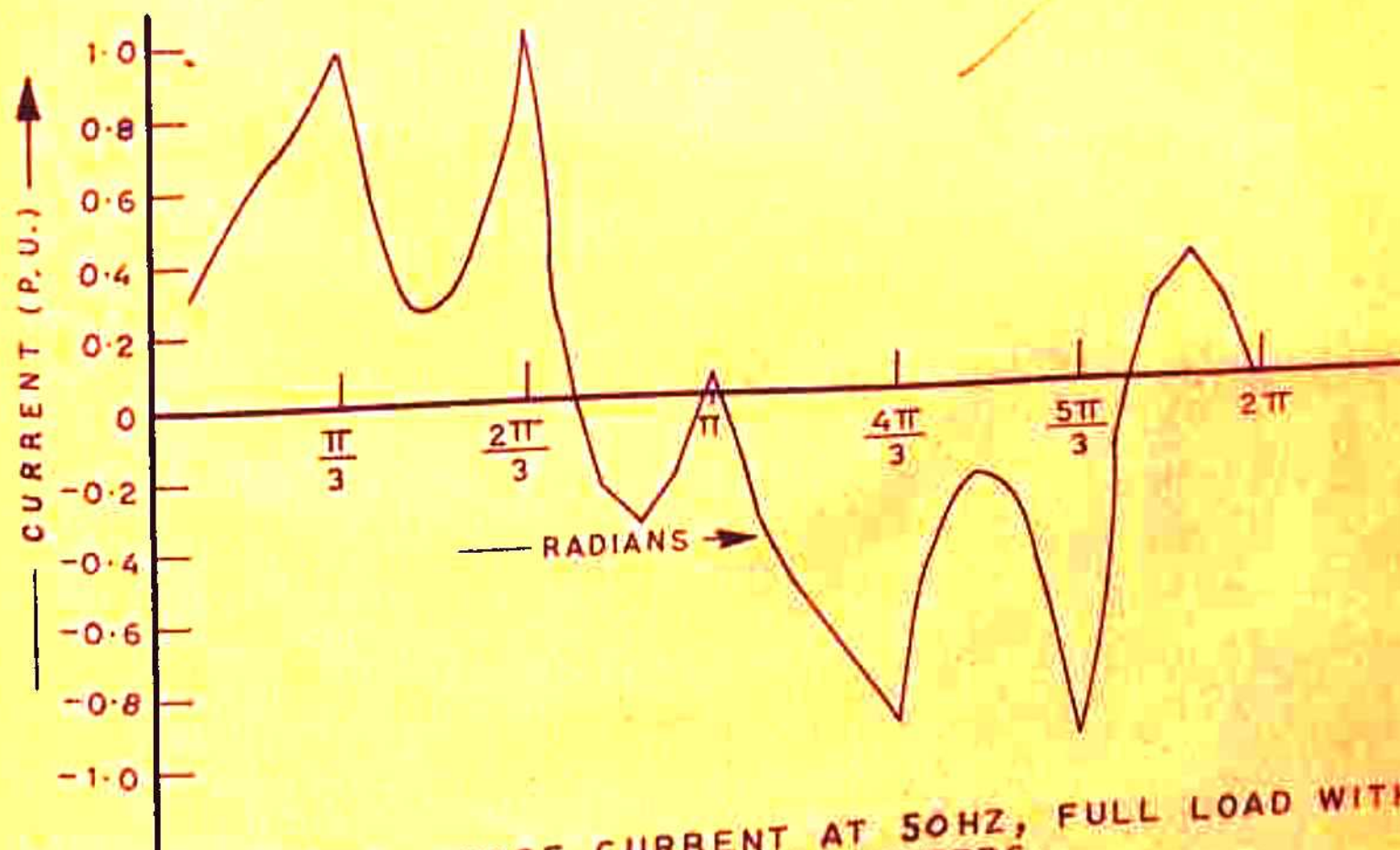
FIG. 6·23 STATOR PHASE CURRENT AT 50HZ, FULL LOAD WITH NORMAL PARAMETERS.

PLATE II
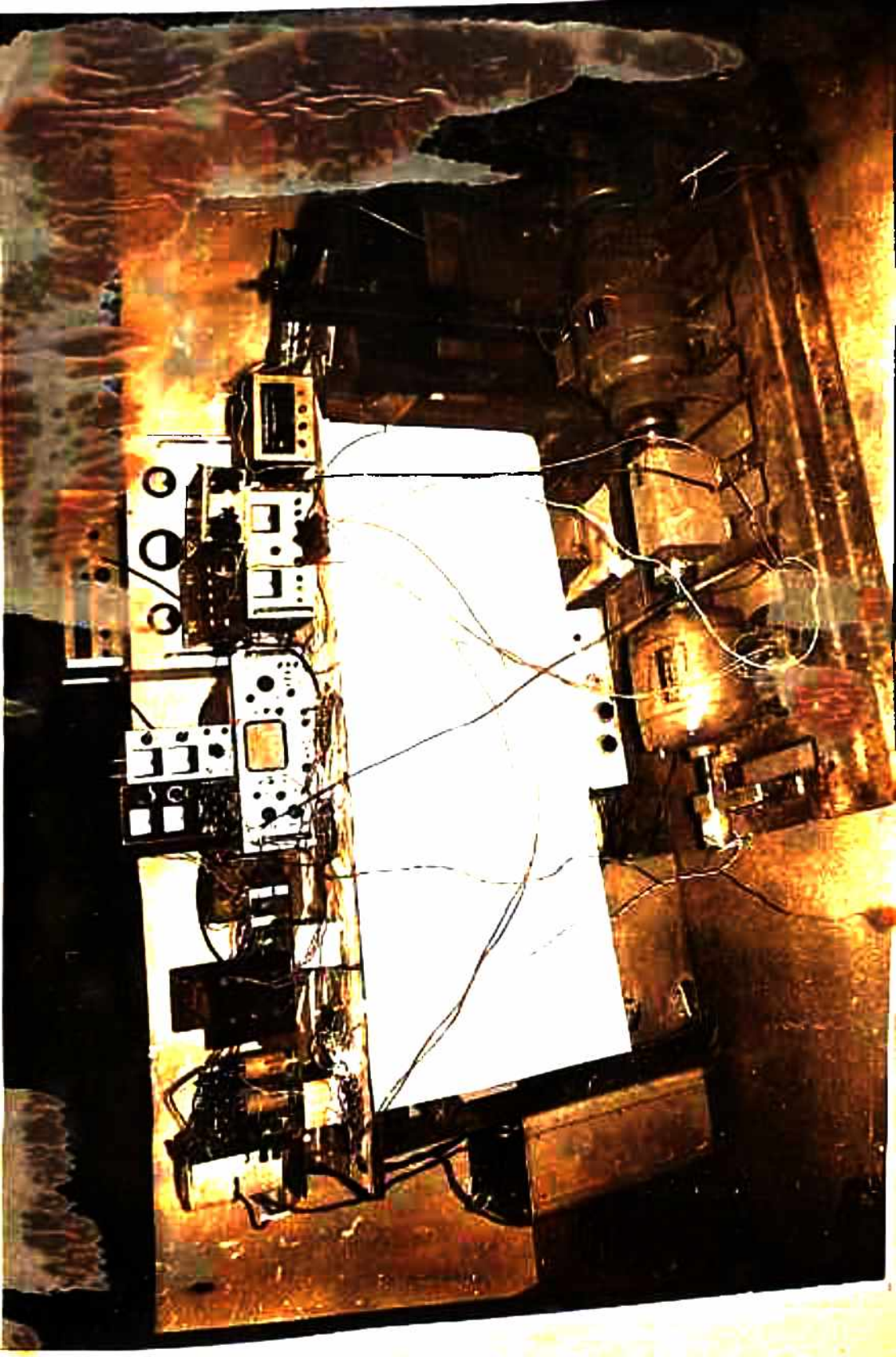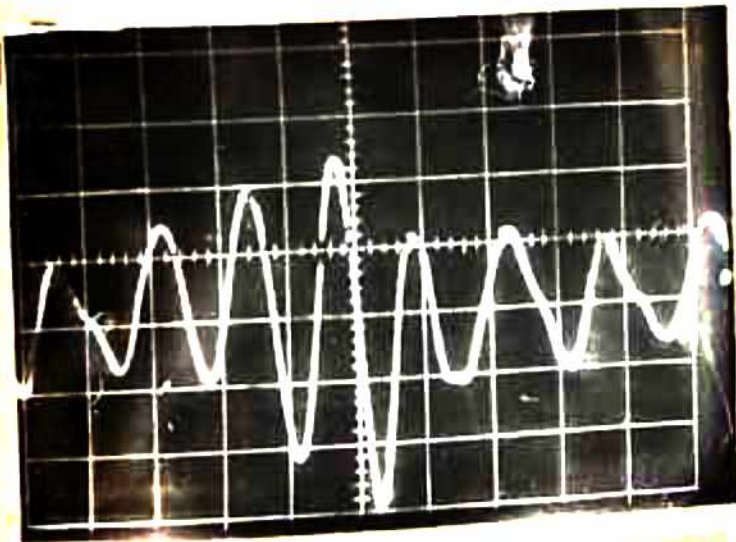
Fig. 6.5 Torque Pulsations 140%
at 15Hz, .45 ft.lb.load torque
X = 6.6 x 10 msec., Y= 5.0 x 0.1
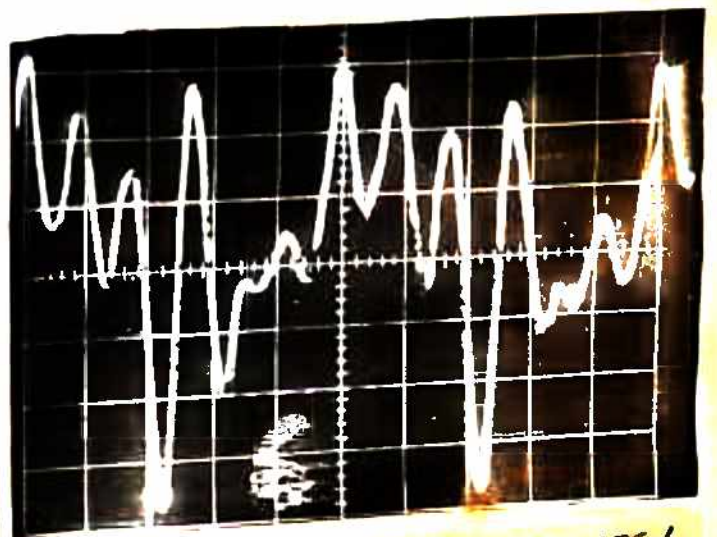
Fig. 6.6 Torque Pulsations 136%
at 20Hz, 0.65 ft.lb load torque
X = 5.0 x 10 msec., Y = 6.8 x0.1

Fig. 6.7 Torque Pulsations 120%
at 25Hz, 0.75 ft.lb load torque
X = 4x10 msec., Y = 3.6 x 0.2

Fig. 6.8 Torque Pulsations 110%
at 30 Hz, 0.75 ft.lb.load torque
X = 3.4 x 10 msec., Y = 6.8x0.1

PLATE III
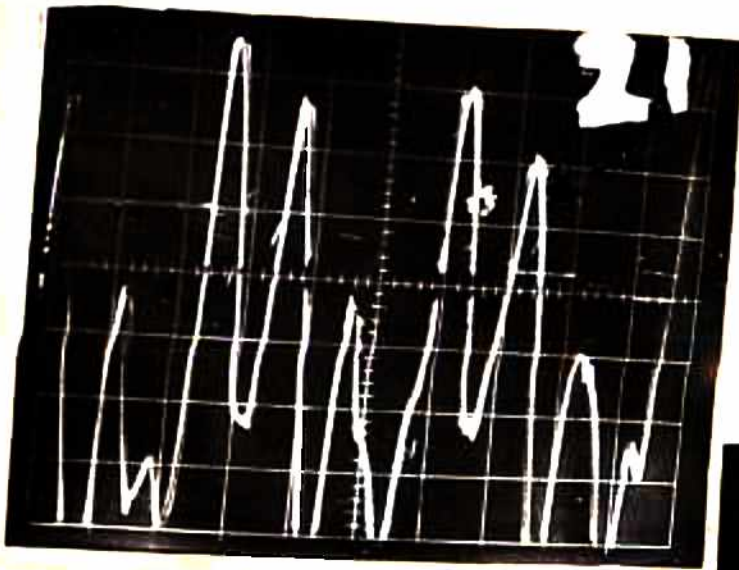
Fig. 6.9 Torque Pulsations 31.7%
at 30Hz, 3.0 ft.lb.load torque
X = 7.0 x 5 msec., Y = 7.6x0.1

Fig. 6.10 Torque Pulsations 30.0%
at 45Hz, 3.0 ft.lb load torque
X = 4.5 x 5 msec., Y = 7.2 x 0.1
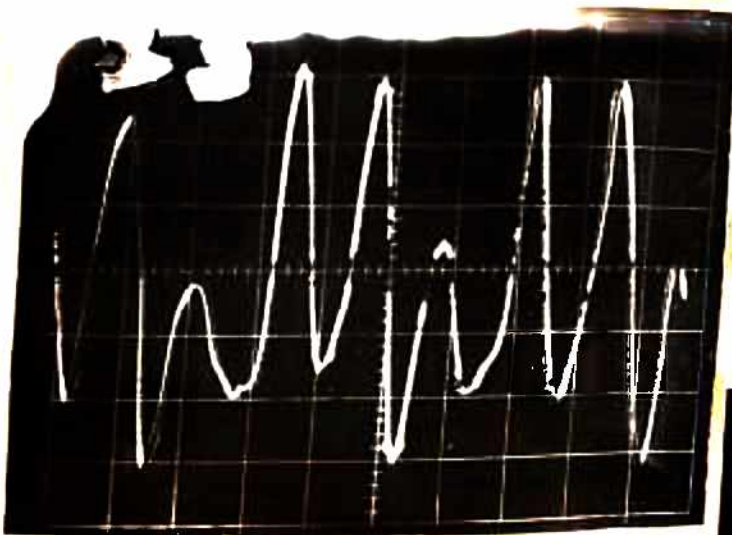
Fig. 6.11 Torque Pulsations 26.7%
at 50Hz, 3.0 ft.lb. load torque
X = 4 x 5 msec., Y = 6.4 x 0.1
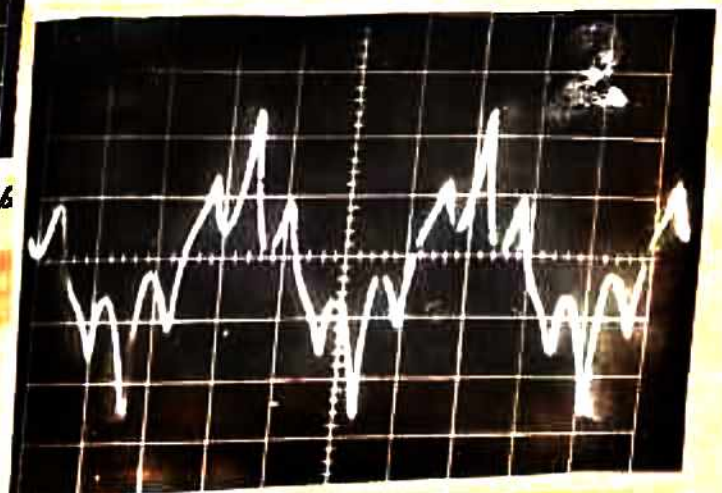
Fig. 6.12 Phase Current at
15Hz, 0.45 ft.lb. load torque

PLATE IV
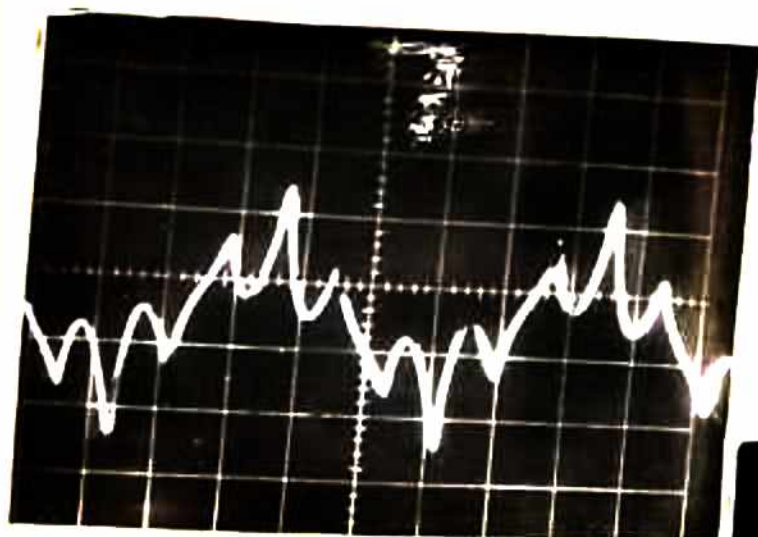
Fig. 6.13 Phase Current at
20Hz, 0.65 ft.lb. load torque

Fig. 6.14 Phase Current at
25Hz, 0.75 ft.lb. load torque
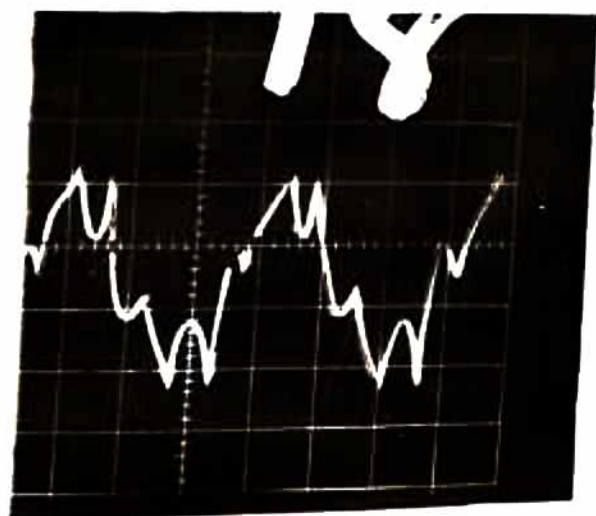
Fig. 6.15 Phase Current at
30Hz, 0.75 ft.lb. load torque
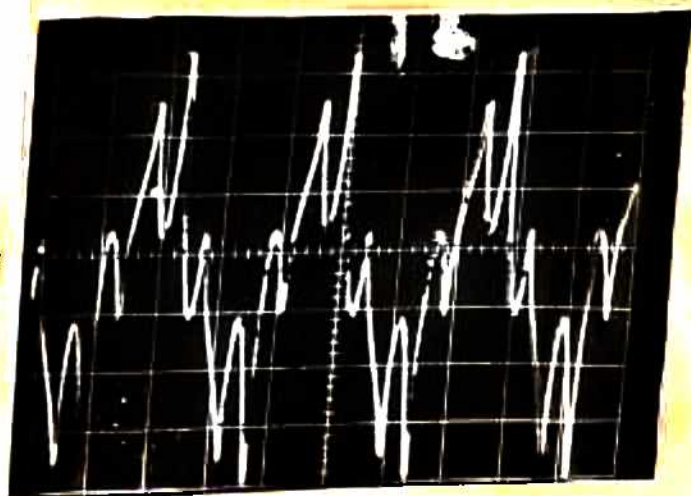
Fig. 6.16 Phase Current at
30Hz, 3.0 ft.lb. load torque

PLATE V
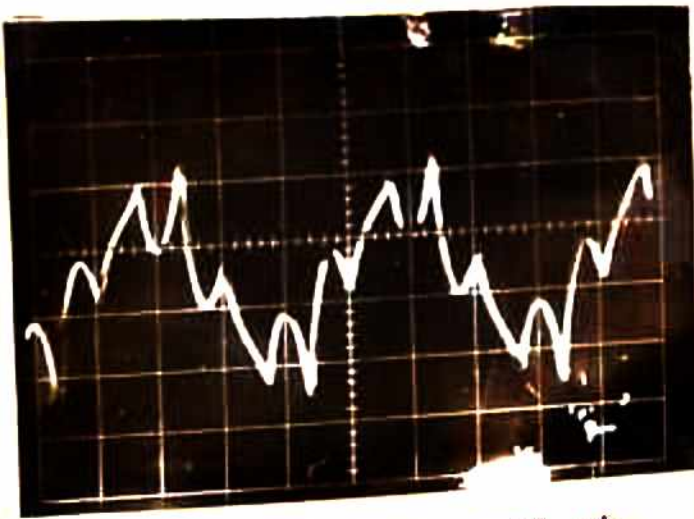
Fig. 6.17 Phase Current at
45Hz, 3.0ft.lb.load torque
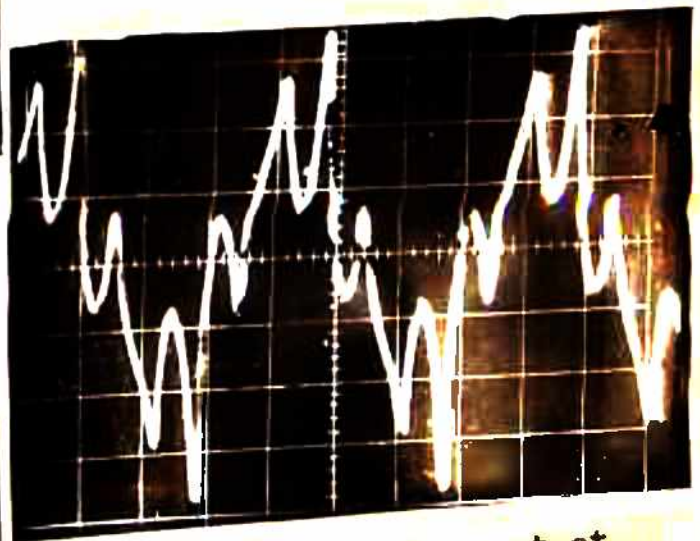
Fig. 6.18 Phase Current at
50Hz, 3.0 ft.lb. load torque
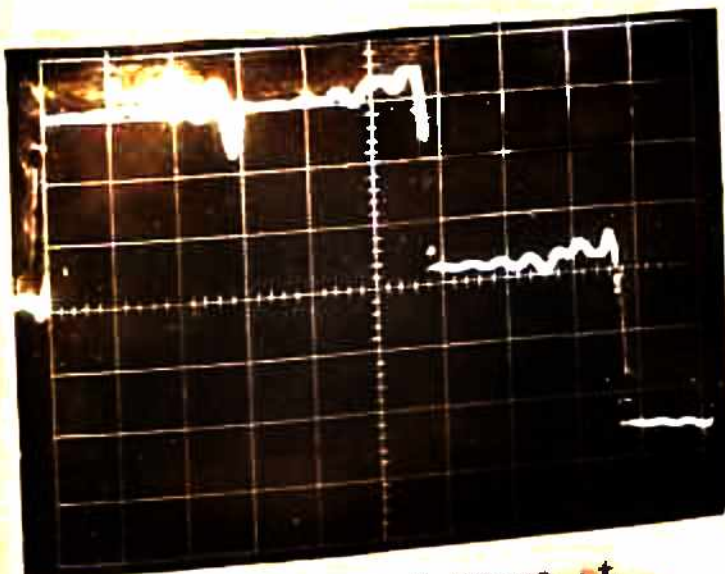
Fig. 6.20 Line Voltage at
50Hz, 3.0 ft.lb. load torque
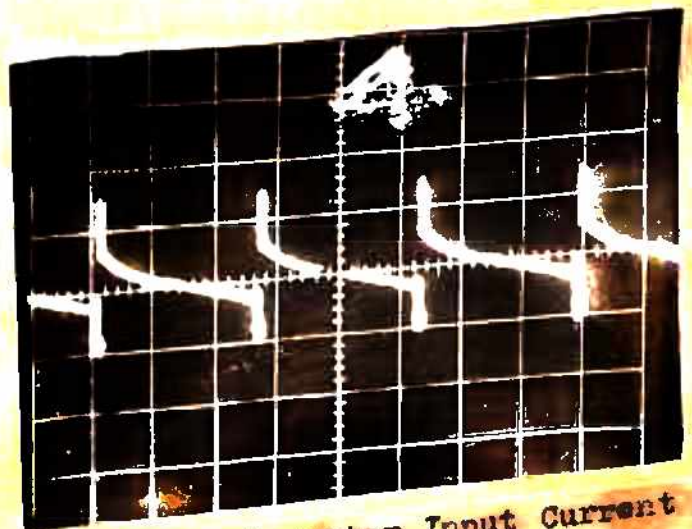
Fig. 6.21 Inverter Input Current

CONCLUSIONS:

With the availability of high power, reliable and efficient frequency converters; it has become possible to make the induction motor a versatile, wide speed range electrical drive. The variable frequency drive has resulted in many new problems relating to the performance of an induction motor. One such problem of importance in the application of a rectifier inverter induction motor drive is that of large speed and torque pulsations specially at low frequencies. In the present work a new methodology, for predicting the performance characteristics of the inverter fed induction motor, has been developed special attention has been paid to the steady state torque pulsations and their minimisation.

A comprehensive but simple mathematical model has been developed for a inverter fed, variable speed drive system. Three axis commutator transformation is used to establish a link between a.c. and d.c. variables. The system equations are formulated at the d.c. terminals of the inverter. The changing network topology of the system due to the periodic switching action of the inverter, is accounted by formulating suitable Kron's connection matrix for each state. The model also duly accounts the effects of filter parameters, ripples present in the rectified output, and the thyristor's forward impedances. The system equations are converted into standard first order state space equations, retaining the phase currents and the capacitor voltage as the state variables

for computational ease and simplicity.

The effects of high frequency harmonic excitations present in the inverter output, over the stator and rotor resistances, and over the various losses are considered. In particular, the importance of losses due to end leakage flux, high frequency flux pulsations and skew leakage flux has been well demonstrated. The methods of calculations of stray load losses with sinusoidal excitations whose accuracy have been well established by earlier researchers; have been used to formulate expressions for such losses with nonsinusoidal excitations.

A systematic study of the effects of machine and filter parameters on steady state torque pulsations and on other relevant performance characteristics is carried out using the developed model. The motor is considered as constant torque drive for all frequencies less than or equal to its normal operating frequency; and constant horse power drive for frequencies greater than normal. Computed results are reported for large sets of system parameters.

It is found, that the large values of leakage and magnetising inductances, tend to decrease the pulsating torques appreciably, with a corresponding marginal decrease in efficiency and power factor values. The large stator resistance also help in dampening the torque pulsations, but at the cost of efficiency. The rotor resistance is proved to be ineffective for torque pulsations. It is also shown

that the pulsating torque can be kept with in a reasonable value, by properly selecting the filter capacitor. The effects of variation of filter inductance are only marginal. It appears that the method of analysis presented herein is adequate to predict the magnitudes of pulsating torques for any change in system parameters.

The other aspect of the work is the search for an optimal set of machine parameters, giving the minimum torque pulsations. A simultaneous search for minimisation with respect to the few selected machine parameters and for maximisation with respect to the frequency, is carried out with in the feasible design constraints on the independent variables. Rosenbrock's HILL CLIMB METHOD has been used as MIN-MAX technique for this purpose.

The feasible optimal machine parameters confirm, that the design considerations for a variable frequency operation of induction motor are far more different than those of normal fixed frequency induction motor. Though the performance is deteriorated a little from the economic point of view but a motor with optimal parameters is certainly preferably to have minimum pulsating torque. The suitable general design recommendations have been evolved to translate the optimal parameters into practice.

The machine with recommended optimal machine parameters, has been tested for any instability using Routh-Hurwitz

criterion over a frequency range of 5 to 200 Hz; and is found to be stable at almost all the frequencies. The transient torque, speed and current characteristics with optimal machine parameters are computed and compared with those obtained with normal machine parameters. The transients are found to be less severe, the motor needs less settling time, and torque speed characteristics are smoother with optimal parameters. Thus it can be concluded that optimal machine parameters and the general design recommendations, yield not only the minimum steady state torque pulsations; but an all round improvement in transient performance too.

The computed results with normal machine parameters at various frequencies are experimentally verified using a recently developed six step bridge inverter by Central Electronics Engineering Research Institute, Pilani. The experimental results are found to be in close agreement with computed ones in general, establishing the correctness of the unified mathematical model.

The FURTHER WORK, of investigation of dynamics of the system, with the available computer programmes; can immediately be taken up. For example, system response for a sudden change in frequency, inverter's input voltage or load torque needs to be probed further. To find the degree of severity of transients under different fault conditions, or due to the partial failure of the commutation or triggering circuits;

is another area where the present mathematical model can be usefully employed. This information may prove to be very useful for the design of protective circuitry of thyristors. The stability studies of the closed loop system by incorporating speed monitored triggering circuitry, is the proposed extension of the present work.

- o -

REFERENCES:

1.   A.I.E.E. Committee Report. 'Stray load loss measurement in Induction machines'. AIEE Trans. Pt III, Vol PAS-78, April 1959, p67-71.

2.   Alger, P.L.; Angst, G.; Davies, E. John 'Stray load losses in polyphase Induction machines'. AIEE Trans., Pt III-A, Vol PAS-78, June 1959, p343-357.

3.   Alger, P.L. 'Nature of polyphase Induction machines'. (book) John Wiley and Sons, Inc. N.Y. 1951.

4.   Aoki, Masano 'Introduction to Optimisation techniques' (book) Macmillan Company, N.Y. 1971.

5.   Barnes, E.C. 'Performance and characteristics of Induction motors for solid state variable frequency' IEEE, IGA group conference record, 1969, p653.

6.   Beathe, W.C.; Monteeth, W. 'Digital modelling of a thyristor' Proc. IEE, Vol-120, No.7, July 1973, p786.

7.   Bedford, B.D.; Hoft, R.G. 'Principles of Inverter Circuits'. John Wiley and Sons, Inc. N.Y. 1964.

8.   Bedford, R.E.; Nene, Vilas D. 'Voltage control of the three phase Induction motor by thyristor switching: a time domain analysis using $\alpha\beta o$ transformation'. IEEE Trans., Vol IGA-6, No.6, Nov./Dec. 1970, p553-561.

9.   Bellini, Armando; Cioffi, Giacoma 'Induction machine frequency control : 3 phase bridge inverter behaviour and performance'. IEEE Trans., Vol IGA-7, No. 4, July/Aug. 1971.

10. Berg, G.J.; Serkar, A.K. 'Speed change of Induction motors with variable frequency supply'. IEEE Trans., Vol PAS-90, March 1971, p500-508.

11. Bradley, D.A.; Clarke, C.D.; David, R.M. 'Adjustable frequency inverter and their applications to variable speed drives'. Proc. IEE, Vol-111, No.11, Nov.1964, p1838.

12. Chalmers, B.J. 'Induction motor losses due to nonsinusoidal supply waveforms'. Proc. IEE, Vol-115, No. 12, Dec. 1968, p1777.

13. Chalmers, B.J.; Narain, C.K. 'High frequency no load losses of cage Induction motors'. IEEE Trans., Vol PAS-89, 1970, p1043.

14. Charlton, W. 'Matrix method for the steady state analysis of inverter fed Induction motor'. Proc. IEE, Vol-120, No.3, March 1973, p364.

15. Cooper, L. 'Heuristic methods for location allocation problems'. SIAM Review, Vol-6, 1964, p1.

16. Corey, P.D. 'Methods for optimising the waveform of stepped wave static inverters'. AIEE paper, CP62-1147, Denver, June 17-22, 1962.

17. Dewan, S.B.; Duff, D.L. 'Optimum design of an input commutated inverter for a.c. motor control'. IEEE Trans., Vol IGA-5, 1969, p699.

18. Dewan, S.B.; Rosenberg, S.A. 'Output voltage in three phase pulse width modulated inverter'. IEEE Trans., Vol IGA-6, 1970, p570.

19. Arlicki, M.S. 'Optimised parameter analysis of an Induction machine'. IEEE Trans., Vol PAS-84, No.11, Nov. 1965, p1017.

20. Fallside, F.; Wortley, A.T. 'Steady state oscillation and stabilisation of variable frequency inverter fed Induction motor drives'. Proc. IEE, Vol. 116, No. 6, June 1969, p991.

21. Griffin, A.; Ramshaw, R.S. 'The thyristor and its applications'. (book) Chapman and Hall Ltd. 1965.

22. Gutzwiller, F.W. and others.'Semiconductor Controlled Rectifiers'. (book) Prentice-Hall, Inc., Englewood Cliffs, N.J. 1964.

23. Hansen, A.; Wilkerson, A.W. 'Automatic speed regulation of d.c. motors using combined armature voltage and motor field control'. IEEE Trans. Vol. PAS-80, 1961, p59-64.

24. Harashima, F.; Uchida, K. 'Analysis of inverter Induction motor system by state transition method'. EE in Japan, Vol-89, No. 12, 1969, p27-34.

25. Hayashi, N. 'State variable analysis of Induction motor controlled by semiconductor switches'. EE in Japan, Vol-91, No. 12, Nov./Dec.1971, p153.

26. Heller, B.; Jokl, A.L. 'Losses in squirrel cage motors due to rotor skew '. IEEE Trans. Vol PAS-90, March/April 1971, p556.

27. Helmick, C.G. 'Present status of adjustable frequency drive applications'. IEEE, IGA group, second annual conference, 1967, p275.

28. Heumann, K. 'Pulse control of d.c. and a.c. motors by silicon controlled rectifiers'. IEEE Trans., Vol CE-83 (Comm. and Elect.), 1964, p397.

29. Humphrey, A.J. 'Constant horse power operation of Induction motor'. IEEE, IGA group conference record, 1968, p743.

30. Jacovides, Linos.J. 'Analysis of Induction motor drives with nonsinusoidal supply voltage using fourier analysis'. IEEE Trans., Vol IA-9, No.6, Nov./Dec.1973, p741.

31. Jain, G.C. 'The effect of voltage waveshapes on the performance of a three phase Induction motor'. IEEE Trans., Vol PAS-83, 1964, p561-566.

32. Johnston, R.W.; Newill, W.J. 'Variable speed Induction motor drive system for industrial applications', IEEE, IGA group conference record, 1970, p581.

33. Jones, C.V. 'Unified theory of electrical machines'. Butter worths, London, 1967.

34. Jordan, H.E. 'Analysis of Induction machine in dynamic systems'. IEEE Trans., Vol PAS-84, Nov.1965, p1080-1088.

35. Kiefer, J. 'Sequential minimax search for a maximum'. Proc. Am. Math. Soc., Vol-4, 1953, p502.

36. Klingshirin, Eugene. A. 'Induction motor losses due to nonsinusoidal voltages'. IEEE Trans., Vol PAS-87, March 1968, p624-31.

37. Krause, P.C. 'Method of multiple reference frames applied to the analysis of symmetrical Induction machinery'. IEEE Trans., Vol PAS-87, Jan. 1968, p218-227.

38. Krause, P.C.; Lipo, T.A. 'Analysis and simplified representation of a rectifier inverter Induction motor drive'. IEEE Trans., Vol PAS-88, No.5, May 1969, p588-596.

39. Kron, G. 'Tensor analysis of networks' (book) John Wiley, 1939, reprinted by Macdonald 1965.

40. Kuester, L.J. 'Optimisation Fortran' (book), McGraw Hill Book Company 1973.

41. Kuhlmann, J.H. 'Design of electrical appratue'. (book) John Wiley and Sons.

42. Kuo, B.C. 'Automatic Control Systems'. (book) Prentice Hall (India), 1961.

43. Lach, K.D. 'A study of the effect of variable frequency operation on Induction motor stability'. IEEE Trans. Vol IECI-15, Nov.1968, p43-47.

44. Lamb, C.S.J. 'Commutatorless a.c. voltage fed variable speed motor'. Proc. IEE, Vol-110, No. 12, Dec. 1963, p2221-7.

45. Lavi, A.; Polge, R.J. 'Induction motor speed control with static inverter in the rotor'. IEEE Trans., Vol PAS-85, No.1, Jan. 1966, p76-84.

46. Landun, I.D. 'Wide range speed control of three phase, squirrel cage Induction motors using static frequency converters'. IEEE, IGA group conference record, 1969, p591.

47. Lawrenson, P.J.; Stephenson, M.J. 'Note on Induction machine performance with a variable frequency supply'. Proc. IEE, 1966, p1617, discussion in Vol-115, 1968, p1540.

48. Li, K.Y.G. 'Induction motor, inverter fed variable speed analysis and operation'. Proc. IEE, Vol-116, 1969, p1571.

49. Lipo, T.A.; Krause, P.C.1 Jordan, H.E. 'Harmonic torque and speed pulsations in a rectifier inverter Induction motor drive'. IEEE Trans. Vol PAS-88, May 1969, p579.

50. Lipo, T.A.; Krause, P.C. 'Stability analysis of a rectifier inverter Induction motor drive'. IEEE Trans., Vol PAS-88, Jan. 1969, p55-66.

51. Liwschitz-Garik, M.M. 'Computation of skin effect in bars of squirrel cage rotor'. AIEE Trans., Power appratus and systems, Vol-74, 1955, p768-781.

52. Louden, R.K. 'Programming the IBM 1130 and 1800' (book) Prentice-Hall, 1367.

53. Ludbrock, Allan 'Basic economics of thyristor adjustable speed drive system'. IEEE, IGA group annual conference record, 1969.

54. McMurray, W.'SCR inverter commutated by an auxiliary impulse'. IEEE Trans., Comm. Elect., Vol-83, 1964, p824-29.

55. McMurray, W.; Shattuck, D.P. 'A silicon controlled rectifier inverter with improved commutation'. IEEE Trans. Comm. Elect. Vol-80, 1961,p531-542.

56. Mclean, G.W.; Mix, G.P.; Alwash, S.R. 'With square wave excitation performance and design of Induction motor'. Proc. IEE 1969, Vol-116, p1405-1412.

57. Molerytyki, B. 'Pulse width modulated inverter for a.c. motor drives' IEEE International, Conference record, Vol-8, 1966, p8-23.

58. Murphy, J.M.D. 'Thyristor control of a.c. motors'. (book) Pergamon Press 1973.

59. Nassar, A. 'Electromagnetic Energy Conversion' (book) McGraw-Hill N.Y. 1971.

60. Nelson, R.H.; Lipo, T.A.; Krause, P.C. 'Stability analysis of a symmetrical Induction machine'. IEEE Trans, Vol PAS-88, No. 11, Nov. 1969, p1710.

61. Novotny, D.W.; Fath, A.F. 'The analysis of Induction machines controlled by series connected semiconductor switches'. IEEE Trans., Vol PAS-87, No.2, Feb. 1968, p597-604.

62. Odok, A.M. 'Stray load losses and stray torques in Induction machines'. AIEE Trans. Vol-77, Pt III, Power appratus and systems, 1958, p43-53.

63. Oliver, L.T.; Wilde, D.J. 'Symmetric sequential minimax search for a maximum'. Chem. Eng. Dept. Tech. Report, The University of Texas.

64. Paice, D.A. 'Speed control of large Induction motors by thyristor converters'. IEEE Trans. Vol IGA-5, No.5, Sept./Oct. 1969, p545-551.

65. Pelly, B.R. 'Thyristor phase controlled converters and cycloconverters'. (book) John Wiley, Interscience, N.Y. 1971.

66. Pipes, Louis. A. 'Applied mathematics for engineers and physicists'. (book) McGraw-Hill 1958.

67. Powell, M.J.D. 'A survey of numerical methods for unconstrained optimisation' SIAM Review, Vol-12, Jan. 1970, p79-97.

68. Ramamoorthy, M. 'Matrix method for the steady state analysis of inverter fed Induction motor'. Proc. IEE, Vol-120, No.9, Sept. 1973, p1015.

69. Ramesh, M. Robertson, S.D.T. 'Induction machine instability predictions based on equivalent circuits'. IEEE Trans., Vol PAS-92, No.2, March/April 1973, p801.

70. Ramshaw, R.S. 'Power Electronics' (book) Chapman and Hall 1973.

71. Revankar, G.N. 'Topological approach to thyristor circuit analysis'. Proc. IEE, Vol-120, No.11, 1973, p1403.

72. Rieberg, R.L. 'A wide speed inverter fed Induction motor drive' IEEE, IGA group, Conference record 1969, p629.

73. Robertson, S.D.T.; Hebbar, K.M. 'A digital model for three phase Induction motor'. IEEE Trans., Vol PAS-88, No.11, Nov. 1969, p1624-34.

74. Robertson, S.D.T.; Hebbar, K.M. 'Torque pulsations in Induction motors with inverter drives'. IEEE Trans, Vol IGA-7, No.2, March/April 1971, p318.

75. Rogers, G.J. 'Linearised analysis of Induction motor transients'. Proc. IEE, Vol-112, No. 10, Oct. 1965, p1917.

76. Rosenbrook, H.H. 'An automatic method for finding the greatest or least value of a function'. Computer.J. Vol-3, 1960, p175-184.

139

77.   Sabbagh, S.M.; Shewan, W. 'Characteristics of an
        adjustable speed polyphase Induction machine'.
        IEEE Trans, Vol PAS-87, March 1968, p613-624.

78.   Salihi, T. Jalal.'An Inverter for traction applications'.
        IEEE Trans. Vol IA-8, Sept./Oct. 1972,p644.

79.   Sarkar, A. De.; Berg, G.J. 'Digital simulation of
        three phase, Induction motor'. IEEE Trans., Vol PAS-89,
        1970, p1031-39.

80.   Say, M.G. 'Performance and design of a.c. machines'.
        (book) English Language Book Society, London.

81.   Schaefer, J. 'Rectifier Circuits'(book) John Wiley and
        Sons. N.Y.

82.   Schwartz, K.K. 'Stray load losses in squirrel cage
        Induction motor'. Proc. IEE 1964, Vol-111, p1565.

83.   Shepherd, W. 'On the analysis of the three phase
        Induction motor with voltage control by thyristor
        switching'. IEEE Trans., Vol IGA-4, No.3, May/June
        1968, p304-311.

84.   Shepherd, W.; Stanway, J.'The silicon controlled
        rectifier a.c. switch for the control of one phase
        series and transformer loads'. IEEE International
        Conference Record, 1964, p155-63.

85.   Smith, I.R.; Sriharan, S. 'Transient performance of
        the Induction motor'. Proc. IEE, Vol-113, No.7,
        July 1966, p1173.

86. Smith, I.R.; Hamill, B. 'Effect of parameter variations on Induction motor Transients'. Proc. IEE, Vol-120, Dec. 1973, No. 12, p1483.

87. Spang, H.A. 'A review of minimisation techniques for nonlinear equations'. SIAM Review, Vol-4, Oct. 1962, p343-65.

88. Stanton, R.G. 'Numerical methods for science and engineering'. (book) Englewood Cliffs, N.J. Prentice-Hall 1961.

89. Still, A.; Siskind, C. 'Elements of electrical machine design'. (book) McGraw-Hill Book Company.

90. Swann, S.A., Salmon, J.W. 'Effective resistance and reactance of a solid cylindrical conductor placed in a semiclosed slot'. Proc. IEE, Vol-109C, 1962, p611-615.

91. Swann, W.H. 'Report on the development of a new direct search method of optimisation'. I.C.I. Ltd., Central Instrument Research Note, 64/3, England 1964.

92. Takeuchi, J.; Madea, A.; Iida, B. 'A three phase Induction motor controlled by a bridge type SCR inverter'. EE in Japan, Vol-88, No.2, 1968, p46.

93. Takeuchi, T.J. 'Characteristics of a.c. motors controlled by general periodic voltage'. EE in Japan, Vol-90, No.6, Nov./Dec. 1970, p26-37.

94. Turnbull, F.G. 'Selected harmonic reduction in static d.c. to a.c. inverters'. IEEE International Conference Record, Vol-83, 1964, p374-378.

95. Turnbull, F.G. 'Wide range, impulse commutated, static inverter with a fixed commutation circuit'. IEEE, IGA group annual meeting, 1966, p475.

96. Tsivitse, P.J., Eugene Killingshirn 'Optimum voltage and frequency for poly phase Induction motors operating with variable frequency power supplies'. IEEE Trans. Vol. IGA-7, No.1, Jan/Feb 1971, p61-68.

97. Ward, E.E.; Kazi, A. 'Time domain analysis of the inverter fed Induction motor'. Proc. IEE, Vol-114, No. 3, March 1967, p361-369.

98. Westinghouse Electric Corporation 'Generalised electric machine'. Lab.manual.

99. White, D.C.; Woodson, H.H. 'Electromechanical Energy Conversion'. (book) John Wiley and Sons 1959.

100. Williams, S.; Smith, I.R. 'Fast digital computations of 3 phase thyristor bridge circuits'. Proc. IEE, Vol-120, No.7, July 1973, p791.

101. Wiederholt, F.; Lawrensen, F.; Fredreri, A.; Wertz, H.Z. 'Motor transients analysis on a small digital computer'. IEEE Trans. Vol PAS-86, No.7, July 1967, p819-824.

- o -

APPENDIX I

PHASE AND TRANSFORMED IMPEDANCES

I-A PHASE IMPEDANCE MATRIX:

$$\left[Z^{s\ r}_{ryb,ryb}\right] =$$

$$\begin{array}{c} \\ r^s \\ y^s \\ b^s \\ r^r \\ y^r \\ b^r \end{array}
\begin{array}{c} r^s \\ \left[\begin{array}{c} R_1+\overline{L}_1p \\ \overline{M}_1p \\ \overline{M}_1p \\ \overline{M}p\cos\theta \\ \overline{M}p\cos\theta_2 \\ \overline{M}p\cos\theta_3 \end{array}\right. \end{array}
\begin{array}{c} y^s \\ \overline{M}_1p \\ R_1+\overline{L}_1p \\ \overline{M}_1p \\ \overline{M}p\cos\theta_3 \\ \overline{M}p\cos\theta \\ \overline{M}p\cos\theta_2 \end{array}
\begin{array}{c} b^s \\ \overline{M}_1p \\ \overline{M}_1p \\ R_1+\overline{L}_1p \\ \overline{M}p\cos\theta_2 \\ \overline{M}p\cos\theta_3 \\ \overline{M}p\cos\theta \end{array}
\begin{array}{c} r^r \\ \overline{M}p\cos\theta \\ \overline{M}p\cos\theta_3 \\ \overline{M}p\cos\theta_2 \\ R_2+\overline{L}_2p \\ \overline{M}_2p \\ \overline{M}_2p \end{array}
\begin{array}{c} y^r \\ \overline{M}p\cos\theta_2 \\ \overline{M}p\cos\theta \\ \overline{M}p\cos\theta_3 \\ \overline{M}_2p \\ R_2+\overline{L}_2p \\ \overline{M}_2p \end{array}
\begin{array}{c} b^r \\ \overline{M}p\cos\theta_3 \\ \overline{M}p\cos\theta_2 \\ \overline{M}p\cos\theta \\ \overline{M}_2p \\ \overline{M}_2p \\ R_2+\overline{L}_2p \end{array}\left]\right.$$

where:

$$\theta_2 = \theta + 120°$$
$$\theta_3 = \theta - 120°$$

I-B TRANSFORMED IMPEDANCE:

$$[Z^s_{ryb,\alpha\beta}] = \begin{bmatrix}
R_1+L_1p & 0 & 0 & \bar{M}p & -\frac{1}{2}\bar{M}p & -\frac{1}{2}\bar{M}p \\[6pt]
0 & R_1+L_1p & 0 & -\frac{1}{2}\bar{M}p & \bar{M}p & -\frac{1}{2}\bar{M}p \\[6pt]
0 & 0 & R_1+L_1p & -\frac{1}{2}\bar{M}p & -\frac{1}{2}\bar{M}p & \bar{M}p \\[6pt]
\bar{M}p & -\frac{1}{2}\bar{M}p+\frac{\sqrt{3}}{2}\bar{M}w_r & -\frac{1}{2}\bar{M}p-\frac{\sqrt{3}}{2}\bar{M}w_r & R_2+\bar{L}_2p & \bar{M}_2p+\frac{L_2}{\sqrt{3}}w_r & \bar{M}_2p-\frac{L_2}{\sqrt{3}}w_r \\[6pt]
-\frac{1}{2}\bar{M}p-\frac{\sqrt{3}}{2}\bar{M}w_r & \bar{M}p & -\frac{1}{2}\bar{M}p+\frac{\sqrt{3}}{2}\bar{M}w_r & \bar{M}_2p-\frac{L_2}{\sqrt{3}}w_r & R_2+\bar{L}_2p & \bar{M}_2p+\frac{L_2}{\sqrt{3}}w_r \\[6pt]
-\frac{1}{2}\bar{M}p+\frac{\sqrt{3}}{2}\bar{M}w_r & -\frac{1}{2}\bar{M}p-\frac{\sqrt{3}}{2}\bar{M}w_r & \bar{M}p & \bar{M}_2p+\frac{L_2}{\sqrt{3}}w_r & \bar{M}_2p-\frac{L_2}{\sqrt{3}}w_r & R_2+\bar{L}_2p
\end{bmatrix}$$

Where :

$$L_1 = \bar{L}_1 - \bar{M}_1$$

$$L_2 = \bar{L}_2 - \bar{M}_2$$

APPENDIX II

PER UNIT VALUES UNDER VARIABLE FREQUENCY OPERATION:

V_{base}	Base Voltage
I_{base}	Base Current
P_{base}	Base Power
V_o, i_o	Actual Voltage and Current
w_o	Operating Frequency
w_{ro}	Actual Speed of Rotation in Electrical Radians per sec.
w_b	Base Frequency
α_o	Actual Frictional Coefficient.

$\left. \begin{array}{c} w, w_R \\ V, T \\ \alpha, X \\ i, J \end{array} \right|$ Per Unit Values of Frequency, Speed, Voltage, Torque, Frictional Coefficient, Reactance, Current and Inertia Respectively.

Transformer EMF:

$$V_o = L \frac{di_o}{dt}$$

$$\frac{V_o}{V_{base}} = w \left(\frac{Lw_b}{V_{base}} I_{base} \right) \frac{di}{dw_o t} = wX \frac{di}{d(w_o t)} \qquad (II.1)$$

Resistive Load:

$$ \qquad (II.2) $$

$$V = Ri$$

204

Capacitive Drop:

$$V_0 = \frac{1}{C} \int i_0 \, dt$$

$$V = \left(\frac{X_C}{w}\right) \int i \, (dw_0 t) \tag{II.3}$$

Speed:

$$w_{ro} = w_0(1-s)$$

$$w_R = w(1-s) = \frac{w_{ro}}{w_b} \tag{II.4}$$

Generated EMP:

$$V_0 = M \, w_{ro} \, i_0$$

$$V = X_M \, w_R \, i \tag{II.5}$$

Torque:

$$T_0 = M \, i_{10} i_{20}$$

$$T_{base} = P_{base}/w_b \tag{II.6}$$

$$T = X_M \, i_1 i_2$$

Inertia:

$$T_{10} = \frac{J_0}{p} \frac{dw_{ro}}{dt}$$

$$T_1 = \frac{1}{p} \left(\frac{J_0 \, w_b^3 \, w}{P_{base}}\right) \frac{dw_R}{d(w_0 t)}$$

$$(II.7)$$

$$J = \frac{1}{p} \left(\frac{J_o \, w_b^3 \, w}{P_{base}} \right)$$

Frictional Coefficient:

$$\alpha_o \, w_{ro} = T_{fo}$$

$$\frac{T_{fo}}{T_{base}} = \frac{1}{p} \left(\frac{\alpha_o \, w_b^2}{P_{base}} \right) \, w_R$$

$$(II.8)$$

$$\alpha = \left(\frac{\alpha_o \, w_b^2}{P_{base}} \right)$$

In the above equations $t_{base} = \frac{1}{w_o}$, since this gives always a constant time period of 2π electrical radians for any frequency, thus simplifying the computations.

- o -

APPENDIX III

NORMAL MACHINE PARAMETERS:

III-A EXPERIMENTAL DETERMINATION:

The following observations were recorded for no load test with the motor driven at synchronous speed and blocked rotor test, over the test motor of 2 H.P., 400 V, star connected, 2360 rpm.

Test	Line Volts	Line Amps.	Power (watts)
NO LOAD	400	1.65	160.0
BLOCKED ROTOR	64	4.0	384.0

Frictional losses as determined by variable voltage test (fig. III.2) are equal to 35 watts.

Stator resistance (d.c.) = 4.32 ohms.

Corrected power at no load = No load input - no load stator resistance losses - frictional losses

= 81.0 watts.

A skin effect ratio k_s of 1.1 is assumed at 50 Hz to get effective stator resistance, giving R_1 = 4.76 ohms. The expressions for effective resistance and reactance from the equivalent circuit (fig. III.1) are -

$$R = R_1 + \frac{(R_2 R_M - X_{12} X_M)(R_M + R_2) + (R_M X_M + R_2 X_M + R_M X_{12})(X_{12} + X_M)}{(R_M + R_2)^2 + (X_{12} + X_M)^2}$$

(III.1)

$$X = X_{L1} + \frac{(R_M + R_2)(R_M X_M + R_2 X_M + R_M X_{L2}) - (X_{L2} + X_M)(R_2 R_M - X_{L2} X_M)}{(R_M + R_2)^2 + (X_{L2} + X_M)^2}$$

Where -   (III.2)

$$X_M = 142.6 \text{ ohms}$$

$$R_M = 1980.0 \text{ ohms}$$

$$R = 8.0 \text{ ohms}$$

$$X = 9.04 \text{ ohms}$$

$$X_{L1} = X_{L2}$$

$$R_1 = 4.76 \text{ ohms}$$

From equations (III.1) and (III.2) with other parameters known, R_2 and X_{L2} can be determined, giving:

$$R_2 = 3.04 \text{ ohms}$$

$$X_{L2} = 4.56 \text{ ohms.}$$

D.C. Rotor Resistance:

Variable frequency blocked rotor test is conducted varying frequency from 75 Hz to 5 Hz keeping short circuit current at constant level of 3 amps. The observations are given in table (III.1). The skin effect ratio k_s approaches unity for frequencies less than 20 Hz[26]. The average of
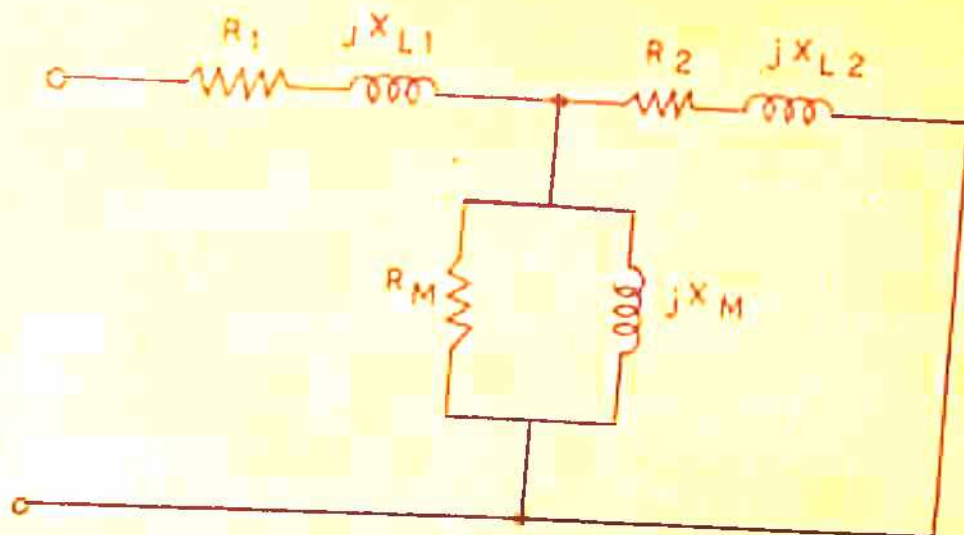
FIG. III·1 EQUIVALENT CIRCUIT UNDER BLOCKED ROTOR CONDITION

WF (50HZ) = 35 WATTS

WF (25HZ) = 10 WATTS
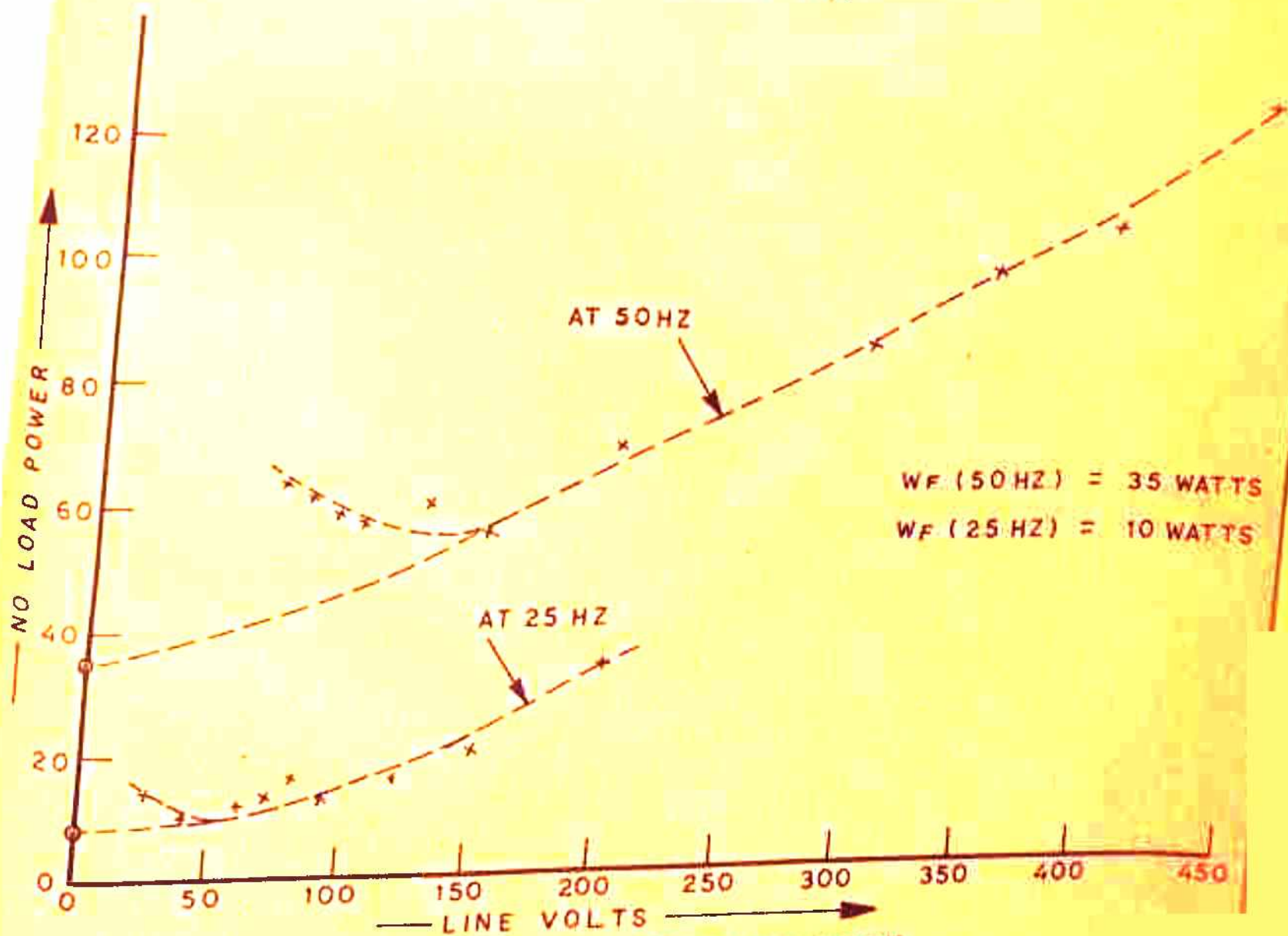
FIG. III·2 VARIABLE VOLTAGE TEST

rotor resistances at 15,10 and 5 Hz may safely be taken as the d.c. rotor resistance, giving $R_{2(d.c.)} = 2.71$ ohms.

Table III.1   Variable Frequency Blocked Rotor Test:

Frequency (Hz)	Line Volts	Input Watts.	$R_1 + R_2$	R_2	Line Amps.
75	89	228	7.90	3.13	3.0
70	86	219	7.75	3.02	3.0
65	80.5	205	7.56	2.79	3.0
60	75	194	7.60	2.83	3.0
55	72.5	186	7.45	2.72	3.0
50	69.0	170	7.65	2.92	3.0
45	65.0	154	8.0	3.27	3.0
40	62.0	144	7.55	2.82	3.0
35	59.5	133	7.52	2.79	3.0
30	55.0	120	7.54	2.80	3.0
25	49.0	97	7.52	2.79	3.0
20	47.0	83	7.45	2.72	3.0
15	43.0	59	7.36	2.63	3.0
10	43.0	38	7.46	2.73	3.0
5	36.0	20	7.51	2.77	3.0

APPENDIX IV

DESIGN OF SINGLE SECTION LC FILTER:

The objective of filter connected between the rectifier and inverter (fig. IV.1) is to attenuate the harmonic ripples present in the rectified output voltage. The basic considerations in designing a filter are as given below[7].

(i) The minimisation of total rectifier output current, by providing a suitable value of shunt filter element.

(ii) The minimisation of voltage regulation with proper value of filter series element.

(iii) The minimisation of filter cost, size and weight.

The attenuation of a given frequency is determined by its relation with the resonant frequency of the filter. It is relatively simple to determine the required LC product[81] to attenuate a harmonic by a given amount. The attenuation ratio $K_{A,n}$ defined as E_R/E_L is given as (an approximate relation).

$$K_{A,n} = \frac{E_R}{E_L} = w_b^2 L_F C_F - 1 \qquad (IV.1)$$

Fig. IV.2 gives the variation of $K_{A,n}$ (for $n = 6$) against a product LC. A large value of L_F and small C_F will give high regulation and a value of rectifier current slightly larger than the load current. On the other hand, a small value of L_F and a large C_F will result in low regulation but a

large increase of rectifier current over the load current value. In either case rating of the rectifier is adversely effected. Thus, a TRADE OFF is required. The power factor of the load as is shown in the subsequent relations has an important bearing on this trade off. It is desirable to consider the effects of the values of both L_F and C_F on attenuation of harmonic ripples present in S_R. This information is needed to determine the circuit relationship required to give a desired attenuation of a given frequency component. From fig. IV.1 for nth harmonic the following relations can be written:

$$X_{LFn} = n \, |X_{LF}| = n \, K_2 \, |Z_L| \qquad (IV.2)$$

$$X_{CFn} = \frac{|X_{CF}|}{n} = \frac{K_1}{n} \, |Z_L|$$

where

$$K_2 = \frac{|X_{LF}|}{|Z_L|} \qquad (IV.3a)$$

$$K_1 = \frac{|X_{CF}|}{|Z_L|} \qquad (IV.3b)$$

$$Z_{Ln} = R_L + jn \, |X_L|$$

$$= |Z_L| \, (\cos\theta + jn\sin\theta)$$

and

$$\frac{S_{Ln}}{S_{Rn}} = \frac{jnK_2 + (Z_{on}/|Z|) - jnK_2}{jnK_2 + (Z_{on}/|Z_L|)} \qquad (IV.4)$$

FIG. IV·1 FILTER

FIG. IV·2

FIG. IV·3
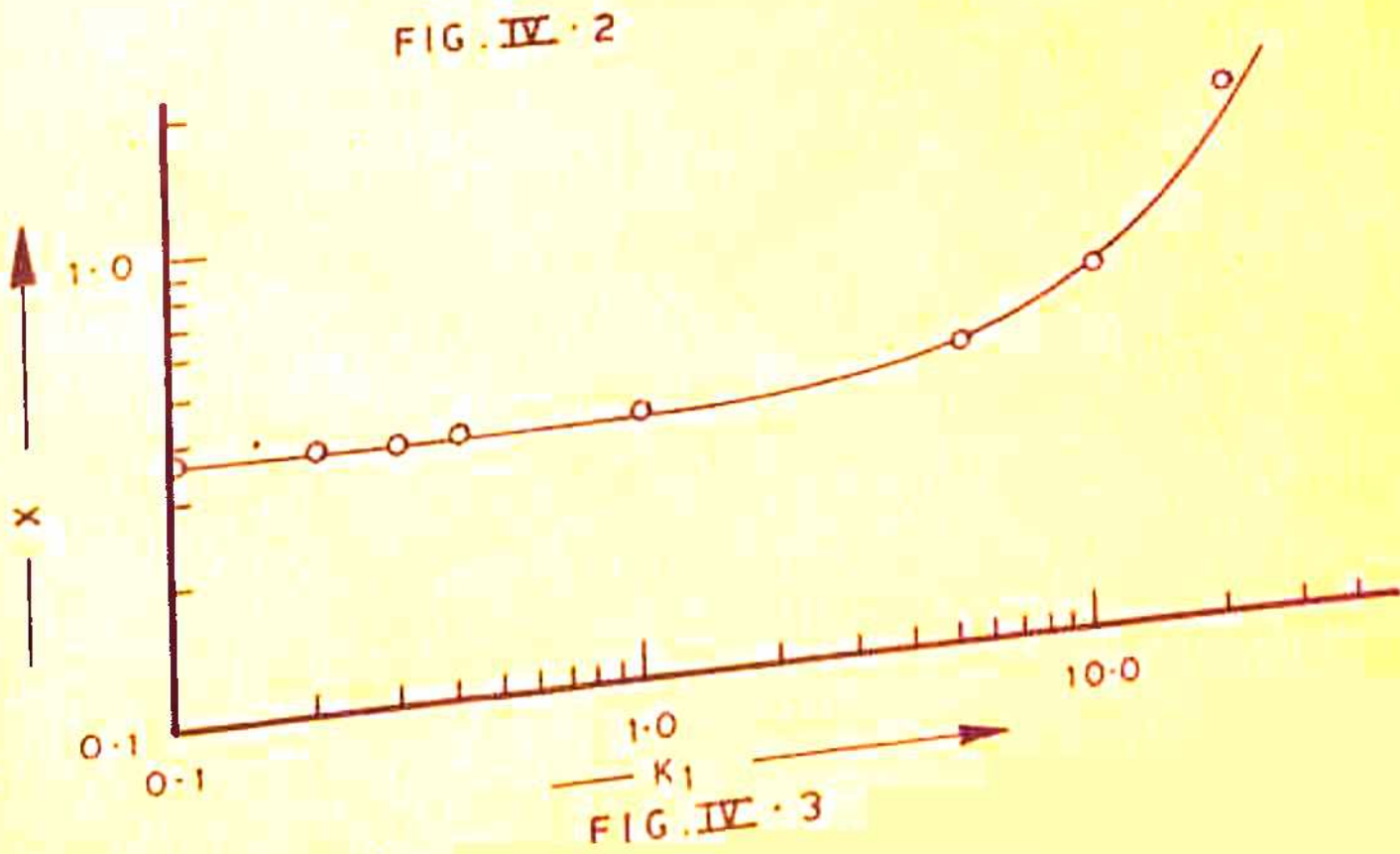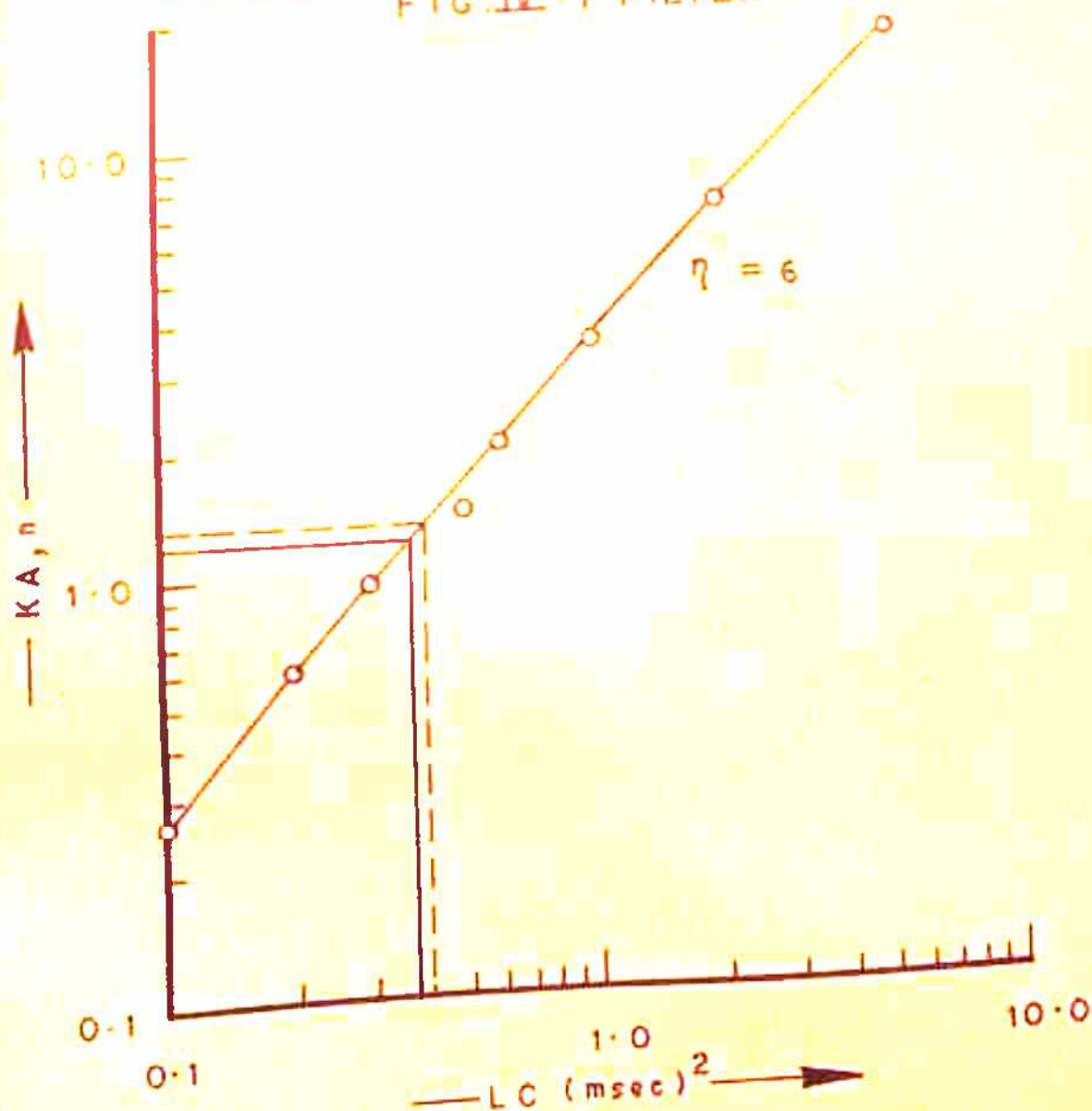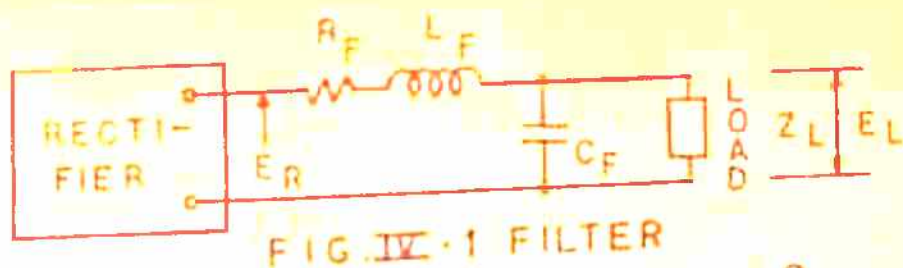
where

$$Z_{on} = \frac{Z_{In} - jX_{CFn}}{Z_{In} + (-jX_{CFn})}$$

Let

$$K_{A,n} = \frac{Z_{Rn}}{Z_{Ln}} \quad \text{(Attenuation constant for nth harmonic)} \quad \text{(IV.5)}$$

$$\frac{Z_{on}}{|Z_L|} = \frac{-j\frac{K_1}{n}(\cos\theta + jn\sin\theta)}{(\cos\theta + jn\sin\theta) - j\frac{K_1}{n}} \quad \text{(IV.6)}$$

where θ is the load impedance angle.

From equations IV.4, IV.5 and IV.6 we get -

$$X = \frac{K_2}{K_1} = \frac{1}{n^2} \left| \frac{\cos\theta + jn\sin\theta}{\cos\theta + j(n\sin\theta - \frac{K_1}{n})} \right| (K_{A,n} - 1) \quad \text{(IV.7)}$$

The variation of X with K_1 is shown in fig. IV.3.

Normal Filter Values:

The apparent fundamental impedance $|Z_L|$ is determined by transforming the a.c. quantities of the machine to synchronously rotating reference frame [37,49,50] and equating the power on d.c. and a.c. side, which give the following relations:

$$v_q^s = \frac{2}{\pi} V_1 \qquad i_q^s = \frac{\pi}{3} I_1 \qquad \text{(IV.8)}$$

$$v_d^s = 0 \qquad\qquad\qquad (IV.9)$$

Thus the apparent load impedance is -

$$Z_q^s = \frac{v_q^s}{i_q^s} = \frac{6}{\pi^2} Z_1$$

$$Z_1 = \frac{\pi^2}{6} Z_q^s$$

where -

Z_1 apparent load impedance on inverter side

Z_q^s apparent load impedance of the motors.

For a three phase motor taking 4 Amps. at 220 Volts (phase) at 0.8 p.f. lag. at full load, the apparent load impedance Z_q^s is equal to $55\,\underline{/-36^0}$ ohms, thus giving an apparent load impedance on inverter Z_1 equal to $91.6\,\underline{/-36^0}$ ohms. Assume $K_{A,6} = 20$ for sixth harmonic ripples. Fig. IV.2 gives a LC product of 36 (msec)^2 and, $X = w_b^2\,LC \times 10^{-6} = .355$. From fig. IV.3, the constant $K_1 = 0.1$ for $X = 0.355$. Here low value of filter inductance has been preferred, as it reduces the dip or overshoot of the output voltage in case of sudden load change. Dissipated power in choke is also less with small filter inductance. Choosing a value of 0.035 for K_1 we get-

$$X_{LF} = .035 \times 91.67 = 3.2 \text{ ohms} = 0.08 \text{ p.u.}$$

$$L_F = 100 \text{ mH} \quad \text{and} \quad C_F = 400 \text{ MF or } 0.2 \text{ p.u.}$$

A reasonable resistance value $R_F = 0.01$ p.u. is attached with the filter choke.

- 0 -

APPENDIX V

SETS OF SYSTEM PARAMETERS:

With the maximum and the minimum limits prescribed in table 3.1 and 3.2 of Chapter 3, the following sets of system parameters (table 5.1) are obtained by varying one at a time and keeping the other fixed at their normal values:

Table V.1   Sets of System Parameters.

Set	R_1	R_2	$X_{L1}=X_{L2}$	X_M	X_F	X_C	R_F
1	0.119	0.081	0.113	3.564	0.08	0.2	0.01
2	0.357	0.081	0.113	3.564	0.08	0.2	0.01
3	0.06	0.081	0.113	3.564	0.08	0.2	0.01
4	0.119	0.138	0.113	3.564	0.08	0.2	0.01
5	0.119	0.034	0.113	3.564	0.08	0.2	0.01
6	0.119	0.081	0.25	3.564	0.08	0.2	0.01
7	0.119	0.081	0.031	3.564	0.08	0.2	0.01
8	0.119	0.08	0.197	7.128	0.08	0.2	0.01
9	0.119	0.08	0.093	2.673	0.08	0.2	0.01
10	0.119	0.08	0.113	3.564	0.25	0.2	0.01
11	0.119	0.08	0.113	3.564	0.02	0.2	0.01
12	0.119	0.08	0.113	3.564	0.08	0.5	0.01
13	0.119	0.08	0.113	3.564	0.08	0.05	0.01

APPENDIX VI

MACHINE CONSTANTS AND LOSS COEFFICIENTS:

VI-1   Machine Constants:

The relevant dimensions (all in cms) and other design information for the TEST MOTOR are given below:

(i)   Diameter at the inner surface D_1 = 10.25

(ii)   Length of the stack L = 6.4 cms.

(iii)   Number of stator slots S_1 = 24

(iv)   Number of rotor slots S_2 = 31

(v)   Stator wire size = 20 swg

(vi)   Number of turns per phase = 344

(vii)   Number of poles = 2

(viii)   Airgap length = 0.175

(ix)   Stator slot opening = 0.3

(x)   Rotor slot opening = 0.1

(xi)   Rotor slot skew = 1.6

(xii) Y_1 (fig. 2.1) = 2.5

(xiii) Y_2 (fig. 2.1) = 187

(xiv)   A (fig. 2.1) = 8.1

(xv)   Rotor tooth width = 0.35

(xvi)   Stator tooth width = 1.1

(xvii)   Stator coil pitch = 8 slots.

VI-2   Loss Coefficients:

(a)   Iron Loss Coefficient:

The hysteresis and eddy losses are separated with the

217

help of usual variable frequency no load test. The no load power is corrected for frictional losses and no load stator resistance losses which are quite substantial, can not be ignored. The test is conducted at constant V/f ratio, to keep the airgap flux density fixed.

From fig. VI.1, we get -

$$k_1 = 0.55 \text{ and } k_2 = 0.0164 \text{ and}$$

$$W_1 = 0.55 \, f_0 + 0.0164 \, f_0^2$$

The other iron loss coefficients as defined in equations (2.15), (2.16), (2.17) and (2.18) are -

$$K_1 = 1.0535, \quad K_2 = 1.0744$$

$$G_1 = 0.03608, \quad G_2 = 0.12865$$

(b) Stray Loss Coefficients:

(i) Loss Coefficients Independent of Frequency:

$$C_S = 0.061$$
$$C_{SL} = 7.2 \times 10^{-4}$$
$$C = 0.114$$
$$C_K = 8.5 \times 10^{-4}$$

(ii) Frequency Dependent Loss Coefficients:

The high frequency surface loss and rotor pulsation loss equations consist of frequency dependent constants $C_{K(n)}$ and k_{sn} respectively. The values of these constants are given in table VI.1.
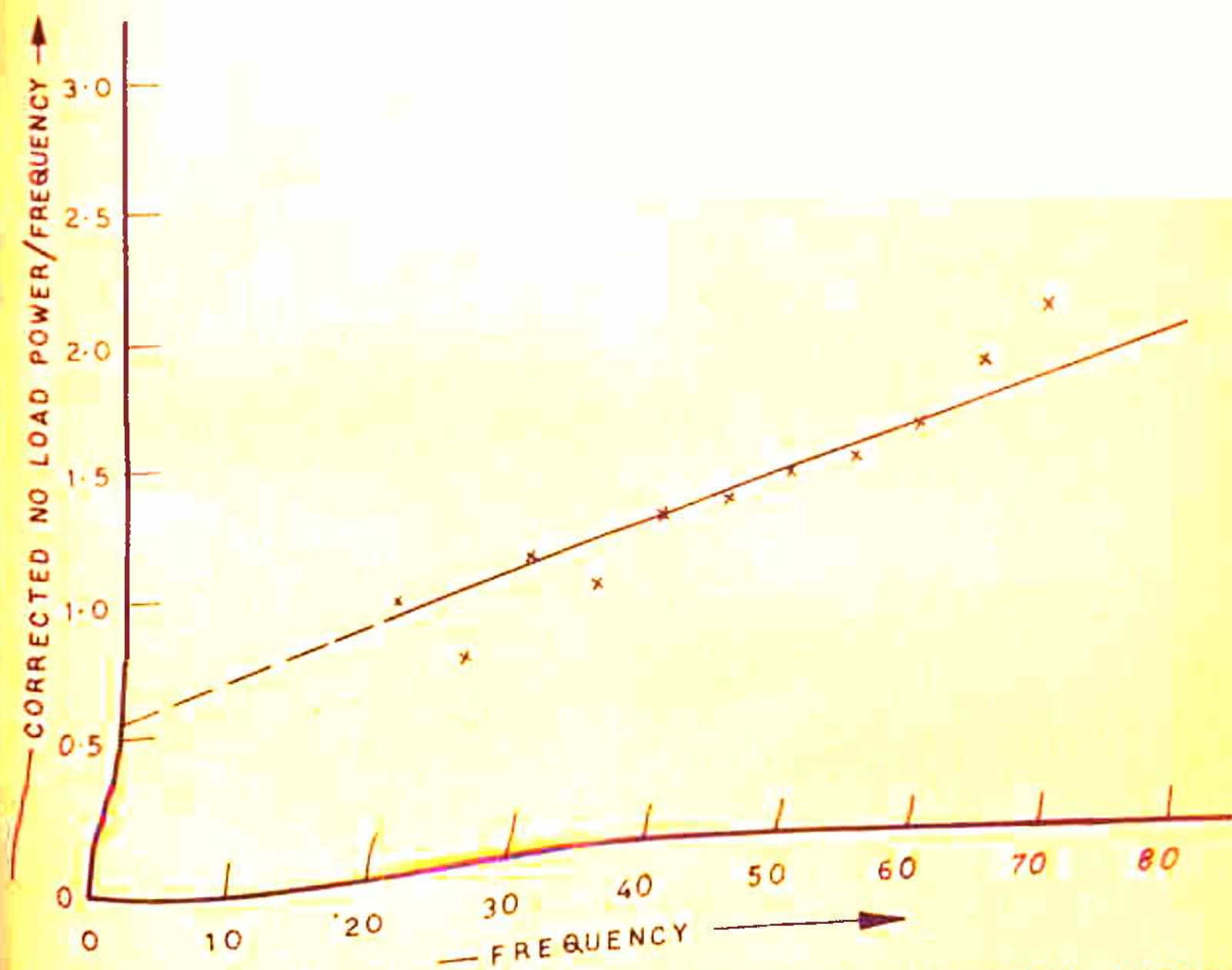
FIG. VI-1 SEPARATION OF HYSTERESIS AND EDDY LOSSES.

Table VI.1 Frequency dependent loss coefficients.

$C_{K(n)}$

n	Per Unit Frequency											
	0.1	0.2	0.3	0.4	0.5	0.6	0.7	1.0	1.5	2.0	3.0	4.0
1				NEGLIGIBLE				17.5	21.0	50	89.3	129
5								163	210	351	548	738
7								247	345	510	778	1015
11								401	538	825	1240	1672
13								481	768	967	1468	1361

k_{sn}

n	0.1	0.2	0.3	0.4	0.5	0.6	0.7	1.0	1.5	2.0	3.0	4.0
1	1.13	1.43	1.80	2.40	2.45	2.70	2.90	3.44	4.1	4.9	6.0	6.95
5	2.45	3.44	4.25	4.9	5.61	6.65	6.65	7.74	8.63	10.9	13.4	15.4
7	2.31	4.11	5.0	5.8	6.65	7.0	7.66	9.2	11.3	12.9	15.8	15.4
11	3.66	5.14	5.31	7.27	6.35	8.88	9.63	11.21	13.4	16.2	13.9	22.8
13	3.36	5.61	6.86	7.2	7.97	9.68	10.7	12.5	14.9	17.6	21.6	25.0

(c) **Frictional loss Coefficients:**

Variable voltage test at 50 and 25 Hz are conducted over the test motor. These observations are given in Fig. III.2 and the loss coefficients of equation (2.48) are determined. The values are: $A_1 = 0.1$, $a_1 = 0.012$

CURRICULUM VITA:

1. Name of Author   O.P. GARG

2. Academic Qualifications:

Degree	Year	University/Institute
B.E.(Electrical)	1963	Rajasthan University
M.E.(Adv.Elect.M/c)	1966	Roorkee University

3. Member of Professional Bodies

    (a)   Member of Institution of Engineers (India) (MIE).

    (b)   Associate Member of Society of Power Engineers.

4. List of Research Papers

    1.   Losses in Inverter Fed, Wide Speed Range
         Three Phase Induction Motor.
         O.P. Garg, R.B. Saxena
         Electrical India, 30th April 1975, p5.

    2.   Effect of Various Machine Parameters on the Torque
         Pulsations of Inverter Fed Variable Speed Three
         Phase Induction Motor.
         O.P. Garg, R.B. Saxena.
         Presented at a Seminar on 'Power Management and
         Energy Conservation' held at Ludhiana on Sept. 12-14,
         1975. Organised by Institution of Engineers (India).